Western Australian School of Mines

Mineral Engineering and Extractive Metallurgy

Investigation of the Reasons for Copper and Gold Loss in the Cleaner Tail, at Ok Tedi, Papua New Guinea

Peter Erepan

This thesis is presented for the Degree of Master of Science
of
Curtin University of Technology

July 2004

Declaration

This thesis contains no material which has been accepted for the award of any other degree or diploma in any university.

To the best of my knowledge and belief this thesis contains no material previously published by any other person except where due acknowledgment has been made.

Signature:

Date: 10-06-04

Acknowledgements

The author wishes to express his appreciation to Ok Tedi Mining Limited for their sponsorship of this research over the past three years. Special thanks also go to the AusAID office at Curtin University of Technology, for the provision of an opportunity to study at the W.A. School of Mines in the Post Graduate Diploma and Masters Programs.

Many people have provided valuable assistance toward the completion of this project. In particular, the support and guidance of my supervisors Dr. Michael Morey, Team Leader, Metallurgy Projects (OTML), and Dr. Denis Yan, Programme Chair of Minerals Engineering & Extractive Metallurgy, W.A. School of Mines, is noted. Dr. Morey contributed significantly with technical assistance and project reviews through the course of this study. Danny Orwe, Senior Development Metallurgist (OTML) is also acknowledged for technical input in the initial stages of the project and for his encouragement toward keeping the project on schedule. I also acknowledge Dr. David Lauder, a consultant metallurgist, for his editorial contribution. This project was first suggested by Mr. Jonathan Glatthaar, (former) Chief Metallurgist, OTML and his technical support is acknowledge with appreciation.

Thanks are also due to the hard working OTML metallurgical laboratory team for their participation in survey sampling, sample preparation and technical assistance. Furthermore, Mr. Ashley Stewart, Senior Technical Sales Representative of Cytec Australia, and Ms. Jennie Coe, Research Mineralogist of Cytec America, are acknowledged for providing free, the mineralogical ore liberation data contained in this thesis.

Finally, I would like to thank my family and church for being a constant source of moral support during the three years it took to complete this study at the W.A. School of Mines, Curtin University of Technology, Western Australia.

Abstract

Ok Tedi Mining Limited generates a copper and gold concentrate from its porphyry and skarn ore deposits located at Mt. Fublian, Western Province, PNG. The predominant porphyry ore-type is blended with high grade skarn ores to optimize copper and gold feed grades to the concentrator. Current operation (2003) is to blend 80% porphyry with 20% skarn ores, resulting in an acceptable concentrate grade and recovery.

However, when the proportion of skarn ore in the plant feed exceeds 20%, low flotation recovery is often observed. Approximately 20% of the copper and 30% gold losses occur through the rougher flotation circuit. However, losses via the cleaner tailing stream are 8% and 9% for copper and gold, respectively, and augment value mineral losses to the final tailing. It may be noted that the cleaner tailing stream contains value minerals which have already been successfully floated in the rougher section of the concentrator, and are therefore recoverable.

This study has the objective of determining the reasons for copper and gold loss in the cleaner tailing. The focus is therefore on the cleaner flotation bank and related streams. The project strategy commenced with characterization of the cleaner circuit performance under various operating conditions. This would provide evidence for any proposed mechanisms to explain the losses of valuable minerals to the cleaner tailing. The second part of the project strategy was to evaluate potential methods for improvement of cleaner flotation performance via laboratory flotation tests. To complete the work, plant trials of methods showing benefit in the laboratory were conducted.

Characterisation surveys of the cleaner flotation bank were conducted as a function of ore blend, pulp and surface chemistry, mineralogy, flotation kinetics, particle size distribution, cleaner flotation cell hydrodynamic characterisation and residence time. These studies indicated that for greater than 20% pyrite skarn in the concentrator feed blend, lower than expected gold and copper recoveries were achieved in the cleaner bank. Pulp and surface chemical analytical techniques indicated layers of oxide coatings existed on all particles, depressing flotation. Oxide coatings had also resulted in the copper activation of pyrite (CuS rimming), making separation from copper sulfides difficult. Losses included coarse composite particles, also suggesting possible liberation issues.

However, liberated copper sulfides were also lost, supporting the notion of depression via oxide coatings. Residence time calculations for the cleaner flotation bank suggested that the flotation capacity was less than adequate, particularly at high mill throughput rates. Hydrodynamic characterisation indicated improvements in cell hydrodynamics were warranted.

In contrast to the oxidised ore feed blend described above, when less than 20% pyrite skarn was contained in the ore blend, high copper and gold recoveries were achieved in the cleaner bank.

Laboratory tests suggested that increasing cleaner feed pH from 10.5 to 11.5, and / or collector addition to the cleaner feed, would result in improved cleaner flotation performance. These changes were trialed in the plant, with the pH adjustment being successful. High cleaner feed pH continues as a permanent modification to plant operating conditions.

TABLE OF CONTENTS

LIST OF FIGURES

LIST OF TABLES

CHAPTER 1: GENERAL INTRODUCTION

1.1 Introduction

Flotation recovery for copper and gold at the Ok Tedi Concentrator has decreased significantly in recent years. Current (2001) plant performance shows an 76 percent copper recovery and 59 percent gold recovery, which is well below the budgeted figures of 82 percent and 64 percent, respectively. Losses of valuable minerals occur via the two final tailings streams, designated as rougher tailing and cleaner tailing. Most of the mineral losses occur through the rougher flotation circuit, owing to the high volumetric flow. Although the volumetric flow through the cleaner circuit is small, a higher loss of copper and gold in the tailings is usually encountered during treatment of a high proportion of skarn ore in the mill feed blend. This augments the final tailings losses and lowers the total plant recovery. Plant results from July 1990 to December 2000 have produced evidence to confirm the problem. The average loss of copper and gold through the cleaner circuit was found to be 8 and 9 percent, respectively. Higher losses were also observed in the rougher circuit (Gron 2001).

The factors that contribute to affect the floatability of copper and gold are not known, at this present time. Therefore, this research project was suggested to investigate the problem with respect to mineral losses occurring in the cleaner tail.

1.2 Aim and Objective

The aim of this research project is to investigate reasons for copper and gold losses from the cleaner tailing. At present, there is very limited relevant information on the cleaner circuit performance. The project objective therefore is to characterize the cleaner circuit performance, and provide causal evidence for the losses of valuable minerals to cleaner tailing.

1.3 Strategy

To achieve the project objectives, the following strategy was put in place. The broad project framework included four stages, conducted in three phases. The stages of the project included:

1 Determination of losses occurring in the cleaner tailing stream.

2 Determination of reasons for copper and gold losses.

3 Laboratory evaluation of methods to improve cleaner flotation recovery.

4 Plant trials of methods showing benefit in the Laboratory.

The three project phases were firstly, characterization surveys of the cleaner bank flotation performance. The cleaner circuit surveys were conducted as a function of:

- Blended ore type.
- Pulp & surface chemistry, including Eh, pH, collector adsorption, valuable mineral surface oxidation and surface contamination, depression of gangue minerals, particularly pyrite.
- Denver DR500 cleaner flotation cell hydrodynamic conditions.
- Residence time.
- Particle size by size.
- Mineralogy.
- Flotation kinetics.

Because of the large range of ore types and blends possible in the Ok Tedi concentrator feed, the cleaner survey work was simplified to include a comparison of cleaner performance for a typical 'good' ore blend (porphyry stocks) and a typical 'difficult' ore feed blend (including sulphide skarn components). This simplification has been justified on the grounds of practicality, and from some mineralogical and pulp chemical evidence which suggests that the major problems of different ore blends largely differ in degree rather than the type of problem encountered (Morey & Grano 2000). Of course there will be exceptions to this generalization. However, it provides an appropriate scope for the project and may provide solutions to poor cleaner flotation performance under a large range of feed conditions.

Project phase two, laboratory test work, was somewhat dependent on outcomes from the survey work. However, obvious tests to be included were:

- Examination of different collector dosage.
- Examination of the effect of pH.
- Examination of the effect of water quality.
- Examination of the effect of aeration.
- Examination of the effect of agitation.
- Examination of the effect of flotation time.

The third and final project phase of plant trials included:

- Lime addition to cleaner circuit.
- Collector addition to cleaner circuit.
- Cleaner flotation response to an unground feed (i.e. without running the regrind mill prior to cleaner flotation).

1.4 Background

1.4.1 Ok Tedi Mine: Overview

The Ok Tedi story began in 1963 when a government patrol officer discovered copper mineralization near Mt. Fubilan. Six years later, in 1969, a Kennecott exploration geologist discovered a mineralized float at the Ok Tedi-Ok Menga confluence and traced its source to the Mt. Fubilan area. A prospecting authority was issued to Kennecott Copper Corporation over the area and a deposit was later discovered at Mt. Fublian. A drilling program was undertaken from 1969 to 1971 to evaluate the deposit and found favourable ore reserves. However, the company withdrew in 1975, when an agreement to develop the project could not be reached, based on government terms and conditions.

In 1976, the Broken Hill Proprietary Company Limited (BHP) successfully negotiated an agreement with the government to develop the project. A consortium was then formed to carry out a project feasibility and pilot plant studies. The National Government accepted the proposals in 1980. Ok Tedi Mining Limited was incorporated in 1981, to develop and mine the deposits. Mining was designed in three phases due to the geometry of the deposits. The first phase involved the mining and processing of the rich gold cap from 1984 to 1987. From then on, both copper and gold ore were mined and processed. However, the gold plant was decommissioned in 1988 when the oxide ore was exhausted, resulting in a final phase of mining and processing of sulphide ore to produce copper concentrate (Rush & Seegers 1990).

Historically, Ok Tedi Mining Limited (OTML) owners have been BHP (52%), the Independent State of Papua New Guinea (30%) and Inmet Mining Corporation of Canada (18%). However, in February 2002, after an agreement was reached with the PNG government and BHP shareholders, BHP withdrew from the company and awarded its 52% stake to the traditional people of Western Province and the National Government. Ok Tedi Mining Limited is now owned by Inmet (18%), National Government (30%) and PNG Sustainable Development Program Limited (52%). The PNG Sustainable Program Limited is an independent company set up to manage the 52% shareholding formerly

owned by BHP, and to develop the mine affected area in the Western province of Papua New Guinea.

1.4.2 Description of Ok Tedi Ore

The regional geology and exploration history has been described by Rush and Seegers (1990). The Ok Tedi deposit at Mt. Fubilan consists of a number of ore types. The main body of copper mineralisation is related to the intrusion and alteration of a monzonite porphyry stock. As a result of many years of weathering, the porphyry stock was subject to oxidation. A leach cap (oxide ore) and an enriched copper zone was thus formed overlaying the primary mineralisation. The leached cap contained significant gold mineralisation, also extending downwards into the copper mineralisation. Surrounding the porphyry stock was the skarn mineralisation, formed by the acidic pneumatolytic fluids contacted with the host country rocks. The country rocks were predominately calc-alkaline basic rocks.

1.4.2.1 Ok Tedi Ore Deposits and Mineralogy

The Ok Tedi porphyry–skarn intrusive system, located within the raised sediments of the Hindenberg ranges in the Star Mountains of the Western Province of Papua New Guinea, has been classified as an hydrothermal deposit. Based on the rock lithology, Fubilan stock was classified as Monzonite and Monzodiorite porphyry intrusive rocks which are acidic in nature. Monzonite porphyry ore is predominately alkali-feldspar and Monzodiorite porphyry ore is predominately plagioclase feldspar. There are a number of different skarn ores formed by contact between the acid intrusive and surrounding host rock and are named according to the rock lithology. These include magnetite skarn, pyrite skarn, oxide skarn and calcium-silicate skarn. Endoskarn is a particular ore type occurring at the contact between porphyry and skarn ores. Endoskarn combines the porphyritic mineralogy with the greater sulphide deposition of skarn ores. Siltstone ore is an additional category based on the country rock prior to intrusion, with copper minerals

deposited along fractures in the country rock at close proximity to intrusion. Figure 1.0 shows a geological plan of the ore bodies currently mined for copper–gold flotation (Rush & Seegers 1990).

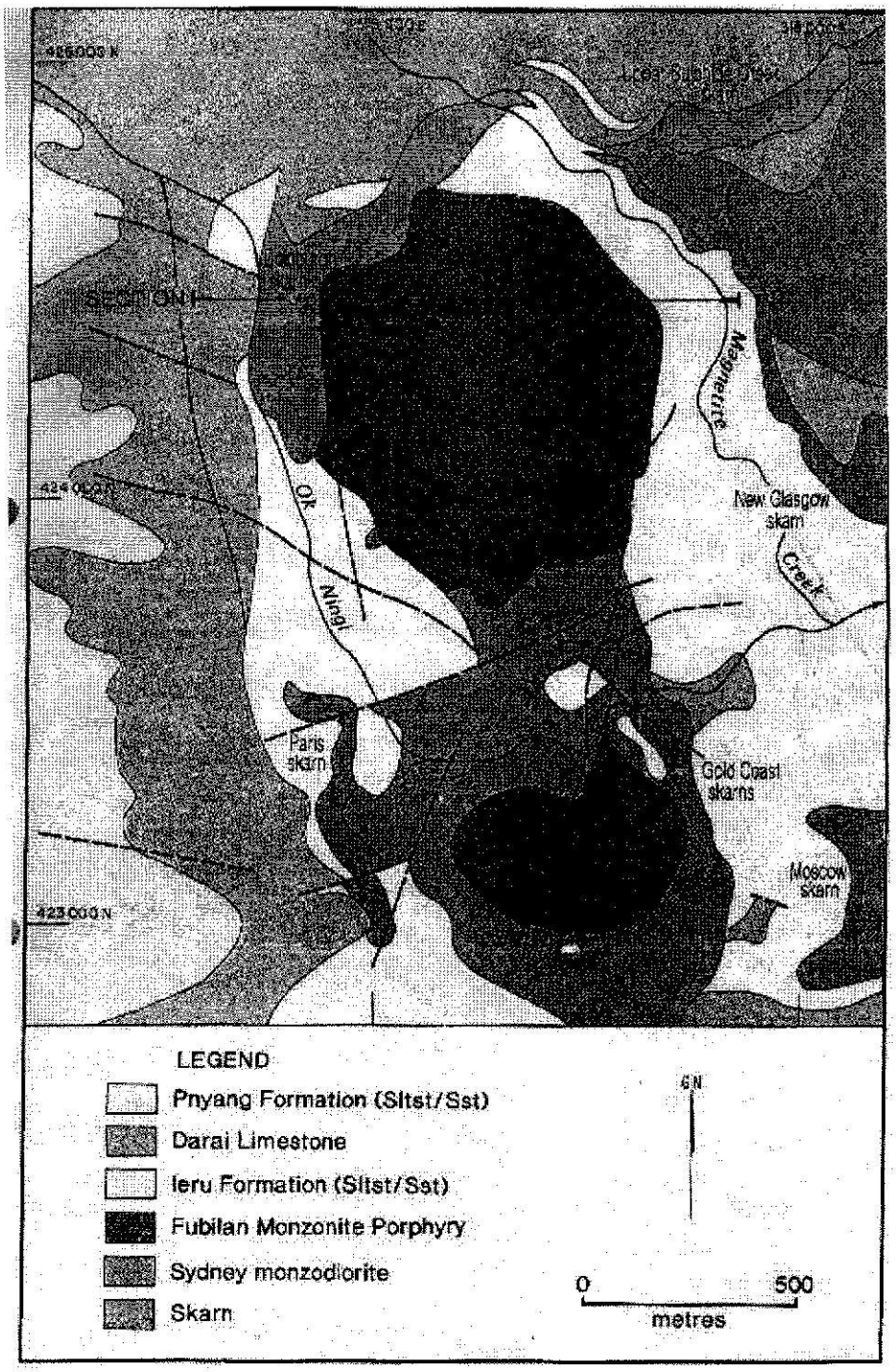

Figure 1.0: Geological mine plan (Rush & Seegers 1990)

Copper mineralization resulted from the intrusion and alteration of monzonite and monzodiorite porphyry stocks. Subsequent leaching and redeposition of copper minerals produced a leached cap of significant gold overlaying a secondary enriched copper ore. Below this was the primary porphyry ore body. Each ore type has it's own mineralization. For monzonite porphyry ore, the primary copper minerals are chalcopyrite, bornite, and native copper. These are disseminated in fractures (veinlets & crack infills). The secondary copper minerals associated with this ore are; chalcocite, covellite, malachite, azurite, cuprite, chrysocolla, turquoise and chalcanthite. These minerals occur predominantly in fractures. Chalcocite and covellite occur both in fractures and as coatings of primary sulphides (chalcopyrite/pyrite).

Chalcopyrite is the primary copper mineral associated with monzodiorite ore and predominately occurs on fractures. The occurrences of secondary copper minerals in monzodiorite are similar to those of monzonite formation.
The mineralogy of skarn ores includes predominately chalcopyrite with pyrite, digenite, chalcocite, covellite and bornite. The copper minerals are disseminated in fractures and as interstitial grains. Chalcopyrite and covellite occur in fractures and as coatings of primary sulphides (chalcopyrite/pyrite). There are traces of oxide copper minerals, malachite, cuprite, chalcanthite, azurite and cupriferous iron minerals formed from oxidation of the sulphide minerals.

The gangue minerals associated with copper sulphides are pyrite, pyrrhotite, silicates, carbonates, goethite, limonite, and magnetite. Pyrite is the most significant gangue mineral in the Ok Tedi deposit. Copper sulphides and gold are associated with pyrite (Ninduara 2002).

The total ore reserves as of June 2000 are 305 million tonnes estimated at 0.87% copper and 0.93 g/t gold. Table 1.0 shows the distribution of the ore reserves.

Oretype	% of Total Ore	Million Tonnes	% Cu	Au (g/t)
Monzonite Porphyry	50.8	155	0.58	0.52
Monzodiorite Porphyry	6.6	20	0.50	1.73
Sulphide Skarn	25.9	79	1.51	1.73
Pyrite Skarn	1.3	4	1.37	2.77
Endoskarn	12.8	39	0.82	0.97
Oxide Skarn	0.6	2	1.84	1.90
Siltstone	2	6	0.79	0.57
Total	100	305	0.87	0.93

Table 1.0: Ok Tedi pit ore reserves at June 2000

1.4.3 Concentrator Flowsheet Description

The Ok Tedi concentrator consists of a crushing and ore delivery system feeding two parallel grinding and flotation circuits that are similar in design and throughput. A schematic flowsheet of the concentrator is shown in Figure 2.0.

1.4.3.1 Crushing and Ore Delivery

The concentrator is located approximately 1 kilometer from the mine. Run of mine ore (ROM) is delivered directly from the mining face to the 'Inpit' and 'Taranaki' crushers. The primary crushing is open circuit through a 60" by 102" Nordberg crusher producing 4,000 to 7,000 tonnes per hour (tph) of minus 250 mm coarse material. The crusher product is carried via overland conveyor belts for 1.5 km to a 300,000 tonne intermediate stockpile. The material from this stockpile is drawn by three 11.6 m by 2.4 m Krupp

apron feeders and discharges onto a 1.8 m wide, single overland conveyor. The conveyor delivers to two 30,000 tonne SAG feed stockpiles.

Figure 2.0: Schematic representation of the Ok Tedi Concentrato

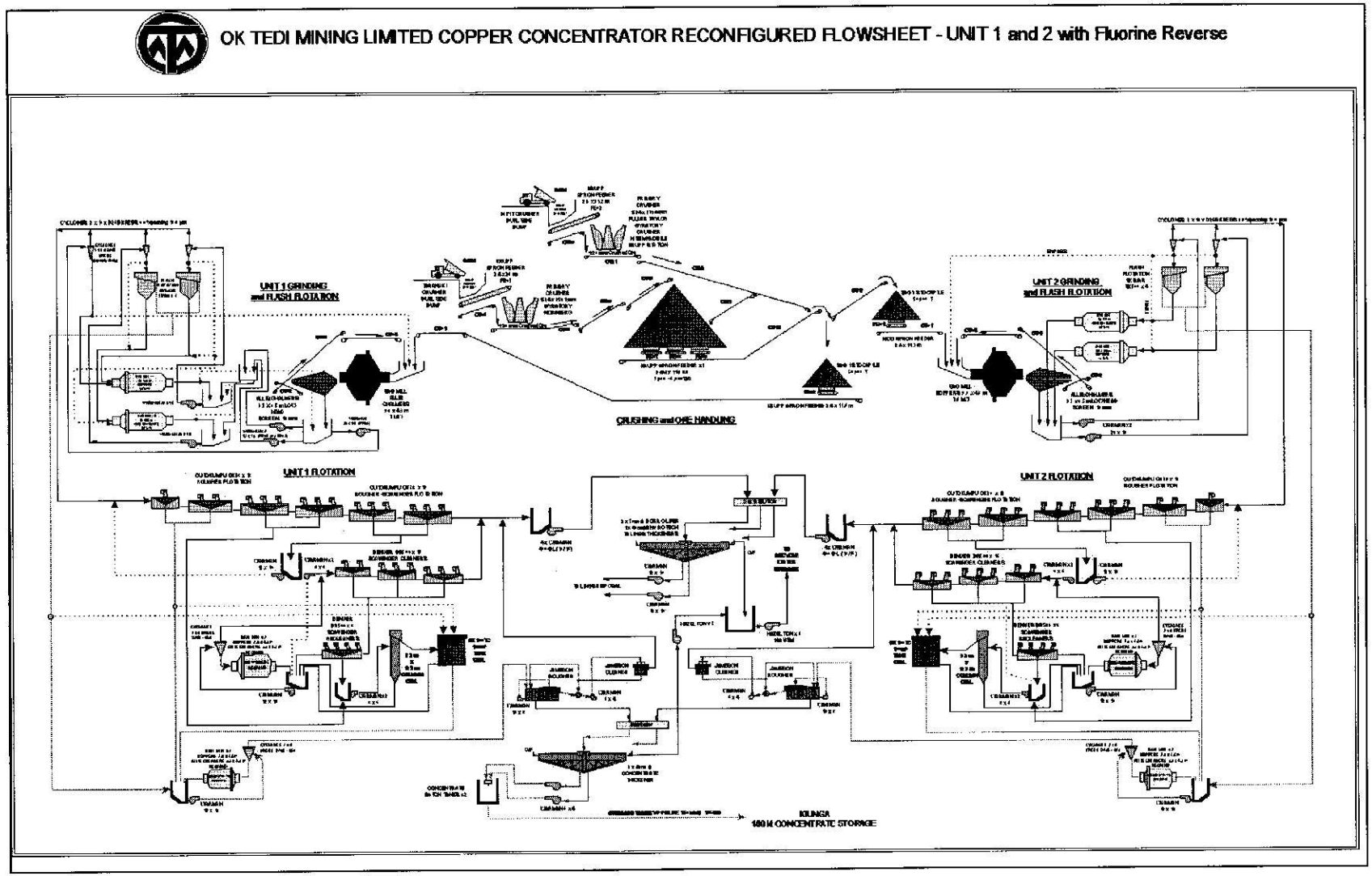

The primary ore blending process is controlled by DISPATCH computerised control of haul truck movements to the crushers. This system attempts to deliver a relatively consistent blend of ROM ore to the crushers. Further blending of the mill feed occurs via mixing of the two-crusher products. A typical ore blend delivered to the mill is as follows:

- Monzonite Porphyry — 60% of total ore blend
- Monzodiorite Porphyry — 20% of total ore blend
- Endo Skarn — 10% of total ore blend
- Pyrite Skarn — 5% of total ore blend
- Magnetite Skarn — 5% of total ore blend

Crusher throughputs are recorded on a daily basis to manage the intermediate stockpile and maintain the balance between mining and milling rates.

1.4.3.2 Milling

OTML has two parallel grinding circuits, similar in design and throughput, each being fed by a dedicated feed stockpile. A detailed description of the circuit and equipment has been presented by Kanau and Katom (1997). The grinding circuits consist of a SAG mill with 'scats' recycle and two ball mills, each in closed circuit with a nest of cyclones. Included in the ball mill circuit are SK500 flash flotation cells that are fed with one third of the cyclone underflow. Implementation of flash flotation at Ok Tedi has been reported by Paki and Erepan (1997). Grinding circuit feed may be up to 3,000 tph of ore. However, throughput is restricted by power and lift pressure limits, resulting from ore hardness and feed size distribution. The grinding circuit product, after grinding and classification, is gravity fed to the associated flotation unit at a sizing of 80% passing 150 to 200 μm.

1.4.3.3 Flotation

The flotation circuit consists of two parallel rougher–scavenger flotation banks, similar in design and capacity. A description of the circuit and equipment was presented by England (1993). The original circuit has been recently reconfigured, including provision of extra cleaning capacity, and the option of bypassing higher rougher grade concentrate to a final

cleaning stage or final concentrate. This has helped to reduce cleaner circuit circulating loads (Cornish 1997). A reverse Flotation process utilizing Jameson Cell Technology was also commissioned in 1998 to treat final copper concentrates containing unacceptable levels of fluorine.

The rougher–scavenger bank for each flotation unit consists of 30 Outokumpu OK38 cells, in parallel lines of 15 cells. The mean residence time at 42% solids is 15-18 minutes. Concentrate from cells 1-3 is fed to a Outokumpu 100 m^3 tank cell for one cleaning stage to produce the final concentrate grade. Concentrate from cells 4-9 is fed to a column cell and concentrate from cells 10-15 can be directed to either the 'low grade' regrind mill or the cleaner bank, depending on operational requirements. The concentrate from both the column and recleaner cells are combined and directed to the tank cell. For reasons of concentrate pipeline rheology, final concentrate from the tank cell is fed to the 'high grade' regrind mill and the product classified in hydrocylones to meet pipe line particle size requirements (d_{80} 31 μm). The tailings from the tank and column cells are combined with the recleaner tails for regrinding in a 'low-grade' regrind mill. The reground product is classified and the cyclone overflow is fed to the cleaner bank, consisting of 16 Denver DR 500 cells. The concentrate from the cleaner cells is fed to a further bank of 8 Denver DR 500 recleaner cells for further cleaning. The scavenger cleaner tail can be either directed to final tail or recycle to the rougher circuit, depending on its copper content.

The Jameson reverse flotation unit comprises rougher and cleaner stages of operation to produce a low fluorine final concentrate, assaying typically 27-31% Cu. The high fluorine Jameson tailings is sent to final tailings. Sodium hydrosulphide (NaHS) is added to control Eh of –600 mV for depression of copper sulphides and the flotation of talc bearing minerals in the Jameson cells.

Final tailings are gravity fed to two Dorr-Oliver 50 m high rate thickeners and one 40 m Envirotech thickener which is a standby duty thickener. The pulp is thickened to 65% solids by mass and is pumped for disposal. Recycled water is used in the plant.
Further more, to produce the required flotation performance, good reagent and pH control is necessary in the concentrator. Slaked lime, produced on site, is added to the SAG feed

at 1-2 kg/t and controlled to a rougher feed pH of 11.5 for pyrite depression and collector absorption on copper sulphides. Cytec S-7249 collector, (a mixture of di-isobutyl di-thio phosphate and di-isobutyl mono-thio phosphate) is added to SAG feed at 20-40 g/t and to the scavenger feed (cell 9 tail) at 10 g/t (relative to plant feed). Approximately 15-30 g/t OTX 140 frother (an alcohol/glycol blend) is added to the SAG feed. The copper feed grade varies between approximately 0.5 and 1.0% Cu.

1.4.3.4 Concentrate Handling

Concentrate from the flotation plant is gravity fed to two 36.6 m Dorr-Oliver thickeners for dewatering to 65% solids, prior to pumping to batch tanks and rheological determinations. Slurry meeting specifications is then discharged into the overland pipeline. The pipeline carries approximately 100 tph of concentrate solids a distance of 88 km under static head until a pump station is reached. There, two pumps boost line pressure to maintain the flow for the remaining 59 km to Kiunga, 150 km from the concentrator.

At Kiunga, slurry is thickened in a 36.6 m Dorr-Oliver thickener, and stored in batch tanks prior to filtering in 3 small 5.49 m by 4.87 m and 3 big 7.70 m by 4.30 m long drum filters which reduce product moisture to 10-11%. The moisture level achievable is dependent upon product sizing and mineralogy. Further moisture reduction to 9.0% is achieved by thermal drying in two Rotary kilns.

The Kiunga concentrate storage capacity is 100,000 tonnes, kept in three stockpiles and two storage sheds. Blending of the stockpiles is performed to meet contract requirements. The location of Kiunga, some 850 river kilometres from the mouth of the Fly river, provides shipping access. A fleet of nine shallow draft barges of 2,500 tonnes capacity trans-ship to a 70,000 tonne storage vessel permanently moored in the Gulf of Papua. Overseas vessels are loaded from the storage vessel by a crane–mounted 'grab' (England 1993).

CHAPTER 2: LITERATURE REVIEW

2.1 CHARACTERIZATION OF FLOTATION CIRCUIT

Due to the large range of ore types and blends possible in the Ok Tedi concentrator feed, flotation performance is variable and problems encountered are dissimilar but largely differ in degree. This situation prompted the need to carry out metallurgical investigations and most recently the Ian Wark Research Institute (IWRI), JKTech and Met Engineers of Canada carried out characterization studies of the flotation circuit. The scope of the work in each case was to characterize the performance of the flotation circuit with respect to current ore types, flotation feed size and cell operating conditions.

2.1.1 Mineralogy and Liberation

Mineralogical and liberation studies were carried out as a function of grind size by JKTech. The study was performed using mineral liberation analysis (MLA). "MLA is a device that utilizes grey level information from a back-scatter electron image to distinguish the minerals present within particles mounted on a carbon resin" (Dunglison et al. 2001, p.7).

Based on the two rougher flotation circuit surveys conducted as a function of grind size it was found that copper recovery increased with fine grind size (F_{80} 206 μm) and decreased with coarse grind size (F_{80} 252 μm). When the results were correlated with liberation analysis, it was found that despite the finer grind size producing slightly better liberation of copper sulphides from the non-sulphides, the liberation effect on floatability was not significantly apparent. Further correlation with the degree of locking (copper mineral) to recovery also indicated a different behaviour. It was found that chalcocite did follow the expected trend (recovery decreasing with increase in locking) whilst a different trend was observed for chalcopyrite. Furthermore, chalcopyrite achieved a significantly poorer recovery at coarser size than would be expected due to locking alone. The reason for the low recovery was attributed to poor surface exposure of the hydrophobic coating by collector, relative to hydrophilic oxy / hydroxy precipitates.

There was no correlation for bornite and covelite with mineral locking. Their recoveries were higher than their degree of locking. It was suspected that these minerals might be associated with chalcopyrite.

Liberation analysis was also carried out on the flotation streams and the following outcomes were found.

- Liberation analysis of the rougher concentrate from cell 1 to 9, showed 70% non-copper bearing mineral. These minerals were found in the intermediate to fine fractions which suggests high entrainment. The concentrate minerals were predominately potassium feldspars, and quartz. Copper sulphide minerals were present in the intermediate to fine sizes and were spread out in different classes of liberation. The pyrites were present in all size ranges and were in a liberated form. This suggested that pyrite was being activated to float in the rougher circuit.

- Liberation analysis of the scavenger feed (rougher cell 9 tail) revealed a predominance of coarse particles. The mode of occurrence of copper minerals was; chalcopyrite and bornite as poorly liberated coarse particles, chalcocite and covellite as fine particles and poorly liberated coarse particles. The scavenger concentrate showed mainly coarse and poorly liberated copper bearing particles. These results suggested that loss of copper minerals was due to liberation issues and insufficient collector.

2.1.2 Pulp Chemistry

Flotation pulp chemical studies were performed by the Ian Wark Research Institute as a function of ore type (skarn and porphyry ores) with respect to recovery and concentrate grade (Morey & Grano 2000). The following reasons were provided for the poor floatability of copper minerals and lower concentrate grades.

- Sulphide minerals in the presence of oxygen were found to be thermodynamically unstable. Measurements of the dissolved oxygen demand at flotation feed showed

high demand, with a declining trend down the circuit. The consequence of chalcopyrite oxidation in the pulp is indicated by equations 1 to 3.

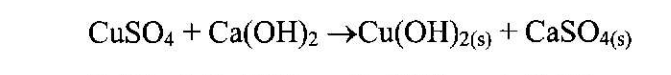

$$CuFeS_2 + 4O_2 \rightarrow CuSO_4 + FeSO_4 \quad (1)$$

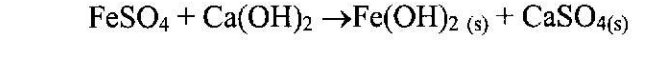

$$CuSO_4 + Ca(OH)_2 \rightarrow Cu(OH)_{2(s)} + CaSO_{4(s)} \quad (2)$$

$$FeSO_4 + Ca(OH)_2 \rightarrow Fe(OH)_{2\,(s)} + CaSO_{4(s)} \quad (3)$$

- EDTA and ToF-SIMS analysis indicated that oxy-hydroxide precipitates of Cu, Ca, and Fe, and also Al_2O_3 / SiO_2 slimes, all contributed to the decreased hydrophobicity and floatability of chalcopyrite and pyrite particles.

- ToF-SIMS analysis indicated that pyrite activation to flotation and final concentrate was due to Cu and dithiophosphate collector adsorption.

- Galvanic chemical reactions between grinding media and minerals were not considered to greatly affect the pulp chemistry of skarn feed blends at Ok Tedi. A relatively high Eh was apparent at the ball mill discharge. The expected result of reducing Eh produced from oxidation of steel balls and reduction of oxygen on noble mineral surfaces was not observed.

2.1.3 Cell Characterization

Cell characterization work was a component of the overall characterization work carried out on Unit 1 flotation circuit by JkTech (Dunglison 2000). The aim of this study was to characterize the hydrodynamic conditions and thus obtain information that can be used for optimization. Different techniques were used to obtain measurements of entrainment, superficial gas velocity, bubble size distribution, bubble surface area flux and air hold up. Brief background information on these techniques is included in the discussions. These are important hydrodynamic parameters that influence the froth recovery process.

2.1.3.1 Entrainment

Bubble attachment and entrainment are two sub processes involved in the recovery of minerals from the pulp, through the froth phase and into the concentrate launder. Entrainment is defined as an unselective process resulting from mechanical carry over of mineral with the water phase. It may contribute to froth stability, but is detrimental to the concentrate grade.

The amount of material entering the froth phase due to entrainment is determined by firstly taking a pulp sample just below the froth phase. This is then compared with the concentrate to assess the amount of gangue material, which does not drain from the froth. The degree of entrainment is calculated by the ratio of solids that report to the concentrate relative to that in the pulp phase (Equation 4) (Ross 1998).

$$ENT_i = \frac{\text{mass of solids suspended in the water in the concentrate}}{\text{mass of solids suspended in the water in the pulp phase}} \quad (4)$$

The degree of entrainment for non-floating particles is usually one for ultrafines (i.e. no drainage back through the froth into the pulp) and zero for coarse particles (i.e. complete drainage back into the pulp).

Entrainment analysis was performed for rougher cells 1 to 3, cells 4 to 9 and scavenger cells 10 to 15 by JKTech (Dunglison 2000). The degree of entrainment of silica was calculated and plotted against particle sizes (Figure 3.0). The calculated values of the degree of entrainment are shown in the figure as entrainment function, which indicates the degree of silica in the concentrate relative to the mass of water, relative to the tail. The results indicate similar entrainment curve trends in all cases. Rougher cells 10 to 15 have a significantly higher rate of entrainment than rougher cells 1 to 3 and 4 to 9 (which were similar). The sharpness of the entrainment curves for cells 1 to 3 and cells 4 to 9 indicates that the froth had good drainage properties. The curves also indicate that the majority of silica is non floatable in the rougher scavenger cells.

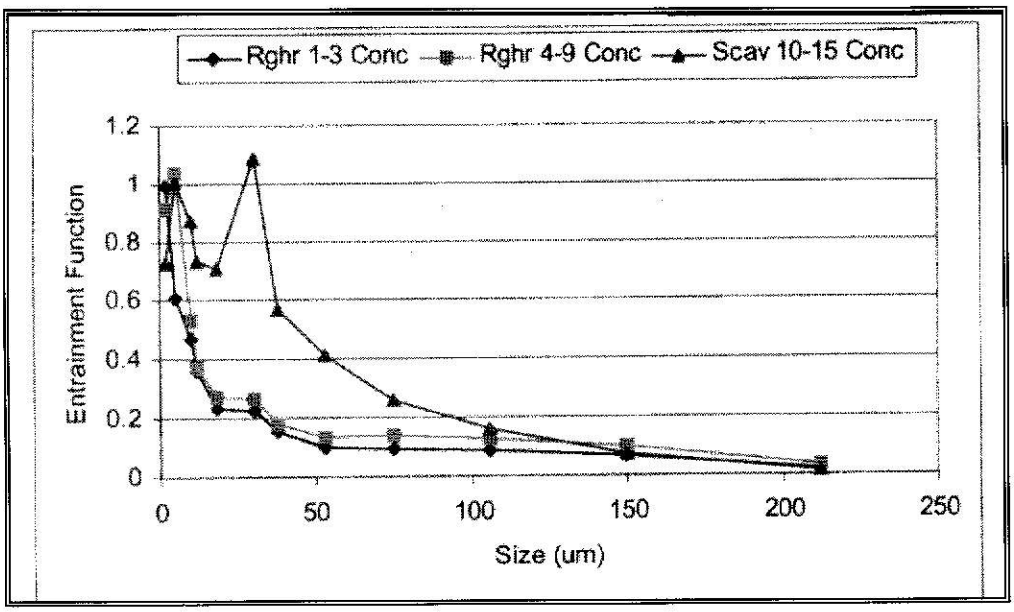

Figure 3.0: Shows degree of entrainment as a particle size (Dunglison 2000)

2.1.3.2 Superficial Gas Velocity

Air dispersion is defined as the distribution of incoming air throughout the volume of cell (Gorain et al. 1996). The contributing factors to the effectiveness of air dispersion in the cell are the impeller speed, airflow, frother dosage, cell dimensions and cell design including baffles and internal launders (Power et al. 2000). Measurements can be performed within the pulp region of the cell to determine the effectiveness of air dispersion. Characteristics generally measured include bubble size, air hold up and superficial gas velocity. These measured values can be combined to calculate bubble surface area flux (Power et al. 2000). These parameters are important as they can be correlated to metallurgical performance.

Superficial gas velocity (Jg) is a measure of the aeration of a cell. It is defined as the volume of air passing a unit cross-section area of a flotation cell in the pulp per unit time (Equation 5) (JKMRC 1988).

$$Jg = \frac{Q}{A} \qquad (5)$$

where:

J_g = superficial gas velocity

Q = volume air flow

A = cross-section area

The superficial gas probe is an instrument used for measuring the rise velocity of bubbles at different positions across the cell pulp.

Measurements performed by JKTech (Dunglison et al. 2000) in the OTML rougher cells (cells 2, 4, 11, 14) indicated that air dispersion was non-uniform. In general, the Jg value was higher in the central area around the impeller and lower towards the feed and tail ends of the cells. The Jg values at OTML were found to be in the lower range when compared to OK 38 cells used in Australia and South Africa. These results suggested a poor dispersion of air across the OTML rougher cells (they were not balanced) and generally low air rates. This could be contributing to lower than optimum metallurgical performance.

2.1.3.3 Air Hold – Up

Air hold-up is defined as the volumetric fraction of air bubbles in the aerated pulp. It is an important cell hydrodynamic condition. The effective cell volume and residence time are determined by the air hold–up factor (JKMRC 1988). An air hold-up device may be used to accurately measure the proportion air in a pulp. The ratio of air volume to total volume of the sample is defined as the air hold–up.

Measurements were taken by JKTech at the same points as the superficial gas velocity (Jg) measurements (See section 2.4.4). The air hold-up increased with increasing in Jg values. Comparison of air hold-up values with other OK38 cells in Australia and South Africa showed significant variation. The air hold - up values for the Ok Tedi OK 38 cells were 5-8%, which was at the lower operating range of other sites, which showed values for OK 38 cells in the range 15 to 21% (Dunglison 2000).

2.1.3.4 Bubble Size Distribution

Bubble size is an important factor governing flotation performance. Smaller bubbles carry more mineral particles per unit volume of air, and increase flotation recovery. In contrast bigger bubbles are unstable. Large bubbles may be caused by high superficial gas velocity combined with poor shearing of bubbles by the impeller (Gorain et al. 1995). JkTech have used a UCT bubble size analyzer (Dunglison 2000) to measure the bubble size distribution in the three-phase systems (solid-water-air) of OTML mineral pulps. The method relies on direct capture of bubble size in a capillary with an electronic sensor detecting bubble dimensions. A software program then interprets the data and calculates the bubble size distribution. The bubble size is normally presented by the Sauter mean bubble diameter (d_{32}) and the arithmetic mean bubble diameter (d_{mean}) (Equations 6 & 7).

$$d_{32} = \frac{\Sigma d_i^3}{\Sigma d_i^2} \qquad (6)$$

where:

d_{32} = Sauter mean bubble diameter

d_i = bubble diameter

$$d_{mean} = \frac{\Sigma d_i}{\eta} \qquad (7)$$

where:

d_{mean} is the arithmetic mean bubble diameter,

d_i is the individual bubble diameter and η is the total number of bubbles.

In OTML rougher cells, the bubble size was found to vary with different air rates. The majority of bubbles were between 1.1 and 1.5 mm diameter. It was observed that there was significant difference between the d_{32} values of cells 2 and 3 with those in cells 7 and 14 (although the d_{mean} values were similar). This difference could be the result of high pulp solids concentration of the hydrophobic valuable mineral particles in the first few

rougher cells. The presence of these value minerals affects bubble coalescence, resulting in an increase in the portion of larger bubbles and a greater Sauter mean bubble diameter (d_{32}). The higher superficial gas velocity values measured at different positions in some cells indicated more bubbles per unit volume in these cells. This may therefore have also contributed to bubble coalescence and larger bubble formation. These measurements were not compared with other known values.

2.1.3.5 Bubble Surface Area Flux

Bubble Surface area flux (S_b) is a term that incorporates both the superficial gas velocity and the Sauter mean diameter (Equation 8). It is an important machine parameter, which gives a measure of the bubble surface area rising up through the cell per unit cross sectional area. The value mineral recovery rate is related to bubble surface area flux. The higher the value of S_b, the better is cell performance (Gorain et al. 1996).

$$S_b = \frac{6J_g}{d_{32}} \qquad (8)$$

where:

S_b = bubble surface area flux

Jg = superficial gas velocity

d_{32} = Sauter mean bubble diameter

The measured values of S_b at OTML were compared against those measured in other OK38 cells operated in Australia. It was observed that the bubble surface area flux of Ok Tedi cells were quite variable, ranging from 15 to 45 s^{-1}. This did not compare favourably with S_b determinations at other sites. These other values were in the range 25 to 48 s^{-1}. It is possible that the low bubble surface area flux values in OTML OK 38 cells are contributing to a loss of value minerals in the rougher circuit.

2.2 CHALCOPYRITE OXIDATION

It has been established that some sulphide minerals can float without collectors when brought into an oxidizing environment. The general conclusion is that the formation of oxidized products can not only influence interactions with flotation collectors, but also impart hydrophobicity or hydrophilicity to the mineral surface. For example, it is well known that the presence of elemental sulphur can render a surface strongly hydrophobic (Finkelstein 1997). However, the presence of metal hydroxides on surfaces was found to depress chalcopyrite (Senior & Trahar 1991).

Chalcopyrite was found to display collectorless flotation under oxidizing conditions (Heyes & Trahar 1977; Trahar 1984), and this phenomenon has been interpreted in terms of the formation of metal-deficient species (sulphur rich layer) on the mineral surfaces (Luttrel & Yoon 1984; Buckley & Woods 1984; Gardner & Woods 1979; Chander 1991, Pang & Chander 1992). The sulphur rich layer has generally been regarded as a metal deficient sulphide, with the sulphide moiety maintained in the –2-oxidation state (Morey & Grano 2000, Smart et al. 2000).

Since flotation is dependant on the formation of a hydrophobic surface, it is important to know the mechanism of sulphide mineral oxidation. In the case of sulphide minerals surface, the "state of surface" is determined by interaction with collectors. Knowledge of the kinetics and mechanism of oxidation of chalcopyrite are reviewed, with respect to flotation behaviour. The importance of pH, Eh and the electrical double layer are included in the review since they are the conditions under which the minerals are treated, and also interactions between collectors is influenced by these parameters.

2.2.1 Mechanism of Chalcopyrite Oxidation

Many chalcopyrite oxidation mechanism studies were conducted in the laboratory to study the behavioural mechanism. Buckley and Woods (1984) studied the oxidation of fractured chalcopyrite in air, ammonium solution, acid and alkaline medium. The oxidation products were analysed using X-ray photoelectron spectroscopy (XPS). XPS is a surface analytical technique, used for quantitative elemental analysis of the outermost

atomic layers of the solid sample, including the chemical state of the elements on the surface (Laajalehto et al. 1997). The XPS results revealed that in the presence of air iron atoms migrated to the surface to form an overlayer of iron hydroxide and the sulfur and the copper atoms of the altered mineral formed a CuS_2 species. Copper sulphate was formed when oxidation time was extended. Chander (1991) provided similar descriptions of the oxidized chalcopyrite surface in air. Oxidation in air saturated with ammonium produced similar species and in acid solution resulted in the dissolution of iron, leaving a copper sulphide product layer. Elemental sulfur and a metal deficient copper sulphide species resulted from oxidation in hydrogen peroxide. Further chalcopyrite oxidation studies were conducted under acid and alkaline conditions and the following reactions were identified by cyclic voltammetry;

In acid solution; $CuFeS_2 \Rightarrow CuS + S + Fe^{2+} + 2e^-$ (9)

In alkaline solution; $CuFeS_2 + 3H_2O \Rightarrow CuS + S + Fe(OH)_3 + 3H^+ + 3e^-$ (10)

The XPS results indicated that in acid the iron component dissolved and in basic media it formed an oxide layer, whilst copper remained bonded to sulphur. From these experimental results, Buckley and Woods concluded that a sulphur rich phase (metal deficient sulphide) is formed when chalcopyrite undergoes oxidation. Lutrell and Yoon (1984) studied the collectorless flotation of chalcopyrite in alkaline solution with controlled potential, and the results with UV spectrophotometry, detected similar products (elemental or polysulphide species). Gardner and Woods (1979) found anodic oxidation of chalcopyrite (equation 9) was responsible for conferring hydrophobicity. Thus, collectorless flotation is induced by the presence of the sulphur rich layer on the surface of chalcopyrite.

A good description of the chalcopyrite oxidation reaction and the various steps involved has been given by Pang and Chander (1992). The steps can be written as:

(i) Release of iron species

The first step in the oxidation is the release of ferric ions by reactions of the following types;

$CuFeS_2 = CuFe_{1-x}S_2 + xFe^{3+} + 3xe^-$ (11)

$CuFeS_2 = (CuS+S) + Fe^{3+} + 3e^-$ (12)

The polysulphide species, $CuFe_{1-x}S_2$ or (CuS+S) is referred to as the iron deficient sulphide (IDS) layer. At higher potential (above open circuit potential (OCP)), reaction 12, was observed.

(ii) Formation of the iron–deficient sulfide layer

Oxidation and the release of ferric ions continued with an increase in potential, leaving a reacted IDS layer. Dissolution of chalcopyrite continues until the potential reached 0.12 to 0.14 V. At that stage, the IDS layer is non-passivating.

(iii) Passivation by the iron–deficient sulfide layer

The IDS layer becomes passivated in the potential 0.12 to 0.24 V.

(iv) Dissolution of the iron–deficient layer–Passivity breakdown

The iron–deficient layer dissolves in the potential range of 0.24 to 0.44 V, according to the reaction:

$$(CuS + S) + 3H_2O = Cu^{++} + S_2O_3^{=} + 6H^+ + 6e^- \quad (13)$$

The reaction makes the reacted layer more porous and the coating resistance decreases substantially.

(v) Precipitation of iron and copper hydroxides in alkaline solutions

Iron and copper hydroxide precipitates to form a product layer in alkaline solutions. The layer is passivating up to 0.53 V and above that it becomes non-passivating.

Chander and Khan (2000) reported that under stirred solution, a significant amount of the iron hydroxide layer went into solution to expose the copper-sulphur (Cu-S) layer. Thus, the rich Cu-S layer has been identified to react with collector more readily than the original chalcopyrite or iron hydroxide covered chalcopyrite. Pang and Chander (1993) reported that the iron hydroxide layer on chalcopyrite was more porous than on pyrite. Under these conditions, it can be seen that the Cu-S layer can be exposed for reaction with collector.

It is clear from the foregoing studies that chalcopyrite can acquire hydrophobicity and become floatable by the presence of a sulphur rich layer on the surface. The presence of the Cu-S layer makes it possible for the application of collectors to increase flotation rate.

However, the presence of hydroxides at higher potentials poses problems for flotation and highlights the need to treat the minerals according to their desired conditions.

2.2.2 Galvanic Interactions in Sulphide Ore System

It has been found that galvanic potential has the capability to oxidize metal and minerals. In a sulphide ore system, when a mixture of two or more minerals are ground and floated, there may be galvanic interactions between the minerals or between grinding media. Redox reactions in a thermodynamic system can form galvanic cells and current flows between these minerals, causing surface oxidation. Their electrochemical activity is indicated by the rest potential of the sulphide minerals. Thus, in principle, minerals with higher rest potential (noble mineral) act as a cathode and minerals with the lower rest potential (active mineral) act as an anode. Majima (1996) studied the galvanic effect on pyrite and galena and found that galena oxidized rapidly in the presence of pyrite. Ekmekei and Demirel (1997) studied the effect of galvanic interaction on collectorless flotation behaviour of chalcopyrite and pyrite and found that at pH 9.2, pyrite had a higher rest potential of 270 mV and a lower rest potential of 119 mV for chalcopyrite. Hence, electrons flowed from chalcopyrite (anodic) to pyrite (cathodic) forming a galvanic cell. For reactions taking place between grinding media and sulphide minerals, the sulphide minerals act as the cathode and the grinding media as the anode (Rao et al. 1976). Yelloji and Natarajan (1989) found that galvanic interaction between a noble mineral such as chalcopyrite and active minerals such as galena and sphalerite or hyper steel ball material, affected the floatability of chalcopyrite significantly. They reported that the rate of anodic or cathodic reactions could be spontaneous depending on the rest potential difference, magnitude of galvanic current density and the difference in relative surface areas.

Subrahmanyam and Forssberg (1993) provided the important galvanic reactions among sulphide minerals:

<u>cathodic reaction (high rest potential)</u>

$$^{1}/_{2}O_2 + H_2 + 2e^- = 2OH^- \qquad (14)$$

anodic reaction (low rest potential)

$$MeS = Me^{2+} + S + 2e^- \quad (15)$$

The overall reaction being:

$$MeS + \frac{1}{2}O_2 + H_2O = Me^{2+} + S + 2OH^- \quad (16)$$

Above galvanic reactions show that elemental sulphur and hydroxyl ion is produced and oxygen is consumed. Further oxidation of these products can proceed, depending on the thermodynamics. Under alkaline conditions, the elemental sulphur can form insoluble metal sulphates (Majima 1969). The hydroxyl ions can react with metal ions in solution to form hydroxides. Studies conducted by Adam and Iwasaki (1984) indicated that iron released from grinding media or from dissociation of pyrrhotite formed iron hydroxides, and precipitated on pyrrhotite. When pyrrhotite was floated, its floatability was adversely affected. Cheng and Iwasaki (1992) provided similar results with chalcopyrite and pyrite interaction. Yelloji and Natarajan (1989) confirmed with X-ray photoelectron spectroscopic analyses that the presence of iron oxy-hydroxide species derived from galvanic interaction with steel grinding material decreased the floatability of sphalerite. From these studies it is clear that surface contamination can affect the floatability of sulphide minerals.

The consumption of oxygen, as expressed by equation 14 can change the rest potential of the mineral and that affects the relationship between rest potential and flotation behaviour. It has been found that grinding in an enclosed mill or in a situation where there is galvanic contact with iron, creates an oxygen-demanding environment (Rao et al. 1976). Wang and Xie (1990) found that activity of oxygen reduction was strongly dependent on the electrode material. They observed that pyrite was the most active mineral for oxygen reduction at a pH between 1 and 9.2. It can be observed that in the presence of pyrite, a reducing environment can be created. Rao et al. (1976) reported that in the presence of pyrite, selectivity of Cu-Pb-Zn was decreased when grinding in steel mill.

A necessary condition for xanthate oxidation and adsorption is that the minerals must display a higher rest potential than the reversible potentials of the dixanthogen. Since the presence of dixanthogen on the surface renders the surface hydrophobic, the effect of rest potential is pronounced in the flotation of sulphide minerals (Poling 1976). Guy and

Trahar (1985) studied the effect of grinding environment on the floatability of chalcopyrite and galena without collectors. They found that the flotation rate of chalcopyrite and galena were lower in a reducing environment (closed steel mill, -0.3 volt) compared with an oxidizing environment (ceramic, stainless steel or glass mill, +0.3 volt). Similar flotation behaviour was observed when xanthate was added. From these studies it was concluded that floatability of chalcopyrite and galena were dependant on pulp potentials and their natural floatability was attributed to elemental sulphur. It is clear from these studies that galvanic interaction is an important factor that affects the rest potential of the mineral.

2.2.3 Collector Adsorption on Surface

The interaction between collectors and surfaces plays an important role and the understanding of the interaction mechanisms of different reagents with mineral surface is significant in achieving selective flotation. It is now widely accepted that there are two separate mechanisms by which collectors adsorb on sulphide minerals. Firstly, there is the chemisorption mechanism where the adsorbed xanthate molecule forms a chemical bond with metal atoms at the sulphide surface. The other mechanism is electrochemical, and involves the electrochemical oxidation of the adsorbed collector molecules to give oxidation product species, which renders the sulphide surface hydrophobic. It is believed that a hydrophobic surface is produced on galena, chalcocite and sphalerite by the chemisorption mechanism while the electrochemical mechanism is responsible for the collection of pyrite, arsenopyrite and pyrrhotite. However, an electrochemical mechanism may still occur to some extent when chemisorption is the major mechanism. Both mechanisms have been observed in chalcopyrite (Kelly & Spottiswood 1982)

2.2.3.1 Importance of Eh and pH

The driving force for adsorption of collector on the mineral surface is the electrical potential. Because the sulphide exhibits some electrical conductivity, (that is it can act as a source or sink for electrons), it develops what is called a rest potential when in contact with an aqueous solution. At its 'rest' potential, the mineral is electrically at equilibrium

with respect to electrochemical processes. However, at any other potential, redox processes occur and the electrochemical potential (Eh) of a mineral in the pulp is regarded as the most important parameter of pulp chemistry. It is defined as the potential difference across the mineral-solution interface and generally it is a measure of the tendency for a solution to be oxidizing or reducing. The potential is determined through the Nernst equation (equation 17) which defines the relationship between redox potential and standard electrode potential (Ralston & Grano 1995).

At the mineral–solution interface, electrons are transferred and the system comes to equilibrium. The potential of the metal is assumed as characteristic of the system. It has been known that the absolute potential is impractical to obtain and consequently the potential across the mineral-solution interface is measured against a reference electrode placed in the same solution. The potential scale is set against the standard hydrogen electrode (SHE) and is applied for the measurement of potential. The SHE is defined as conceptual electrode in which hydrogen ions and hydrogen gas are in equilibrium at their standard states (Ritchie et al. 1999).

$$Eh = E^{o} - (RT/\eta F) \ln [O_x]/[R] \qquad (17)$$

where: E_o = Rest potential at standard state. This parameter is related to the free energy difference between the reactants and products; $\Delta G = \eta FE$

R = Gas constant

T = Absolute temperature

η = Number of moles of electrons involve in reaction

F = Faraday constant

$[R]$ = concentration of reduced species

$[O_x]$ = concentration of oxidized species

The rest potential provides information regarding the possible processes taking place on its surface. A solution with a given Eh will oxidize minerals, which have an E° less than E. Conversely, the same solution will reduce minerals which have an E° greater than Eh (Rao et al. 1992).

Extensive research on electrochemical potential has shown a strong correlation between pulp potential and recovery of sulphide minerals (Chander 1988; Woods 1984; Ralston 1991). Chalcopyrite has been found to float without collector at an Eh of 0-100 mV (SHE) (Gardner & Woods 1979; Heyes & Trahar 1977; Heyes & Ralston 1988). From these studies it was established that flotation was strongly dependant on electrochemical potential owing to the following effects:

1. Surface oxidation of sulphide minerals to form hydrophobic and hydrophilic species depends strongly on potential.
2. Precipitation of metal ions in solution onto the mineral surface is affected by potential.
3. The adsorption of thiol type collectors often occurs through an electrochemical mechanism.
4. Selective flotation of sulphide minerals can be achieved by potential control (Hintikka & Leppinen 1995).

The electrochemical potential is greatly influenced by pH because of the presence of hydrogen and hydroxide ions in the solution. The pH is defined as the measure of the hydrogen ion concentration in the solution and the potential is related to the ionic species present in solution and their concentration (Hayes 1993). Hydrogen and hydroxides are potential determining ions and one of the major sources of these ions is from the composition of the ore. From studies conducted by Ritcey (1989), ores that contained more pyrite generated surplus hydrogen ions and ores that had high metal sulphur ratio as found in chalcocite rich ore, generated surplus hydroxyl groups. Therefore, the resultant pH is dependant on the metal to sulphur ratio of the minerals.

The concentration of hydroxyl and hydrogen ions is related to the Eh, which influences collector adsorption. This effect resulted from the modification of the electrical double layer and zeta potential (Wills 1997). It is well established that solution pH is of particular importance. Variation of the pH value can cause the following:

1. Selective precipitation or dissolution of components present in the solution.

2. Enhance or weaken the competition betweens ions of the liquid phase of the pulp and the collector in occupying a place on the surface of the mineral.

Therefore there will be a critical pH above which the surface will appear to be insufficiently hydrophobic and the mineral will not float. Thus the control of the pH of the pulp is important to flotation recovery of sulphide minerals (Hayes 1993).

2.2.3.2 The Importance of the Electrical Double Layer

The electrical double layer is important to flotation since collector adsorption, depressant adsorption, activator adsorption and bubble particle attachment depends on it.
It was found that there are a number of ways the flotation process can be affected by the electrical double layer (Fuerstenau 1982b);

- The sign and magnitude of surface charge controls the adsorption of physically adsorbing flotation reagents.
- A high surface charge can inhibit the chemisorption of chemically adsorbed collectors.
- The flocculation and dispersion of a mineral suspension is controlled by the electrical double layer.
- Flotation kinetics is related to the effect of electrical double layers on the kinetics of film thinning.

The electrical double layer is formed by the presence of potential determining ions in the mineral-solution system. The potential determining ions may be ions of collector, depressants, activators, metal ions from mineral surfaces and hydrogen or hydroxyl. An electrified interface is created under the influence of the potential and the ions redistribute themselves near the interface. Thus, organization of the ions is responsible for the electrical double layer formation (Ritchie et al. 1999). Figure 4.0, presents a schematic representation of the electrical double layer (Wills 1997). This figure also shows the drop in potential across the double layer.

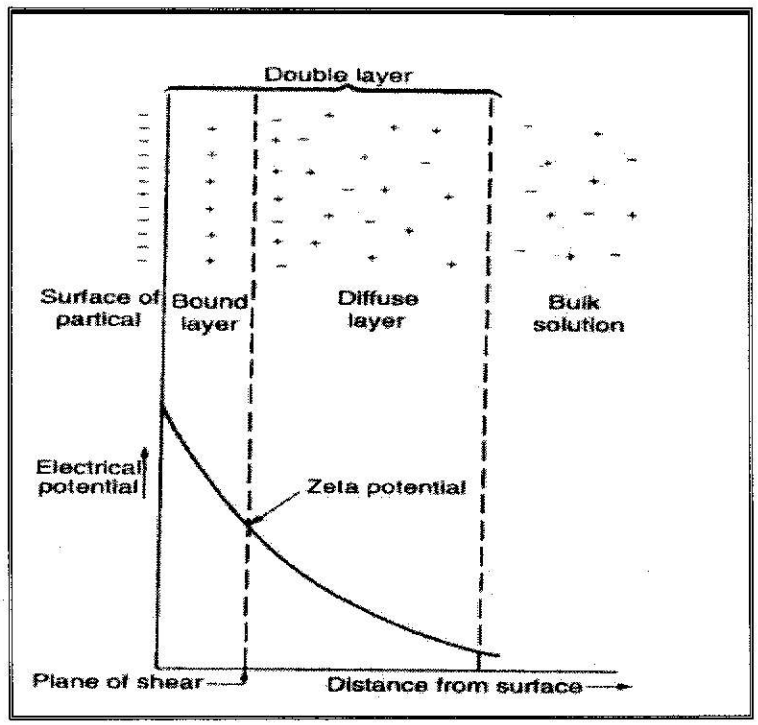

Figure 4.0: Schematic representation of the electrical double layer (Wills 1997)

The electrical double layer is made up of the charged surface, that is, there is a layer of positive charge and a layer of negative charge with the whole system electrically neutral. The excess neutralizing counter ions are distributed in a diffuse manner in the polar medium resulting in two regions formed in the vicinity of the charged surface, the inner region adjacent to the solid surface, which may include potential determining ions, and a diffuse region in which counter ions occur. The inner layer is called the Stern layer and consists of a single layer of hydrated ions rigidly held to the solid surface. In comparison the diffuse layer extends out into the liquid phase. From Figure 4.0, it can be seen that the potential drops linearly in the fixed layer while in the diffuse layer the potential gradually and exponentially decreases to zero in the bulk of the solution. The potential at the shear boundry of the two electrical layers, that is, the potential difference across the diffuse layer is called the zeta potential (Yan 1999).

Since the electrokinetic phenomenon is responsible for the electrical double layer, zeta potential measurements are taken to understand the adsorption phenomena occurring in the system. When hydrogen and hydroxyl are potential determining ions, the pH controls

the zeta potential and there is a relationship. Figure 5a, represents the relationship between surface potential and pH and shows that the zeta potential may reduce to zero and even the reverse sign. The point at which the surface charge is zero is known as the 'point of zero charge' (PZC) and the point at which the zeta potential is zero is the 'iso electric point' (IEP). Figure 5b, represents the associated effect on recovery using goethite as the mineral with anionic and cationic collectors. It can be seen that when the zeta potential is positive, that is for pH values less than IEP, the anionic collector will adsorb on the surface and flotation is possible. However, the anionic collector does not adsorb when the surface is negative. Under this condition a cationic collector may adsorb on the goethite surface (Kelly & Spottiswood 1982).

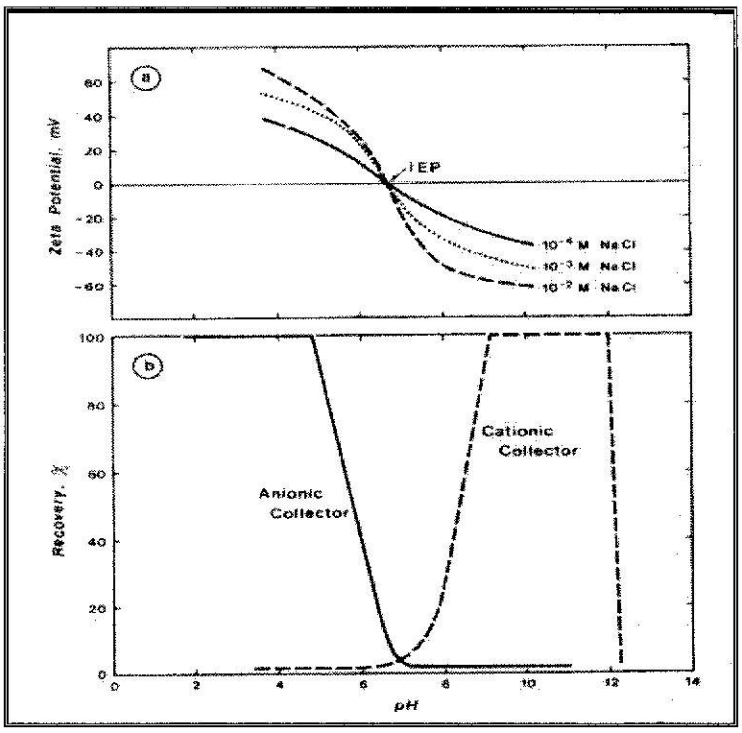

Figure 5 .0: (a) The effect of pH on zeta potential and (b) its influence on the flotation of goethite (Kelly & Spottiswood 1982).

2.3 PYRITE ACTIVATION

In a flotation system, most sulphide minerals are thermodynamically unstable and undergo oxidation, which leads to the release of metal ions into the pulp. The metal ions are potential determining ions; hence adsorption onto the surface of sulphides can change the zeta potential, which is related to flotation. It has been found that these species can either depress the target mineral or activate unwanted minerals (Allison et al. 1982; Healy 1984; Shannon & Trahar 1986; Senior & Trahar 1991; Kant et al. 1994; Basilio et al. 1996; Zhang et al. 1997).

Adsorption of ions such as the Cu^{2+} ion onto pyrite is common and originates from dissolution of Cu^{2+} from the sulphide ore or through the addition of copper sulphate (Senior & Trahar 1991; Finkelstein 1997; Fuerstenau 1982a; Sui et al. 1995). Since flotation is implemented by selective attachment of hydrophobic collector molecules onto the valuable metal sulphide, pyrite can be rendered hydrophobic through this mechanism.

At the Ok Tedi and Hellyer concentrators, the inadvertent activation of pyrite and sphalerite has been reported. On the basis of XPS, ToF-SIMS and in conjunction with EDTA analysis, Morey and Grano (2000) found pyrite activation by cupric ion and collector in the Ok Tedi flotation circuit. A similar scenario has been observed at Hellyer concentrator, where Greet et al. (1994) found sphalerite activation by lead ions.
It can be seen that control of a metal ion with respect to pyrite activation is necessary to improve selectivity during treatment of complex ore. Knowledge of the activation mechanism and the conditions which influence the behaviour of minerals must be known so that measures can be taken to counter the effects.

2.3.1 Activation with Copper

Copper sulphate is the common activator for sphalerite due to the fact that zinc xanthate is highly soluble and could not induce hydrophobicity (Finkelstein 1997; Finkelstein & Allison 1976). It is also an activator for pyrrhotite and pyrite (O'Connor et al. 1988; Dichmann & Finch 2001; Allison et al. 1982).

Sphalerite activation with copper has been extensively studied and the widely accepted mechanism is an ion exchange reaction between cupric ion (Cu^{2+}) and Zinc ion (Zn^{2+}). It has been found that the driving force for activation is approximated by the following chemical reaction.

$$Cu^{2+}_{(aq)} + ZnS_{(s)} = CuS_{(s)} + Zn^{2+}_{(aq)} \quad (18)$$

$$\Delta G = -62.83 \text{ kJ per mole } Cu^{2+} \text{ or } K = [Zn^{2+}] / [Cu^{2+}] = 10^{11}$$

The above reaction show that the free energy is negative, which indicates that the reaction can proceed until equilibrium is attained when $[Zn^{2+}]$ / $[Cu^{2+}]$ ratio is equal to 10^{11} in solution. The rate of reaction has been observed to follow two distinct stages:
An initial stage of activation is observed to be rapid when Cu^{2+} is taken up and eventually slows down when Cu^{2+} diffuses through the product layer (CuS) (Finkelstein 1997; Fuerstenau 1982a; Laskowski 2001; Allison et al. 1982).

In general, studies have shown that at low pH, Cu^{2+} and Zn^{2+} followed the ion exchange mechanism. It has been observed that longer conditioning time is not needed at low pH. However, with alkaline conditions, longer conditioning time is needed due to the effect of Cu^{2+} ion being slowly released from the copper hydroxide product.

Many studies have been carried out with different minerals to study the ion exchange mechanism. It has been found that ion exchange mechanism was responsible for Pb^{2+} ion activation of galena (Basilio et al. 1996; Morey et al. 2001). Allison et al. (1982) found that while pyrrhotite followed the ion exchange mechanism, pyrite was observed to be different. Because the behaviour of pyrite was different to pyrrhotite, it has been studied extensively using particle surface techniques. A most recent study by Weisener and Gerson (2000a) with X-ray photoelectron spectroscopy (ARXPS) found that when copper was adsorbed, S_2^{2-} species were formed and Cu (II) was reduced to Cu (I). The results indicated that the Cu (I) layer was covered by Cu(II), followed by the hydroxide layer. The EDTA analysis did not indicate any iron in solution and it was concluded that pyrite activation by copper was not by ion exchange but by adsorption of copper onto sulphur species. Voigt et al. (1994) and Smart (1991) found similar mechanisms with XPS and concluded that copper adsorption was attributed to the Cu-S surface species. When ethyl

xanthate was used at pH 6-9, Cu (II) and Cu(I) adsorption on pyrite resulted in formation of Cu(I) ethyl xanthate. However, Allison et al. (1982) showed that copper adsorption on pyrite, was through physical adsorption of precipitated $Cu(OH)_2$ and not ion exchange with the lattice cation. Zhang et al. (1997) provided similar results and stated that the increase in zeta potential of pyrite from adsorption of $Cu(OH)_2$ onto the negatively charge pyrite surface was responsible for activation.

It is clear from these studies that in order to control pyrite activation, an alkaline environment is needed. The formation of copper hydroxides can slow down the flotation rate of pyrite. Sui et al. (1997) investigated the effect of xanthate adsorption on Pb^{2+} ion contaminated pyrite, using soda ash as modifier (pH at 10.5) and found $PbCO_3$ ions had a suppressive effect on Pb^{2+} ions. It was observed that $PbCO_3$ is negatively charged and was not able to adsorb onto the negatively charge pyrite, hence caused the Pb^{2+} ion to be dispersed. The results were confirmed by voltammograms, which showed no peak for dixanthogen on the Pb contaminated pyrite. It can be seen that pyrite activation can be controlled using soda ash at pH 10.5. However, when lime was used as the pH modifier, more xanthate was adsorbed and it was suggested that Ca^{2+} has an activating effect. Zhang et al. (1997) provided similar results and stated that with a single mineral, the presence of Cu^{2+}, $Fe^{2+}$and Ca^{2+} can activate pyrite. Zeta potential measurements confirmed the results and it was suggested that the adsorption of cations provided a high density of surface actives sites, which electrostatically attract negatively charged xanthate.

It can be seen from these findings that inadvertent activation is an issue and corrective measures such as altering the zeta potential by adding potential determining ions can be of practical use. The mechanism of copper activation of pyrite is by direct adsorption of cupric ion onto the pyrite surface. When xanthate is used as the collector, it reacts with cupric ion and is reduced to cuprous ion which forms a Cu(I) xanthate metal complex.

2.4: IMPORTANCE OF HYDRODYNAMICS IN FLOTATION PROCESSES

The efficiency of the flotation process is influenced by the flotation cell hydrodynamics. Studies have shown that the flotation processes are actually governed by the particle-bubble interactions, including collision and adhesion mechanisms (Ahmed & Jameson 1989). These mechanisms are influenced by gas dispersion properties such as gas hold-up, bubble size, and superficial gas velocity (Power et al. 2000; Gorain et al. 1997b; Ahmed & Jameson 1989; Ramadan et al. 1998). A sound understanding of these properties is needed because the flotation process depends on it.

2.4.1 Flotation Process

In the turbulent conditions of flotation cells, there are a number of sub-processes that occur. The efficiency or effectiveness of these processes is a function of the flotation machine performance. Schubert and Bischofberger (1978) considered the following sub processes:

- Suspension of particles in the pulp.
- Feeding of air into the pulp and dispersion of air into bubbles.
- Mixing of the aerated pulp for reagent distribution and conditioning, and to bring about particle-bubble collisions as the basic requirement for bubble attachment.
- Rising of the loaded bubbles and removal of the froth.

These sub-processes are considered the basic dynamic processes in mineral froth flotation and govern the metallurgical performance of the process. Flotation commences under intensely turbulent conditions. Schubert and Bischofberger (1998) studied the turbulent flow around an impeller and suggested the following stages, which lead to bubble formation, collision and dispersion:

- In the absence of air, a vortex is formed behind the impeller blades.
- When air is introduced at a low flow rate, bubbles form in the low-pressure region which results from pressure differences between the flow against the blade and turbulent pressure fluctuations.

- When air flow is increased, cavitation occurs and bubbles disconnect from the vortex.
- Bubble collision occurs around the impeller.
- Gas precipitates impact with solid particle surfaces and attachment is accomplished.

This study showed that when air is supplied under pressure to the flotation cell, air bubbles are produced by the effect of shearing forces and cavitation. In parallel, bubble collision and dispersion occur along turbulence stream lines, with precipitation occurring on the particle surface after collision. It can be seen from the foregoing studies, that bubble formation and attachment are driven by the hydrodynamics of the flotation cell.

2.4.2 Particle-Bubble Collision Mechanism

It is generally agreed that the collision mechanism is the dominant factor controlling flotation recovery. However, not all collisions between particles and air bubbles result in flotation. Only the hydrophobic particles adhere to the bubble surfaces. Therefore, the probability of adhesion will determine the selectivity of a flotation process; the probability being a function of particle hydrophobicity and detachment forces. Some particles will detach from the bubble surface due to the weak inertia forces and turbulent conditions of the flotation cell. The recovery of relatively coarse particles is limited due to the effect of inertia forces in bubble-particle detachment.

Fine particle flotation recovery, on the other hand, depends predominantly on the collision probability. The difficulty in floating fine particles is attributed to the low probability of bubble-particle collisions, as both bubbles and fine particles follow the same stream lines (Yoon 2000; Nguyen et al. 1997; Rubinstein & Samygin 1998). These limitations in the hydrodynamic conditions of froth flotation cells have effectively narrowed the particle size range of easily floated materials to between 10 and 100 μm (Heyes & Trahar 1997).

The universal particle-bubble collision theory is based on the Derjaguin and Dukhin model, which describes all interactions as due to forces (Derjaguin & Dukhin 1961; Dai et al. 2000). The model suggests that before a particle can adhere on the surface of an air bubble, it must pass through three distinct zones. The three zones are categorized as hydrodynamic, diffusiophoertic and wetting zones and constitute the forces that influence

the particle to collide and adhere to the bubble. When a big particle moves toward a bubble, the hydrodynamic force is dominant. The force acting on such particles is based on particle inertial and gravitational forces.

For small particles near to the bubble, diffusiophoretic forces are dominant, acting on the particles as a result of adsorbed ions or surfactants on the bubble surface. An electrical field is formed between the bubble and particle, which implies that reduction of the particle zeta potential can promote collision. Hence, the motion of fine particles toward bubbles is controlled by diffusional and electrophoretic forces, along with hydrodynamic forces. For fine particles in the wetting zone, it was considered that relatively weak forces such as van der Waals and electrostatic forces act to encourage collision. Due to their small inertia, fine particles may adhere on the surface of the air bubbles without penetrating the wetting film (Dai et al. 2000; Ahmed & James 1989; Yoon 2000; Nuguyen et al. 1997).

It is apparent that the flotation process is controlled by factors governing the particle–bubble collision and adhesion mechanism. Flotation performance may deteriorate if anything affects the factors that control the probability of particle and bubble coming into contact, and the probability of this contact resulting in attachment. Important variables, which impact on the mechanisms occurring in the turbulent pulp region are given by Ahmed and Jameson (1989):

- With increased agitation, the particle-bubble collision probability increases in order of increasing bubble size. For the same gas flow rate and agitation, however, the actual number of collision increase with decreasing bubble size because of the increase in the number of bubbles.
- Bubble–particle attachment probability is inversely proportional to the bubble diameter and increases with particle density, particle size and agitation.
- Detachment probability is inversely proportional to the bubble diameter and directly proportional to the particle density, particle size and agitation.

Thus, the flotation rate in the pulp zone is a fine balance between the mechanisms due to the compensating effects from bubble size, particle size and agitation.

2.4.3 Air Dispersion

Gas dispersion properties do not exist within the pulp, but are created by machine factors, including impeller type, impeller speed, mixing and aeration. In sub-aeration machines, the impeller is required to perform the triple function of pulp circulation, particle suspension, and aeration. The impeller must produce a degree of circulation of fluid and solids within the cell such that all particles have a chance to pass through the impeller zone, to collide with and attach to bubbles, and report to the concentrate. Hence, the axial and radial flow within the impeller periphery is designed to perform this role. The radial component of the flow enables dispersion of the air to all parts of the cell whilst the axial flow provides the required circulation of the fluid (Power et al. 2000; Harris 1976; Harris & Khandrika 1985).

Effective aeration is achieved when there is dispersion of fine air bubbles through the cell, in such an amount that there is more than enough air bubbles available for contact by hydrophobic particles. Accordingly, air dispersion is a measure of how well the air entering a flotation cell is dispersed throughout the volume of the cell. The major contributing factors to the effectiveness of gas dispersion in the cell, are the impeller speed and air flow rate. Generally an impeller speed is chosen which could effectively shear the incoming air into fine bubbles and then disperse these bubbles into all parts of the cell. Thus, peripheral speed is an important parameter and its velocity must be higher than the gas rising velocity, so that big bubbles can be broken up into small bubbles. It can be seen that impeller speed and bubble size are intimately connected (Gorain et al. 1995; Arbiter 1984)

Air dispersion is related to metallurgical performance in terms of the flotation rate constant. For a given flow rate of air to a cell, an increase in impeller speed should cause more air dispersion and precipitation, with a breakage of all undissolved air into air bubbles. It has been found that when an impeller speed is increased, this increases the rate of flotation. The probability of attachment of particle to bubble increases, due to the enhanced momentum of the particles. However, flotation rate decreases under severe turbulence when the agitation is so intense that it disrupts the bubble-particle attachment (Schubert & Bischofberger 1998; Ahmed & Jameson 1989; Laplante et al. 1983).

2.4.4 Air Dispersion Properties

The particle-bubble collision mechanism is dependant on air dispersion in a cell. The parameters which describe air dispersion include: air hold up, bubble size and superficial gas velocity. These properties are responsible for the mass transfer of hydrophobic particles from the pulp zone to the froth phase. The flotation capability of the cell depends on the effectiveness of the mass transfer sub-processes.

2.4.4.1 Air Hold – Up

Air hold-up is an important hydrodynamic characteristic of a flotation cell. Air hold–up is a basic measure of the effectiveness of bubble-particle contacting and mixing. When air is introduced into a cell, slurry is displaced and the volumetric fraction displaced is called the air hold-up, ϵ_g (Finch & Dobby 1990).

Air hold-up affects flotation performance via the related parameter, bubble area flux (Finch et al. 2000). Ahmed and Jameson (1989) suggested that an increase in air hold up may produce greater bubble size. Ramadan et al. (1998) studied the parameters affecting hydrodynamics of a conventional flotation cell and found that gas (air) hold-up was increased with an increase in impeller speed. This effect was due to the creation of small bubbles, which have a slower rise velocity. However, Gorain et al. (1995) conducted a series of test as a function of impeller design and speed, and found that bubble size was variable. Deglon et al. (2000) provided similar results from gas dispersion studies on cells in South Africa. It was observed that South African cells were run at high aeration rates to get recovery whilst Power et al. (2000) found that cells in Australia operated at lower aeration rates to get selectivity. It is apparent that to a certain extent, airflow and impeller speed can be adjusted to achieve metallurgical grade and recovery.

Other physical conditions in the cell can have an effect on air hold–up. Since solid particles distribute between the liquid phase and air phases, high solids density and viscosity may increase the air hold–up (Finch & Dobby 1990). Furthermore, an increase in air hold-up decreases the effective cell volume, which impacts on the residence time of the flotation pulp (Bentli & Kaya 2000).

2.4.4.2 Bubble Surface Area Flux

The success of the flotation process depends on the capture and transfer of hydrophobic particles by bubbles to the froth phase. The sub-processes of these phenomena are dominated by two factors, namely, superficial gas velocity and bubble size. In principle, this process can be adjusted to control the recovery rate. Recent studies have found a strong correlation between bubble surface area flux (S_b) and flotation rate constant (k). Bubble surface area flux (S_b) is a term, which incorporates the superficial gas velocity (J_g) and bubble size (D_{32} - Sauter mean bubble diameter). Superficial gas velocity (J_g) is a measure of the aeration ability whilst bubble size (D_{32}) is a measure of air dispersion in the flotation cell (Gorain et al. 1995). Hence, the effectiveness of particle-bubble collision and the rate of recovery are expressed by bubble surface area flux. The implication is that the cell should be operated to achieve a higher bubble surface area flux number (Gorain et al. 1995, 1997a). However, Gorain et al (1995, 1997a) did not establish the effect of bubble surface area flux on particle sizes and it is not known if the correlation is valid (Heiskanen 2000). It is clear that bubble area flux has an effect on recovery rate and that it is important to control the air flow rate and impeller speed to produce correct bubble size. Earlier studies on the effect of bubble size indicated that flotation rate constants for different particle sizes were dependant on bubble size and impeller speed (Ahmed & Jameson 1989; Schubert & Bischofberger 1978).

A most recent study on the effect of flotation frothers on bubble size by Cho and Laskowski (2002) suggests that the size of the bubble strongly depends on frother concentration. Their results generally showed that bigger bubbles were produced at low frother concentration. It was believed that coalescence was a significant mechanism determining the bubble size. They suggested that coalescence could be prevented at frother concentrations exceeding the critical coalescence concentration. Previous studies by Finch and Dobby (1990) had found that increasing frother dosage produced smaller bubble sizes.

The most common bubble size is 1-2 mm for the flotation of large particles (Dobby & Finch 1990). However, Ahmed and Jameson (1989) have suggested a bubble size diameter of 500 μm for different particle sizes. Schubert and Bischofberger (1978)

claimed 600 μm, and observed better flotation kinetics with smaller bubble size. A more recent study on the effect of particle and bubble size on flotation kinetics by Rubinstein and Samygin (1998) provided similar results. However, reduction of the buoyancy force was found to be associated with smaller bubble sizes, and it was noted that buoyancy force was an important factor in the flotation process. This indicated that smaller bubbles may not have been able to lift the particles due to insufficient buoyancy force.

The air dispersion properties have been found to be key hydrodynamic variables in flotation cells. Most recent studies conducted on industrial cells have advocated bubble surface area flux as a key machine variable (Yianatos et al. 2001; Power et al. 2000; Deglon et al. 2000; Gorain et al. 1997b). However it is important to note that flotation processes are a function of hydrodynamics, pulp chemistry and surface chemistry effects. Solutions to flotation problems are increasingly dependent on a sound understanding of every aspect of the process.

2.5 CLEANER FLOTATION CIRCUIT BEHAVIOUR

Cleaner circuit flotation is similar in principle to rougher flotation. Flotation performance is expressed by the relationship of two parameters, grade and recovery. Generally, the rougher flotation circuit is operated to achieve valuable mineral recovery at the expense of grade. In contrast, the cleaner circuit is designed to improve the concentrate grade by re-floating the rougher concentrate in one or more stages of cleaner cells. The product of the cleaner circuit is the final concentrate, graded according to the proportion of metals present. The metal recovery indicates the proportion of the valuable metal recovered from the original feed.

The inclusion of a regrind stage in the cleaner circuit is generally important. Regrinding of a flotation concentrate is commonly applied in the treatment of complex ores, which include a significant proportion of locked particles. The effect of regrinding is shown in improved cleaner circuit grade and recovery responses (Lynch et al. 1981).

A sound understanding of the cleaner circuit performance parameters is vital. Knowledge gained on factors affecting grade and recovery may be applied to problem solving and enhanced flotation performance.

2.5.1 Effect of Regrind Mill on Cleaner Performance

A flotation circuit in its simplest form may be represented as a circuit in which there is a countercurrent flow of valuable and waste minerals. An apparent limitation is that there is nothing done during processing to improve the separation characteristics of the slow floating particles. These tend to report to the scavenger concentrate and cleaner tailings, and include coarse composites and fine-grained minerals. Due to the presence of these components in cleaner circuit streams, a regrinding stage may be incorporated to enable further liberation of the coarse composites, with consequent improvement in flotation characteristics (Lynch et al. 1981; Morizot et al. 1997).

A study by Sutherland et al. (1988) on the influence of mineral locking on flotation behaviour indicated that particle size and mineral concentration significantly affected flotation characteristics. The authors found that for a 30 μm mineral particle size,

liberated chalcopyrite showed the highest recovery, whilst locked particles with low chalcopyrite composition produced lower recovery. Similar particle size behaviour was observed at the Elura lead flotation circuit by Frew and Davey (1993). The authors observed that the recovery of lead was limited by the low recovery of composite lead particles. Also Morizot et al. (1997) studied liberation and its role in flotation flowsheet development and found that recovery of locked chalcopyrite was lower than for liberated chalcopyrite.

It is apparent from all these flotation studies, that mineral liberation (particle composition) significantly influenced the flotation behaviour of particles of the same size. Regrinding to liberate the valuable minerals from locked particles was therefore necessary to improve flotation recovery.

Although little has been published on the effect of regrinding, some interesting results have been presented. Weller et al. (1997) conducted an assessment of the role of regrinding in lead cleaner flotation at the Hellyer concentrator and found that liberation of lead was improved, but that the benefits were offset by poor selectivity in the cleaner circuit. The poor selectivity during lead flotation was examined via EDTA Extraction and X-ray photoelectron (XPS) analysis methods. Results indicated that the galena particle surfaces were contaminated with lead hydroxides and that the sphalerite particle surfaces were activated by lead hydroxide precipitates. It was observed that the regrind product oxidized rapidly, especially in the presence of pyrite which promoted galvanic reactions, and was also due to the effect of a high recirculating load, which prolonged oxidation.

Most recently, Harbort et al. (2000) studied the impact of regrind on the metallurgical performance of the cleaner circuit at Bajo De Alumbrera. No benefits from the application of regrind to cleaner flotation were found. The size by size analysis and liberation analysis showed considerable loss of copper and gold in the ultrafine fraction. Mineral liberation analysis performed by JKMRC on the scavenger cleaner concentrate indicated 70% liberation of chalcopyrite. Based on these results, a solution was proposed to coarsen the cleaner feed size by not regrinding the scavenger cleaner concentrate.

From these studies it is apparent that regrind involves a possible trade-off between liberation and particle size effects, both of which affect particle floatability in the cleaner

circuit. The importance of studying cleaner circuit flotation performance on a 'size by size' basis is noted.

2.5.2 Particle Size

The major constraint on separation efficiency in mineral froth flotation is particle size. The pattern of behaviour is quite consistent, and includes a plateau region covering a range of sizes over which the separation efficiency is at a maximum. For sizes larger and smaller than this range the efficiency decreases. This is illustrated with respect to behaviour of Monzodiorite sulphide ore at Ok Tedi in Figure 6.0, in which the response of particle sizes was studied as a function of pH (Orwe 2000).

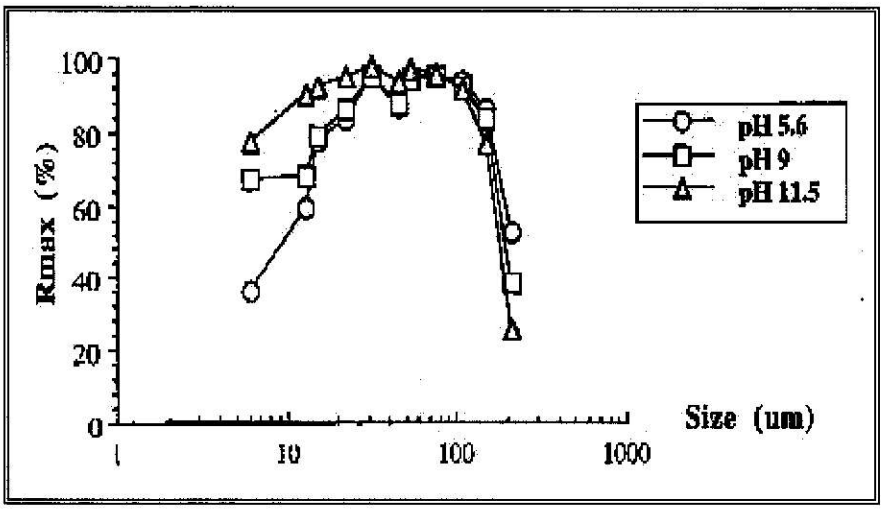

Figure 6.0: Effect of pH on the floatability of Monzodiorite sulphide ore (Orwe 2000)

The reasons for lower flotation rate constants of the valuable minerals, at finer (<20 μm) and coarser (>100 μm) particle sizes, are largely due to limitations in hydrodynamics. During the interactions of particle–bubble collision and attachment, fine particles have much lower probability of particle–bubble collisions, whilst coarse particles are affected by disruption of bubble-particle aggregates in turbulent zones, and also a decrease in buoyancy of the particle-bubble aggregate. The recovery of fines may therefore be primarily due to water recovery or entrainment mechanisms, rather than genuine flotation via bubble attachment (Ahmed & Jameson 1989; Yoon 2000; Heyes & Trahar 1997).

Sulphide minerals of fine particle sizes may also be prone to oxidization in flotation pulps, becoming hydrophilic in nature. Moreover, because of their disproportionate particle surface area, they consume reagents more rapidly compared to coarse particles. Their presence in significant quantities may lead to insufficient collector coverage of larger particle sizes. Considerable work has been undertaken to improve the recovery rates of these fine, slow floating particles. Orwe et al. (1998, 1997) investigated the use of sodium hydrosulphide (NaHS) in the flotation of two Ok Tedi ores and found that use of this reagent could increase the flotation rate and recovery of the sulphides. Sulphidization by NaHS improved recovery in finer sizes, which were more oxidized than the coarse particles.

Oxidized fines may form slime coatings on the valuable minerals. Chen et al. (1999) investigated the effect of high intensity conditioning (HIC) on the flotation of nickel ore and found improvement in nickel recovery, after removing slimes from the surfaces of coarse mineral particles. Song et al. (2001) studied the effect of floc flotation, on 20 μm sized galena and sphalerite minerals using potassium amyl xanthate at pH 8. Flocculation followed by flotation was found to increase the flotation rate constant for both mineral types. The floc flotation effect was explained via the formation of hydrophobic floc aggregates, which increased the probability of collision with bubbles. Castro and Mayta (1994) studied the effect of particle size on the flotation of molybdenite, from the perspective of flotation kinetics. They found that when higher concentrations of frother (MIBC) and collector (iso propyl xanthate, IsopX) were applied, fine particles of molybdenite (10 μm) responded more positively to the frother than the collector. This behaviour was interpreted as an effect of the decreasing bubble size with increasing frother addition. Inversely, coarse particles (51.7 μm), were shown to be more sensitive to collector addition rate than frother addition rate. Win and Yan (1992) studied the factors affecting the recovery and grade of complex lead-zinc ores by flotation. Similar behaviour to the results of Castro and Mayta were found for coarse zinc and lead particles (63 μm), with a high concentration of collector (sodium ethyl xanthate, NaEX). From the above studies it is apparent that the floatability of fine particle sizes in froth flotation may be improved. However, for much coarser particles (>106 μm), it may be preferable to reduce the size of the particles by improving the efficiency of grinding and classification processes, rather than attempting to improve floatability (Senior et al. 1995).

The foregoing studies demonstrated high flotation efficiency for mineral particles of a relatively narrow size range. However, outside that size range, flotation efficiency decreased substantially. Grindability of different minerals within an ore body, will also affect the overall particle size distribution and flotation performance, via bubble attachment and entrainment mechanisms.

2.5.3 Effect of Froth Depth on Flotation

When hydrophobic particles are conveyed from the pulp phase to the froth phase by the action of the rising bubbles, they become subjected to the phenomena occurring in the froth zone. In this froth zone, there are several mechanisms that occur, and their interactions produce the froth behaviour. The two most important mechanisms that occur in the froth phase are particle detachment and re-attachment mechanisms. The detachment mechanism is defined as the loss of hydrophobic particles from the bubble surfaces in the froth. The effect is decreased froth recovery. Detachment is promoted when bubbles crowd together at the pulp-froth interface, causing hydrophobic particles to be sheared from the bubble surfaces. When bubbles rise in the froth, the drainage of liquid from the surrounding films causes the bubbles to coalesce. The more frequently a bubble coalesces the greater the probability that a floating particle will become detached. In contrast, the re-attachment mechanism occurs when hydrophobic particles are detached from the froth phase, but become re-attached again to the surface of the bubbles rising in the froth. The probability of such particles attaching to the bubbles will depend on the particle characteristics and the availability of free bubble surface area (Finch & Dobby 1990; Ross 1998).

Ross (1998) has provided a generic description of the mechanisms occurring in the froth where no wash water is added. The Ross generic model of the froth phase explains bubble mobility, as shown in Figure 7.0.

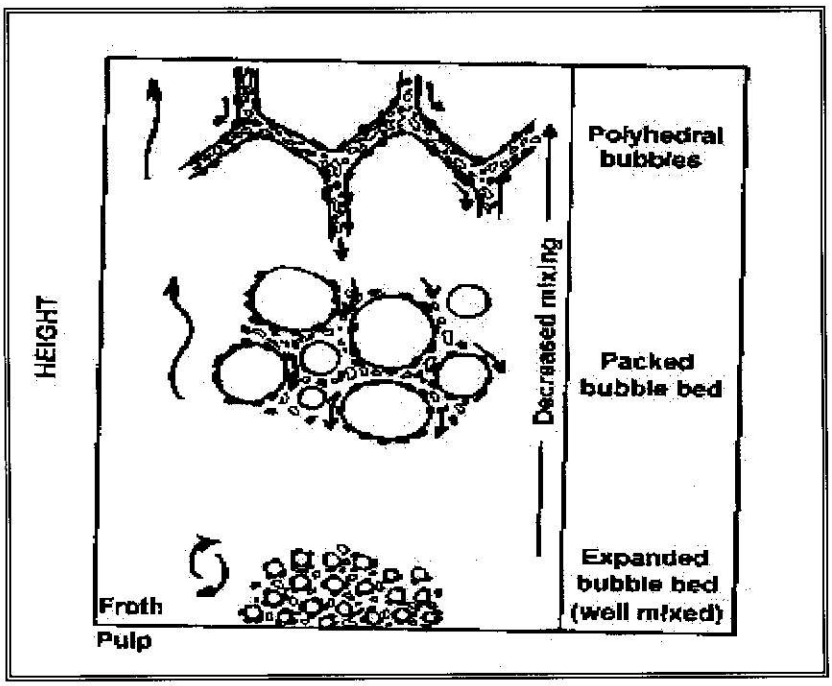

Figure 7.0: A generic model of the froth phase (Ross 1998)

When bubbles enter the froth, they slow down and crowd together. This causes the drainage of a large proportion of entrained particles and water from the slurry layers surrounding the bubbles. Because of the interaction of the draining slurry and the bubbles arriving at the interface, it is believed that good mixing occurs at the bottom layer of the froth. From the pulp/froth interface, the bubbles rise into the froth phase, a region characterized by an increase in air hold–up (packed bubble bed). While most of the bubbles retain a spherical shape in the froth, some distortion towards a more angular bubble size occurs. In this phase, mixing is reduced and the bubbles rise in a more uniform fashion, similar to a plug-flow transport mechanism. The layers of slurry that separate the bubbles are relatively thick and drainage of slurry from the froth continues freely. As the bubbles rise further in the froth, bubble structures change from spherical to an angular polyhedral bubble shape. At this stage, the bubbles are separated by thin liquid films (of slurry) or lamellae. The drainage process occurs from these bubble films into the Plateau borders, i.e. the intersection of three bubbles. In this higher froth region of the lamellae, the drainage of entrained material is small, and upgrading of the froth ceases. The mobility of the froth also decreases because of an increased rigidity brought about by the high ratio of hydrophobic solid to water.

The overall kinetics of froth flotation is a function of the transfer of material from the pulp into the froth phase across the pulp-froth interface and also the transfer of material from the main body of the froth into the concentrate launder. Cutting et al. (1986) and Ross (1998) provided similar descriptions of the mechanisms involved. They concluded that the froth structure is a function of drainage mechanisms and mobility factors. Furthermore, Neethling and Cilliers (2002) studied the entrainment of gangue in the froth and found that solid particles tend to move in two ways. The hydrophobic particles followed bubble lamellae and hydrophilic particles tended to follow liquid flows by means of a hindered settling mechanism. For the flotation practitioner, correlation of these mechanisms with froth stability, froth depth, and particles size effects is important.

Based on experience in Mount. Isa flotation circuits, Lynch et al. (1981) reported that increasing froth depth improved flotation selectivity. The authors observed a 3% gain in copper grade when froth depth was increased to 30 cm in the copper rougher cells. When froth depth was increased from 100 to 140 mm in the galena circuit, a sharp decrease in galena recovery was observed as a result of coarse composite particles detaching from the bubbles. When considering this effect, it is apparent that particle size and liberation significantly affects particle hydrophobicity and attachment to bubbles. A significant reduction in non–sulphide gangue recovery was also observed, being due to preferential drainage with water. There was no further benefit in flotation selectivity observed when the froth depth was increased beyond 140 mm. It was believed that at that froth depth, only liberated and highly hydrophobic galena particles were present in the upper region of the froth, and no increase in water drainage occurred. This also suggested an increased retention time of hydrophobic particles in the froth zone. Engelbrecht and Woodburn (1975) also studied the effect of froth depth on pyrite recovery and provided similar results. The authors suggested that recovery and grade could be optimized based on identifying at which froth depths the gangue drainage and bubble loading regions occurred. They also noted the entrainment mechanism as indicated by the linear relationship between fine silica recovery and water recovery.

The studies of Lynch et al. (1981) and Engelbrecht and Woodburn (1975) have provided a practical demonstration of the effect of froth depth on rejection of gangue minerals and the resultant improvement in concentrate grade up to a certain degree. However, Gorain et

al. (1998) have noted that increased froth depth may also decrease recovery by increasing froth retention time. They studied the effect of this froth residence time on the kinetics of flotation. Their findings indicated that the flotation rate constant decreased exponentially with froth residence time. It is therefore apparent that for the operation of mineral flotation circuits, there is a trade-off between concentrate grade and recovery, determined by the setting of the froth depth.

CHAPTER 3: EXPERIMENTAL PROCEDURE

Based on a review of previous technical reports at Ok Tedi and the technical literature, it was recognized that two approaches were needed to determine the possible reasons that could contribute to losses of copper and gold in the cleaner scavenger tail. The first approach was to conduct experimental work in the laboratory and the objective was to establish preliminary results that could provide directions for further experimental work in the plant. Cleaner circuit charaterisation studies were the major experimental work and it also includes examination of collector and lime addition to the cleaner circuit, and the effect of the low grade regrind mill.

Cytec (USA) and Ian Wark Research Institute (Australia) were respectively engaged to perform mineralogical and mineral surface analyses. EDTA extracted solution & solids, was analyzed by AMDEL.

This chapter details the experimental equipment and reagents, and procedures for the laboratory and plant work.

3.1 Laboratory Studies

The following tests were conducted in the laboratory;

1. Examination of the effect of pH
2. Examination of the effect of Collector dosage
3. Examination of the effect of Cleaner Feed Oxidation in Tap Water
4. Examination of the effect of Water quality
5. Examination of the effect of Extended Flotation of Cleaner Tail
6. Examination of the effect of Aeration Rate
7. Examination of the effect of Agitation Rate

The description of the test procedures and the equipment and reagents used are discussed in the following sections.

3.1.1 Equipment and Reagent

The laboratory batch flotation units were an ESSA machine and Denver D12 machines equipped with 2 litre and 4 litre cells, respectively.

Reagent sourcing for the laboratory test work consisted of both plant and analytical supplies. Where the reagent was not available from plant samples, it was sourced from analytical supplies.

Reagent specifications are as follows:

Collector: Cytec 7249–a blend of di-isobutyl di-thio phosphate and di-isobutyl mono-thio phosphate. Used as a pure solution, as supplied, and added via a micro syringe.

Frother: Oreprep OTX-140-a mixture of higher alcohols and polyglycols. Used as a pure solution, as supplied, and added via a micro syringe.

Lime [$Ca(OH)_2$]: produced at Folomian from Geneva Ridge limestone deposit, typically 76-80% CaO. Added in the laboratory as a solid.

Sodium Hydroxide (NaOH): Pellets, 97% minimum NaOH, Technical Reagent Grade.

Hydrochloric Acid (HCL): 39% w/w, Technical Grade.

Ethylene diaminetetraacetic acid, disodium salt (EDTA), Technical Reagent Grade.

Salt: Cooking Salt (Sodium chloride)

Water: Untreated tap water, typically less than 100 ppm of any particular ion.

3.1.2 Flotation Pulp Sample Preparation

Flotation pulp samples were collected from the low-grade cyclone overflow (classified scavenger cleaner feed) and scavenger cleaner tail steams in Unit 2 cleaner flotation circuit. The pulp samples were taken to the laboratory on the same day and filtered. The filtered solids (cakes) were collected and a wet mass of 1420 gm was weighed and transferred to a 4 litre flotation cell. About 3383 mls of filtered water was added to the cell to make up 30 percent solid, which was maintained constant for all the tests. All the experiments were conducted on the same day, to avoid sample aging.

3.1.3 Examination of Flotation Variables

3.1.3.1 Effect of Water Quality

A feed sample as described in section 3.1.2 was re-pulp with either Tap or Process water in a standard 4 litre ESSA cell. The mixture was agitated at an impeller speed of 600 rpm for 2 minutes to obtain a good suspension of solids. After mixing, the pH for the tap water was raised to 10.5, using 0.1 M NaOH and conditioned for another 1 minute. The adjustment of pH was needed to ensure that the pH was similar to the Process water. After the 2 minutes conditioning period, a pH probe was inserted into the pulp and the reading was taken with a portable Hanna pH-Eh meter (Hl 8424 microcomputer), which had been calibrated at pH 7 and 12. After pH adjustment, 5 g/t of collector and 10 g/t of frother was applied for the test with tap water and conditioned for 1 minute. The addition of reagents was necessary to simulate plant conditions. The air flow valve was open and the aeration rate was set at 10 l/min for flotation. Then concentrates were scraped every 10 seconds and collected at 1, 3, 5 and 10 minutes intervals. After collection, the concentrates and tailings were filtered and dried in an oven at 80 °C. The dry weights were recorded and a representative sample was submitted for elemental analysis. In the chemical laboratory, the samples were pulverized before the analysis was carried out. Samples of tap water and process water were also submitted to characterize the chemical species present in each type.

3.1.3.2 Effect of pH 10, 11 & 12

Similar feed samples and flotation conditions as described in section 3.1.3.1 were applied to carry out flotation tests at pH 10.0, 11.0 and 12.0. In these tests, process water was used and that was selected to simulate plant conditions. Considering the pH adjustments, 0.1 M HCL and 0.1 M NaOH were used and were manually added into the pulp using a graduated dispenser. The pH was again measured using the same pH meter as described in section 3.1.3.1. In addition, the Eh of the pulp was also measured by using platinum and Ag/AgCl electrodes, which was calibrated with calomel solution at 430 mV. Concentrates were again collected at 1, 3, 5 and 10 minutes interval. After collection, the products were again filtered, dried, weighted and assayed in the standard manner.

3.1.3.3 Effect of Collector Dosage

Similar feed samples and flotation test conditions to those described in section 3.1.3.1 were applied, except for the application of different collector dosages. While the collector dosage was varied the pH was maintained constant at 10.5. The collector used was the Ok Tedi standard collector, which is Cytec S-7249 (a blend of di-isobutyl di-thio phosphate and di-isobutyl mono-thio phosphate) and is supplied in solution form. The test dosages were 9, 18 and 27 g/t, and for each dosage a micro syringe was used to add the collector into the pulp. After adding the collector it was conditioned for 2 minutes to ensure sufficient interaction with minerals. Concentrates were again collected at 1, 3, 5 and 10 minutes interval. After collection, the products were filtered, dried, weighted and assayed in the standard manner.

3.1.3.4 Effect of Aeration Rates

Similar feed samples and flotation conditions as those described in section 3.1.3.3 were followed, except for the application of variable aeration rates and an impeller speed of 600 rpm. The addition of collector was avoided in order to examine the effect of aeration rates under collectorless condition. Airflow rates of 10, 15 and 20 l/min were examined using the ESSA flotation machine. A conditioning time of 2 minutes prior to flotation was used to ensure that the pulp was saturated with air. Similar timed concentrate products as those described in the previous sections were collected and filtered, dried, weighted and assayed in the standard manner.

3.1.3.5 Effect of Agitation Rates

The flotation test conditions and feed sample as described in section 3.1.3.4 were applied, except for the application of varied agitation rates and an airflow rate of 10 l/min. The addition of collector was again avoided in order to examine the effect of agitation rates under collectorless condition. Agitation rates of 500, 600, 700 and 800 rpm were tested using the ESSA flotation machine. Further agitation increase beyond 800 rpm was not possible due to severe turbulence. Flotation was carried out after 2 minutes conditioning

and at a pH of 10.5. As usual, the flotation products were filtered, dried, weighted and assayed in the standard manner.

3.1.3.6 Extended Flotation of Cleaner Scavenger Tail

Similar flotation conditions as those described in section 3.1.3.2 were applied, except for a change in sample to cleaner tail. The sample was again mixed with process water in a 4 litre cell and floated at 30% solid and pH of 10.5. No additional collector was used and again that was to simulate plant conditions. After collecting the flotation products at 1,3,5 and 10 minutes, they were filtered, dried, weighted and assayed in the standard manner.

3.1.3.7 Effect of Cleaner Feed Oxidation in Tap Water

A mineral dissolution test was carried out for the cleaner feed sample using a 4 litre Denver flotation machine. The impeller speed was 1100 rpm and no air was applied. Tap water was used as the medium for the dissolution of the sulphide minerals present in the sample. Prior to the test, the plant sample was filtered and rinsed with tap water 5 times to clean the surface of the minerals. The reason was to remove any traces of chemical on the surface of the minerals that could cause interference. For the test, 1000 gm of plant sample was agitated at 20 percent solids. During agitation, sub samples of the pulp were extracted using a 10 ml syringe at 10 minutes interval and lasted 1 hour. The sub samples were subjected to two filtering stages, using a Whatman No. 91 filter paper and a 0.45 μm Millipore filter to remove colloidal particles. The filtered liquor were collected in test tubes and submitted to the chemical laboratory for ICP analysis of dissolved species.

3.1.4 EDTA Extraction of Flotation Pulp Samples

Before extraction was carried out, a 3% (w/v) stock solution of ethylene diamine tetra acid (EDTA) was prepared a day earlier. The reason is that it is a slow dissolving solvent (Rumball & Richmond 1996). The solution was contained in a 20-litre bucket that was thoroughly cleaned with acid and rinsed with acetone to remove organic substances. A thoroughly clean stainless steel stirrer was used to mix the salt to dissolution. During mixing, sodium hydroxide pellets were added to raise the pH from 4

to 7. It has been known that an alkaline pH was required as EDTA does not complex strongly with metal ions at acidic pH values (Morey 1998). After making the stock solution, it was purged with a nitrogen gas and that was to remove any dissolve oxygen. From the stock solution, 90 ml of 3% EDTA was placed in a clean beaker, which was gently stirred, with nitrogen gas bubbled through the solution. After thoroughly mixing the slurry to suspend particles, a 10 ml sample was extracted using a syringe and transferred into the EDTA solution. Then the solution was placed on a magnetic stirrer and leached for 5 minutes. After leaching, the solution was filtered using a Buchner funnel, and the liquor was collected then re-filtered using a sartorius 0.45 μm, Millipore filter. The final filtrate was placed in labeled bottles. The filtered solids were dried, weighed and placed in bags. Both solids samples and EDTA extract solutions were sent to Amdel (Adelaide) for chemical analysis. EDTA extractions were carried out on cleaner feed, tail and concentrate streams.

3.1.5 Size by Size Analysis

Samples from plant surveys were sized using a Tyler Rotap sieve shaker and Warman Cyclosizer. Operation of the Cyclosizer is described in section 3.1.6. The size fractions were +215 μm, -212+150 μm, -150+106 μm, -160+75 μm, -75+53 μm, -53+38 μm, -31+31 μm, -31+22 μm, -22+15 μm, -15+13 μm and -13 μm. These sizing products were assayed, with some size fractions selected for mineralogical examination.

3.1.6 Particle Size Analysis by Cyclosizer

A standard Warman cyclosizer was used for cycloning the slime fraction. Initially, a sample was wet screened with a 38 μm screen and the screen undersize (-38 μm) was filtered and the solids were collected for the cycloning process.

A sample weight of 100 gms at a time was slurried with water in a beaker and transferred to the sample container of the Warman cyclosizer. The sample was bled from the container into the water stream by opening the sample valve so that the whole of the sample was released over a period of 5 minutes. The cyclosizer products collected were:

+C2	(-38+31 μm)
C3	(-31+22 μm)
C4	(-22+15μm)
C5	(-15+13 μm)
C6	(-13 μm)

Size ranges of the Cyclosizer fractions were specified as quartz equivalent size according to the manufacturer, Warman International Ltd (1981). After sizing, the fractions were collected, including the slimes (-13 μm) and were filtered, dried and weighed. The products were submitted to the chemical laboratory for assay.

3.2. Cleaner Circuit Characterization Studies

Plant surveys were performed as a function of 'good' and 'bad' feed blends. In addition, plant testing of collector and lime addition to the cleaner circuit, and the effect of the low grade regrind ball mill was also examined. The following sub-sections discuss the specific conditions and methodology of the plant surveys conducted.

3.2.1 Metallurgical Sampling

At 0700 am, before sampling, the plant operational conditions were stabilized to ensure that there was no disturbance. Stabilization of the plant conditions were carried out in the following manner.

- The ore delivery to grinding were strictly monitored and controlled to deliver a steady feed-rate to the flotation circuit.
- All recycle spillage pumps in the flotation building were shut down to prevent recycling of material on the flotation basement. This step was taken to avoid contamination of the fresh feed with oxidized material.
- The cleaner circuit was operated in an open circuit mode. In this situation the cleaner scavenger tail was directed to the final tailings.

- A one hour period was allowed for the plant to stabilized and during this period the process conditions were monitored using the process trends, graphically displayed on the Bailey control system.

After establishing steady conditions, pulp chemical measurements were carried out at 0900 am and the procedure is described in section 3.2.2. When pulp chemical measurements were completed, metallurgical sampling was then carried out at 0930 am. Samples were collected at 15 minute interval, for a period of one hour. Dip samplers were used for taking samples inside the flotation cells whilst cereal containers were used for taking concentrate lip samples. Figure 8.0 shows the sample points and its descriptions which included scavenger cleaner feed (1), cleaner cell 1-2 concentrate (2), cleaner cell 1-2 tail (3), cleaner cell 3-5 concentrate (4), cleaner cell 3-5 tail (5), cleaner cell 6-8 concentrate (6), and cleaner cell 6-8 tail (7). All the samples were taken to the laboratory and wet masses were taken. The samples were filtered, dried and prepared in the standard manner. Dry masses of the sample were recorded and the samples were rolled and mixed 10 times before it was further mixed using a rotary splitter. After mixing 5 times with the rotary splitter, representative samples were weighed and submitted to the chemical laboratory for assays. The remaining split samples were weighed and stored in plastic bags. These samples were used for sizing as per procedure described in section 3.1.5 and 3.1.6.

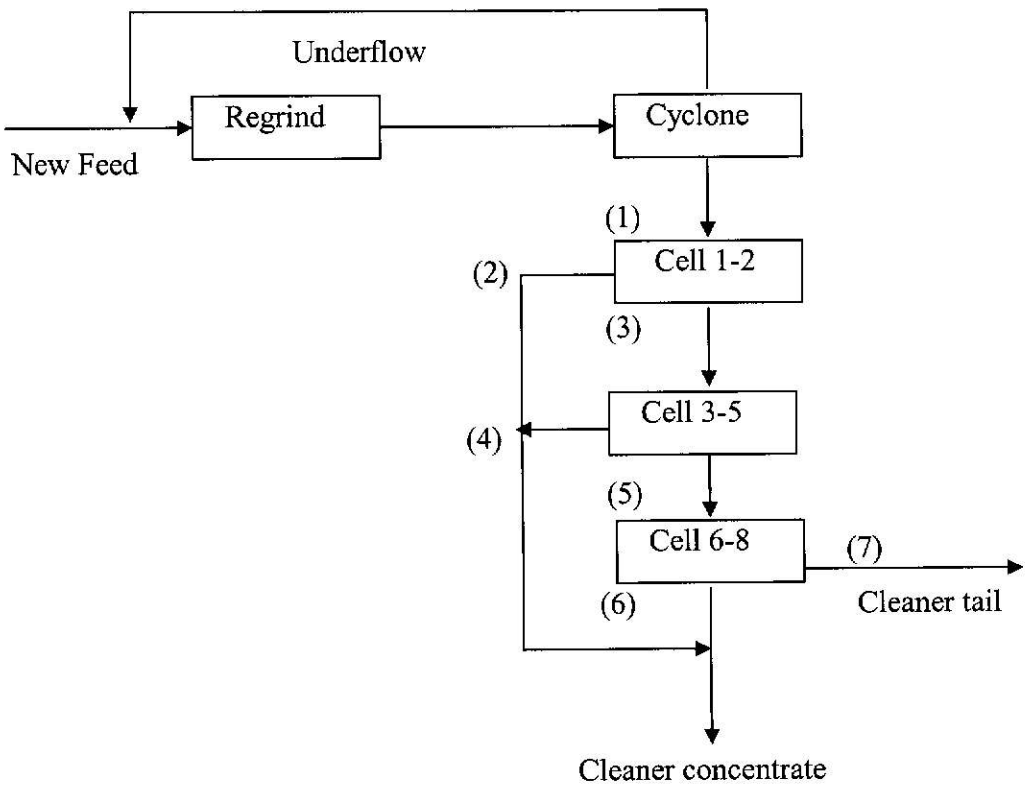

Figure 8.0: Block diagram of the cleaner circuit with sampling points

3.2.2 Pulp Chemical Measurements

As stated in the previous section, pulp chemical measurements of pH, Eh, temperature and dissolve oxygen (D.O.) were carried out. The pH and Eh of the pulp were measured using a Hanna pH-Eh meter whilst dissolved oxygen and temperatures were measured using a dissolved oxygen-temperature meter (Model Wp-82). The Eh probe was composed of a platinum-Ag/AgCl electrode and was calibrated with calomel solution at 430 mV. The dissolve oxygen (D.O.) meter was calibrated at zero using a 0.2M sodium sulphite solution. The temperature probe was calibrated at room temperature using tap water and a thermometer.

A sample was collected using the same method as that described in the previous sections. The sample was then transferred into a clean 2 litre bucket and mixed gently. Immediately after mixing, the probes were inserted in the pulp, and measurements were taken at cumulative times of 0, 10, 20, 30, 40, 50, 60, 70, 80, 100 and 120 seconds. After taking

measurements for the cleaner feed streams, the probes were cleaned with water and further measurements were carried out in the same manner for cleaner concentrate and tail streams. When the measurements were completed, the buckets were closed with lids and were immediately taken to the laboratory. In the laboratory, an EDTA extraction test was carried out on the samples by applying the same procedure as described in section 3.1.4.

3.2.3 Time of Flight Secondary ion Mass Spectrometry (ToFSIMS) Sample Analysis

When the pulp chemical measurements were carried out, additional samples were also taken of cleaner scavenger tail, feed and concentrate streams. These samples were dedicated for ToFSIMS analysis. At the sampling point, the samples were purged with liquid nitrogen to prevent oxidation. After purging with liquid nitrogen, the samples were immediately taken to the laboratory. In the laboratory, the samples were thoroughly mixing with a magnetic stirrer and a sub sample was extracted into a 10 ml vial. The sub sample was immediately frozen in liquid nitrogen, which was contained in a thermos flask. The samples were then stored in a freezer. When it was ready for transportation to its destination, the samples were transferred to an esky that contained solid ice blocks. On the same day, the samples were flown to Adelaide and were delivered to the Ian Wark Research Institute by following standard procedures.

3.2.4 Effect of Unground Cleaner Feed

Metallurgical sampling was again performed on the Unit 2 Cleaner circuit to determine the function of the regrind ball mill. Two surveys were performed under the conditions, with and without the regrind ball mill. The survey under condition with regrind ball mill was carried out first using a similar method as described in section 3.2.1, including pulp chemical measurements, EDTA extractions and ToFSIMS samples.

In order to carry out the survey under the condition without the regrind ball mill, the circuit was set up in the following manner.

- The underflow of two cyclones were blanked off from the main low grade Cyclone manifold. The blanked cyclones were dedicated for feeding the cleaner circuit with ungrounded material.
- The cleaner circuit was operated in open circuit mode.
- The low grade regrind ball mill was isolated and feed was introduced to the circuit.
- The rougher scavenger concentrate stream was diverted from the low grade regrind circuit to the rougher circuit. This step was taken as a result of an increase in volumetric feed to the cleaner circuit which consequently caused unsteady pulp level conditions in the cleaner circuit.
- A conditioning time of 4 hours was provided for the circuit to stabilized. During this period all the process trends were monitored using the Bailey Control System.
- When steady conditions were established, pulp chemical measurements, including EDTA and ToFSIMS samples were taken.
- Metallurgical sampling was carried out in the same manner as those for the condition 'with' regrind ball mill.
- After completion of the survey, the regrind ball mill circuit was returned to normal operating conditions.

Sample preparation and assaying were again carried out in the standard manner.

3.2.5 Effect of Additional Lime

Addition of lime to the cleaner circuit for improved flotation performance was trialed. Since there was no existing lime addition line to Unit 2 low grade cleaner circuit, a new line was installed and lime was introduced into the low grade cyclone underflow. The pH of the cyclone overflow was measured using a portable Hanna pH-Eh meter and lime flow was manually regulated using a control valve until the cleaner feed pH was stabilized at 11.0. A conditioning time of 1 hour was provided for the lime to saturate in the circuit. After 1 hour conditioning period, pulp chemical measurements and EDTA samples were taken. The sampling was carried out in the standard manner as described in section 3.2.1. A total of six comparative snap shot surveys were carried out. Each comparison included

lime-off and lime-on surveys. All the samples were prepared and assayed in the standard manner.

3.2.6 Effect of Additional Collector

Addition of S-7249 to the scavenger cleaner circuit for improved flotation performance was also trialed. A fresh sample of S-7249 collector, about 20 litres was collected in a clean bucket. The bucket was sealed with a lid and was placed next to the low-grade hydrocyclone pack. A portable Watson reagent pump was used to transfer collector from the bucket to the low-grade cyclone underflow box. The reagent pump was rammed to pressurize the flow through the tubes before the collector flow was adjusted to 15 ml/min (5 g/t). A one hour conditioning and circuit stabilization was allowed. Like the lime trials, 6 collector on-off tests were carried out, including pulp chemical measurements and EDTA extractions.

3.2.7 Residence Time Measurement by Salt Tracer Method

Residence time measurements for the scavenger cleaner flotation bank were performed using common salt as the tracer. Approximately 15 kg of cooking salt (solid powder) was added into the scavenger cleaner feed drop box. Immediately, sub-samples of the cleaner tailing stream from the last cleaner cell (cell 8) were collected at 1 minute intervals, spanning a total time of 21 minutes. The samples were filtered in the same manner as described in section 3.1.4. The filtrates were submitted to the chemical laboratory for sodium analysis.

3.2.8 Hydrodynamic Characterization of Cleaner Cell

Hydrodynamic conditions of the first two scavenger cleaner cells were characterized using a JKTech designed Air Hold-Up and Superficial Gas Velocity devices. A detailed description of the technique has been reported by Power et al (2000). The following sub – sections discusses the methodology that was applied to carry out the measurements.

3.2.8.1 Air Hold Up Measurement

The air hold-up device consists of a 3-inch flexible hose, with air operated pinch valves on the two ends. When the air lines were connected, the pinch valves were closed and the device was placed in the vertical position above the flotation cell. It was then inserted into the pulp, below the froth level, and the pinch valves were immediately opened to collect a sample. After a sampling time of 30 seconds, the valves were closed and the device was removed from the cell and placed above a discharge bucket. The sample was transferred from the device into a graduated cylinder and the volume was measured. In the same manner, several measurements were taken at different locations in the cell. After completion of measurements, the device was calibrated with water to determine the correct volumetric capacity.

3.2.8.2 Superficial Gas Velocity (Jg) Measurement

Superficial gas velocity (Jg) measurements were performed using the Jg probe. The device consisted of a Perspex tube with a pneumatic pinch valve at the bottom end with water addition. After connecting air and water lines, the valve was closed and the probe was placed in a vertical position above the cell. It was then inserted into the pulp phase and the water valve was open to fill the tube. At the same time, the air bleed valve was opened to atmosphere. When the tube was full with water, the air bleed valve was closed to prevent water escaping. Then the water valve was closed and the pinch valve was opened, to allow the pulp air bubbles to rise and fill the Perspex tube, thus displacing the water. A stopwatch was used to record the time taken for the air bubbles to evacuate the tube between the two marks. After flushing with water, further measurements were undertaken at different locations in same manner. For a known volume of air and Perspex tube diameter, the superficial gas velocity can be calculated.

CHAPTER4: LABORATORY EXPERIMENTAL RESULTS AND DISCUSSION

4.1 Introduction

During the processing of porphyry ore, the cleaner circuit is generally operated in open circuit. This means that the cleaner tail is part of the final tail when the Amdel in-stream analysis (ISA) unit indicates less than 2% Cu. However, as the proportion of skarn ore in the plant feed increases, the cleaner tail assay tends to exceed 2% Cu and the cleaner tails are recycled to the rougher circuit. As the mass percent of copper in the cleaner tails increases, copper and gold losses in the final tail increase also. Based on the current plant performance as reported by Gron (2001b) on the cleaner tail from July 1999 to July 2000 indicated that around 26% of the copper and 34% of the gold entering the mill was lost to the final tails. This situation has provided the scope for metallurgical investigation.

4.2 Laboratory Examination of Flotation Variables

As part of the cleaner circuit characterization work in the plant, laboratory work was conducted to seek avenues that could lead to further investigation. This work involved examination of the effect of the following variables; pH, collector dosage, agitation rate, aeration rate, water quality and flotation time. The results of this work were used to assist in providing directions for improvement work in the plant.

The methodologies applied to carry out these experiments were discussed in section 3.1.3. The focus of this chapter is to present the results of the preliminary work, including suggestions for further work in the plant.

4.2.1 Sample Characteristics

All the flotation variables were studied as a function of the plant cleaner feed. The test sample was collected from Unit 2 cleaner flotation circuit and all the tests were performed on the same day. This measure was taken to minimize oxidation and more importantly to

compare the laboratory results with the plant performance. Furthermore, it is important to establish the sample characteristics and pulp conditions to assist in explaining the results.

4.2.1.1 Chemical Composition

The nature of the feed will naturally influence the flotation response. A typical cleaner feed sample was therefore analysed with a Philips PW 1660 XRF instrument and the results are shown in Table 2.0

Table 2.0: Chemical composition of cleaner circuit feed

Sample	Cu %	Fe %	S %	SiO_2 %	Al_2O_3 %	K_2O %	TiO_2 %	CaO %	MgO %	F ppm
Feed	9.39	19.87	19.16	21.02	6.39	2.26	0.33	0.60	0.73	587

The results show that the sample is rich in sulphide minerals and is predominately iron sulphide. The presence of the iron sulphides is attributed to the high percentage of sulphide skarn component in the plant feed, as the feed blend on that day (10/01/03) was 16% sulphide skarn ore and 84% porphyry ore. The presence of SiO_2, Al_2O_3, CaO, MgO, TiO_2 and F suggest magnesium-iron silicate and feldspar gangue minerals. It is known that, these minerals are inert to collector (Gaudin 1939). Although, talc is a magnesium silicate mineral and inert to collector, it is naturally floatable. In general, the chemical composition suggests that the feed has the necessary properties for flotation and that the separation of copper from gangue should not be difficult. Further mineralogical characteristics for porphyry and skarn ores are discussed in section 5.2.1.

4.2.1.2 Metal Distribution

The cleaner circuit feed is the reground product of tank cell tail, column tail, recleaner tail and rougher scavenger concentrate. The particle size for this particular feed sample shows a product size (p80) of 53 μm and Figure 9.0 shows the metal distribution.

Figure 9.0: Metal distribution of cleaner flotation feed sample

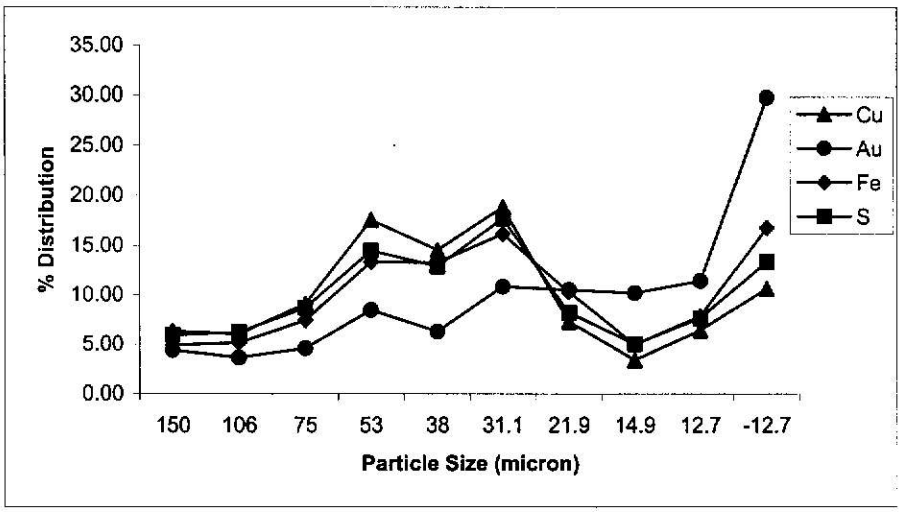

The results show a good flotation feed sizing with most of the sulphides distributed in the floatable size ranges (75–22 μm). However, there is considerable distribution of metal in the very fine size ranges (15–13 μm) and these fractions would probably be slower floating. When comparing these results with a recent liberation analysis as shown in Table 3.0, it can be seen that the product size of p80 = 53 μm is normal (Met Engineers 1999). More importantly, it was observed that the sulphides are well liberated from the gangue at these product sizings. Thus, separation from gangue should be relatively easy. However, selectivity may be a problem with the high proportion of pyrite in the cleaner flotation feed.

Table 3.0: Liberation characteristics (Met Engineers 1999)

Survey Period	Process Stream	Product size (p80) microns	Mineral Liberation – Percent Complete		
			Copper Sulphides	Pyrite	Gangue
20/11/99	Cleaner feed	42	90	78	89
11/12/99	Cleaner feed	47	88	75	75

4.2.2 Pulp Solution Analysis

Pulp solution analysis was carried out to examine the chemical properties of the pulp that could influence the flotation behaviour of particles in the cleaner circuit. Measurements were carried out for the pulp parameters; dissolved oxygen, pulp potential and pH. The results are discussed in the following sections.

4.2.2.1 Measurements of Pulp Parameters: Dissolved oxygen, pH and Eh

Sulphides are thermodynamically unstable in the presence of oxygen and potential determining ions such as Fe^{2+}, Fe^{3+}, OH^- and H^+. Since flotation recovery is influenced by pH, Eh and dissolved oxygen concentration, it is important to understand the conditions of the cleaner circuit streams. For instance, oxygen is necessary for the collector adsorption to occur, through either the electrochemical or chemical adsorption mechanisms (Kelly & Spottiswood 1982; Kuopanportti et al. 1997).

Measurements were carried out in the plant following the methodology as described in section 3.2.2. The dissolved oxygen readings are expressed as a percentage of saturation. These readings were used to produce oxygen demand curves. Figure 10.0 shows the data collected from both the cleaner feed and tail streams. The dissolved oxygen demand curves may be compared with previous results (Ok Tedi oxygenated mill water) which trend from 100% to 80% saturation (Morey & Grano 2000). It is apparent that this trend correlates with the natural de-oxygenation of quiescent water. These authors stated that any stream which consumes dissolve oxygen at a significantly greater rate than this has a high dissolved oxygen demand. Mineral sulphide particles in the stream would therefore be oxidizing (consuming oxygen). That means the particles would be rapidly developing oxide coatings.

Figure 10.0: Oxygen demand curves for cleaner feed and tail streams

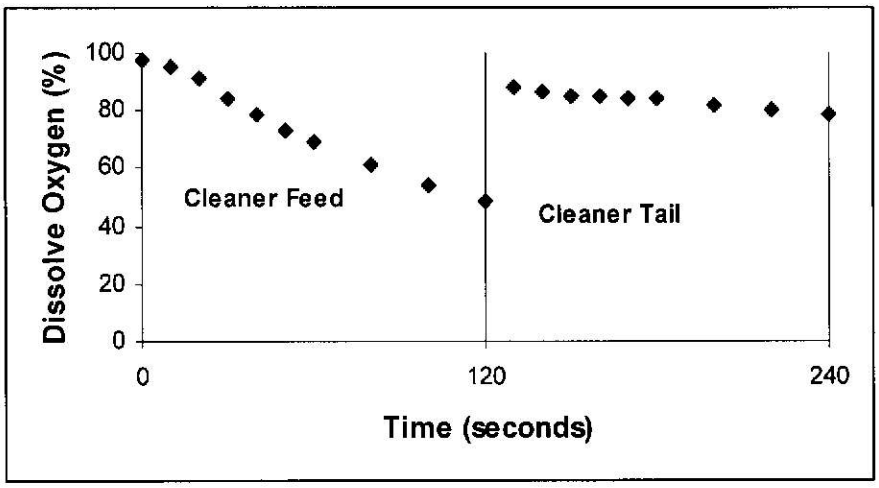

The results have indicated that the feed stream is showing below 80% saturation, while the tail stream appears to be reasonably steady at 80% saturation. The interpretation is that the feed stream has a higher demand for oxygen and the pulp is therefore oxidizing, while this trend is not shown for the tail stream. Therefore the feed stream is not electrochemically passivated and perhaps the sulphide particles could adsorb more collector and perhaps become more hydrophobic, with a higher flotation rate constant. On the contrary, the cleaner tail stream with low oxygen demand suggests that the particles are coated with oxides. These trends indicate that the sulphide particles in the stream were progressively oxidized in the cleaner circuit.

Figure 11.0 and 12.0 shows typical measured values of the pulp parameters Eh and DO in cleaner feed and cleaner tail. The pH was observed to be reasonably steady at 10.7 for the cleaner feed and 10.5 for the cleaner tail while the Eh and DO were variable. The pulp potential measurements have been converted to the standard hydrogen electrode (SHE) scale by the addition of 199 mV and the dissolved oxygen (DO) is again expressed as a percentage of saturation. The Eh of the pulp was measured by using a platinum and Ag/AgCl electrode, which was calibrated with calomel solution at 430 mV.

Figure 11.0: Cleaner feed pulp potential and dissolve oxygen data

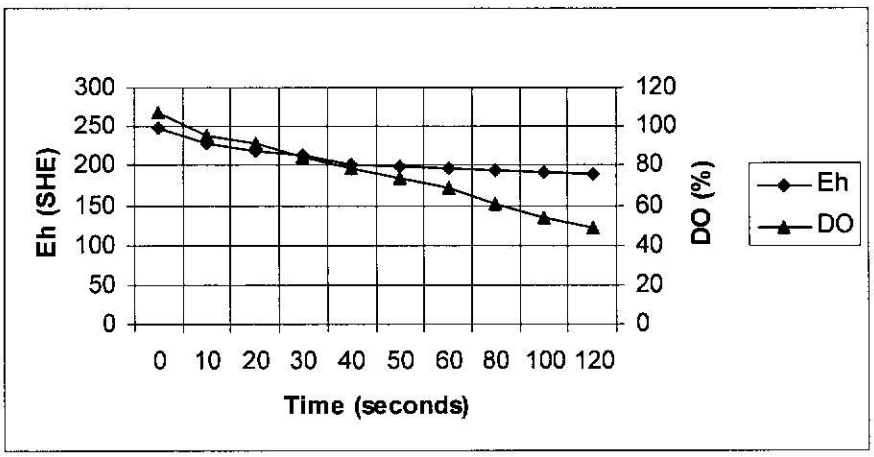

Figure 12.0: Cleaner tail pulp potential and dissolve oxygen data

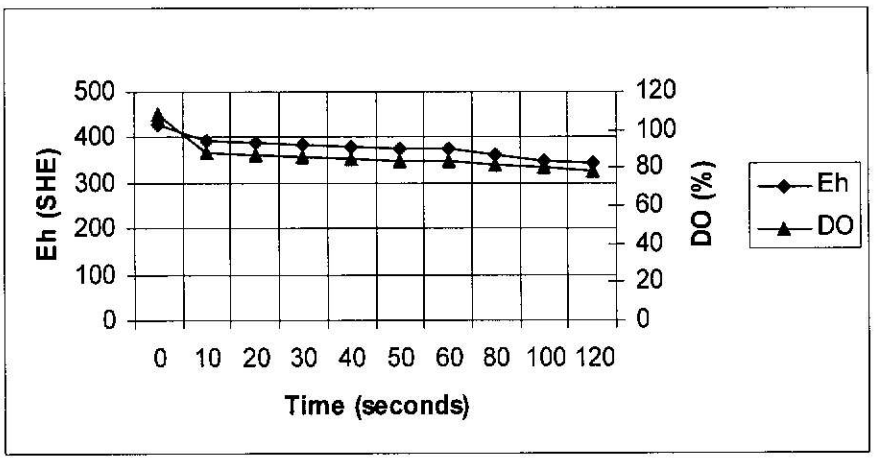

It is apparent from Figures 11.0 and 12.0 that the pulp potential is dependant on dissolved oxygen concentration. As with the data of Figure 10.0, the cleaner feed stream (Figure 11.0) shows a decreasing dissolve oxygen trend coupled with a reasonably steady potential of approximately 200 mV (SHE). In contrast, the cleaner tail stream shows high potentials (300-400 mV SHE) coupled with steady dissolve oxygen concentration (80%). These trends show that the sulphide particles in the cleaner feed stream are consuming oxygen whereas this is not shown in the cleaner tail stream. The implication is that the particles in the cleaner feed stream are not coated but are reactive. They could most likely adsorb further collector and become more hydrophobic.

4.2.2.2 EDTA Extraction Analysis

Before EDTA extraction was performed, a dissolution test was conducted for cleaner flotation feed pulp. The objective was to examine if sulphides can dissolve in the pulp under the absence of air and with tap water (pH 8.0). The methodology is described in section 3.1.3.7. Figure 13.0 show that the concentration of the copper, iron and sulphur as a function of dissolution time. From this graph, it is observed that copper and iron can dissolve under these conditions. It is believed that these metals may dissolve in the pulp under the alkaline conditions of the cleaner circuit. Consequently, they may precipitate out as hydroxides as found by Grano and Morey (2000). A study by Orwe (2000) on the copper dissolution from Ok Tedi monzonite ore also indicated that the rate of dissolution was high below pH 5 (acid) and low at an alkaline range. Since the natural pH for most ore at Ok Tedi lie between 5 and 7, it is reasonable to assume that copper is dissolving from the mine pit to the mill.

Figure 13.0: Dissolution of sulphide minerals

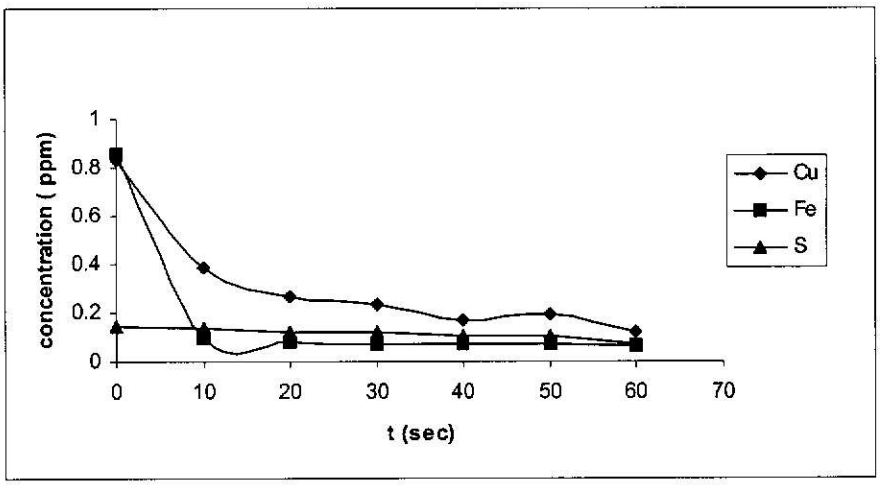

In order to establish that oxidized products are present in the pulp, EDTA extraction techniques were applied according to the methodology described in section 3.1.4. Ethylene diamine tetra acid (EDTA) is a powerful chelating reagent and it has been found by numerous authors (Greet et al 1994; Rumball & Richmond 1996; Grano et al. 1994; Clarke et al. 1995) to solubilise the oxidation products of sulphide minerals. This technique was therefore applied to extract any divalent metal hydroxides from coated

surfaces. The percent EDTA extractable copper (or percent oxidised copper) is determined by:

$$\% \text{ EDTA extractable Cu} = \frac{\text{Mass of EDTA Extracted Cu}}{\text{Mass of Cu in solids}} \times 100$$

Calculations were performed for copper, iron, calcium and sulphur for a typical cleaner feed and tail streams. The results are shown in Table 4.0. The metal ions are expressed as a percent of total metal in the pulp solids.

Table 4.0: EDTA extractable metal ions as percent of element in solids analysis

Stream	% Cu	% Fe	% S	% Ca
Cleaner feed	0.169	1.57	0.163	45
Cleaner tail	1.32	3.53	0.643	65

The immediate conclusion drawn from these results is that the cleaner tail stream contains a higher relative concentration of EDTA extractable ions, suggesting that the cleaner tail stream is passivated and the particles are covered with oxide layer or slimes. Combining these results with the oxygen demand curves (Figure 10.0), forms a good agreement, i.e., the low oxygen demand is attributed to the oxide layers on the particle surfaces. Furthermore, if the results are compared with previous results of the plant streams (Table 5.0) it is apparent that, tailing streams show a higher EDTA extractable copper than the other streams. It is therefore reasonable to conclude that the oxidation products are making value minerals less floatable and therefore concentrating in the tailings.

Also, Morey and Grano (2000) found that the EDTA extractable copper level at Ok Tedi was unusually high when compared with other mines in Australia. These authors confirmed by XPS studies, the presence of $Cu(OH)_2$ and concluded that the high EDTA copper level was attributed to the presence of $Cu(OH)_2$ in the pulp.

Table 5.0: EDTA extraction test results from Unit 2 survey (Orwe 2000)

Stream	% EDTA extractable copper
Rougher feed	2.10
Final tailing	15.40
Cleaner feed	0.45
Cleaner tail	3.80
Cleaner concentrate	0.25
Final concentrate	0.20

Orwe (2000) also carried out EDTA conditioning tests on Ok Tedi monzonite ore as a function of pH (pH 5 to 12) and found that the concentration of EDTA extractable copper increased at low pH and decreased at high pH. Further, Orwe carried out zeta potential measurements for single minerals (chalcocite, covellite and bornite) and found that the surface charge for these mineral particles changed from positive to negative at high pH, showing formation of surface hydroxides at high pH. Copper sulphides are thermodynamically unstable at high pH and the Orwe's conditioning tests confirm this, however passivation by surface precipitation of hydroxides will limit this effect.

Based on these preliminary indications, it is apparent that the flotation behaviour can be influenced not only by the nature of the ore but also the prevailing thermodynamic conditions in the plant pulp. Considering these effects, analysis of Eh and DO are good diagnostic tools, indicating passivation effects and hinting that the loss of copper and gold in the cleaner scavenger tail stream could be associated with oxide/hydroxide formation on the particle surface.

4.2.3 Cleaner Circuit Performance

During the processing of the same particular feed blend as in section 4.2.2 (sulphide skarn/porphyry ore), survey samples were collected from Unit 2 cleaner flotation circuit. The objective was to examine the plant performance and compare with the laboratory results.

Copper and gold assays for the feed, concentrate and tail were data-smoothed using the computer MATBAL program. Table 6.0 shows the data-smoothed results for the cleaner flotation circuit.

Table 6.0: Cleaner flotation performance in the plant

Stream	Mass %	Assay		Recovery (%)	
		Cu (%)	Au (g/t)	Cu	Au
Cleaner Feed	100	9.39	10.68	100	100
Cleaner Con	73.59	12.26	13.32	96.12	93.35
Cleaner tail	26.41	1.38	2.61	3.88	6.65

From Table 6.0 copper and gold recoveries were 96 and 93 percent respectively, while the cleaner concentrate grade shows 12.2% copper and 13.3 g/t gold. These results are typical and acceptable in terms of the metallurgical performance. Also, the copper level in the tails is below the 2% control limit and on that day, the cleaner circuit was operated in an open circuit mode, i.e., the cleaner tail was directed to the final tailings.

It may be noted however, that the cleaner tail showed relatively high copper and gold content. The potential for improvement in cleaner flotation performance to minimize copper and gold losses in the cleaner tail is apparent.

4.2.4 Examination of Flotation Variables in Bench Flotation

Laboratory flotation of the plant cleaner feed was performed as a function of pH, collector dosage, agitation rate, aeration rate and water quality. In addition, the effect of flotation time on cleaner tail grade was also examined. The objective of these experiments was to optimise these variables and improve copper and gold recoveries. Furthermore, the results could be compared with the plant performance to indicate possible adjustments in the plant.

4.2.4.1 Effect of pH

The plant cleaner feed sample was floated as a function of pH and without additional collector. The results are shown in Table 7.0 and Figure 14.0.

Table 7.0: Flotation test conditions and results as a function of pH

Test Condition		Head Grade		Cumulative Concentrate grade		Cumulative Recovery (%)	
pH	Eh SHE (mV)	Cu (%)	Au (g/t)	Cu (%)	Au (g/t)	Cu	Au
10	312	8.57	8.46	11.21	10.59	94.31	90.26
11	215	8.91	8.65	10.09	12.15	96.30	92.11
12	163	8.16	8.22	10.84	10.43	98.61	94.13

Figure 14.0: Copper and gold recoveries as a function of pH

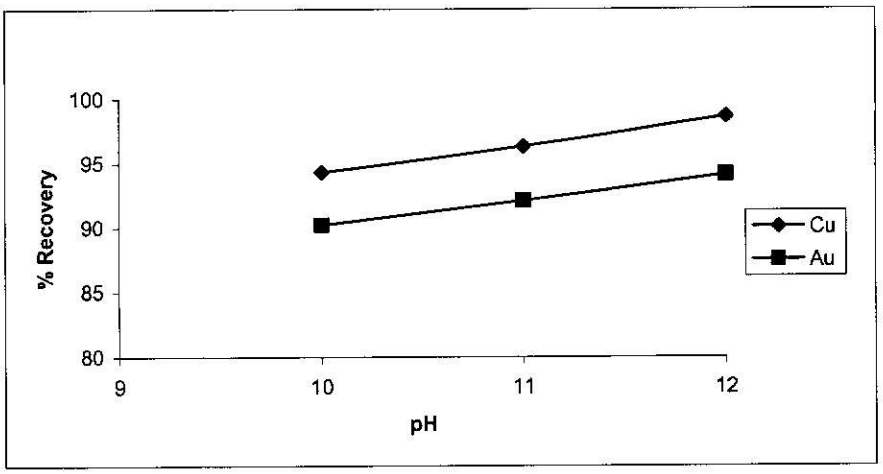

It is apparent from Table 7.0 and Figure 14.0 that copper and gold recoveries are increasing linearly with pH. That is, as the pH is increased from 10 to 12, there is a corresponding increase in copper and gold recoveries. The best results are observed at pH 12 with 98% copper and 94% gold recoveries. When compared to the plant results (Table 6.0), it is observed that the concentrate grades are similar while recoveries appear to be

much better. An improvement of 2% for copper and 1% for gold is obtained and this shows that the effect of pH on copper and gold recovery is significant.

While the results show that the effect of pH is more profound for copper, the small increase in gold recovery could mean that the gold is difficult to float. This problem could be associated with particle size because Figure 9.0 showed that 50 percent of the gold is distributed in the fine particle size ranges (22-13 μm). Mineralogical investigation of a cleaner tail sample by Amdel (1999) also indicated that 50% of the gold was distributed in the –20 μm size range. Therefore, it is reasonable to assume that gold losses could be attributed to a lower flotation rate constant.

Another interesting observation shown by the results is that, there is a change in pulp potentials when pH is increased. For this particular feed blend (sulphide skarn/porphyry ore), pH appears to decrease the pulp potentials. When plotting the pH against Eh and recovery, it can be observed from Figure 15.0 that, as pH is increased the Eh decreases and copper and gold recoveries appear to increase inversely. These results indicate that the increase in copper and gold recoveries is attributed to the increase in pH.

Figure 15.0: Copper and gold recoveries as a function of pulp potential

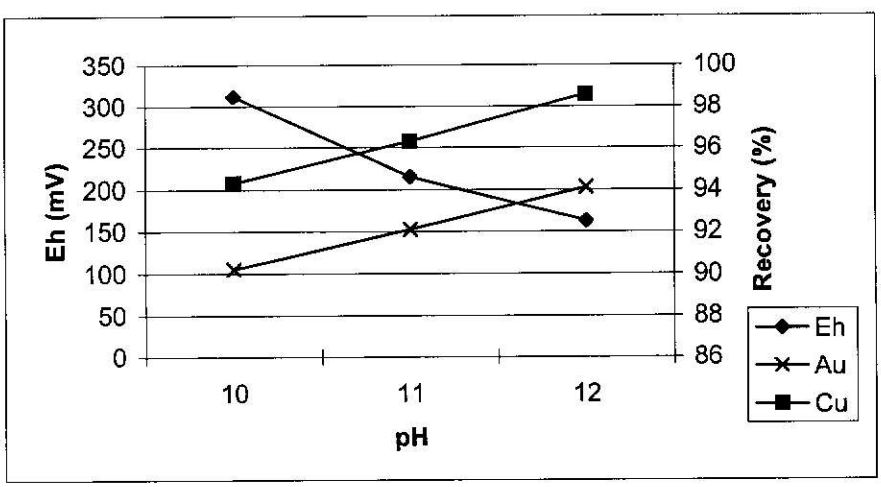

However, when considering the oxygen demand curve (Figure 10.0) for the feed pulp conditions, it also shows a decreasing pulp potential coupled with high oxygen demand. These results could also suggest that the increase in copper and gold recoveries is

influenced by both pulp parameters (pH and dissolve oxygen). A recent study by Kuopanportti et al. (1997) also showed that the dissolved oxygen had a strong influence on the pulp potential and the rate of xanthate adsorption on a sulphide minerals surface. The author found that chalcopyrite recovery was poor when dissolve oxygen concentration was at lowest level. Further investigations were carried out on these conditions in the plant and the results are discussed in Chapter 5.

It is also known that pH helps to modify the electrical double layer for fine particles, which consequently helps to increase the probability of bubble-particle contact (Fuerstenau, 1982b; Nguyen et al. 1997). When comparing the flotation feed sizes in the plant, (that is, cleaner flotation feed size (p80, 53 μm)) with rougher flotation feed size (p80, 180 μm), it can be seen that the cleaner feed stream is the finest stream. It is assumed that under the high pH conditions, the colloidal particles in the cleaner feed stream may have dispersed. Previous work by Orwe (2000) on the size by size recovery of Ok Tedi monzonite ore found that an increase in pH from 6.0 to11.5 resulted in a significant increase in the maximum recovery of the –31 μm fraction, coupled with an increase in the flotation rate constant. Since the feed blend was predominantly porphyry ore (84% monzonite ore), it is possible that a similar effect could have occurred.

The work of Kuopanportti et al. (1977) is consistent with classic thermodynamic theory. This work indicated that collector adsorption onto value minerals decreased with increasing pH. Therefore floatability should decrease with increasing pH. Possible reasons for the reverse actually be true is the cleaning of particle surfaces by the dispersion of precipitates (as $CuOH_3^-$ species for example). However, it has been shown that for pyritic ores, a major effect of increasing pH above 10 is to transfer collector from pyrite surfaces to other sulphide mineral particle surfaces (Morey 1998).

It is apparent from these results that increasing the pH and increasing collector addition could be useful methods to enhance copper and gold recoveries and possibly selectivity against pyrite in the cleaner flotation circuit. This concurs with the conclusion on page 69 that copper sulphide particles were not passivated and could probably adsorb more collector.

4.2.4.2 Effect of Collector Dosage

After the pH test, the same sample was used for the examination of the effect of collector dosage. The collector used was the standard Ok Tedi collector, which is Cytec S7249 and is a blend of di-isobutyl dithiophosphate and di-isobutyl monothiophosphate. The flotation test results are shown in Table 8.0 and Figure 16.0.

Table 8.0: Flotation test conditions and results as function of collector dosage

Collector Dosage (g/t)	pH	Eh (mV)	Head Grades		Cumulative Concentrate grade		Cumulative Recovery (%)	
			Cu (%)	Au (g/t)	Cu (%)	Au (g/t)	Cu	Au
0	11.0	215	8.57	8.46	11.21	10.59	96.3	92.1
9	11.0	229	7.78	8.17	10.90	11.34	98.4	97.5
18	11.0	233	8.57	8.73	10.77	10.92	98.8	98.4
27	11.0	230	8.22	8.74	9.99	10.58	98.9	98.6

Figure 16.0: Copper and gold recoveries as a function of collector dosage

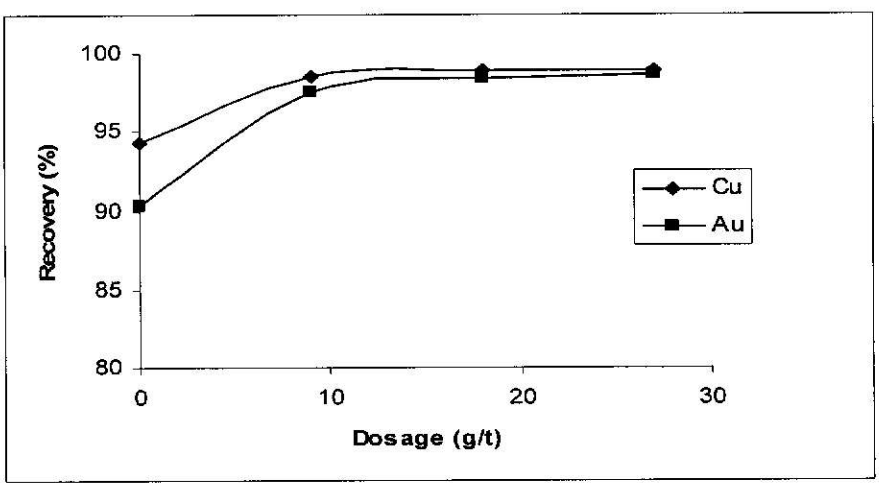

The results show that as the collector dosage is increased from a nominal coverage from rougher flotation to an additional 27 g/t, then copper and gold recoveries also increases. Copper recovery increased from 96.3 to 98.9% and gold recovery increased from 92.1 to

98.6%. When compared with the plant results (Table 6.0), it can be observed that an improvement of 5.2% is obtained for gold and 2.8% for copper. This suggests that additional collector is needed to improve flotation performance in the plant. When the concentrate grades were compared with the plant, a slight decrease is observed for both copper and gold. That could suggest that selectivity is not seriously affected for this particular feed and more importantly it show that the collector is very selective at high dosage at pH 11. This observation supports previous studies which have shown that dithiophosphate is selective against pyrite (Sutherland & Wark 1955; Poling & Beattie 1984; Nagaraj & Brinen 2001; Erepan 2000).

When relating these results to the feed conditions, some concluding remarks can be drawn. Since the oxygen demand for the feed indicates that the particle surfaces were not passivated, it is probably significant, that the collector had induced the particles to be more hydrophobic and that could have resulted in enhancing the copper and gold recoveries. In addition, the 'fresh' surfaces generated from the regrind mill could also be adsorbing the collector.

4.2.4.3 Effect of Agitation and Aeration Rates

Following the pH and collector tests, further tests were carried out to examine the effect of agitation and aeration rates. It is known that these two factors influence the gas dispersion properties such as gas hold-up, bubble size, and superficial gas velocity which influence the bubble-particle collision and adhesion mechanisms (Power et al. 2000; Gorain et al. 1997b; Ahmed & Jameson 1989; Ramadan et al. 1998; Schubert & Bischofberger 1978; Lins & Adamian 1993; Yoon 2000).

The agitation tests were conducted using an ESSA flotation machine with an aeration rate of 10 l/minute and without additional collector. The results are shown in Table 9.0 and Figure 17.0.

Table 9.0: Flotation test conditions and results as a function of agitation rates

Agitation Rates (rpm)	pH	Eh (mV)	Head Grades		Cumulative Concentrate grade		Cumulative Recovery (%)	
			Cu (%)	Au (g/t)	Cu (%)	Au (g/t)	Cu	Au
500	11.0	226	8.20	7.32	12.24	10.93	94.70	92.63
600	11.0	235	8.27	8.12	12.15	11.68	97.70	95.61
700	11.0	238	8.69	7.88	12.87	11.75	94.56	95.22
800	11.0	234	8.04	7.65	12.46	11.80	93.51	93.12

Figure 17.0: Copper and gold recoveries as a function of agitation rates

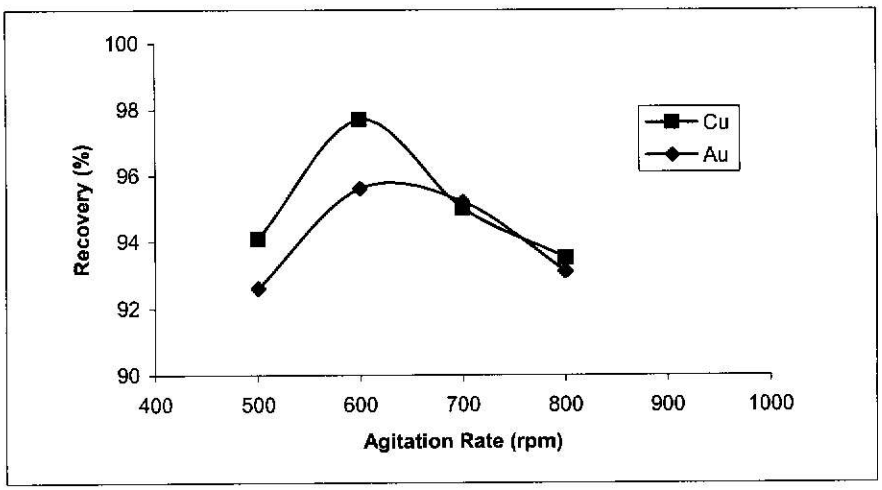

The results show that increasing the agitation speed increases copper and gold recoveries until an optimum point is reached. The optimum rate appears to be 600 rpm and, at this point, copper and gold recoveries were 98% and 95%, respectively. Agitation rates above 600 rpm show poor recoveries and that is probably due to the turbulent conditions. It has been stated that under turbulent conditions, the particle detachment mechanism becomes dominant to the particle bubble collision and adhesion mechanisms (Ahmed & Jameson 1989; Schubert & Bischofberger 1978).

When compared with the plant results (Table 6.0), the results are again better than plant. The cleaner flotation machine (Denver DR500) has an impeller speed of 975 rpm (driven by a 30 kW motor). However, for this particular feed the lab results are better. Thus, it is apparent that hydrodynamic conditions may differ between plant and laboratory flotation cells. It has been shown that pulp turbulence is a function of energy input rather than RPM or impeller tip speed.

Aeration and bubble dispersion is also an important variable, which is influenced by the hydrodynamic conditions of the cell. Schubert and Bischofberger (1998) stated that the precipitation of gas on solid particles for the attachment process is influenced by the aeration rates, bubble size and dispersion.

Based on the importance of aeration rate, the cleaner feed sample was again floated as a function of this variable, using the ESSA cell. The flotation conditions were similar to those for the agitation test. The results are shown in Table 10.0 and Figure 18.0.

Table 10.0: Flotation test conditions and results as a function of aeration rate

Aeration Rates (l/min)	pH	Eh (mV)	Head Grades		Cumulative Concentrate Grade		Cumulative Recovery (%)	
			Cu (%)	Au (g/t)	Cu (%)	Au (g/t)	Cu	Au
10	11.0	246	8.12	8.21	12.71	12.33	94.20	90.38
15	11.0	245	8.69	8.73	13.47	12.92	97.76	93.32
20	11.0	244	8.85	8.48	13.29	12.17	92.46	88.36

Figure 18.0: Copper and gold recoveries as a function of aeration rate

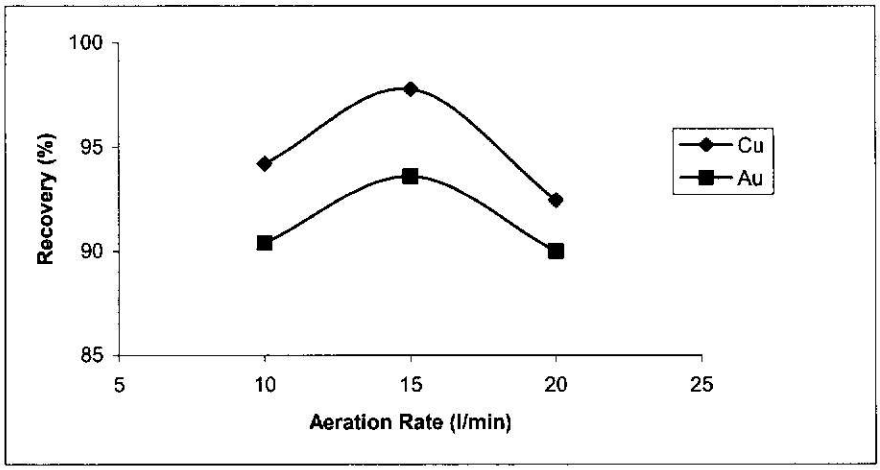

The results show a similar flotation response to the effect of agitation. In both tests (agitation & aeration), the results show an optimum rate. It can be observed from Figure 18.0, that at an optimum aeration rate of 15 l/min, copper and gold recoveries are 97.8% and 93.3%, respectively. When comparing again with the plant results (Table 6.0), it can be observed that copper recovery has improved by 2 percent, while gold appears to show no improvement and the concentrate grade appears to be similar. Possible reasons for the loss in recovery at very high aeration rates include bubble coalescence, bubble collapse and froth instability. It is apparent that for fine particle attachment to bubble surfaces, bubble size must be of the same order of magnitude as the particles so that the probability is greater (Gorain et al. 1995, 1997b; Ahmed & Jameson 1989).

When considering both agitation and aeration, the results appear to show that there is an optimum rate for each which will be a function of cell geometry, particle size and specific gravity, particle hydrophobicity, etc. Recent studies by Gorain et al. (1996) found that at higher agitation speed and low airflow rate, the dispersion of air as fine bubbles was found to be uniform with different flotation machine types. This may provide a starting point for further optimization studies of the cleaner circuit using these parameters.

In conjunction with the laboratory work, a preliminary investigation was conducted in the plant to examine the hydrodynamic conditions of the cleaner cell. The specific objective was to measure the superficial gas velocity (Jg) and gas (ϵ_g) hold up and determine if

these parameters were within specifications. The methodology is also included in section 3.2.8. Figure 19.0 shows the geometrical view of measurements inside the Denver DR500 cell, while Figure 20.0 and 21.0 shows the trends of the superficial gas velocitiy (Jg) and gas hold up (ϵ_g).

Figure 19.0: Geometrical view of the measurement locations inside cleaner cell number one

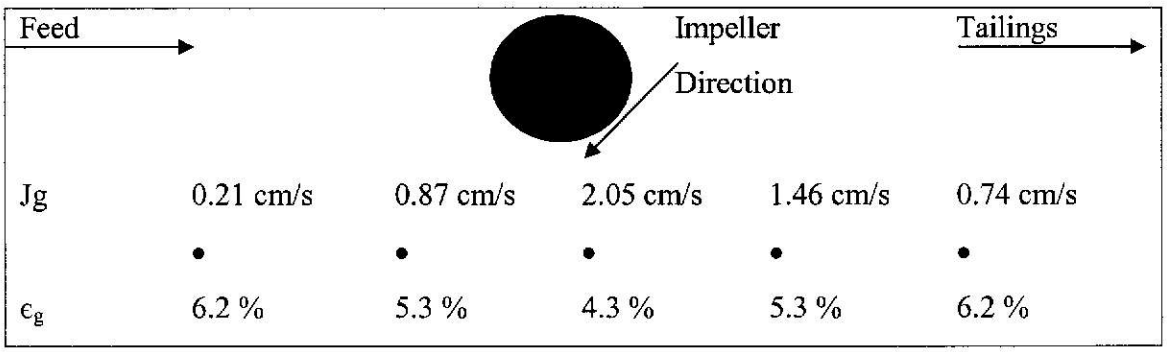

Figure 20.0: Superficial gas velocity (Jg) measurement for cleaner cell number one

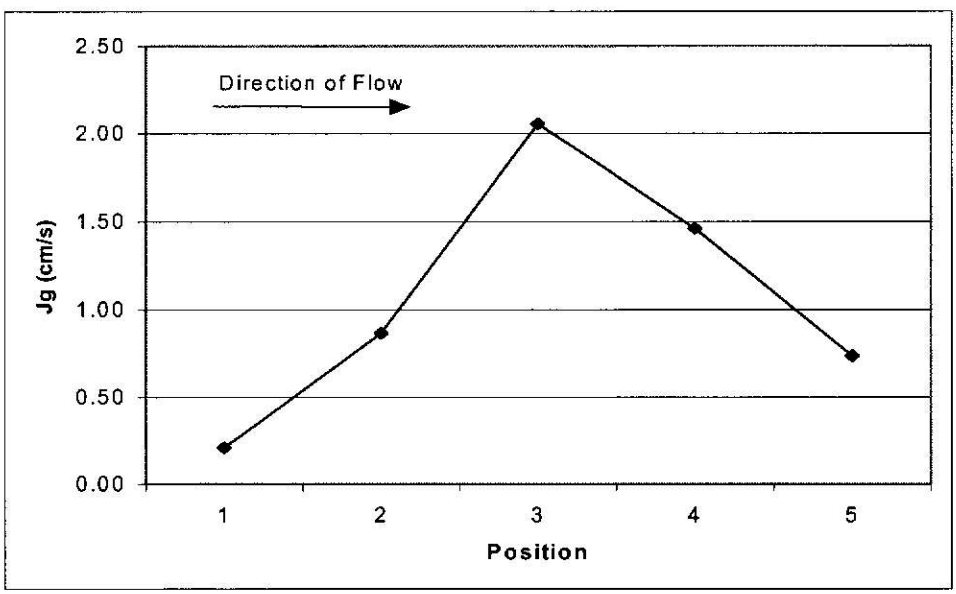

Figure 21.0: Air hold up (ϵ_g) measurement for cleaner cell number one

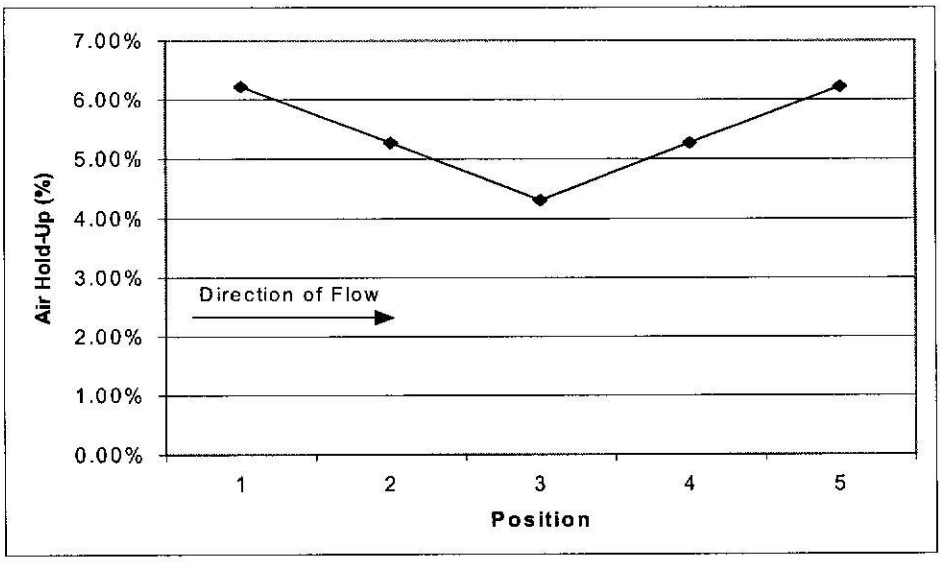

From the above Figures (19.0, 20.0, 21.0), the results show that the superficial gas velocity (J_g) is high and gas hold up (ϵ_g) is low at position number 3, which is closer to the impeller. It can be seen that, the J_g is 2.05 cm/s and the ϵ_g is 4.3%. The results show that as the locations are moved further away from the impeller, a low J_g and a high ϵ_g are shown. Schubert and Bischofberger (1978) stated that the superficial gas velocity at different locations in a flotation cell gives an indication of the air dispersion characteristics. Such results could suggest that there is high air rate for this machine type. It could also suggest a low impeller speed or a worn out impeller and stator condition.

Thus, the results suggest that the dispersion of gas is not uniform in the cell. However, all cells need turbulent zones for bubble attachment and quiescent zones for bubble transportation to the froth zone. Furthermore, the average J_g and ϵ_g for the cleaner cell were calculated and compared with typical operating values (Alexander 2002). It can be seen from Table 11.0 that the measured values are within the operating range. However, further measurements on all the cells are needed to ensure that the overall values are realistically within the typical operating ranges.

Table 11.0: Comparison of average J_g and ϵ_g with typical operating values

Variable	Measured values (Ok Tedi)	Typical range
Superficial velocity	1.06 cm/s	0.8 – 2.0 cm/s
Air hold up	5.5 %	5 – 15 %

4.2.4.4 Effect of Water Quality

Tests were performed to examine the effect of water quality on flotation performance in the cleaner bank. In the plant, process water is re-used because it is advantageous in that it contains residual frother and has a high pH of 10. However, recycle process water for flotation process may affect collector performance, especially when it contains high concentration of dissolved ions. For instance, lime addition to the zinc circuit at the Hilton Concentrator increased the concentration of Ca^{2+} ions in the circuit water and was found to form calcium sulphate which depressed the floatability of galena (Grano et al. 1990).

Before the test was carried out, water samples were characterized using ICP. The results are shown in Table 12.0. The concentrations of anions were not measured due to limitations of the ICP.

Table 12.0: Concentration of major cations in solution

Water Source	Cations (ppm)							
	Cu^{2+}	Fe^{2+}	Ca^{2+}	Mg^{2+}	K^{+}	Na^{+}	Al^{3+}	S
Tap	0.045	0.074	15.81	0.448	0.357	0.373	0.064	203
Process	0.013	0.014	39.3	6.88	0.118	0.01	0.098	167

From this analysis, it is observed that both water sources contain similar cations and their concentrations are relatively low. Therefore it is less likely that the flotation process would be affected by the dissolve ions in the process water. When flotation test was performed with process water, the results (Table 13.0) show that both water sources

produce similar flotation response. Therefore the results reflect that the process water is good quality and it is suitable for plant use.

Table 13.0: Effect of water quality on copper and gold recoveries

Water Type	Head Grade		Cumulative Con Grade		Cumulative Recovery	
	Cu (%)	Au (g/t)	Cu (%)	Au (g/t)	Cu (%)	Au (%)
Tap	8.76	8.95	10.91	10.78	98.3	95.0
Process	8.15	8.01	12.15	11.68	97.7	95.6

4.2.4.5 Effect of Flotation Time

To examine the effect of flotation time, the extended flotation of the cleaner tail was undertaken. The method is shown in section 3.1.3.6. Since the plant results (Table 6.0), show that the cleaner tail contained 1.38% copper and 2.61 g/t gold, a laboratory flotation test was conducted to examine the flotation recovery of the cleaner tailing. Table 14.0 shows the results for 10 minutes flotation and it is apparent that good recoveries and grades were obtained.

Table 14: Copper and gold recoveries as a function of extended flotation time

Total Flotation Time (Min)	Cleaner Tail Grade (Plant)		Cleaner Tail Grade (Laboratory)		Cumulative Concentrate Grade		Cumulative Recovery (%)	
	Cu (%)	Au (g/t)	Cu (%)	Au (g/t)	Cu (%)	Au (g/t)	Cu	Au
10	1.39	2.26	0.652	1.55	4.88	5.64	61.1	43.3

Furthermore, the results show that the extended flotation of the plant cleaner tail resulted in reduced metal content in the tailings. The results suggest that additional flotation time is needed to increase recovery in the cleaner bank under typical operating condition.

In order to translate this laboratory improvement in copper and gold recoveries to the plant, the computer METBAL program was used to simulate the plant effect. The results are shown in Table 15.0. It is apparent that the effect of the lower laboratory cleaner tail grade has resulted in higher copper and gold recoveries. When compared with the original plant results (Table 15.0), an improvement of 2.25% for copper and 2.86% for gold is obtained. These results show that loss of copper and gold in the plant cleaner tailings could be attributed to insufficient residence time.

Table 15.0: Effect of extended flotation of the plant cleaner tail

Plant Results					
Stream	Mass %	Assay		Recovery (%)	
		Cu (%)	Au (g/t)	Cu	Au
Cleaner Feed	100	9.39	10.68	100	100
Cleaner Con	73.59	12.26	13.32	96.12	93.35
Cleaner Tail	26.41	1.38	2.61	3.88	6.65
Simulated Plant Results using the laboratory cleaner tail assay					
Cleaner Feed	100	9.39	10.68	100	100
Cleaner Con	75.44	12.32	13.32	98.37	96.21
Cleaner tail	24.56	0.65	1.55	1.63	3.79
Improvement in recovery of copper and gold				2.25	2.86

In conjunction with the laboratory work, preliminary work was conducted in the plant to determine the residence time in the cleaner circuit. Residence time was measured by applying the salt tracer method as described in section 3.2.7. The method follows the plug flow concept, where the initial concentration of salt is measured at the output of the last cleaner scavenger cell. Figure 22.0 show the results of the sodium concentration as a function of time and the mean residence time is indicated by the peak. The analysis indicates that the mean residence time of the cleaner flotation bank was 12 minutes at a given SAG throughput of 2148 dry tonnes per hour. When this result was compared with the design value of 13.8 minutes for a dry tonnage of 1879 (Gron 2001a), it shows that the residence time has decreased. It is most likely that at a higher SAG throughput and

combined with higher cleaner feed head grades, increased copper and gold losses would occur in the cleaner tail. Both laboratory and plant results indicate that residence time could be an issue, for further work.

Figure 22.0: Concentration of salt tracer showing residence time of cleaner circuit

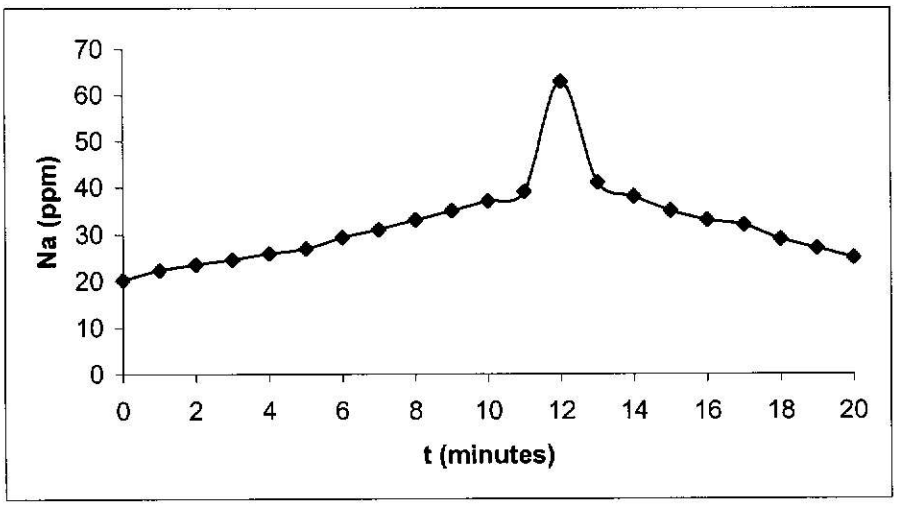

4.2.5 Conclusions and Recommendations

The laboratory flotation tests of the effect of the flotation variables on metallurgical performance indicated potential improvements from optimization of a number of parameters. It was recommended that the addition of lime and collector to the cleaner feed, along with an examination of cleaner residence time.

CHAPTER 5: CLEANER CIRCUIT CHARACTERISATION

5.1 Introduction

Metallurgical performance of the cleaner circuit is variable because of the large range of ore types and blends possible in the Ok Tedi concentrator feed. During the processing of porphyry ore the cleaner circuit is generally operated in open circuit. This means that the cleaner tail is directed to plant final tail when Amdel in-stream analysis (ISA) unit indicates a cleaner tail of less than 2% Cu. However, as the proportion of skarn ore in the ore blend increases (> 20%), the cleaner tail assay will at times exceeds 2% Cu and the cleaner circuit is then operated in closed circuit mode, with the cleaner tail recycled to the head of the rougher circuit. In general, as the mass percent of copper and gold in the cleaner tail increases, copper and gold losses from the plant increases also. Monthly recovery from May 1999 to January 2001, indicates that 26% of the copper and 34% of the gold entering the concentrator was lost to the final tails on average (Figures 23.0 and 24.0).

Figure 23.0: Copper losses in Unit 1 rougher (RGH) and cleaner (CLN) flotation circuit

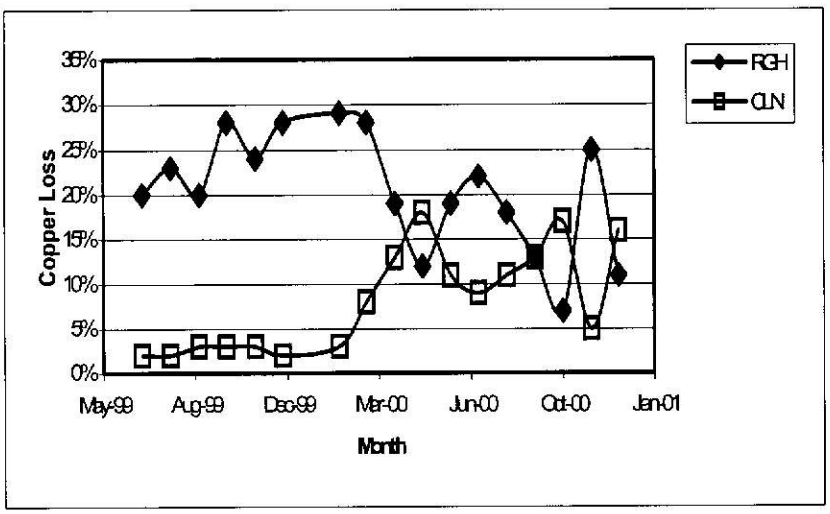

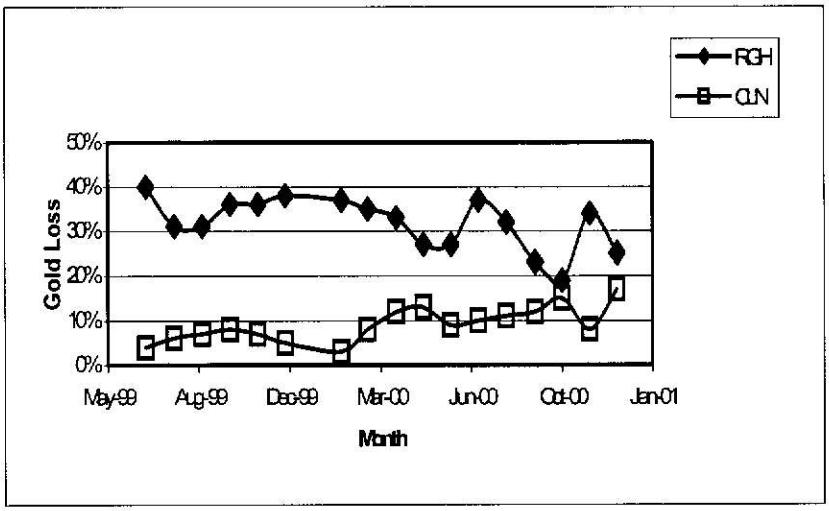

Figure 24.0: Gold losses in Unit 1 rougher (RGH) and Cleaner (CLN) flotation circuit

It may be noted that previous studies on mineralogical and pulp chemical aspects of Ok Tedi Flotation pulps have provided evidence which suggests that the major problems of different ore blends largely differ in degree rather than the type of problem encountered (Morey & Grano 2000; JKTech 2001).

These previous studies and the production trends shown in Figures 23.0 and 24.0 provided the justification for carrying out characterization studies of the cleaner circuit as a function of a 'good' feed and a 'bad' feed blend. The objective was to determine the pulp chemical reasons that could contribute to the loss of copper and gold in the cleaner tail.

This chapter discusses the results of the cleaner circuit characterization studies, as conducted for the 'good' and 'bad' feed blend.

5.2 Cleaner Circuit Studies as a Function of 'Good' Feed Blend

A series of 'snap shot' surveys were carried out on Unit 2 cleaner flotation circuit as a function of 'good' feed. The objective was to chemically characterize particle samples and pulps collected during the surveys via particle surface analysis by ToFSIMS, particle surface chemical and bulk chemical analysis by the EDTA extraction and size by size kinetic analysis. Analysis was also performed for chemical pulp parameters (pH, Eh & DO) during the surveys.

5.2.1 Ore Feed Blend Description

Two surveys were performed at different times when the concentrator was treating a high proportion of porphyry ore in the plant feed. The descriptions of the ore blends are showed in Table 16.0. The feed blends contained 94% porphyry ore and 6% pyrite skarn ore in both ores. Such porphyry ore feeds are known to give good grade and recovery in flotation. They may be classified as a 'good' ore feed blend.

Table 16.0: Plant feed blend condition, showing percentage of different ore proportion

Survey #	Period	Ore Blend Condition	% Proportion in Feed Blend	Feed Grade % Cu	g/t Au
1	02/08/01	Pyrite Skarn / Porphyry	6/94	0.85	1.08
2	23/08/01	Pyrite Skarn / Porphyry	6/94	0.91	0.60

There are two types of porphyry ore at Ok Tedi. They are classified as monzonite and monzodiorite, accordingly to feldspar mineral proportions. The proportions can be observed from a recent QEM*SEM analysis by CSIRO Minerals (Jenkins & Adair 1996b), as shown in Table 17.0. From the QEM * SEM analysis of this particular sample, it was observed that monzonite sulphide was richer in copper sulphides than monzodiorite sulphide. The analysis appeared to show that chalcopyrite was the major copper sulphide mineral for monzodiorite ore, while the richer secondary copper sulphide minerals were found with chalcopyrite in the monzonite ore. In regard to gangue minerals, it was also

evident that monzodiorite sulphide contained more goethite, hematite, silicates, quartz and apatite than monzonite. The presence of these minerals may indicate that the Monzodiorite sample was closer to the surface of the orebody. However, mineralization may differ when mining increases deeper into the ore deposits. In general, both sulphides were rich in feldspars. Monzonite ore was predominantly K- feldspar whilst monzodiorite predominantly (Na/Ca)- feldspar.

Table 17.0: QEM *SEM analysis, showing proportions of the main mineral phases & groupings for porphyry sulphides (Jenkins & Adair 1996b)

Mineral Weight %	New Rougher Feed			
	-212+150 µm	-150+75 µm	-75+31 µm	-31+13 µm
Chacocite/Degenite	0.06	0.27	0.28	0.24
Covellite	0.01	0.04	0.06	0.11
Bornite/Fe-Degenite	0.16	0.33	0.30	0.18
Chalcopyrite	1.20	1.85	1.66	1.07
Cu_Metal	0.03	0.00	0.00	0.00
Cu_Ox (Cuprite)	0.00	0.00	0.00	0.00
CuFe_Metal/Ox	0.00	0.02	0.01	0.00
Cu_CO_3(Malachite)	0.02	0.00	0.01	0.00
CuFe_Ox/CO_3	0.03	0.06	0.06	0.09
Cu_Silicates(chrys)	0.00	0.00	0.00	0.00
Cu_Phosphates(Turq)	0.00	0.00	0.00	0.00
Other_Cu_Minerals	0.06	0.07	0.09	0.08
Fe_Sulphides	1.67	3.75	3.84	3.30
Mg_Silicates	1.07	1.00	1.09	1.44
(Na/Ca)_Feldspars	23.12	21.19	18.75	16.03
K_Feldspars	36.68	31.77	35.66	44.24
Mica	3.45	3.37	4.82	5.39
Quartz	15.74	14.45	11.46	9.79
Ca_Fe_Silicates	3.23	3.20	3.18	2.87
Fe_Ox/CO_3(Hematite)	3.43	7.81	7.12	1.90
Fe_Ox/CO_3(Goethite)	4.53	5.55	6.70	7.92
Apatite	0.62	0.69	0.53	0.43
Others	4.88	4.57	4.41	4.91
Total	100.00	100.00	100.00	100.00

5.2.2 Cleaner Circuit Flotation Performance

The assays of the surveys were data-smoothed using the computer MATBAL program (Wiseman 1997). The objective was to assess the cleaner flotation performance. The results are shown in Table 18.0 with the data included in the appendix (section 2.1.10).

Table18.0: Cleaner flotation metallurgical performance as a function of 'good' feed blend

Survey Period	Feed Assay		Tail Assay		Cumulative Con Grade		Cumulative Recovery (%)	
	Cu (%)	Au (g/t)	Cu (%)	Au (g/t)	Cu (%)	Au (g/t)	Cu	Au
02/08/01	7.11	4.29	0.53	0.81	19.4	10.6	95.14	87.85
23/08/01	2.74	3.74	0.25	0.33	15.0	10.0	92.42	94.29
Average	4.93	4.01	0.39	0.57	17.2	10.3	93.78	91.07

These results show that the performance of the cleaner circuit was reasonable with relatively low values of copper and gold in the cleaner tail and concentrate grades and recoveries within acceptable metallurgical ranges. Plant flotation results were compared with parallel laboratory flotation results from the same feed (Table 19.0). A reasonable correlation was observed. The laboratory flotation tests involved floating the plant cleaner feed pulp during the survey. It is apparent that the laboratory results are slightly better than those for the plant. However, the results reflect that even with a 'good' feed blend, there are still losses to be accounted for, particularly for gold.

Characterisation work was undertaken to characterize particle surface and pulp variables that could affect the flotation performance. Results are presented in the following sections.

Table 19.0: Laboratory cleaner flotation recoveries and grades as a function of 'good' feed blend

Survey Period	Feed Assay		Tail Assay		Cumulative Con Grade		Cumulative Recovery (%)	
	Cu (%)	Au (g/t)	Cu (%)	Au (g/t)	Cu (%)	Au (g/t)	Cu	Au
02/08/01	7.13	4.24	0.311	0.76	19.13	10.48	96.12	88.50
23/08/01	2.74	3.26	0.265	0.380	15.85	11.59	95.08	94.10
Average	4.94	3.75	0.288	0.57	17.49	11.04	95.6	91.30

5.2.3 Size by Size Recovery Analysis

Size by size recovery analysis for copper and gold was conducted on survey samples to examine the flotation response as a function of particle size. Figures 25.0 and 26.0 show low recoveries at the two extremes of the particle size ranges. That is, copper and gold recoveries were reduced for particle sizes above 75 μm and below 22 μm. However, 95 to 98% recovery for copper and gold was obtained for the immediate size ranges. Similar results were shown previously by Met Engineers (1999) from their mineral deportment assessment of the Ok Tedi cleaner circuit. The report stated that the recovery of chalcopyrite and chalcocite were 95% and 98%, respectively, in the 20-80 μm size range.

Figure 25.0: Size by Size copper and gold recoveries (survey on 02/08/01)

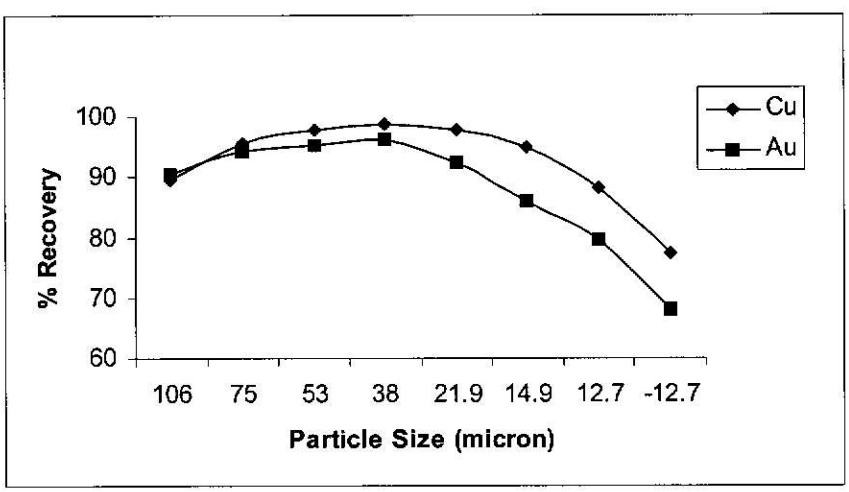

Figure 26.0: Size by Size copper and gold recoveries (survey on 23/08/01)

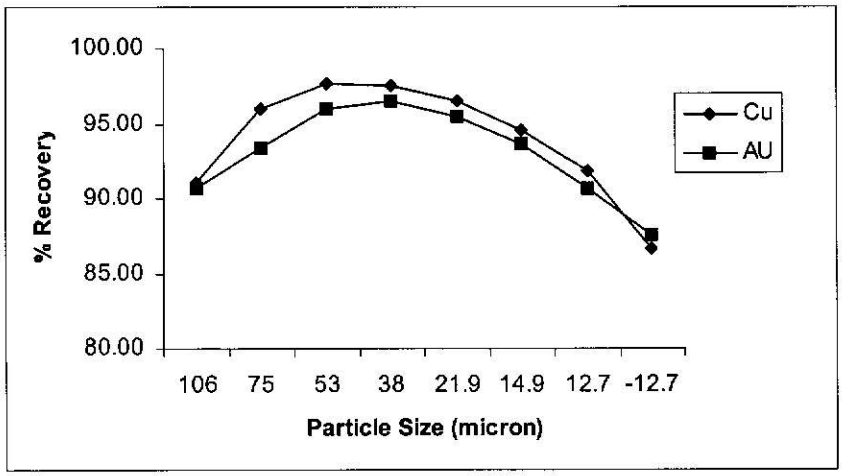

Further, size by size copper and gold recoveries were compared with size by size kinetic analysis (Figures 27.0 and 28.0). The flotation rate constants were calculated from size by size recoveries and residence time of the cleaner circuit using the recovery equation [$R = R_{max}$ [1 - exp (-k t)], which assumes first order kinetic behaviour (Lynch et al. 1981). The residence time of the cleaner bank was determined by using a tracer method, as described in section 3.2.7. The data is shown in the appendix (section 1.1 & 1.2) and, includes residence times for the 'bad' feed surveys.

Figure 27.0: Flotation rate constants as a function of particle size (survey on 23/08/01)

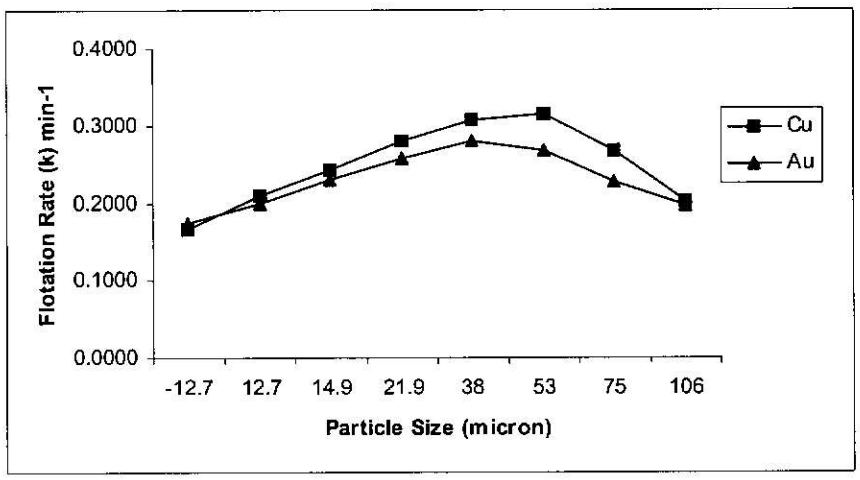

Figure 28.0: Flotation rate constants as function of particle size (survey on 02/08/01)

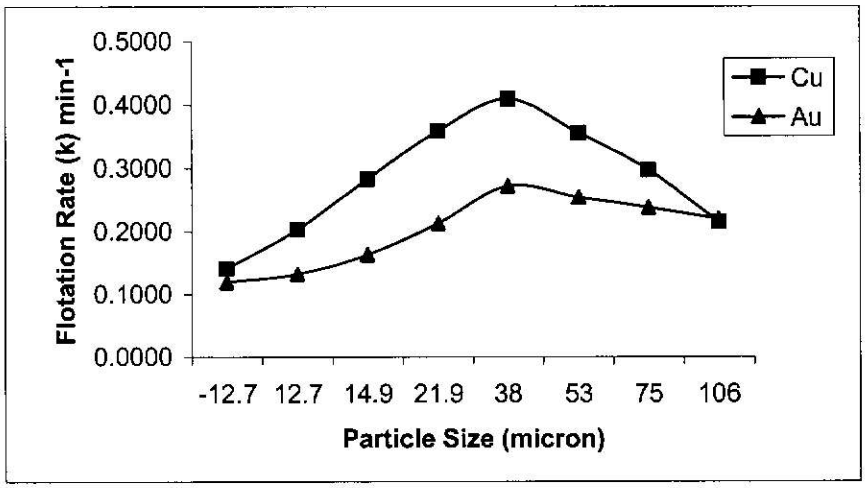

The calculated results show high flotation rate constants at the intermediate size ranges (22-75 μm), suggesting that maximum copper and gold recoveries are achievable in the cleaner circuit at these size ranges. It is also observed that lower flotation rate constants were associated with coarse (> 75 μm) and fine (< 22 μm) particle sizes. It is suspected that the loss of coarse particles is most likely related to lack of liberation whilst the loss of fine particles may be due to the low probability of bubble- particle collision. In summary, the results show that cleaner flotation performance is greatly influenced by particle size.

5.2.4 Pulp Solution Analysis

As part of the cleaner circuit characterization studies, measurements were taken of the pulp parameters; Eh, pH and DO. These measurements were performed at the same time as the circuit survey was conducted, following the methodology described in section 3.2.2. The specific objective was to establish the optimum pulp chemical conditions in the cleaner flotation circuit for sulphide mineral flotation.

The dissolved oxygen concentration data was used to produce the dissolve oxygen demand curves shown in Figures 29.0 and 30.0, with results shown for the two 'good' feed surveys. The dissolved oxygen (DO) is expressed as a percentage of saturation. The pulp parameters are plotted as a function of time to indicate oxygen consumption along the circuit. The following Figures (31a, 31b, 31c and 32a, 32b, 32c) show details for the related pulp chemical parameters, which were measured simultaneously. During the survey of pulp solution analysis, it was observed that the pH was steady at 10.0, whilst Eh and DO were varying. The pulp potential measurements have been converted to the standard hydrogen electrode (SHE) scale by the addition of 199 mV.

Figure 29.0: Oxygen demand curves for 'good' feed blend (survey on 02/08/01)

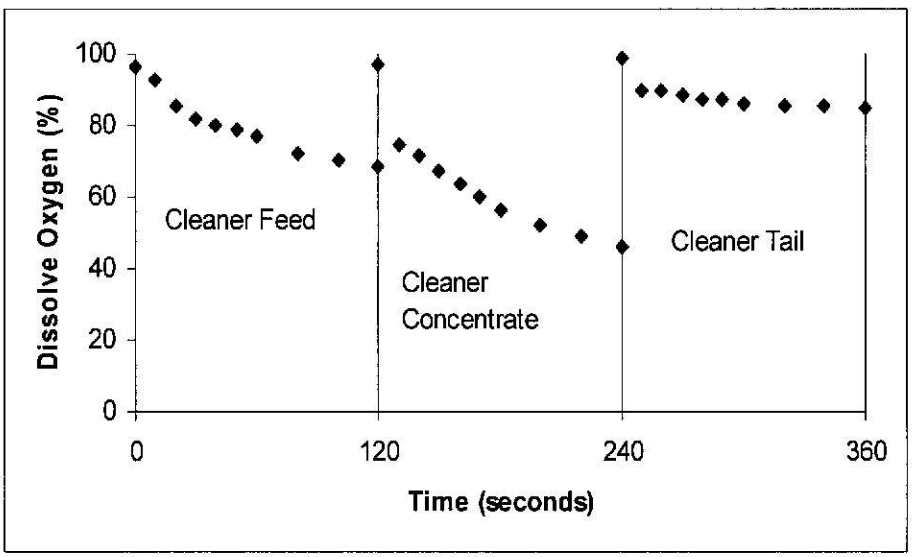

Figure 30.0: Oxygen demand curves for 'good' feed blend (survey on 23/08/01)

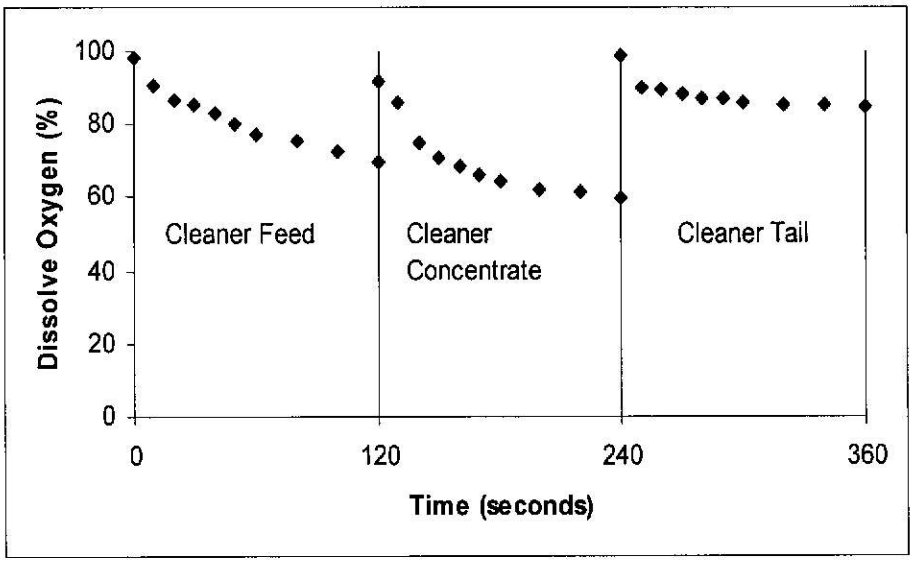

Figure 31a: Eh and DO analysis for cleaner feed stream (survey on 02/08/01)

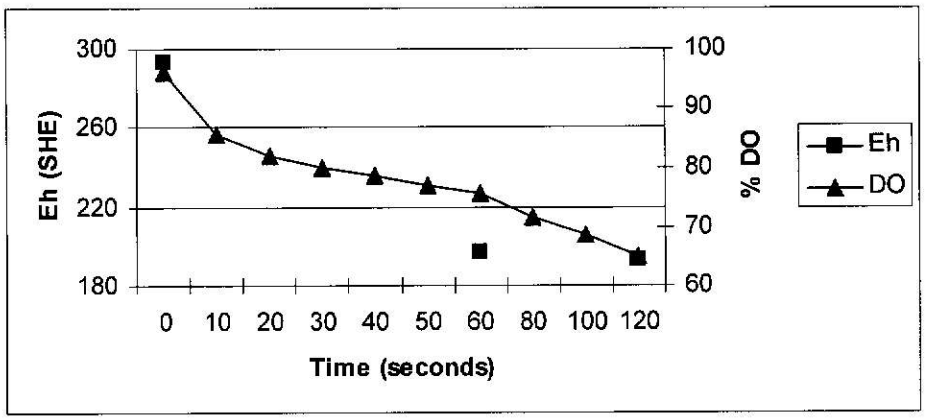

Figure 31b: Eh and DO analysis for cleaner tail stream (survey on 02/08/01)

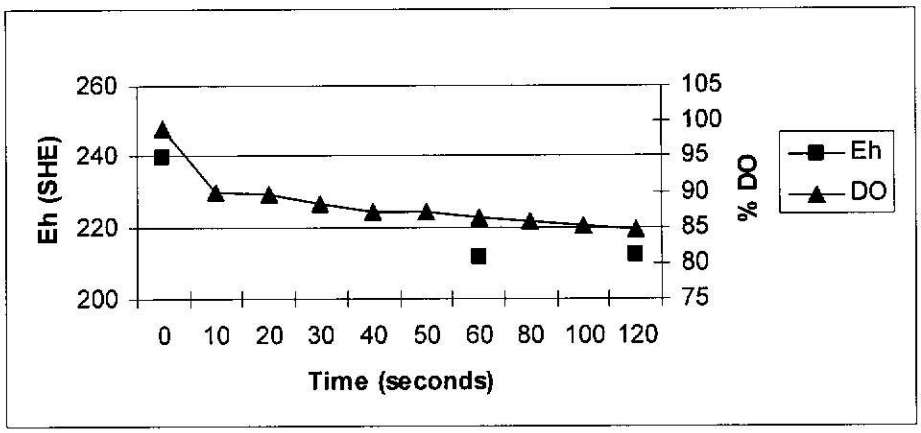

Figure 31c: Eh and DO analysis for cleaner concentrate stream (survey on 02/08/01)

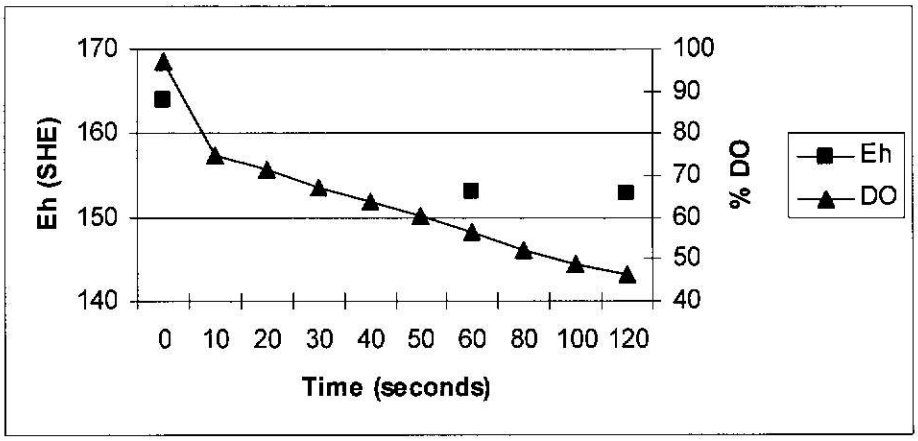

Figure 32a: Eh and DO analysis for cleaner feed stream (survey on 23/08/01)

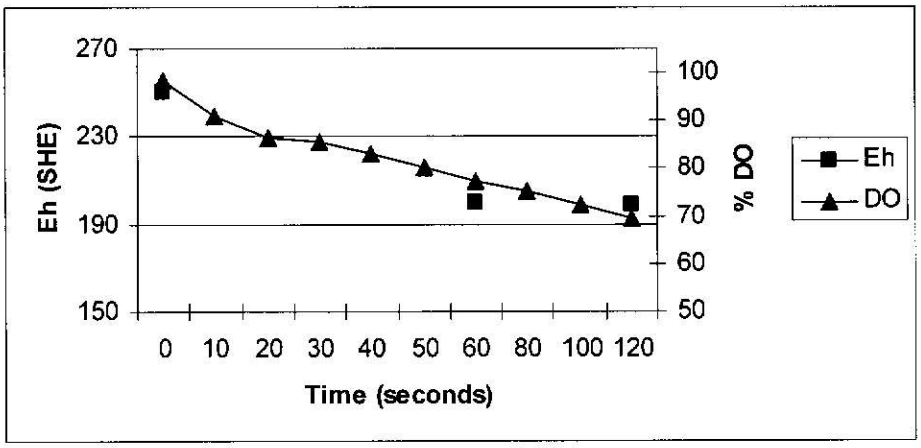

Figure 32b: Eh and DO analysis for cleaner tail stream (survey on 23/08/01)

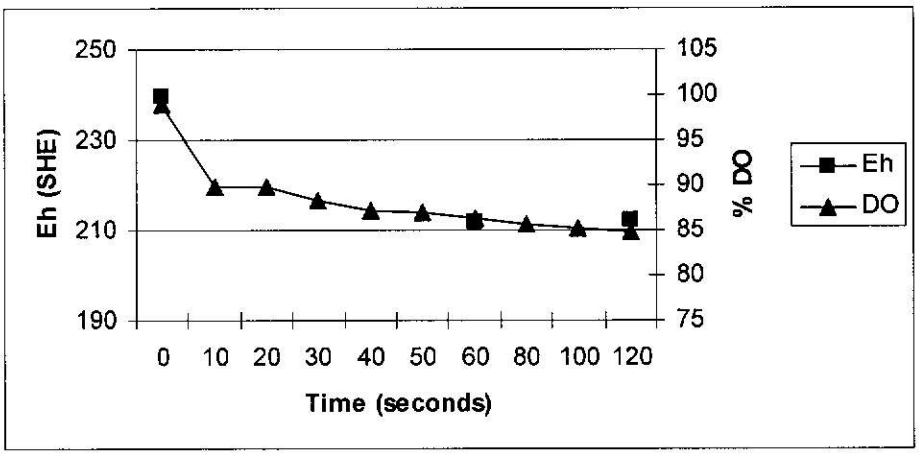

Figure 32c: Eh and DO analysis for clean concentrate stream (survey on 23/02/01)

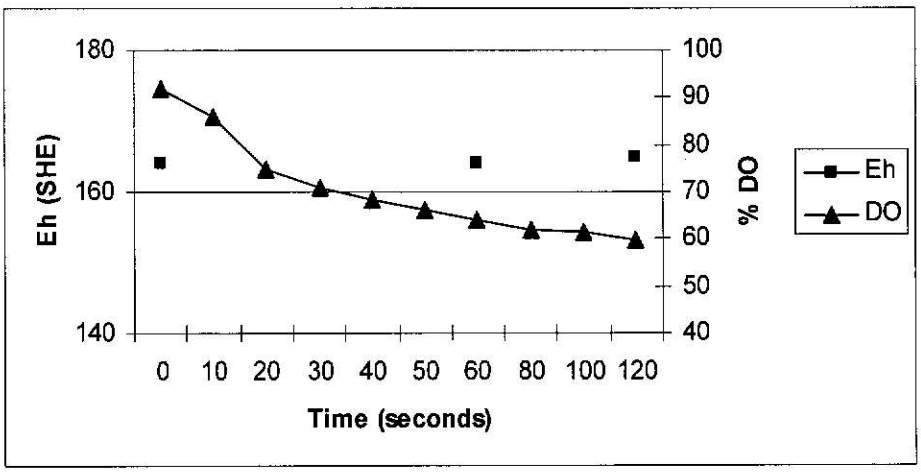

In order to understand the effect of the changing pulp dissolved oxygen with respect to floatability of the particles, a comparison was made with previous results for Ok Tedi mill water only. It has been observed that mill water trends from 100% to 80% saturation (Morey & Grano 2000). It is apparent that this trend correlates with the natural de-oxygenation of quiescent water. These authors stated that any stream which consumes dissolve oxygen at a significantly greater rate than this has a high dissolved oxygen demand. Mineral sulphide particles in the stream would therefore be oxidizing (consuming oxygen). That means the particles would be both reactive and developing oxide coatings. Based on this benchmark, it can be observed from Figures 29.0 and 30.0 that the cleaner feed and concentrate show relatively fresh particle surfaces still undergoing oxidation while the cleaner tail was oxidized or passivated. The interpretation of the comparison is that the concentrate and feed streams are not passivated. That means sulphide particle surfaces are not fully coated with either oxide or fully coated with collector and oxidation is still occurring. Under such conditions, it is possible that the concentrate particles may possibly adsorb more collector and become more hydrophobic, with a higher flotation rate constant. In contrast, the cleaner tail appears passivated, indicating that the particles are covered with oxide layers.

From Figures 31a, 31b, 31c and 32a, 32b, 32c, it is apparent that the Eh of the cleaner feed and concentrate streams varies with the dissolve oxygen concentration, indicating that the pulp potential in the plant is depended on the pulp oxygen concentration. The feed stream showed initial pulp potentials, in the range for electrochemical collector adsorption

to sulphide minerals and optimum flotation and the passivated stream (tail) shows relatively high pulp potentials. The more reactive cleaner concentrate stream showed lower potential than the other two.

In order to form a reasonable understanding of the pulp chemical conditions at Ok Tedi, a comparison was made with an Eh/pH diagram (Figure 33.0), which has recently been developed from measurements taken in the Ok Tedi grinding and flotation circuit (Morey & Grano 2000). Since the current low grade regrind ball mills have the same grinding media (high chromium) as the ball mills in circuit module number 2, it is expected that the cleaner feed stream could show similar conditions. Figure 33.0 shows the Eh/pH diagram for some selected streams, as well as the oxygen/water line. The diagram also includes mineral speciation and a black dotted line which shows the approximate thermodynamic equilibrium for the hydrophobic entity, CuX.

Figure 33.0: Eh/pH diagram for ball mill discharge and rougher feed pulp

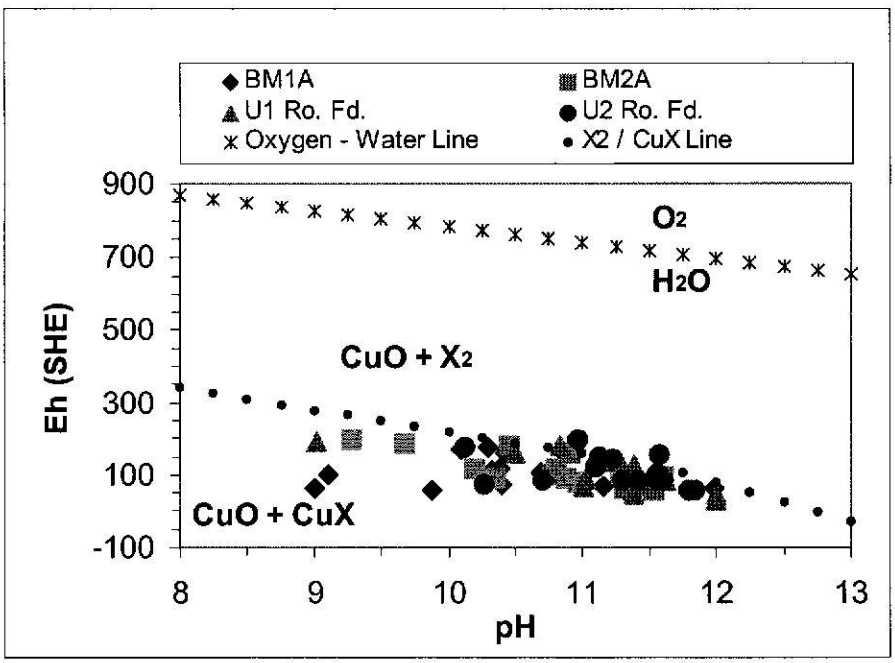

The symbols in the diagram represent the following things;

BM1A - Ball mill (a) on Unit 1 grinding circuit

BM2A - Ball mill (b) on Unit 2 grinding circuit

U1 Ro. Fd. - Unit 1 rougher feed stream

U2 Ro. Fd. - Unit 2 rougher feed stream

2X/CuX - Hydrophobic species

When comparing the pulp potentials for the cleaner feed stream (Figure 31a and 32a) with Figure 33.0, it can be seen that the cleaner feed stream falls close to equilibrium line, which follows the trend for the rougher feed stream on Unit 2 (U2). This suggests that the pulp potentials and dissolved oxygen are within the optimum range for chalcopyrite flotation.

In regard to the chemical changes occurring at the optimum Eh range, a study by Ralston (1991) highlighted these chemical changes, using chalcopyrite as a single mineral and xanthate as a collector. The author suggested that the formation of copper xanthate with a single chalcopyrite mineral is attributed to the following reaction;

$$CuFeS_2 + X^- \Leftrightarrow CuX + FeS_2 + e^- \qquad E° = -0.096\ V \qquad (19)$$

Ralston found that when xanthate was used the maximum recovery of chalcopyrite occurred at 200 mV. However, when the potential was increased further than 200 mV, the recovery decreased. The decrease in recovery was found to be attributed to the decomposition of the Cu (I) – xanthate complex by the following reaction;

$$2CuX + 4H_2O \Leftrightarrow 2HCuO_2 + X_2 + 6H^+ + 4e^- \qquad E° = -1.402\ V \qquad (20)$$

Although the potential for xanthate decomposition does not apply to other collectors, such as DTP (S-7249) used at OK Tedi, similar electrochemical potentials are apparent for adsorption of other collectors because the dominant potential required in each case is the potential for chalcopyrite oxidation.

5.2.5 Particle Surface Chemical Analysis

Comparative particle surface chemical analysis of cleaner streams was conducted as part of the cleaner circuit characterization. The specific focus of this work was to compare the solution chemistry of the cleaner circuit tail and concentrate streams and to correlate the flotation characteristics with the surface chemical characteristic shown by the time of flight secondary ion mass spectrometry (ToFSIMS) results and EDTA Analysis. Following the method as described in section 3.1.4, EDTA extractions were performed to determine the state of oxidation of minerals in the pulp. The results would indicate whether particles in the cleaner tail were more oxidised than those in the cleaner concentrate.

The calculations for EDTA extraction analysis were completed for copper, iron, calcium and sulphur for cleaner feed, tail and concentrate streams, using the same formula as given in section 4.2.2.2. The results for the two surveys are shown in Tables 20.0 and 21.0.

Table 20.0: EDTA extractable metal ions as percentage of element in solids analysis ('Good' feed survey on 02/08/01)

Stream	% Cu	% Fe	% S	% Ca
Cleaner feed	0.144	0.370	0.039	84.83
Cleaner concentrate	0.052	0.374	0.010	55.04
Cleaner tail	1.593	1.767	0.238	87.08

Table 21.0: EDTA extractable metal ions as percentage of element in solids analysis ('Good' feed survey on 23/08/01)

Stream	% Cu	% Fe	% S	% Ca
Cleaner feed	0.159	1.54	0.153	47.09
Cleaner concentrate	0.012	0.41	0.005	39.62
Cleaner tail	1.22	3.63	0.543	51.80

The immediate conclusion drawn from these results is that the cleaner tail stream contains a higher relative concentration of EDTA extractable ions, suggesting that the cleaner tail

stream is passivated and the particles are covered with an oxide layer or more slimes. When compared with the oxygen demand curves (Figures 29.0 and 30.0), a reasonable correlation is observed, i.e., the low oxygen demand of the tail stream could be related to the presence of oxides on the particle surface. It is apparent that the oxide covered particles would be depressed and report to the tailings whilst the less oxide covered minerals, i.e., particles in the concentrate stream with low concentration of EDTA extractable ions would be recovered.

Comparison of the EDTA results with ToFSIMS results (Figures 34.0-36.0, see pages 109-111), shows that there is a greater coverage of chalcopyrite with hydrophilic species (O, OH), with the tailing compared to concentrate, suggesting that surface oxidation of chalcopyrite particles resulted in decreased hydrophobicity, low flotation rate constant and depression. Morey and Grano (2000) conducted pulp chemical studies of different feed blends from skarn and porphyry ores and reported similar results. A study by Senior and Trahar (1991), also suggested that the floatability of chalcopyrite was affected by the presence of hydroxides on the surface. These studies suggest that the floatability of chalcopyrite is reduced by the presence of hydrophilic oxy and hydroxy species on the particle surfaces.

In addition, results from EDTA and ToFSIMS (Figure 34.0), indicates that chalcopyrite coverage with calcium in the cleaner tail is considerably higher than the concentrate. This suggests that the floatability of chalcopyrite is also depressed by calcium slimes (possibly lime or gypsum). Morey and Grano (2000) suggested that the adsorption of calcium precipitates on the chalcopyrite surface might have resulted from gypsum precipitation after Ca from lime reacted with SO_4^{2-} from sulphide oxidation, as indicated by Equations 21 to 23.

$$CuFeS_2 + 4O_2 \Rightarrow CuSO_4 + FeSO_4 \quad (21.0)$$

$$CuSO_4 + Ca(OH)_2 \Rightarrow Cu(OH)_2 + CaSO_4 \quad (22.0)$$

$$FeSO_4 + Ca(OH)_2 \Rightarrow Fe(OH)_2 + CaSO_4 \quad (23.0)$$

Although the high level of calcium is intended for pH of 11.5 for optimum copper flotation and also pyrite depression, it may also indiscriminately adsorb on chalcopyrite. A

recent study on the effect of calcium ions and citric acid on the flotation separation of chalcopyrite from galena using dextrin also found that calcium ion adsorbed preferably on chalcopyrite surface and not galena (Liu & Zhang 2000). These studies suggest that calcium ion adsorbs onto chalcopyrite surface and it is a topic that needs further study.

In summary, the results show that oxidation is taking place in the pulp with oxide coated particles being transported to the cleaner tail stream due to a lower hydrophobicity. Results produced from ToF-SIMS confirm the coverage of chalcopyrite with hydrophilic oxy and hydroxyl species and also with calcium. In conclusion, oxidation and slimes precipitation has been found to be a factor that affects the floatability of copper in Ok Tedi flotation pulp.

5.2.6 Particle Surface Analysis by ToFSIMS

As part of the cleaner pulp characterization, particle surface analysis was performed by the Ian Wark Research Institute (IWRI) using ToF-SIMS (time of flight secondary ion mass spectrometry). ToF-SIMS is a highly surface specific analytical technique (to a couple of atomic layers). It can determine atomic and molecular species on the particle surfaces, although it cannot determine their oxidation state (Piantadosi & Smart 2002; Boulton et al. 2003; Smart et al. 2000; Cecile 1985). The measurements were done using a PHI model TRIFT 2100 spectrometer equipped with Ga liquid metal ion gun. This allows spectroscopy for characterisation of chemical composition and imaging for mass spectra to be taken from the pre-selected areas. The measurements and analysis were performed accordingly to the standard procedure (Jasieniak 2003).

The specific focus of the study was to determine if there were differences in the surface chemistry of pyrite and chalcopyrite particles in cleaner concentrate & tails samples and to correlate results with the surface characteristics as suggested from the pulp solution analysis. Cleaner tail and concentrate samples from cleaner cell 1 were selected from the survey conducted on the 23/08/01 for examination.

About 45 pyrite and 42 chalcopyrite particles were examined and the data statistically analysed. The ToF- SIMS statistical data for the concentrate and tail are shown in Figures 34.0 - 36.0. In Figures 34.0 and 35.0, error bars are provided to give an indication of 95% confidence. Where error bars for the same element do not overlap for concentrate and tail, then there is a genuine difference. Intensities are also normalized relative to a mineral substrate, indicating that intensities of chalcopyrite can be compared between samples. The actual values of surface intensities for each species examined are given in the Table below the bar graphs. Figure 36.0 shows the 'overall hydrophobicity index', which is a ratio of averaged, normalized intensities for predominant hydrophobic species (PO and S, but not sulphate) relative to averaged normalized intensities for predominant hydrophilic species (O and OH). Figure 36.0 also shows the collector 'exposure' or surface concentration. It is noted that the hydrophobicity index is a tool developed at the IWRI and has been found to be useful to describe the behaviour of recovery of particles by flotation (Morey & Grano 2000).

Interpretation of data has been based on comparison of the ToF-SIMS normalized intensities. Figure 35.0 (pyrite) indicates that the normalized intensity for copper on pyrite in the concentrate is 6.4 times greater than for Cu on pyrite in the tailing, suggesting that the copper ions have adsorbed onto pyrite surfaces, causing activation. From Figure 34.0 (chalcopyrite), it can be seen that the intensity of the 'PO' species (collector) on chalcopyrite are less in the tailing and greater on the concentrate, suggesting that the loss of chalcopyrite in the tail could be associated with low hydrophobicity level. Based on the same Figure (pyrite), a similar trend is observed for pyrite, which suggests that some copper had become adsorbed onto pyrite and interacted with the dithio phosphate collector (S-7249). It should be noted that the intensity of 'CH' is not related to collector and is identified as adventious carbon. The source of carbon is believed to be the natural air surrounding the analytical measurement (Morey & Grano 2000).

It has been mentioned above that the presence of copper ions on the pyrite surface could be the catalyst for the adsorption of collector onto the pyrite. Recent studies have found the presence of Cu (II) and Cu (I) on the surface of pyrite. The presence of Cu (I) indicated that copper was adsorbed as Cu-S surface species (Boulton et al, 2003; Weisener & Gerson 2000a; Voigt et al.1994; Smart 1991). Furthermore, it was reported

that the change in zeta potential of the negatively charged pyrite from adsorption of Cu $(OH)_2$, may also contribute to the adsorption mechanism (Zhang et al. 1997). The work of Weisener and Gerson (2000b) suggests that electrochemical adsorption of collector onto CuS may be possible on pyrite surfaces, enhancing pyrite hydrophobocity.

On the other hand, the formation of hydrophilic species in the flotation pulp has been found to affect the floatability of sulphide minerals (Shannon & Trahar 1986; Senior & Trahar 1991; Guy & Trahar 1985). Similar phenomenon is likely in Ok Tedi flotation process. Figure 34.0 provides some evidence to support the proportion. A comparison of ToFSIMS normalized intensities for O and OH species from Figure 34.0 (chalcopyrite), shows higher exposure on chalcopyrite in the cleaner tail than in the cleaner concentrate. There is also high exposure of O and OH on pyrite surface. The presence of these hydrophilic species on sulphide mineral surfaces correlates with the transport of value minerals to tailings.

In order to explain the flotation behaviour of chalcopyrite and pyrite, the hydrophobic /hydrophilic index was derived from the spectral data and is shown by Figure 36.0. It is observed that hydrophobic index for chalcopyrite in the cleaner tail was 0.29, compared to 0.48 in the cleaner concentrate. Although the indices are quite high, the collector exposure on the chalcopyrite is significantly low, i.e., about 0.002 is observed for chalcopyrite in the cleaner concentrate and 0.0001 is observed for chalcopyrite in the cleaner tail. This suggests that the presence of the hydrophilic species on particle surfaces may have limited collector adsorption. Consequently, the hydrophobicity of chalcopyrite was reduced. This may have contributed to the loss of chalcopyrite in the cleaner tail. Furthermore, there is 2 times more calcium exposure on the chalcopyrite in the cleaner tail, suggesting that the chalcopyrite is also depressed by precipitation of insoluble calcium salts on its surface. Similar hydrophilic species were found on the chalcopyrite in the tailings for Ok Tedi ore systems by Piantadosi et al. (2001).

From these studies, it can be concluded that the coverage of chalcopyrite by hydrophilic species (O, OH) and calcium salts, along with decreased collector coverage are most likely to be responsible for the loss of liberated chalcopyrite to the cleaner tail. The

presence of higher copper concentrations on pyrite in the cleaner concentrate indicates activation to be the mechanism responsible for the flotation of pyrite.

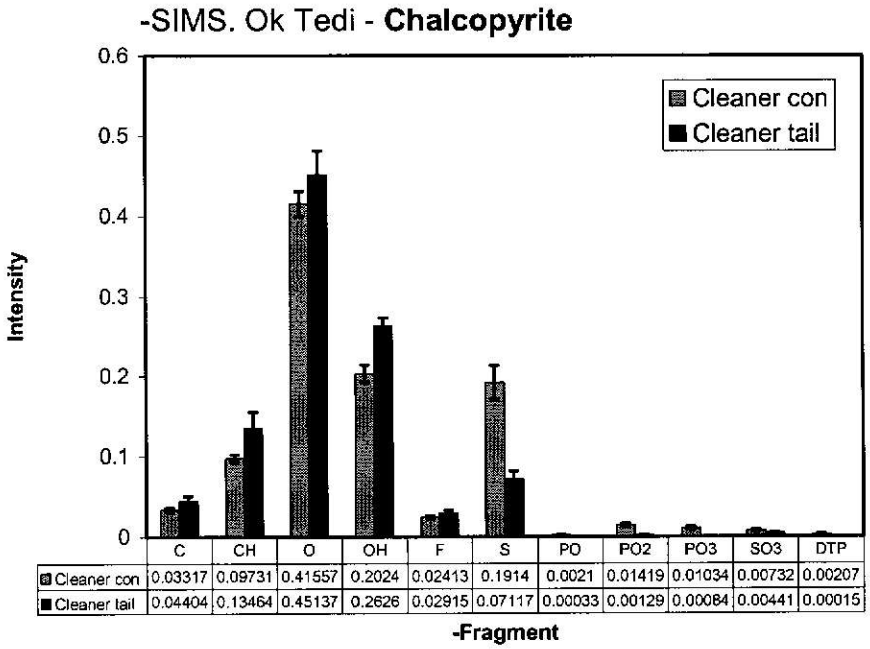

	C	CH	O	OH	F	S	PO	PO2	PO3	SO3	DTP
Cleaner con	0.03317	0.09731	0.41557	0.2024	0.02413	0.1914	0.0021	0.01419	0.01034	0.00732	0.00207
Cleaner tail	0.04404	0.13464	0.45137	0.2626	0.02915	0.07117	0.00033	0.00129	0.00084	0.00441	0.00015

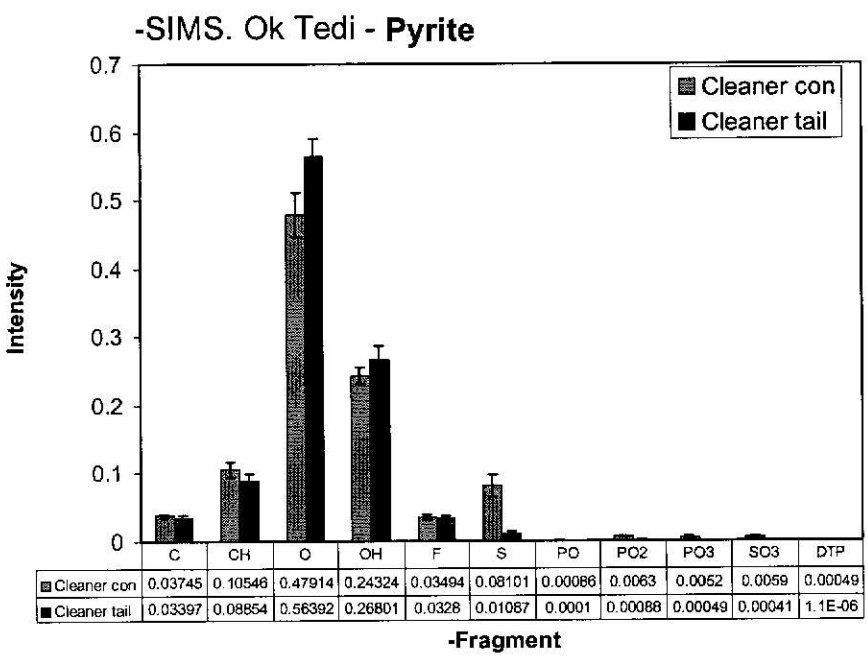

	C	CH	O	OH	F	S	PO	PO2	PO3	SO3	DTP
Cleaner con	0.03745	0.10546	0.47914	0.24324	0.03494	0.08101	0.00086	0.0063	0.0052	0.0059	0.00049
Cleaner tail	0.03397	0.08854	0.56392	0.26801	0.0328	0.01087	0.0001	0.00088	0.00049	0.00041	1.1E-06

Figure 34.0: (+) SIMS. Shows mass spectra for chalcopyrite and pyrite particles in the cleaner con and cleaner tail (confidence intervals calculated for P=95%).

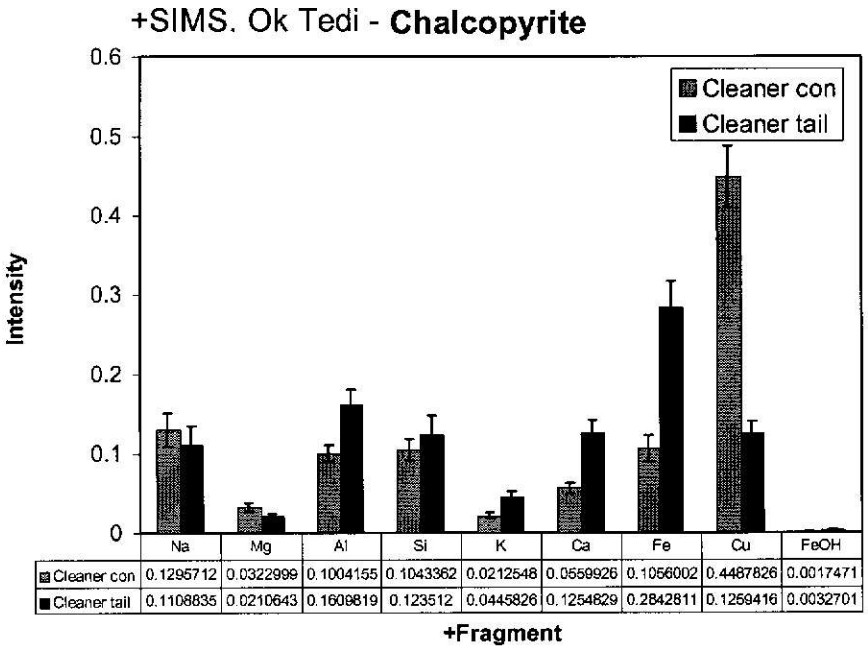

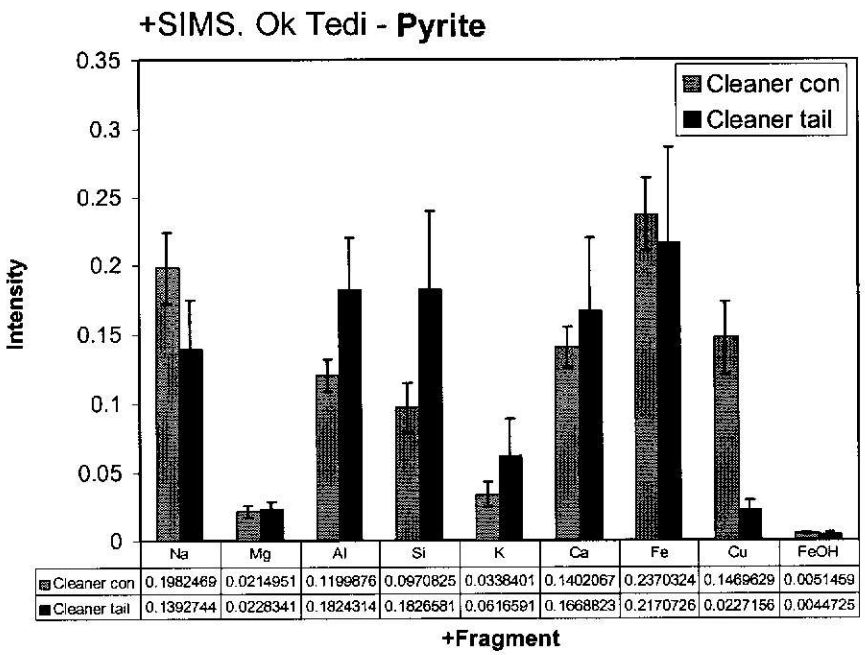

Figure 35.0: (+) SIMS. Shows mass spectra for chalcopyrite and pyrite particles in the cleaner tail and cleaner concentrate (confidence intervals calculated for P=95%).

Figure 36.0: Shows selected spectral characteristics of pyrite and chalcopyrite in cleaner tail and cleaner concentrate (confidence intervals calculated for P=95%).

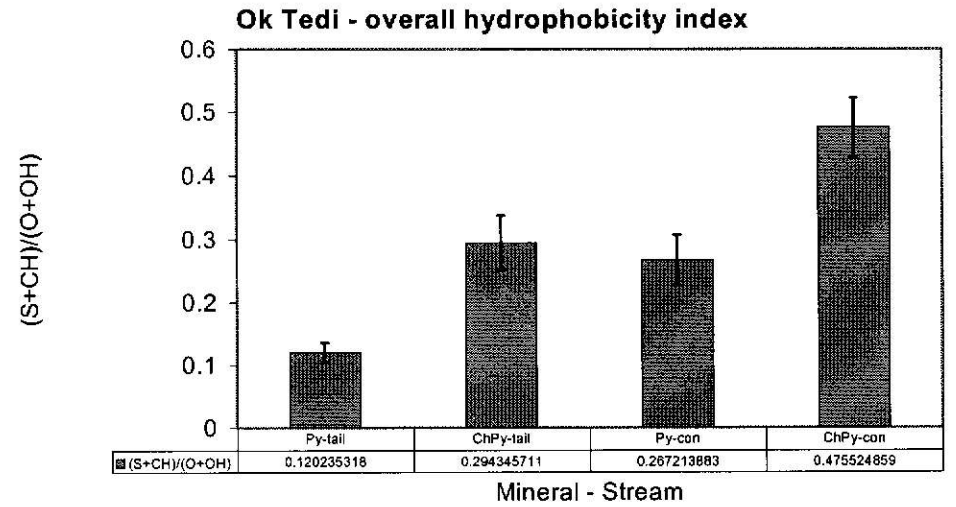

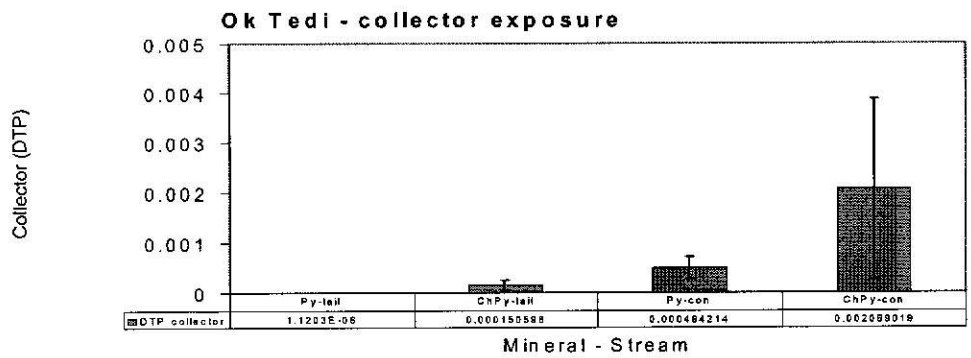

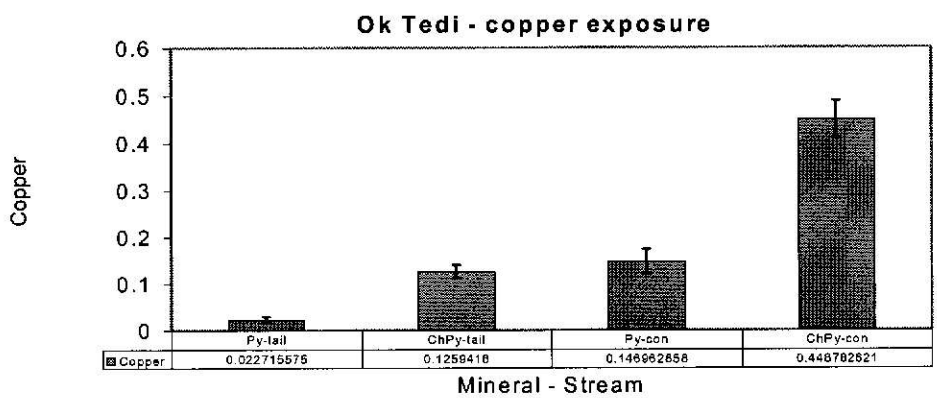

5.3 Cleaner Circuit Studies as a Function of 'Bad' Feed Blend

The performance of the cleaner flotation process was again studied as a function of 'bad' feed. 'Bad' feed is characterized as greater than 20% pyrite or magnetite skarn in the total mill feed blend. Similar characterization work was carried out as for the good feed case, with the inclusion of mineralogical investigations.

5.3.1 Ore Feed Blend Description

Two surveys were again conducted at different periods when the concentrator was treating greater than 20% skarn ore. The descriptions of the ore blends are showed in Table 22.0. It is characterized as a 'bad' ore feed blend.

Table 22.0: Ore blend, showing percent proportion in total feed blend

Survey #	Period	Ore Blend	% Proportion in Feed Blend	Head Grade % Cu	g/t Au
1	31/12/01	Pyrite Skarn/ Porphyry	21/79	1.16	1.02
2	27/11/01	Magnetite Skarn/Porphyry	24/76	1.10	1.00

The mineral compositions typical of pyrite skarn and magnetite skarn are shown in Table 23.0 (Jenkins & Adair 1996a). When compared to the porphyry sulphide (Table 17.0), it can be seen that there is a substantial difference in mineralization. For the skarn ores the feldspar content is very low but they are rich in iron. The pyrite skarn ore is richer in iron sulphides, whereas the magnetite skarn is richer in iron oxides and iron sulphides. In addition, the pyrite skarn examined contained predominantly chalcopyrite mineral with very little trace of secondary minerals. The magnetite skarn examined showed traces of secondary minerals with chalcopyrite as the main copper mineral. Because of the difference in host mineralization, the flotation response for the two types of feed blend may be different. Pyrite skarn is predominately iron sulphide mineralization whilst the magnetite skarn is predominately iron oxide mineralization.

Table 23.0: QEM*SEM analysis, showing proportions of mineral phases & groupings for magnetite (S1) and pyrite (S2) skarn ore (Jenkins & Adair 1996a).

Mineral Weight %	Magnetite Skarn Ore (S1)				Pyrite Skarn Ore (S2)			
Size Fraction (μm)	31+13	75+31	150+75	212+150	31+13	75+31	150+75	212+150
Chalcocite/Digenite	0.04	0.00	0.06	0.02	0.00	0.00	0.00	0.00
Covellite	0.16	0.04	0.02	0.01	0.00	0.00	0.00	0.00
Bornite/Fe-Digenite	0.88	0.34	0.22	0.19	0.01	0.00	0.02	0.00
Chalcopyrite	1.88	1.30	1.15	1.20	2.25	2.26	1.08	0.55
Cu_Metal	0.00	0.00	0.00	0.00	0.00	0.00	0.00	0.00
Cu_Ox(Cuprite)	0.00	0.00	0.00	0.00	0.00	0.00	0.00	0.00
CuFe_Metal/Ox	0.00	0.00	0.00	0.00	0.00	0.00	0.00	0.00
Cu_CO_3(Malachite)	0.00	0.00	0.00	0.00	0.00	0.00	0.00	0.00
CuFe_Ox/CO_3	0.04	0.01	0.01	0.02	0.00	0.00	0.00	0.00
Cu_Silicates(Chrys)	0.00	0.00	0.00	0.00	0.00	0.00	0.00	0.00
Cu_Phosphates(Turq)	0.00	0.00	0.00	0.00	0.00	0.00	0.00	0.00
Other_Cu_Minerals	0.11	0.07	0.05	0.08	0.09	0.06	0.03	0.02
Fe_Sulphides	25.61	19.87	29.31	39.34	88.78	93.40	96.08	93.91
Mg_Silicates	2.05	0.72	0.67	0.78	0.67	0.23	0.08	0.06
(Na/Ca)-Feldspars	0.23	0.08	0.14	0.21	0.53	0.08	0.03	0.17
K-Feldspars	0.45	0.13	0.13	0.22	0.82	0.20	0.08	0.15
Mica	5.53	1.94	1.63	1.43	0.76	0.21	0.08	0.12
Quartz	0.57	0.22	0.15	0.29	3.02	2.34	1.78	2.17
CuFe_Silicates	1.46	0.68	0.69	0.75	1.31	0.45	0.14	0.14
Fe_Ox/CO_3	59.53	73.79	65.07	54.91	0.92	0.45	0.23	2.29
Apatite	0.50	0.12	0.15	0.018	0.04	0.00	0.01	0.00
Others	0.88	0.66	0.58	0.47	0.80	0.32	0.38	0.42
Total	100.00	100.00	100.00	100.00	100.00	100.00	100.00	100.00

5.3.2 Cleaner Circuit Flotation Performance

Survey data was examined after data-smoothing with the computer MATBAL program with results shown in Table 24.0. The mass balance data is included in the appendix (section 2.1.15). The results show that the magnetite skarn blend responded better in flotation with 90% copper and gold recoveries, indicating that the flotation behaviour was different for each feed blend. In order to confirm the plant results, a comparison was made with the laboratory results (Table 25.0). Both Tables 24.0 and 25.0 show similar copper and gold recoveries, for the same feed, but a greater recovery for magnetite. This confirmed that the flotation responses of the two feed blends were different. The laboratory flotation results were again derived from floating the cleaner feed pulp from the plant during the survey.

Table 24.0: Plant cleaner flotation recoveries and grades as a function of 'bad' feed blend

Feed Blend	Feed Assay		Tail Assay		Cumulative Con Grade		Cumulative Recovery (%)	
	Cu (%)	Au (g/t)	Cu (%)	Au (g/t)	Cu (%)	Au (g/t)	Cu	Au
Pyrite skarn/ porphyry	19.40	12.75	7.86	4.98	28.71	15.60	81.11	88.01
Magnetite skarn/porphyry	18.03	7.82	3.60	2.21	26.06	10.70	92.86	90.41

Table 25.0: Laboratory cleaner flotation recoveries and grades as a function of 'bad' feed blend

Feed Blend	Feed Assay		Tail Assay		Cumulative Con Grade		Cumulative Recovery (%)	
	Cu (%)	Au (g/t)	Cu (%)	Au (g/t)	Cu (%)	Au (g/t)	Cu	Au
Pyrite skarn/porphyry	17.46	12.48	7.30	3.78	24.72	18.59	82.59	87.38
Magnetite skarn/porphyry	19.56	12.43	2.19	3.18	27.14	16.25	95.07	90.01

5.3.3 Size by Size Recovery Analysis

Copper and gold recovery analysis was again conducted with respect to particle size. Similar calculations to those applied for the 'good' feed survey were followed and Figures 37.0 and 38.0 show the results. When comparing these results, it appears that the magnetite/porphyry feed blend shows high copper and gold recoveries between 22 and 75 μm, whereas the pyrite skarn/ porphyry feed blend shows high copper and gold recoveries between 22-53 μm, highlighting again that their flotation behaviour is different.

Figure 37.0: Size by size copper and gold recoveries for pyrite skarn/porphyry feed blend

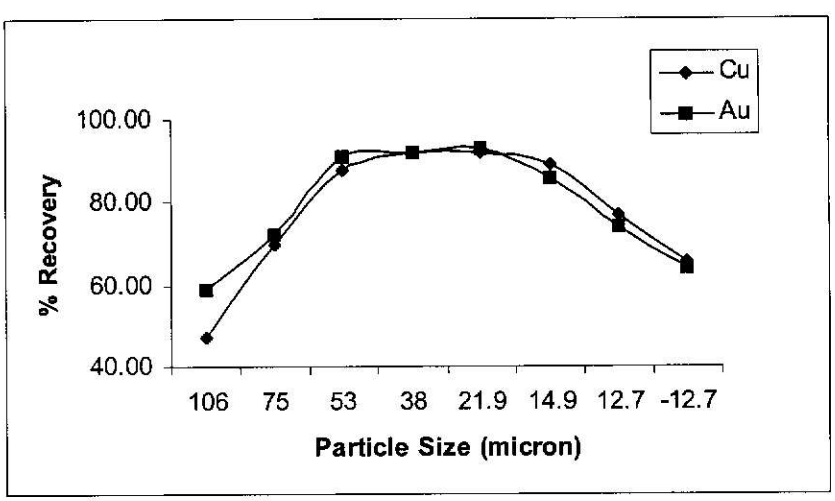

Figure 38.0: Size by size copper and gold recoveries for magnetite skarn/porphyry feed blend

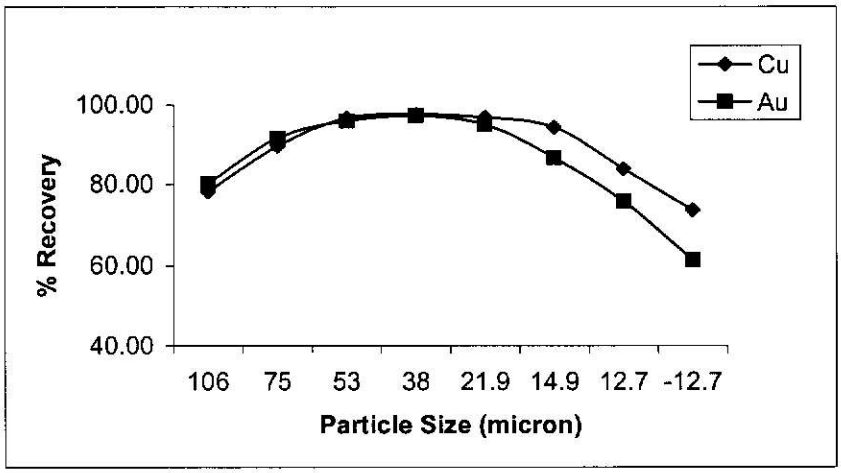

Further comparison of the two skarn blend survey can be observed from Figure 39.0 and 40.0, which shows the flotation rate constants as a function of particle size. It is observed that a relatively high flotation rate constant is observed in the 22-75 μm for the magnetite skarn/porphyry feed whilst the pyrite skarn/porphyry feed appears to show slightly lower flotation rate constants at the same size range.

Figure 39.0: Flotation rate constant as a function of particle size (pyrite skarn/porphyry ore)

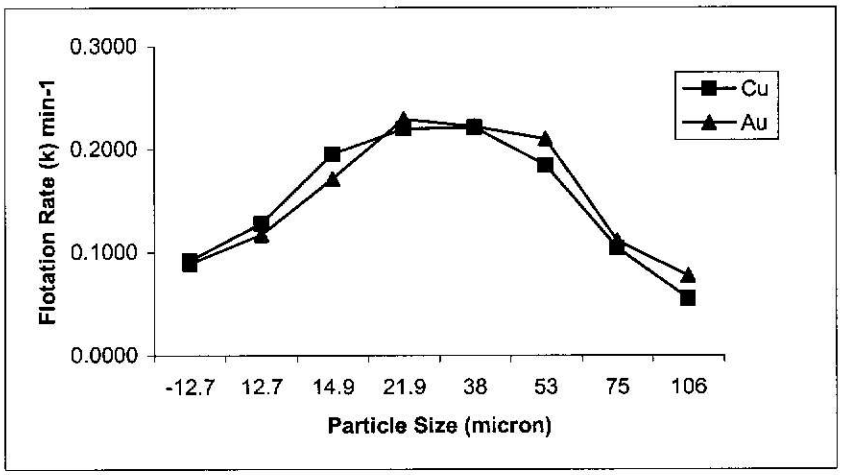

Figure 40.0: Flotation rate constant as a function of particle size (magnetite skarn/porphyry feed)

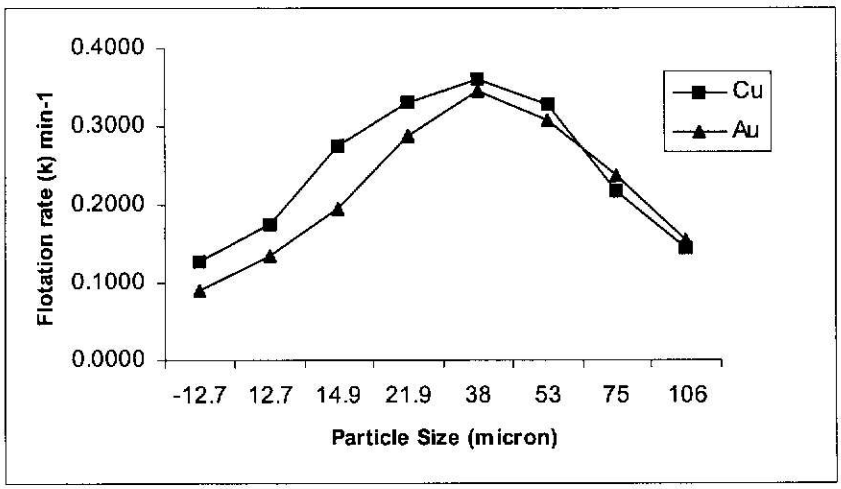

5.3.4 Pulp Solution Analysis

Similar procedures to those for the 'good' feed surveys were applied to measure the pulp parameters as a function of 'bad' feed. Figures 41.0 and 42.0 show the oxygen demand curves for pyrite skarn/porphyry and magnetite skarn/porphyry surveys, respectively. The oxygen demand curves are shown to be different for each condition. The results for pyrite skarn/porphyry feed blend (Figure 41.0) show an 80% saturation limit for the cleaner feed and tail streams. This indicates a low oxygen demand and therefore suggests that the stream particles are passivated. However, the concentrate stream shows a higher oxygen demand with less than 80% saturation, indicating that the concentrate pulp is not passivated and that the sulphide particle surfaces are either not coated with oxide or not fully coated with collector. In contrast, Figure 42.0 shows the magnetite skarn/porphyry feed with a high oxygen demand (<80% saturation) for the cleaner feed and concentrate streams and a low oxygen demand (>80% saturation) for the cleaner tail stream. This suggests that, it is possible for the concentrate and feed particles to adsorb more collector and become more hydrophobic, with a higher flotation rate constant. However, the low D.O. demand of the cleaner tail particles suggests heavier oxide coatings on these particles.

The results show the effect of ore characteristics on pulp chemical conditions. The oxygen demand curves show cleaner feed streams as passivated for a pyrite skarn/porphyry feed blend and as non passivated for the magnetite skarn/porphyry ore feed blend. Passivation of particle surfaces may occur due to oxide or collector coatings. An oxygen hungry sulphide particle (not passivated) however, may react with more collector. It is apparent therefore that this pulp chemical parameter is an indicator to particle floatability.

Figure 41.0: Oxygen demand curves for pyrite skarn/porphyry feed blend

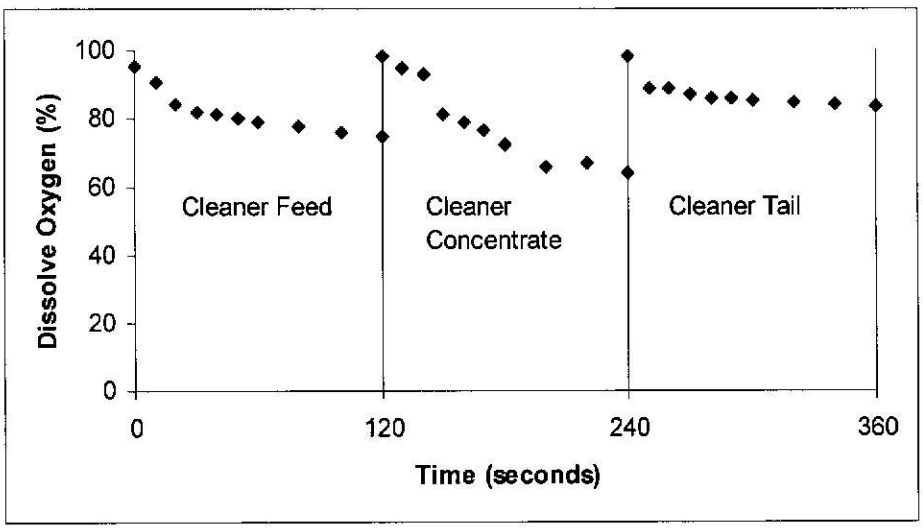

Figure 42.0: Oxygen demand curves for magnetite skarn/porphyry feed blend

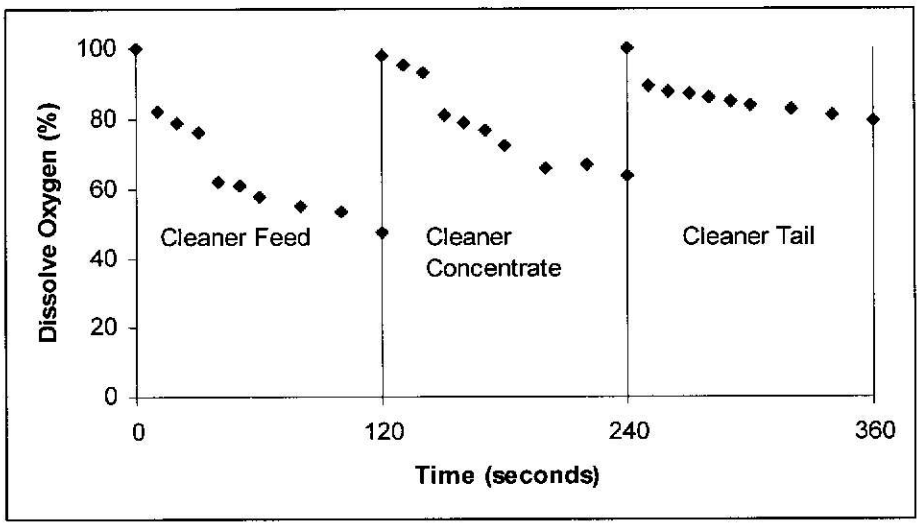

In addition, the following Figures (43a, 43b, 43c and 44a, 44b, 44c) show the trends of the pulp parameters (Eh, DO) for the two surveys. These results show the correlation between the Eh and dissolved oxygen. As oxygen demand increases (DO% decrease) the Eh also decreases. During the pulp chemical plant survey, pH of 10 was observed throughout the cleaner circuit streams. From the graphs was also observed that the Eh for the pyrite skarn/porphyry ore survey remained relatively high compared to the magnetite skarn /porphyry ore survey. When compared with the pH/Eh diagram of Figure 33.0, it may be seen that the cleaner feed stream Eh from the pyrite skarn/porphyry ore survey is outside the optimum range (equilibrium line), whilst the Eh with the magnetite skarn/porphyry ore survey appears to be within the optimum range. This suggests that sulphide oxidation is not contributing to the pulp mixed potential for collector adsorption (surfaces are thoroughly passivated).

Figure 43a: Eh and DO analysis for cleaner feed stream (pyrite skarn/porphyry feed survey)

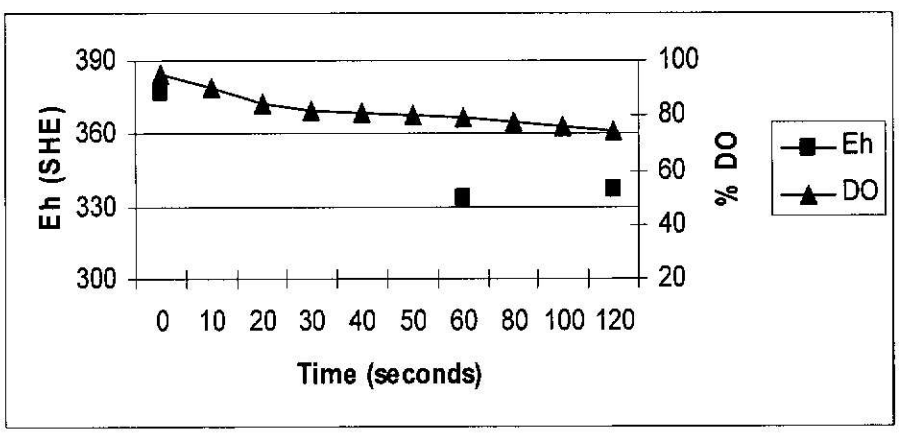

Figure 43b: Eh and DO analysis for cleaner tail stream (pyrite skarn/porphyry feed survey)

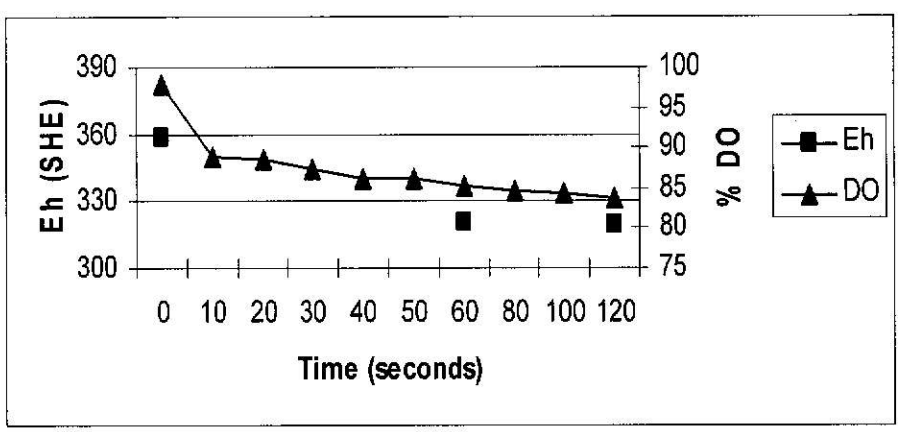

Figure 43c: Eh and DO analysis for cleaner concentrate stream (pyrite skarn/porphyry feed survey)

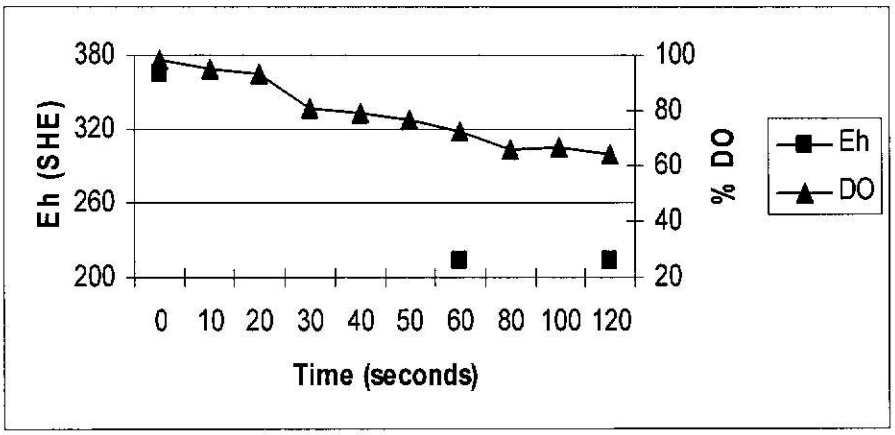

Figure 44a: Eh and DO analysis for cleaner feed stream (magnetite skarn/porphyry feed survey)

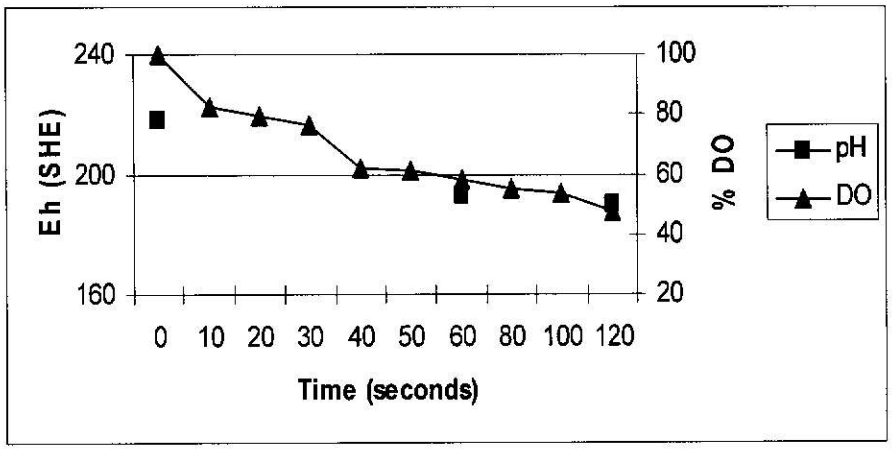

Figure 44b: Eh and DO analysis for cleaner tail stream (magnetite skarn/porphyry feed survey)

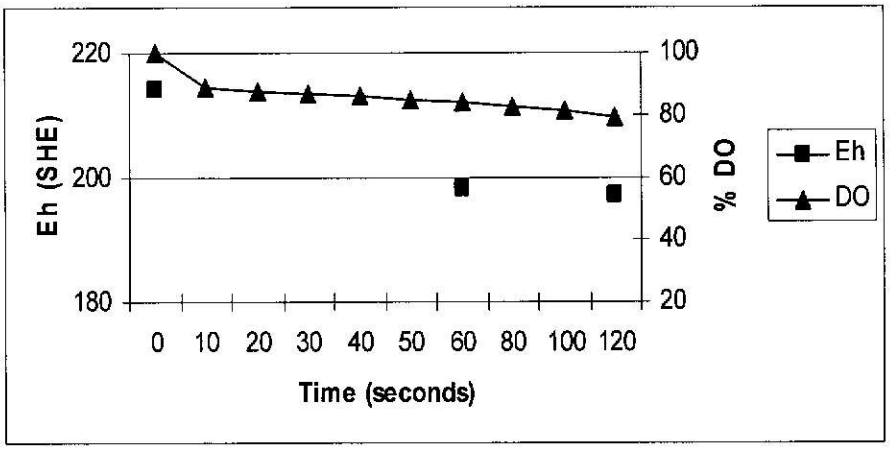

Figure 44c: Eh and DO analysis for cleaner concentrate stream (magnetite skarn/porphyry feed survey)

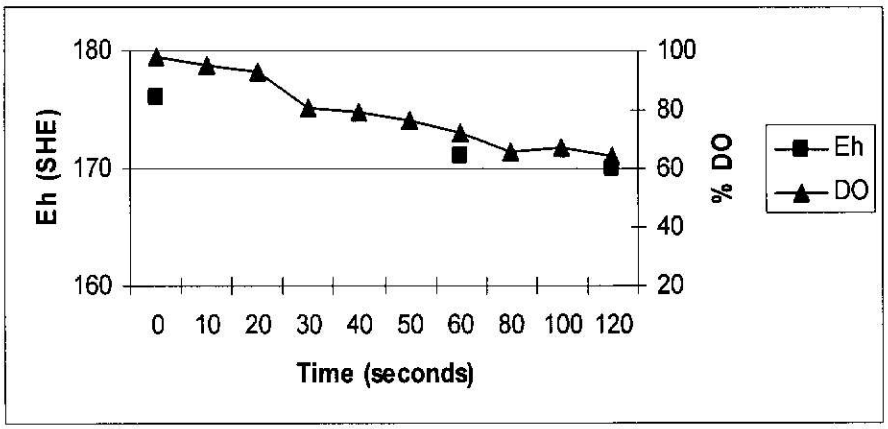

5.3.5 Particle Surface Chemical Analysis

EDTA analysis was again performed on cleaner circuit feed, tail and concentrate streams for the 'bad' feed surveys. Similar procedures to those described for the 'good' feed surveys were followed. The objective was to determine the oxidized species on the surface of the particles. Tables 26.0 and 27.0, shows the EDTA extractable results for the two respective surveys.

Table 26.0: EDTA extractable metal ions as a function of pyrite skarn/porphyry feed blend

Stream	% Cu	% Fe	% S	% Ca
Cleaner feed	0.951	0.744	0.017	65.15
Cell 1 concentrate	0.050	0.386	0.023	62.52
Cleaner tail	3.02	1.45	0.067	67.59

Table 27.0: EDTA extractable metal ions as a function of magnetite skarn/porphyry feed blend

Stream	% Cu	% Fe	% S	% Ca
Cleaner feed	0.021	0.583	0.014	54.07
Cell 1 concentrate	0.010	0.397	0.005	51.06
Cleaner tail	0.055	0.801	0.044	59.39

The immediate conclusion drawn from these results is that the particles from the pyrite skarn/porphyry feed blend showed relatively high EDTA extractable metal ions compared to the particles from the magnetite skarn/porphyry feed blend. These results correlates with D.O. demand and Eh results (cf Figure 43a), a higher level of oxide coating (pyrite skarn/porphyry blend) occurred with high Eh and low D.O. demand, all pointing to particle surface passivation. Therefore, these trends suggest that a decrease in the floatability of sulphide minerals is likely to occur at higher oxidizing pulp potentials with pyrite skarn/porphyry feed blend.

5.3.6 Particle Surface Analysis by ToFSIMS

Particle surface analysis was again performed for the 'bad' feed surveys by the Ian Wark Research Institute (IWRI). Similar measurements and statistical analysis were carried out for the chalcopyrite and pyrite particles in the cleaner feed and concentrate streams. The samples selected were for the pyrite skarn/porphyry feed survey, since low copper and gold recoveries were observed.

The examination was conducted based on the same number of particles as for the 'good' feed. Figures 45.0 and 46.0 (see pages 124-125) show the presentation of the data with the error bars indicating 95% confidence in the results. Intensities were again normalized relative to a mineral substrate for comparison. The actual values of surface intensities for each species examined are included below the bar graphs.

From Figure 45.0, the results show that there is greater exposure of copper on chalcopyrite in the cleaner concentrate, suggesting a cleaner copper sulphide surface with less contamination by iron. There also appears to be some trace exposure of $Fe(OH)_3$ probably from the oxidation of chalcopyrite. Apart from iron, calcium exposure is 2 times higher on tails suggesting lime or gypsum precipitation on these particles. It is also evident that there is a high exposure of sulphur on chalcopyrite indicating less oxidation. There is more collector (2-3 times) on the concentrate chalcopyrite, suggesting that oxidation of chalcopyrite could have prevented collector adsorption on chalcopyrite found in the tailing. It is also evident that the exposure of OH, O species is high and that could suggest an oxidized chalcopyrite surface or suggest the presence of oxidized slimes

adsorbed on surfaces. Other recent studies on the Ok Tedi flotation circuit have provided similar results (AMTEL 2000; Morey & Grano 2000). Adsorbed oxidized slimes are hydrophilic species, which may contribute to depression of chalcopyrite.

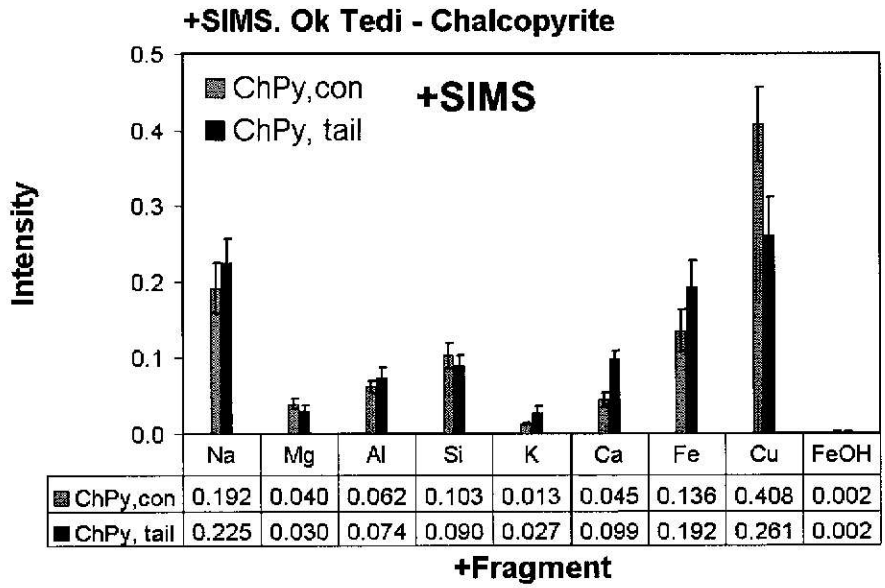

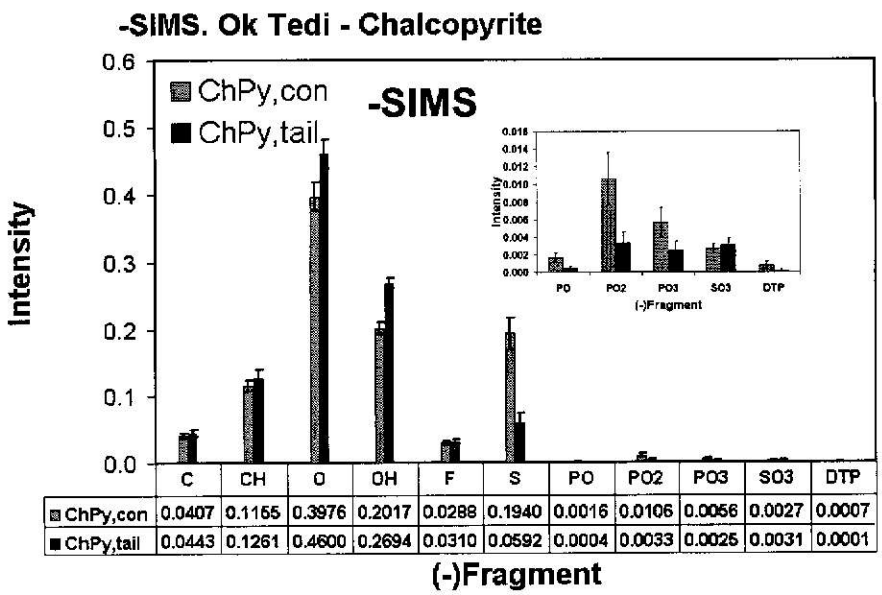

Figure 45.0: Shows (+) and (-) mass spec spectra for chalcopyrite in the cleaner concentrate and tail samples (confidence intervals calculated for P=95%)

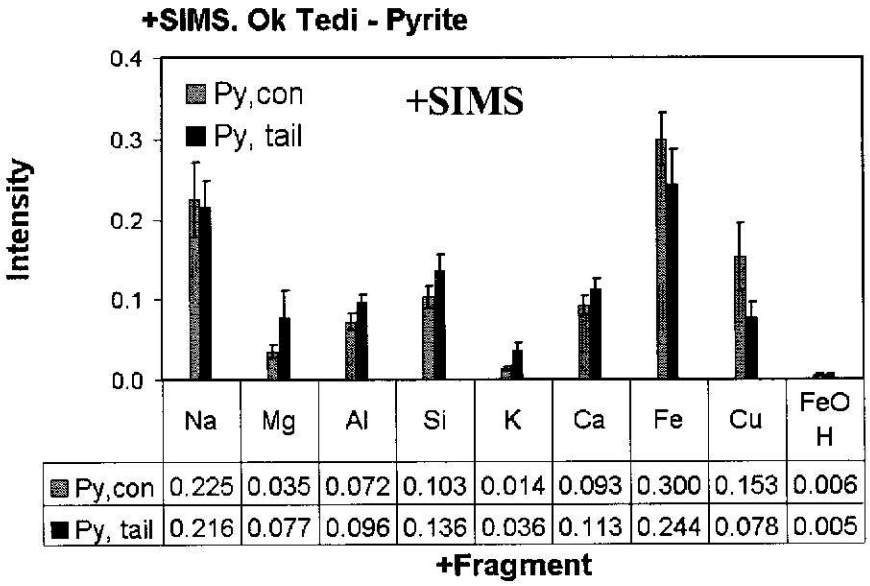

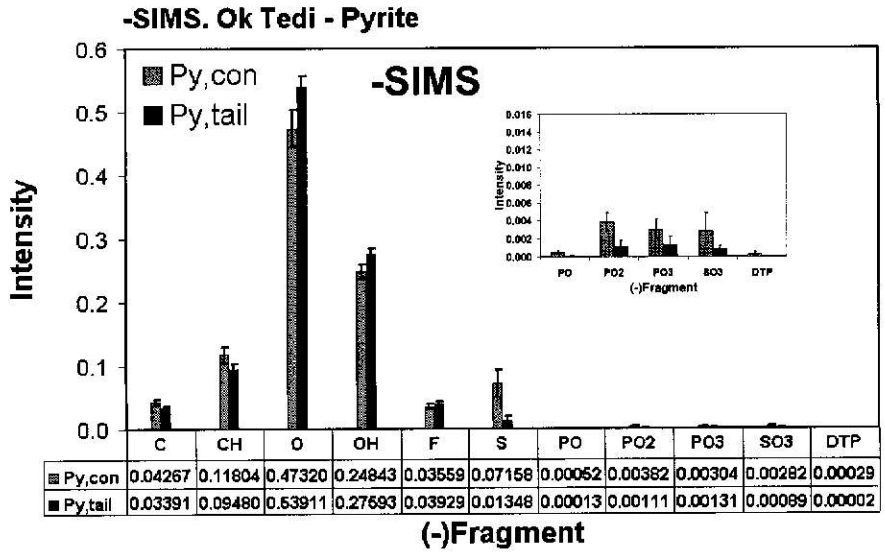

Figure 46.0: Shows (+) and (-) mass spectra for pyrite in the cleaner concentrate and tail samples (confidence intervals calculated for P=95%)

Figure 46.0, shows ToFSIMS analysis for pyrite particles from concentrate and tails streams for the same survey (pyrite skarn/porphyry feed). The results show that pyrite in the concentrate has two times more copper exposure than pyrite in the tail, suggesting copper activation of pyrite. The iron exposure on pyrite in the concentrate was greater, indicating a clean pyrite surface. Evidence of higher exposure of sulphur further shows that the surface was indeed clean. Therefore the pyrite in the concentrate was a clean activated mineral. This suggests that the pyrite was activated in the pit as opposed to activation originating in the pulp. It is apparent that the floatability difference between chalcopyrite and copper activated pyrite may not be sufficient for good separation (particularly as collector was also adsorbed).

Calcium exposure on pyrite is slightly higher in the tail but it appears that it does not have a great affect on pyrite floatability, suggesting that the major influence on pyrite floatability was copper activation.

In general, ToFSIMS analysis for the 'bad' feed cleaner concentrate and tail samples indicated that there were chemical differences on the surfaces of both the chalcopyrite and pyrite in concentrate and tailing samples. Pyrite in the concentrate was found to be activated by copper and collector. The presence of activated pyrite in the pulp that has been activated in the pit, is a difficult problem to address. Chalcopyrite in the cleaner tail was found to be depressed significantly by calcium precipitation and possibly other hydrophilic species.

5.3.7 Mineralogical Examination

Mineralogical examination was conducted on samples from the 'bad' feed surveys. Since the pyrite skarn/porphyry ore feed blend showed lower copper and gold recoveries (Table 24.0), its cleaner tail was selected for mineralogical examination to determine the mode of copper losses in the cleaner tail.

Cytec Industries Limited (Stamford) conducted microscopic examination accordingly to their standard procedures (Coe 2002). The results of the point counting analysis are shown in Table 28.0 and are expressed as percentage of the total copper sulphide occurrences in each of the selected size ranges.

Table 28.0: Estimated percentages of total copper mineral occurrence in the cleaner tail (Coe 2002)

Category	Total copper sulphide distribution (%)		
	-150+106	-106+38	-38+13
Copper minerals associated with non-sulphide minerals.	39	44	43
Copper minerals associated with other sulphide minerals	46	34	22
Free copper minerals	15	22	35
Total	100	100	100

The result shows that the majority of the copper losses occurred as either liberated copper grains or as binary composites with non-sulphides. Also there were traces of native copper and cuprite present, suggesting copper losses in the form of oxides. Their mineralogical structures are shown by the Figures 47.0-52.0. It can be observed that copper mineral losses occurring in the coarse size fractions were relatively simple structures, suggesting that it can be liberated and subsequently recovered.

Figure 47.0: Shows two copper sulphide middlings with non-opaque and magnetite (-150+106 μm).

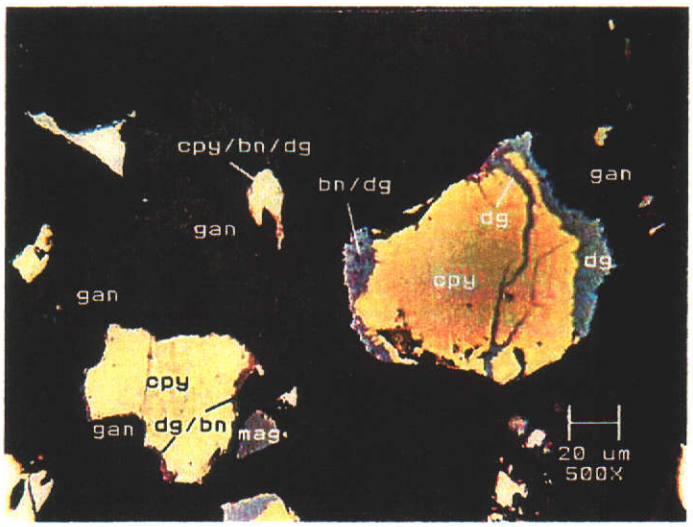

Figure 48.0: Shows native copper and chalcopyrite rimmed with digenite (-150+106 μm).

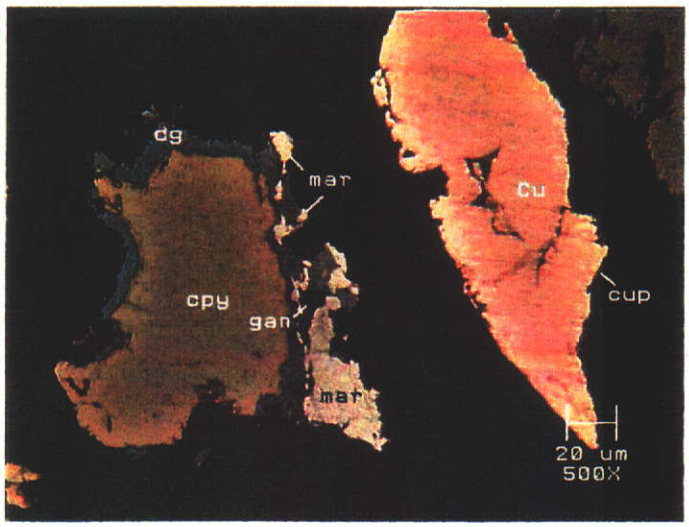

Figure 49.0: Shows digenite rimming pyrite and copper sulphide locked with non-opaque gangue (-106+38 μm)

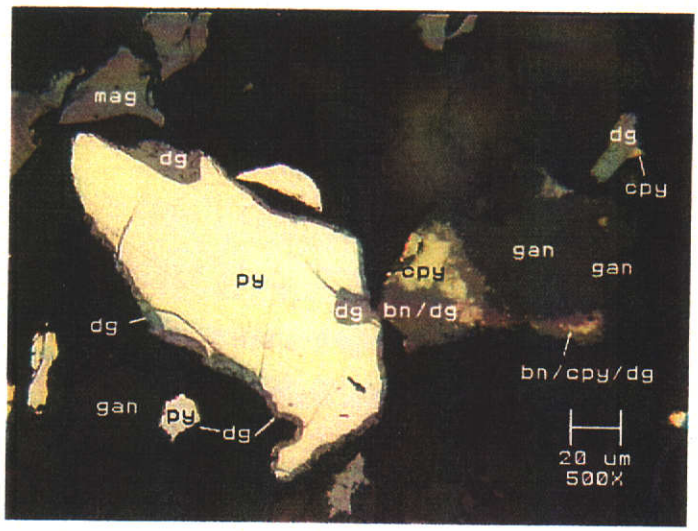

Figure 50.0: Shows a gold locked particle with pyrite/non-opaque gangue (dark grey) (-106+38 μm)

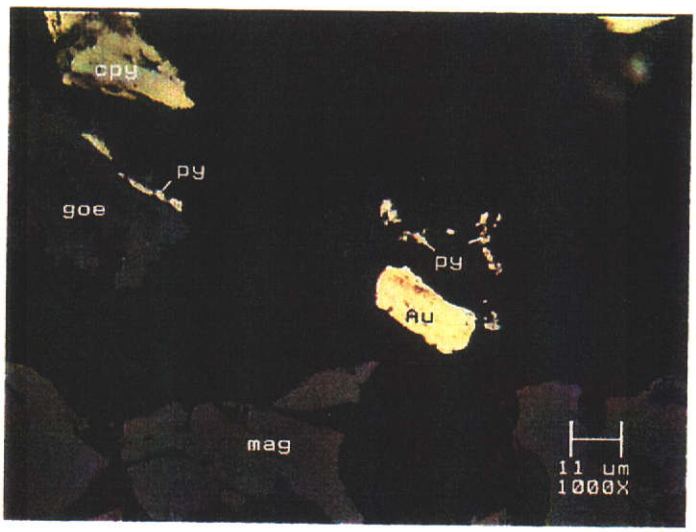

Figure 51.0: Shows a free digenite/covellite particle (-38+13 μm)

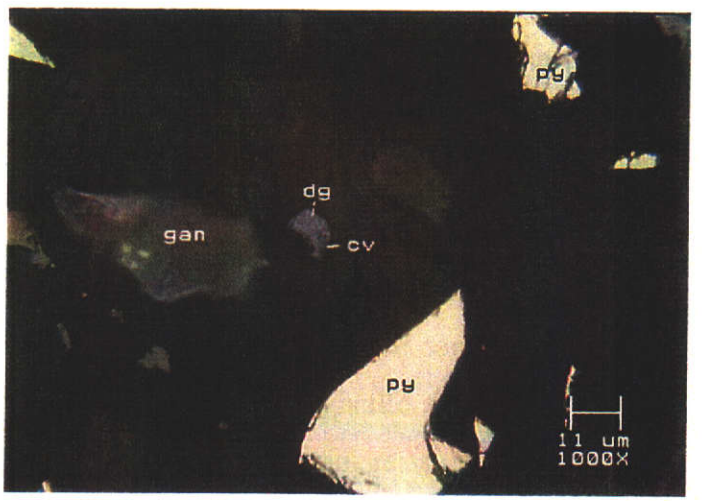

Figure 52: Shows digenite locked with non-opaque gangue and digenite locked with pyrite (-38+13 μm).

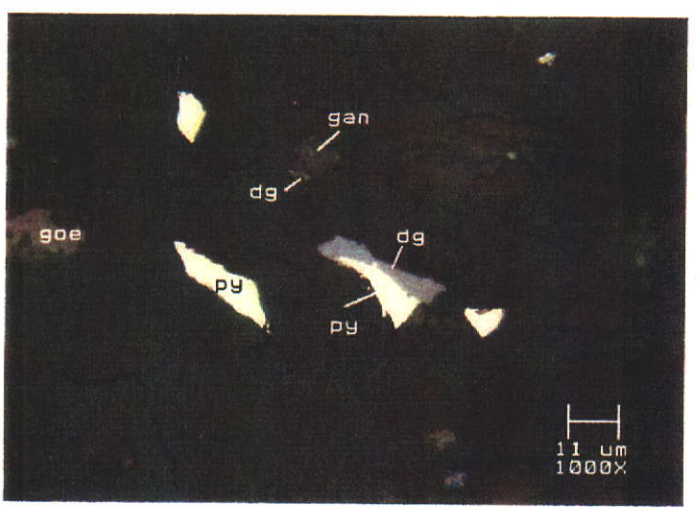

The major copper minerals found were chalcopyrite and digenite, and to a lesser amount, native copper, cuprite, bornite and covellite occurring in all size fractions. It was observed that the majority of the chalcopyrite occurred as either liberated grains or associated with digenite. The majority of digenite occurred in association with chalcopyrite and pyrite. It was evident also that bornite and covellite were mainly associated with chalcopyrite and digenite grains.

From these mineral occurrences, it is likely that pyrite rimmed with digenite (Figure 49.0) will float and decrease the concentrate grade. Furthermore, the presence of native copper (Figure 48.0) may also increase copper losses due to non floatability. The major gangue minerals were pyrite, magnetite and goethite, observed to contain fine chalcopyrite and digenite inclusions. This suggests that fine copper sulphides could be lost in the form of middlings. There was only one grain of gold observed (Figure 50.0), occurring as a fine gold grain locked with a gangue mineral. Such observations are supported by a report by AMTEL (2000), which examined the mineralogy of the Taranaki zone. This report indicated that gold occurs as inclusions and solid solution with pyrite and goethite.

Furthermore, analysis of the total percent loss of copper and gold in each size fraction in the cleaner tail and size by size recovery is shown in Figure 53.0. It is apparent from the figure that poor recoveries associated with these size ranges is indeed contributing significantly to the losses.

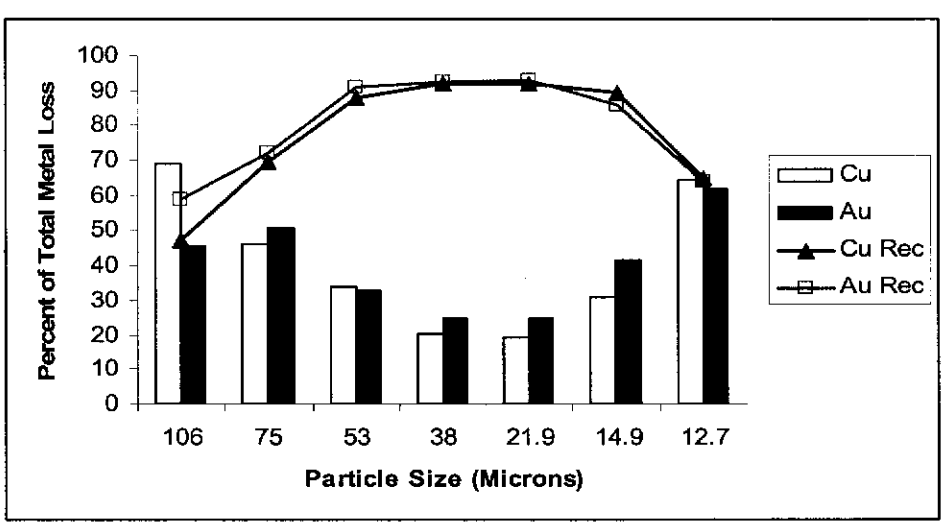

Figure 53.0: Distribution of total percent copper and gold losses in the cleaner tailing.

5.3.8 Concluding Remarks

The examination of 'good' and 'bad' feed ore blends flotation performance and pulp chemistry have shown that the ore blend has a significant impact on the cleaner flotation performance. It was found that the pulp chemistry changed with the ore blend and consequently the flotation behaviour was different for each ore type. For the 'bad' feed case, the magnetite skarn/porphyry blend responded better than the pyrite skarn porphyry blend due to less oxidation of copper sulphides and less activation of pyrite.

The major cleaner flotation issues observed from the characterization studies are as follows:

- ◊ Mineral oxidation and pyrite activation is taking place in the pit. The degree of oxidation was much higher for the 'bad' feed float with the pyrite skarn/porphyry feed blend and correlates with poorer flotation performance.
- ◊ Surface analysis for both feed blends indicated the presence of activated, but clean pyrite in the cleaner concentrate. This suggested pyrite activation within the pit. This is indicated by high copper and sulphur intensities by ToFSIMS analysis of pyrite particles in concentrate. The high sulphur exposure suggests activation layers are not oxide coatings adsorbed during processing, but sulphide coatings generated over geological time in the ore body. Mineralogical analysis confirmed digenite rimming of pyrite particles.
- ◊ Oxidation and slimes precipitation has been found to be a factor that affects the floatability of copper in Ok Tedi flotation pulp.
- ◊ ToFSIMS results indicated the presence of hydrophilic species on chalcopyrite in the tail. It indicated that floatability of chalcopyrite was reduced by hydrophilic oxide coatings and calcium salts.
- ◊ ToFSIMS results indicated decreased collector coverage on chalcopyrite in the cleaner tail.

- ◊ Size by size recovery analysis for both feed blend conditions shows that copper and gold recovery were limited by poor recovery of coarse (53-106 μm) and fine (13-20 μm) particle sizes. In particular, the pyrite skarn/porphyry feed blend showed lower copper and gold recoveries in the coarse size ranges (53–106 μm). These particles would have been marginally floatable and easily depressed by hydrophilic oxide precipitates.
- ◊ Mineralogical analysis indicate, copper loss occur as either liberated and binary composites with non sulphides. This suggests inadequate liberation and poor floatability as factors contributing to affect copper and gold recovery.

CHAPTER 6: PLANT TRIAL OF LIME AND COLLECTOR

6.1 Introduction

Laboratory flotation of cleaner feed pulp, shown in Chapter 4 indicated improved copper and gold recoveries with increased collector and lime addition. Furthermore, the pulp chemical surface analysis and EDTA extraction results of Chapter 5 suggested the presence of reactive sulphide surfaces in the pulp.

Based on these results, plant trials were conducted to examine the effect of collector and lime addition to the cleaner circuit of Unit 2 module via additions to the regrind hydrocyclone underflow. The objective was twofold: to improve copper and gold recovery and to improve concentrate grade via depression of pyrite flotation. This Chapter discusses the results from the plant trials.

6.2 Lime Addition to Cleaner Circuit

A total of six comparative 'snap shot' surveys were performed, each comparing 'lime-off' and 'lime-on' to low grade regrind process. The methodology was discussed in section 3.2.5. The focus of the work was to determine the effect of lime, with respect to cleaner circuit recovery and grade. Sections 6.2.1 and 6.2.2 describe the circuit conditions and discuss the cleaner flotation performance results.

6.2.1 Circuit Condition and Ore Blend

Metallurgical surveys were conducted during normal plant operating conditions and Table 29.0 show the approximate daily ore blends and cleaner circuit conditions for each trial day. A close circuit condition (Table 29.0) means that the cleaner tail was recycled to the rougher circuit, i.e., the copper level in the cleaner tail exceeded 2%. In contrast, an open circuit condition means the cleaner tail stream was directed to the final tailings being less than 2% copper. It is apparent from Table 29.0 that the mode of cleaner circuit operation may be strongly affected by the feed blend characteristics as the majority of the tests were conducted in closed circuit condition.

Table 29.0: Daily feed blend and circuit condition for lime addition tests

Test #	Trial Period	Circuit Condition	Ore Blend (% Skarn/Porphyry)
1	03/04/02	Closed circuit	26/74
2	05/04/02	Closed circuit	24/76
3	01/05/02	Closed circuit	10/90
4	16/07/02	Closed circuit	14/86
5	18/07/02	Open circuit	10/90
6	25/07/02	Open circuit	15/85

6.2.2 Cleaner Circuit Flotation Performance

The cleaner circuit flotation performance as a function of lime addition is shown in Tables 30.0 and 31.0. Hydrated lime was added to the cleaner feed stream and pulp pH was increased from 10.6 to 11.6. The increase in pH was attributed to the dissociation of calcium ions (Ca^{2+}) and hydroxyl ions (OH^-) and the reactions can be represented by the following equations:

Dissociation of lime,

$$CaO_{(s)} + H_2O \leftrightarrow Ca(OH)_{2\,(S)} \quad (24)$$

$$Ca(OH)_{2(S)} \leftrightarrow Ca^{2+}_{(aq)} + 2OH^-_{(aq)} \quad (25)$$

As the pH is increased,

$$Ca^{2+}_{(aq)} + OH^-_{(aq)} \leftrightarrow CaOH^+_{(aq)} \quad (26)$$

$$CaOH^+_{(aq)} + OH^- \leftrightarrow Ca(OH)_{2\,(aq)} \quad (27)$$

Further reactions with air,

$$CO_{2\,(aq)} + H_2O\,(l) \leftrightarrow H^+_{(aq)} + HCO_3^-{}_{(aq)} \quad (28)$$

$$Ca(OH)_{2\,(aq)} + Ca^{2+}_{(aq)} + 2HCO_3^-{}_{(aq)} \leftrightarrow 2\,CaCO_{3\,(s)} + 2H_2O_{(l)} \quad (29)$$

Table 30.0: Copper recovery and grade as a function of lime addition to the cleaner circuit

Test #	No Lime pH	With Lime pH	Head Grades Cu (%)		Copper Recovery (%)		Copper Concentrate Grade (%)	
			No Lime	With Lime	No Lime	With Lime	No Lime	With Lime
1	10.10	11.92	22.45	26.51	76.95	99.33	29.14	30.11
2	10.85	11.12	25.24	8.35	85.24	94.34	34.80	34.42
3	10.89	12.01	10.57	10.73	93.22	95.48	19.98	19.84
4	10.70	11.50	10.48	11.8	96.35	97.43	27.79	23.01
5	10.50	11.50	7.55	7.28	97.36	97.36	17.34	18.19
6	10.46	11.60	5.84	4.74	94.58	92.61	22.96	25.13
Mean	10.59	11.61	13.69	11.57	90.62	96.09	25.34	25.12
Stdev	0.29	0.32	7.41	7.06	7.96	2.43	5.89	5.65

Table 31.0: Gold recovery and grade as a function of lime addition to the cleaner circuit

Test #	No Lime pH	With Lime pH	Head Grades Au (g/t)		Gold Recovery (%)		Gold Concentrate Grade (g/t)	
			No Lime	With Lime	No Lime	With Lime	No Lime	With Lime
1	10.10	11.92	10.33	11.22	80.26	94.51	15.29	16.05
2	10.85	11.12	10.11	6.10	77.10	83.13	15.63	20.89
3	10.89	12.01	6.36	6.87	88.74	89.56	10.74	12.12
4	10.70	11.50	10.95	11.25	85.96	92.83	19.43	18.66
5	10.50	11.50	6.46	6.34	87.67	89.20	12.00	13.75
6	10.46	11.60	4.93	4.51	84.42	80.56	15.75	16.74
Mean	10.59	11.61	8.19	7.72	84.03	88.30	14.80	16.37
Stdev	0.29	0.32	2.34	2.59	4.51	5.44	2.82	2.91

The above reactions show that pH increases with the concentration of calcium oxide (lime) because the CaO becomes hydrolyzed to form $Ca(OH)_2$ (aqueous) species. This hydrolyzed species then dissociates to form hydroxide ions in solution. Further, $Ca(OH)_2$ ions reacts with HCO_3^- ions to form $CaCO_3$ and with SO_4^{2-} to form $CaSO_4$ (gypsum). Bicarbonate ions (HCO_3^-) exist in solution due to the dissolution of carbon dioxide from the injection of air into the pulp for bubble formation. Sulphate ions are present in the pulp from the oxidation of sulphide minerals. The conversion of lime to calcium carbonate or gypsum helps to increase the pH of the pulp by releasing OH^- (DiFeo et al. 2004). However, at high pH it has been established that calcium ions act as a depressant for iron sulphides and gold due to the >50% precipitation of un-dissolved lime (Ball & Rickard 1976; Kimpel 1999). The presence of OH^- ions in pulp solution also contributes to the pulp potential, which is critical for collector adsorption (Hayes 1993; Ralston & Grano 1995). It is therefore apparent that control of pH is critical to the flotation of copper and gold minerals.

As a result of increasing pH from 10.6 to 11.6, copper and gold recovery improved significantly in the cleaner bank, whilst the concentrate grade was not affected. The average recovery improvement was 5% and 4% for copper and gold, respectively. The mechanism for increased copper and gold recovery is unclear, but could be of at least 2 origins. At pH 11.6, the thermodynamically stable oxy species for Cu is $Cu(OH)_3^-$, which is likely to be dispersed from particle surfaces. However, at pH 10.6, the predominant oxy species is likely to be $Cu(OH)_2$, which when adsorbed to copper sulphide particle surfaces would both impede electrochemical reaction of collector with sulphide, and also act as an hydrophilic depressant. The other possible cause of increased recovery, is the transfer of collector from pyrite to copper sulfide at higher pH. The thermodynamic stability of collector adsorption onto pyrite decreases rapidly beyond pH 10 (Morey, 1998). However, without pulp chemical data it is difficult to conclude what chemical mechanism was dominant.

Another reason attributed to the increase in copper and gold recovery after lime addition, could be improved 'froth stability'. This was the reason given in studies at the Chuquicamata concentrator, Chile (Bulatovic et al. 1998). The authors found that copper recovery was increased from 60 to 85% when lime was added to the cleaner circuit. Most

recent studies suggest high froth recovery is associated with strongly hydrophobic particles (Ata et al. 2002, Sis & Chander 2003).

Although the Chuquicamata plant in Chile treated a porphyry ore, the presence of clay in the ore blend had a detrimental effect on frothy stability. In contrast, Ok Tedi skarn ore produces a viscous and stable froth as opposed to the Ok Tedi porphyry ore which provides a drier and more brittle froth. Thus the presence of different minerals may have a detrimental effect on froth stability. In this test work, results show that cleaner flotation performance improved with lime addition. The effect was more profound with test 1 compared to 2. This test pulp had a relatively high skarn proportion in the feed blend, and contained higher levels of oxidized minerals.

Gold in this test work floated at high pH without any adverse effect of calcium ions, in contrast to Kimpel (1999). Again, this may be due to the dispersion of hydroxyl species from particle surfaces. Similar flotation behaviour for gold under high pH has been reported for Freeport concentrator, which treats a porphyry ore and use an identical collector to Ok Tedi (Hartati et al. 1997). Furthermore, Forrest (1998) also using the same collector with a different ore, found that gold recoveries was optimum at pH 12.0. It is apparent that gold from Ok Tedi ore floats well with OMTL standard collector at alkaline pulp conditions.

In order to determine whether lime addition gave significantly improved copper and gold recoveries a students't' test statistical analysis was performed. Students't' tests indicated that the observed increases in copper and gold recoveries were significant at the 90% confidence level.

However, lime addition did not appear to improve cleaner concentrate grade, although marked increases in Tank cell concentrates grade were observed (Table 32.0). The results show that for most surveys the Tank cell concentrate grades increased by 3% (copper) and 3 g/t (gold) (Results for tests 1 to 3 are not included and due to lack of sampling during the survey). It is possible that the recirculation of lime within other stages of cleaning enhanced overall plant performance. Thus, improvements in Tank cell concentrate grades attained at the high pH condition suggest that the floatability of pyrite was impaired. Such

improvement in selectivity could be attributed to calcium and hydroxyl ion displacement of collector on pyrite as suggested by Ball & Rickard (1976).

Table 32.0: Tank cell concentrate grade as a function of lime addition to the cleaner circuit

Test #	Copper Concentrate Grade (%)		Gold Concentrate Grade (g/t)	
	No Lime	With Lime	No Lime	With Lime
4	28.36	32.26	24.74	28.76
5	24.91	28.47	16.55	21.83
6	28.70	27.95	18.59	18.29
Mean	27.32	29.56	19.96	22.96
Stdev	2.10	2.35	4.26	5.33

When comparing individual test results, tests 1 and 2 with higher skarn proportion (>20%) show higher recovery increases as a result of lime addition. Size by size analysis was performed on these tests to study the effect of lime addition on particle sizes transferring to the concentrate. It is apparent from Figures 54.0 and 55.0 that increased lime addition to the cleaner circuit increased copper and gold recoveries across all the particle size ranges. These results indicate that when the pH was increased from 10.6 to 11.6, it improved the floatability of all copper sulphide particles. As mentioned previously, it is possible that the change in pH may have altered the thermodynamically stable hydroxyl species on copper sulphide particle surfaces, resulting in dispersion of negatively charged hydroxy species from particle surfaces, and improved flotation behaviour.

Figure 54.0: Copper recovery as a function of lime addition to the cleaner circuit

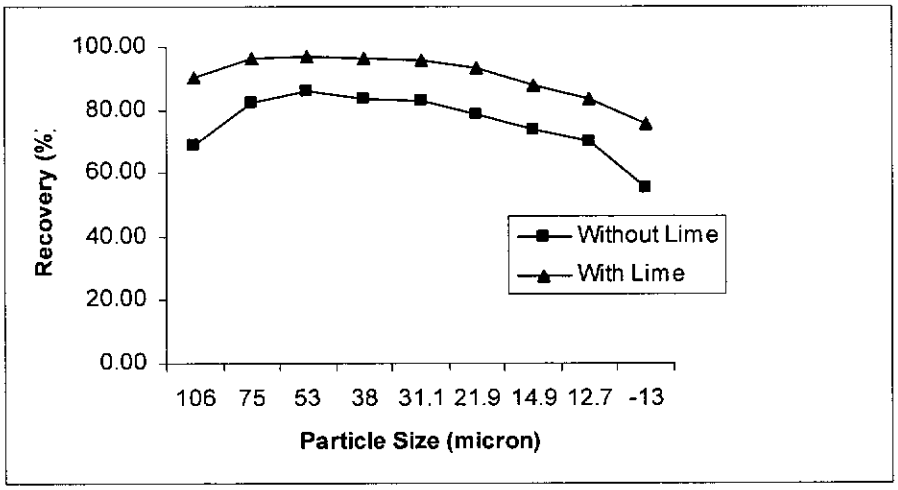

Figure 55.0: Gold recovery as a function of lime addition to the cleaner circuit

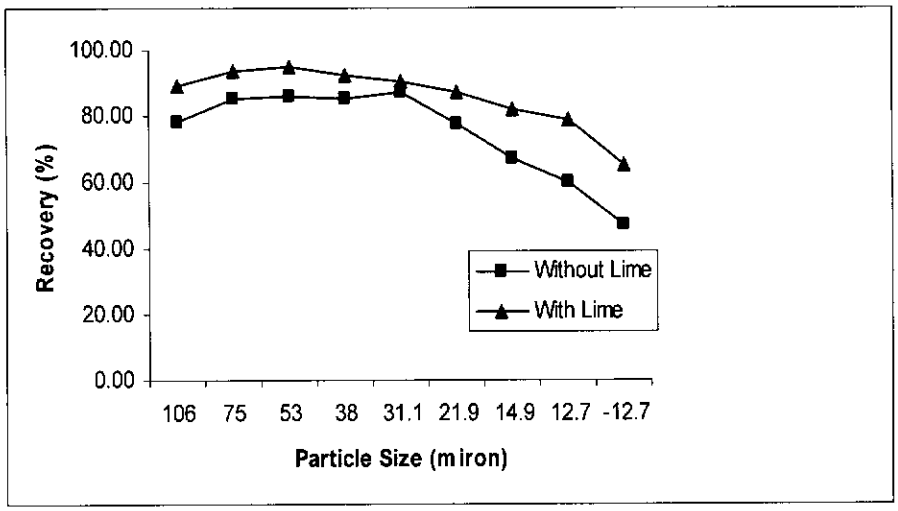

In summary, the addition of lime to the cleaner circuit was found to improve cleaner flotation performance, especially with higher proportions of the more oxidised skarn ore in the feed blend. It was also apparent that increased lime significantly improved the Tank cell concentrate grade.

6.3 Collector Addition to Cleaner Circuit

In a similar approach to the lime trials, a total of six comparative 'snap shot' surveys were again conducted to examine the effect of collector addition to cleaner pulp on flotation grade and recovery. Each trial included 'collector-off' and 'collector-on' comparative surveys. The methodology is discussed in section 3.2.6. Sections 6.3.1 and 6.3.2 provide a description of the circuit conditions and discussion of results.

6.3.1 Circuit Condition and Ore blend

Collector trials were conducted under different circuit and ore blend conditions as shown by Table 33.0.

Table 33.0: Daily ore blend and circuit conditions for collector tests

Test #	Trial Period	Circuit Condition	Ore Blend (% Skarn/Porphyry)
1	28/05/02	Open circuit	17/83
2	29/05/02	Closed circuit	10/90
3	07/06/02	Open circuit	30/70
4	05/08/02	Closed circuit	28/72
5	15/08/02	Open circuit	15/85
6	23/08/02	Open circuit	15/85

6.3.2 Cleaner Circuit Flotation Performance

Standard Ok Tedi collector (dithiophosphate/monothiophosphate blend) was added to the cleaner circuit, to render copper and gold minerals more hydrophobic and thus increase their flotation rate constant. The collector addition rate was 5 g/t to the regrind cyclone underflow stream. The practice of applying additional collector after regrinding is common because the regrinding produces fresh particle surfaces, which may not be

covered by residual collector remaining in the pulp. Reagent additions to cleaner circuits have been found to increase both recovery and selectivity (Bulatovic et al. 1998; Runge et al. 2004).

The process of rendering mineral surfaces hydrophobic involves two mechanisms, including electrochemical oxidation of the mineral surface, and chemisorption of the collector molecule (Buckley et al. 2003; Buckley & Woods 1997). The following reactions in a chalcocite/DTP system were provided by these authors to illustrate the mechanisms occurring in the presence of oxygen in an aqueous solution.

Anodic oxidation of the mineral surface in the presence of oxygen (without the presence of collector),

$$Cu_2S+0.14H_2O \rightarrow 0.07Cu(OH)_2 + Cu_{1.93}S + 0.14H^+ + 0.14e^- \qquad (30)$$

When collector is added, the $Cu(OH)_2$ is expected to react with DTP through an ion exchange step represented by the reaction,

$$2Cu(OH)_2 + 4\ DTP^- \rightarrow 4OH^- + 2\ CuDTP + (DTP)_2 \qquad (31)$$

As a result of this ion exchange process, the DTP_2 (dithiolate) is expected to react with copper in the chalcocite surface to form CuDTP species which renders the mineral surface hydrophobic. The formation of CuDTP is possible since the free energy difference was negative (ΔG = -51.7kJ per mole of $(DTP)_2$) for the reaction,

$$Cu_2S+0.035(DTP)_2 \rightarrow Cu_{1.93}S + 0.07CuDTP \qquad (32)$$

The above reactions for the chalcocite/DTP system serve as a guide to understanding the collector–mineral adsorption reaction in the floatability of sulphide minerals. The extent and kinetics of these reactions is influenced by many factors, such as dissolved oxygen concentration, pulp potential, pH, and grinding conditions (Kuopanportti et al. 2000, Guo & Yen 2003, Goncalves et al. 2003, Peng et al. 2003).

The results of the collector addition to the cleaner circuit are shown by Tables 34.0 and 35.0. Table 35.0 suggests that in contrast to the results for the lime tests, there were only negligible differences in copper recoveries and concentrate grade between the two conditions. When comparing mean recoveries and concentrate grades using a Students't' test statistical analysis, it was found that the recovery and concentrate differences were not significant, even at a 70% level of confidence.

Table 34.0: Copper recovery and grade as a function of collector (S7249) addition (5g/t) to the cleaner circuit

Test #	Head Grade Cu (%)		Copper Recovery (%)		Copper Concentrate Grade (%)	
	No Collector	With Collector	No Collector	With Collector	No Collector	With Collector
1	5.11	4.77	97.67	98.16	21.24	17.09
2	8.00	9.57	97.90	98.87	22.75	25.39
3	9.16	9.36	98.59	99.15	25.14	24.11
4	5.54	4.99	96.96	95.97	12.38	13.96
5	6.58	7.84	96.76	88.58	21.19	20.89
6	10.28	9.11	98.55	98.58	19.54	17.21
Mean	10.13	7.61	97.24	96.55	20.37	19.78
Stdev	6.46	2.20	1.81	4.07	3.97	4.07

Table 35.0: Gold recovery and grade as a function of collector (S7249) addition (5g/t) to the cleaner circuit

Test #	Head Grade Au (g/t)		Gold Recovery (%)		Gold Concentrate Grade (g/t)	
	No Collector	With Collector	No Collector	With Collector	No Collector	With Collector
1	4.27	5.02	87.10	92.03	18.87	13.48
2	7.28	7.98	90.45	92.98	19.47	21.95
3	5.91	8.14	89.61	95.43	16.41	18.52
4	4.83	4.56	89.66	85.58	9.37	10.81
5	4.79	6.18	87.37	87.87	15.78	14.84
6	8.55	8.73	94.72	94.99	15.64	19.19
Mean	5.94	6.77	89.82	91.48	15.92	16.47
Stdev	1.67	1.76	2.75	3.94	3.28	3.77

In respect to the gold flotation (Table 35.0), the average recovery difference with collector addition was marginal (1%) and there was no change to concentrate grade. It is suggested that the lack of recovery improvement, may be studied via particle surface analysis, size and mineral liberation analysis.

A comparison with laboratory flotation results as reported in Chapter 4 (section 4.2.4.2), shows greater improvement in copper and gold recoveries in lab flotation tests with collector addition. Grade and recovery increased linearly with collector dosage. This contrast with plant results suggests that the 5 g/t addition to the plant cleaner feed, may have been too low to impact the cleaner flotation performance. It is suggested that further plant tests with a higher collector addition rate of between 10–20 g/t may be trialed.

Another possible reason that could affect the test results is the collector addition point. As collector was added to the regrind mill, it is apparent that there may be a trade off between rapid adsorption of collector onto fresh copper sulphide minerals, and also collector addition onto fresh pyrite surfaces. It is possible that an improved result would be achieved by a collector addition after milling. This change would allow the pyrite surface to oxidize before the collector is added. Recent studies have shown that the floatability of pyrite was depressed by the presence of calcium, magnesium and iron hydroxides (Piantadosi et al. 2002; Boulton et al. 2003). It is apparent therefore that a change in collector addition point from regrind mill to cleaner flotation feed stream may be worth investigation.

6.4 Conclusions and Recommendations

The examination of lime and collector addition to the cleaner feed have shown improved flotation performance in the cleaner bank. In particular, lime addition to pH 11.6 was found to significantly impact cleaner flotation performance. Under the condition of increased lime, both copper and gold recoveries increased by 5% and 4% respectively on average, for a more oxidized, skarn ore blend. Furthermore, an increase in final cleaning (Tank cell) concentrate grades of 3% for copper and 4 g/t for gold was observed with cleaner concentrate grades remaining unchanged.

The effect of a 5 g/t collector addition to the cleaner circuit showed no significant change to concentrate recovery and grade. A 1% increase in gold recovery was observed (but without statistical confidence). This poor result may be attributable to insufficient collector addition or perhaps the quality of plant feed at the time of surveying.

Results for the lime addition tests were significantly improved on baseline results. It is therefore recommended that further metallurgical surveys be conducted to confirm the results. In conjunction with metallurgical surveys, pulp chemical samples should be taken for pulp and surface chemical analysis to provide chemical information that will help explain the results.

As tests of 5 g/t collector addition to cleaner feed (via regrind cyclone underflow) showed no significant impact on cleaner flotation performance, it is recommended that further tests be conducted at higher collector dosages. Collector additions in the range 10-20 g/t in conjunction with difficult skarn blends are recommended, along with metallurgical surveys, and pulp and surface chemical analysis. Furthermore, it is recommended that the collector addition point be changed from the regrind mill cyclone underflow stream to the cleaner feed stream.

CHAPTER 7: EFFECT OF UNGROUND CLEANER FEED

7.1 Introduction

Size by size kinetic results for the cleaner flotation circuit have shown that copper and gold recovery were limited by particle size (Chapter 5). The results indicated poor recovery of particle sizes above 75 μm and below 21 μm. Mineralogical analysis indicated that the mode of copper and gold losses were in the form of middlings (sulphide/non sulphide) and to a greater amount as fine liberated particles. These results prompted an investigation into the effect of unground cleaner feed, with respect to copper and gold recovery in the cleaner circuit.

Cleaner circuit characterization studies were conducted under two different feed conditions. i.e., in the absence of regrind (unground feed) and in the presence of regrind (ground feed). The methodology is similar to that described in section 3.2.1.

The objective was to determine if regrinding the cleaner feed was necessary to improve cleaner flotation performance. This chapter presents the test results and discussion.

7.2 Characterization Studies of Cleaner Circuit

Characterization studies were conducted with and without regrind. The aim of the study was to examine the effect of regrind on the pulp parameters (Eh, DO & pH), particle size, particle surface oxidation, other surface chemistry effects and mineralogy of copper and gold in the cleaner tail, as it pertains to cleaner flotation performance. Results and discussion are presented in sections 7.2.1 to 7.2.5.

7.2.1 Description of Feed Blend

The feed blend as provided to the concentrator during the survey is shown in Table 36.0. It is predominantly of 87% porphyry and 13% magnetite skarn ore. The mineralogical description is very similar to the description provided for the 'bad' feed survey (section 5.3.1).

Table 36.0: Feed blend, showing percentage of different ore proportions

Survey #	Period	Ore Blend Condition	% Proportion in Feed Blend	Feed Grade % Cu	g/t Au
1	08/01/02	Magnetite skarn / Porphyry	13/87	0.64	0.82

7.2.2 Cleaner Circuit Flotation Performance

The cleaner flotation performance during surveys, as a function of regrind, is shown in Table 37.0.

Table 37.0: Cleaner circuit performances as a function of regrind

Test Condition	Feed Assay		Tail Assay		Cumulative Con Grade		Cumulative Recovery (%)	
	Cu (%)	Au (g/t)	Cu (%)	Au (g/t)	Cu (%)	Au (g/t)	Cu	Au
Ground feed	11.94	9.63	0.62	1.26	19.74	12.38	97.88	96.76
Unground feed	11.54	9.94	1.78	1.56	16.50	12.63	94.80	96.18
Difference in recovery							3.08	0.58

The results show better copper recovery to cleaner concentrate in the presence of regrind. By comparing flotation performance between the two conditions, it was observed that copper recovery was reduced by 3.08% in the absence of regrind. Gold recoveries appear steady at 96% for both conditions. In order to explain the effect on flotation performance, survey samples taken with and without regrinding were sized and subjected to kinetic and mineralogical analysis. Pulp solution analysis was also conducted to provide pulp chemical information. Results and discussion are presented in sections 7.2.3 to 7.2.5

The relationship between particle size and recovery for the two surveys is shown in Figures 56.0 and 57.0 for copper and gold respectively.

Figure 56.0: Copper recoveries as a function of particle size

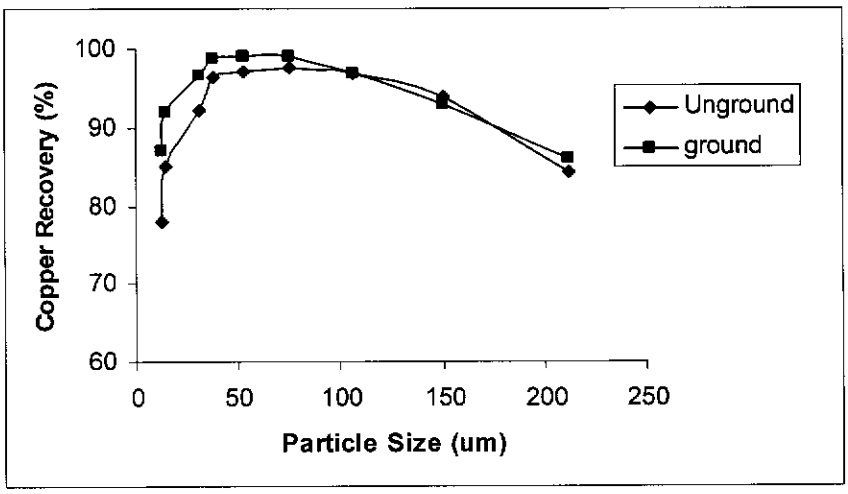

Figure 57.0: Gold recoveries as a function of particle size

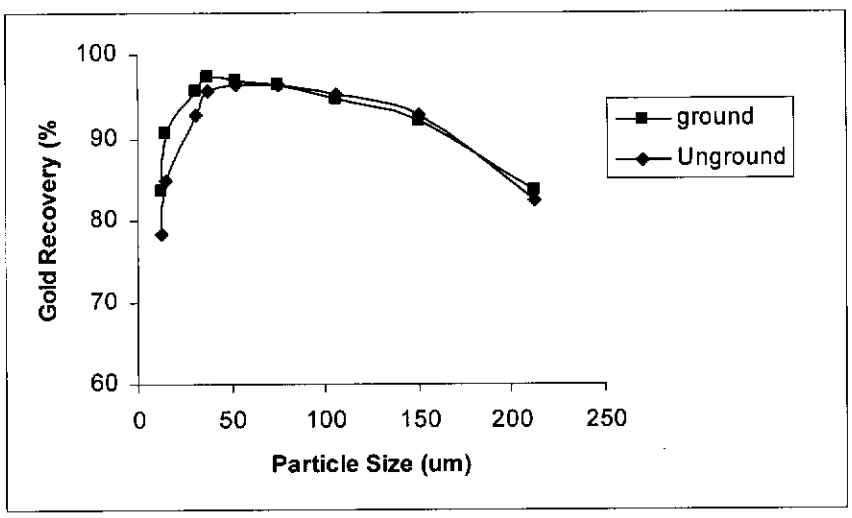

The results show for copper an enhanced recovery in the more floatable size ranges, probably due to the liberation of locked grains on grinding. Gold recovery improved slightly in the presence of regrind.

Further comparisons were made as a function of the first order flotation rate constant, as shown in Figures 58.0 and 59.0.

Figure 58.0: Copper flotation rate constants as a function of particle size

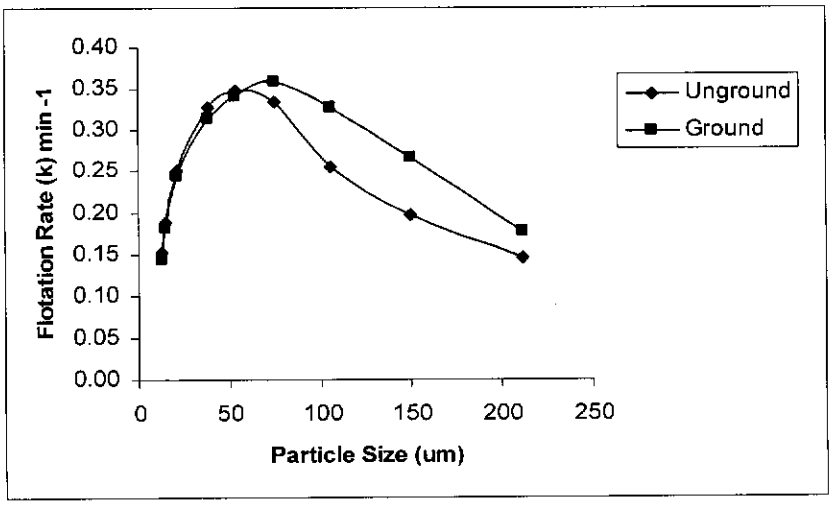

Figure 59.0: Gold flotation rate constants as a function of particle size

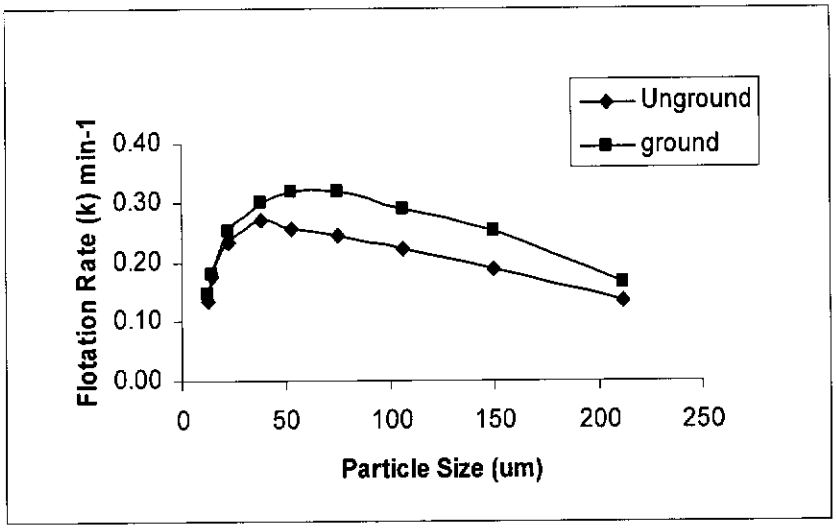

From figures 56.0 to 59.0, the effect of particle size on cleaner flotation rate and recovery is apparent. The most floatable size envelope is clearly seen. Higher flotation rate constants are found in the intermediate size ranges whilst at both coarse and fine size ranges, lower flotation rate constants for both copper and gold were observed. The reason for poor floatability of coarse and fine particle sizes has been widely studied. Fine particles are not readily attached to bubbles because they lack sufficient inertia or

momentum to establish the necessary contact with air bubbles and hence have a lower probability of collision. In contrast, recovery of coarse particles is affected by the disruption of the bubble-particle aggregate in the turbulent zone (due to their high inertia), as well as their decrease in buoyancy force relative to the pulp. Furthermore, insufficient coverage of collector on the coarse particles may occur as a result of the indiscriminate consumption of collector by fine particles (Trahar 1981; Yoon 2000; Nguyen et al. 1997, Dai et al.2000, Ahmed & Jameson 1989).

A comparison of Figures 56.0 and 57.0 with Figures 58.0 and 59.0 shows an interesting contrast. The first two figures show an increase in copper recovery in the fine fractions, due to regrind, whereas the second two figures show an increase in flotation rate of the coarse fractions as a result of regrind. In explanation of the change in flotation rate, for coarse particles the fresh surfaces caused by regrind have enhanced floatability, via enhanced hydrophobicity (buoyancy). However, fresh surfaces on fine particles will not change their lack of inertia and therefore limited contact with bubbles. As regards the increased recovery of fine Cu (and not coarse) after regrind, this may be explained via the shift in grade of the size fractions (to higher grade at finer fractions) due to regrind. Therefore, for a lower head grade for higher fractions after regrind, even with higher flotation rate, overall recovery may be similar. And for smaller size fractions with higher head grades after regrind, a similar flotation rate will produce a higher recovery relative to the same tailings value.

In summary, it is apparent that with an increase in copper in the finer, more liberated size fractions after grinding, overall recovery of copper was increased. It may be noted that recent studies confirm that regrinding of the intermediate products not only increased liberation of the particles but more significantly, increased the particle floatability (Sutherland et al. 1988; Morizot et al. 1997; Frew & Davey 1993; Lynch et al. 1981; Runge et al. 1997).

7.2.3 Pulp Chemical Measurements

Pulp chemical analysis was conducted with and without regrind of the cleaner survey samples. The methodology applied was similar to that described in section 3.2.2. Results are plotted in Figures 60-63. The dissolved oxygen (DO) readings of Figure 60.0 and 61.0 are expressed as a percentage of saturation. The DO demand curves may be compared with previous results (Ok Tedi oxygenated mill water) which show trends from 100% to 80% saturation for aerated mill water (Morey & Grano 2000). Figures 60.0 and 61.0 show that the cleaner feed stream after regrind has a higher oxygen demand than without regrind. The dissolve oxygen drops from 100 to 55% compared to a 100 to 70% decrease in the absence of regrind. This indicates a greater consumption of oxygen by the fresh sulphide particle surfaces generated by regrind. It should be noted that the oxygen demand was not affected by the regrinding media which was of high chromium content.

Figure 60.0: Dissolve oxygen demand curves for the cleaner feed and tail streams in the presence of regrind

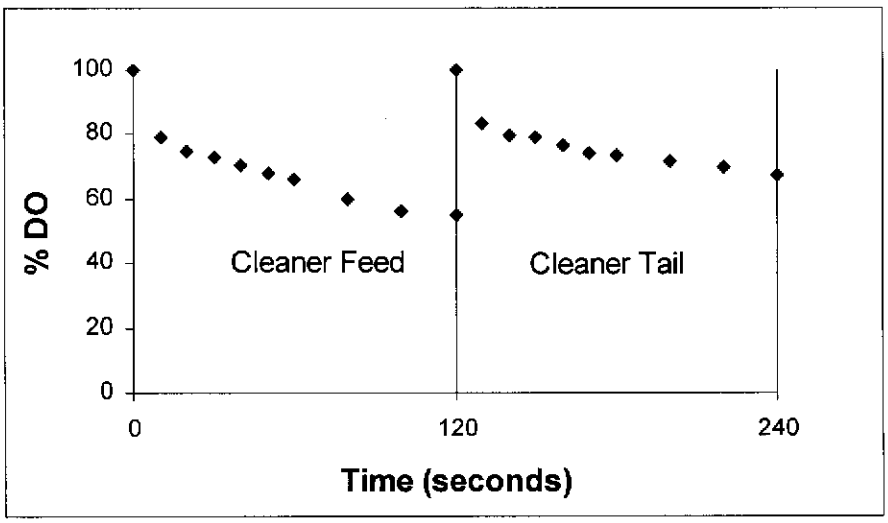

Figure 61.0: Dissolve oxygen demand curves for the cleaner feed and tail streams in the absence of regrind

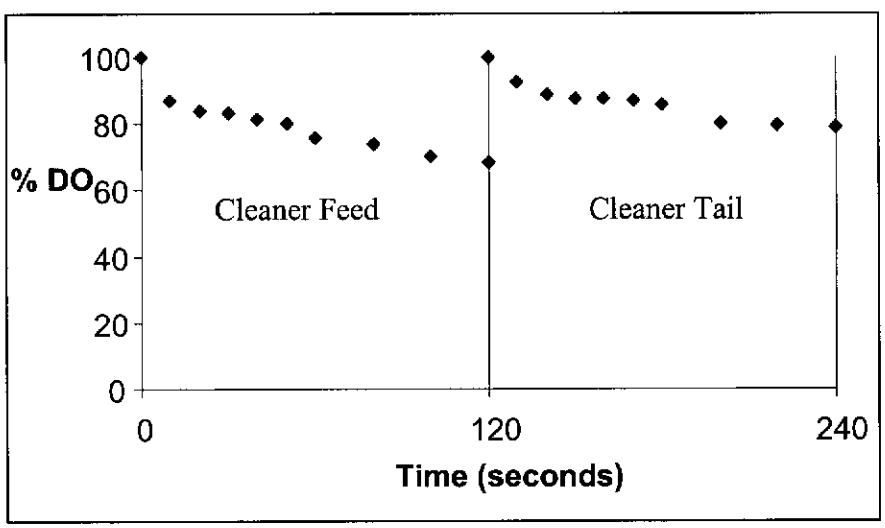

Similar trends for pulp potential are shown in Figures 62.0-63.0. It is apparent from these figures that cleaner feed pulp aeration was adequate to maintain an optimum pulp Eh of +200 mV (vs SHE) with and without regrind (cf. Ralston 1991; Trahar 1984).

Figure 62a: Eh and DO analysis for the cleaner feed stream in the presence of regrind

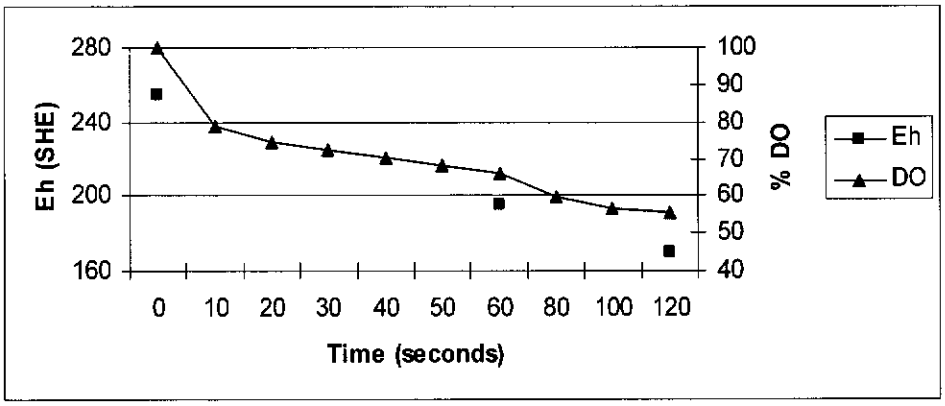

Figure 62b: Eh and DO analysis for the cleaner tail stream in the presence of regrind

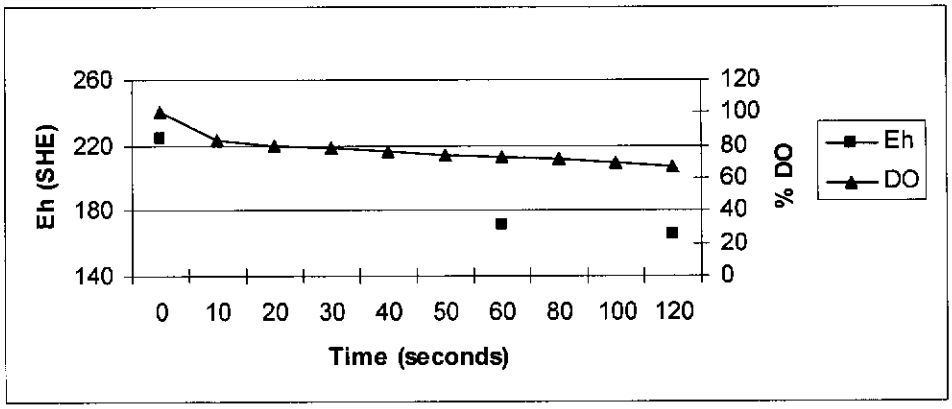

Figure 63a: Eh and DO analysis for the cleaner feed stream in the absence of regrind

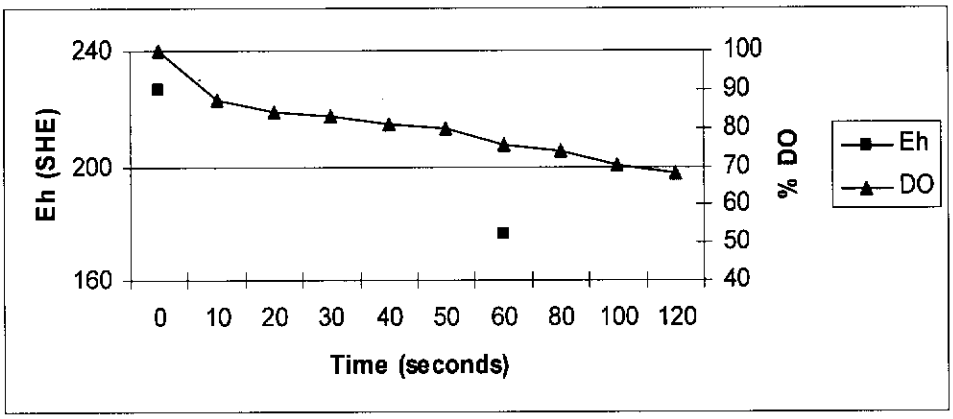

Figure 63b: Eh and DO analysis for the cleaner tail stream in the absence of regrind

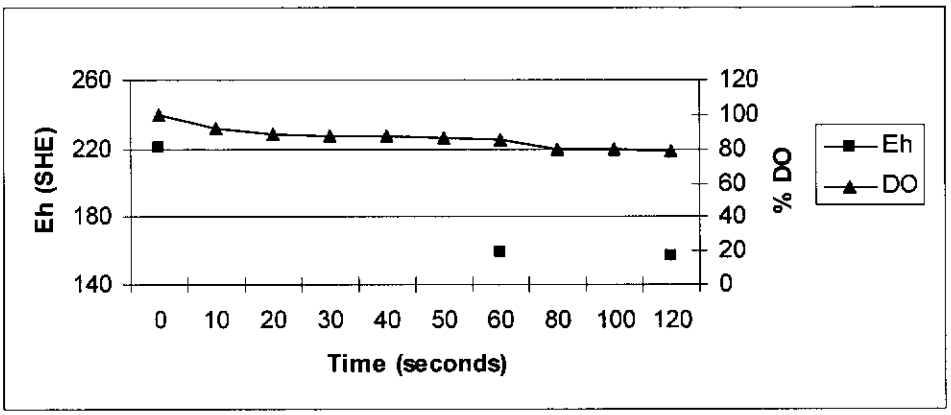

From these figures it is apparent that the Eh was influenced by the DO, showing a strong correlation under a steady pH of 10.0 for the cleaner feed and tail stream during the surveys. The presence of oxygen, of course, will affect the oxidation potential. Figure 60.0 shows a dissolved oxygen decrease from 100 to 50% in two minutes, and indicates a strong oxygen demand of the pulp particles after regrind. This suggests that particle surfaces are fresh and reactive and would react with oxygen and chemical agents. Such fresh particle surfaces are likely to react with collector, adsorbing collector via electrochemical reaction, particularly at the Eh of the pulp (+200 mV SHE) (Poling 1976; Chander 1988, Pang & Chander, 1992).

In contrast, Figure 61.0 shows dissolved oxygen decreasing from 100 to 70% over the two minute interval. This indicates a weaker oxygen demand in the absence of regrind. This suggests that particles in this stream are probably electrochemically passivated with coatings of hydroxide or collector or both. Under this condition the sulphide mineral surface would be less available for electrochemical reaction with the collector molecule. Furthermore, the cleaner tail streams for both test conditions showed similar trends with low oxygen demand. This suggests that particles in the cleaner tailing were passivated with oxide coatings (hydrophilic). In order to verify the formation of oxide coatings, EDTA extraction tests were performed with the results shown in Tables 38.0 and 39.0. Results are presented as % extraction relative to that chemical elements concentration in the solids sample extracted from the pulp.

Table 38.0: EDTA extractable metal ions in the presence of regrind

Stream	% Cu	% Fe	% S	% Ca
Cleaner feed	0.094	1.83	0.049	2.54
Cleaner concentrate	0.049	3.72	0.010	0.673
Cleaner tail	1.08	2.78	1.50	8.76

Table 39.0: EDTA extractable metal ions in the absence of regrind

Stream	% Cu	% Fe	% S	% Ca
Cleaner feed	0.108	1.46	0.053	3.24
Cleaner concentrate	0.065	3.45	0.012	0.689
Cleaner tail	1.31	2.68	0.847	8.13

A comparison of Tables 38.0 and 39.0 show that the cleaner feed pulp in the absence of regrind contained more EDTA extractable metal ions, suggesting surface coatings of hydroxides. The less EDTA extractable metal ions after regrind suggests that regrinding of the cleaner feed has resulted in cleaner particle surfaces with less oxide coatings. This would enable better flotation than for the un-ground particles. The cleaner tail stream for both test conditions showed increased EDTA extractable metal ions compared to feed or concentrate streams. This also correlated with lower oxygen demand. The increase in EDTA extractable metal ions suggests greater surface coverage by metal hydroxides on the tailings mineral particles (and hence reduced hydrophobicity and depressed flotation response). In order to ascertain the formation of hydroxide coatings on the mineral surfaces, ToFSIMS analysis was performed on the first cleaner concentrate and tail of each survey and is described below.

7.2.4 Particle Surface Analysis by ToFSIMS

ToFSIMS analysis of cleaner cell 1 concentrate and cleaner tail was performed for each surveys with and without regrind. The specific objective was to derive statistical differences in surface concentration of hydrophobic and hydrophilic species, comparing concentrate and tail samples. For each sample, approximately 40 chalcopyrite particles were examined and the data statistically analyzed. The results for the concentrate and tail samples with regrind are shown by Figures 64.0 and 65.0. These results are quantitative regarding the surface characteristics of the chalcopyrite. Error bars are shown in Figure 64.0, indicate 95% confidence in the results. The actual values of surface intensities for each species examined are also given in the Tables below the bar graphs. Since the intensities are normalized relative to the mineral substrate, comparison can be made between like species from different analyses. Figure 65.0 shows the 'overall hydrophobicity index', which is a ratio of the surface concentrations of predominant hydrophobic species relative to predominant hydrophilic species. It also shows collector 'exposure' or surface concentration on the samples examined. Collector 'exposure' or surface concentration is measured by the normalized intensity of collector chemical compounds such as PO_2 and PO_3.

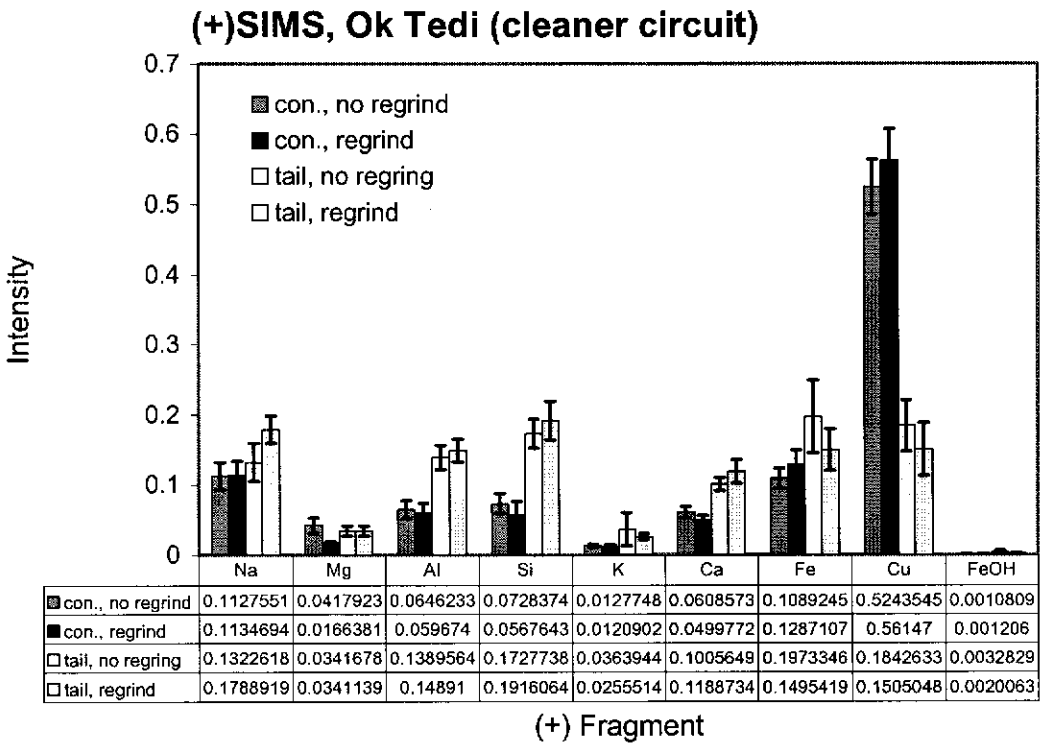

	Na	Mg	Al	Si	K	Ca	Fe	Cu	FeOH
con., no regrind	0.1127551	0.0417923	0.0646233	0.0728374	0.0127748	0.0608573	0.1089245	0.5243545	0.0010809
con., regrind	0.1134694	0.0166381	0.059674	0.0567643	0.0120902	0.0499772	0.1287107	0.56147	0.001206
tail, no regring	0.1322618	0.0341678	0.1389564	0.1727738	0.0363944	0.1005649	0.1973346	0.1842633	0.0032829
tail, regrind	0.1788919	0.0341139	0.14891	0.1916064	0.0255514	0.1188734	0.1495419	0.1505048	0.0020063

(+) Fragment

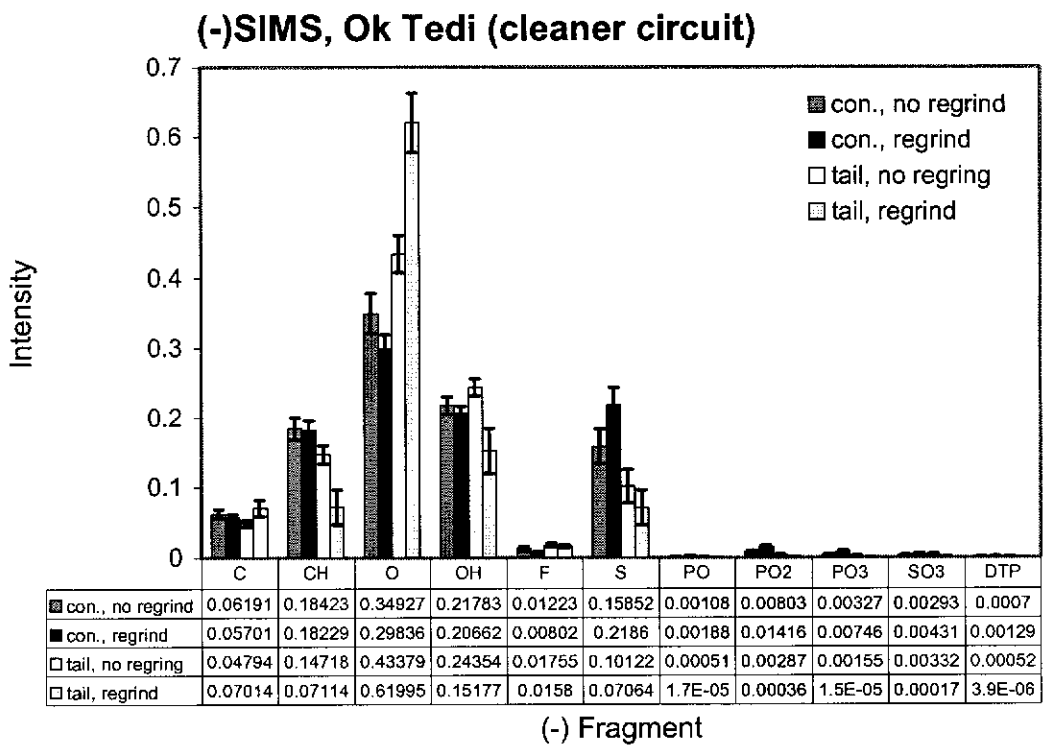

	C	CH	O	OH	F	S	PO	PO2	PO3	SO3	DTP
con., no regrind	0.06191	0.18423	0.34927	0.21783	0.01223	0.15852	0.00108	0.00803	0.00327	0.00293	0.0007
con., regrind	0.05701	0.18229	0.29836	0.20662	0.00802	0.2186	0.00188	0.01416	0.00746	0.00431	0.00129
tail, no regring	0.04794	0.14718	0.43379	0.24354	0.01755	0.10122	0.00051	0.00287	0.00155	0.00332	0.00052
tail, regrind	0.07014	0.07114	0.61995	0.15177	0.0158	0.07064	1.7E-05	0.00036	1.5E-05	0.00017	3.9E-06

(-) Fragment

Figure 64.0: (+) and (-) mass spectra for chalcopyrite in cleaner concentrate and cleaner tail – effect of regrind (confidence intervals calculated for P=95%)

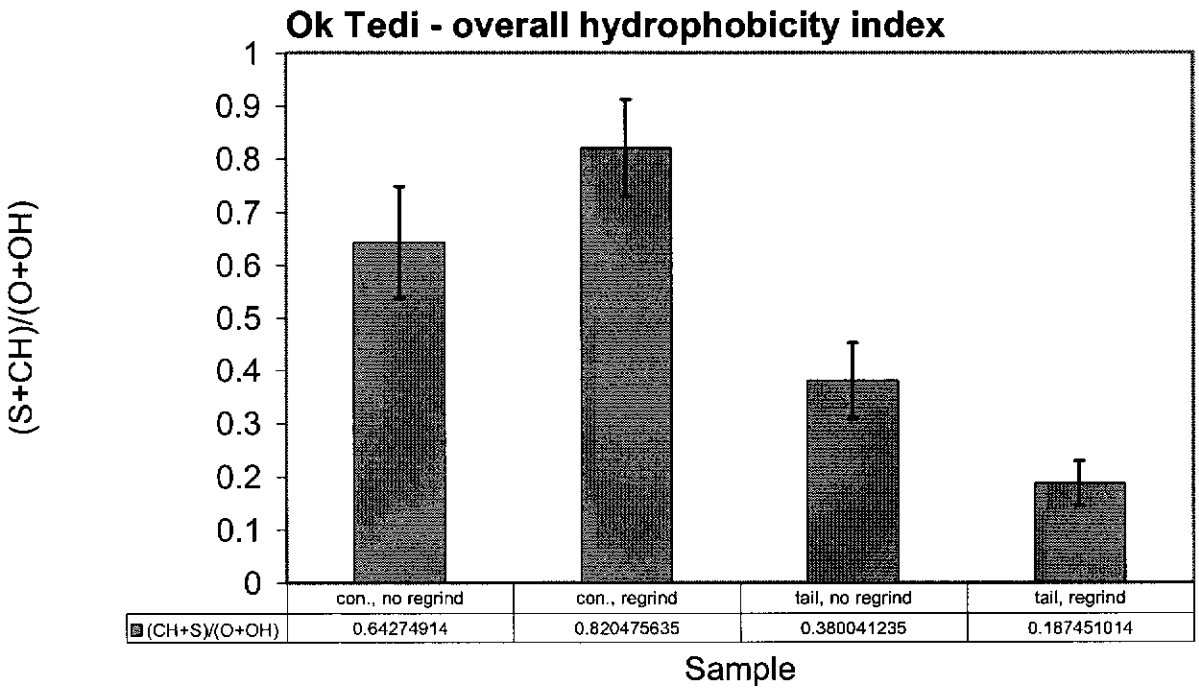

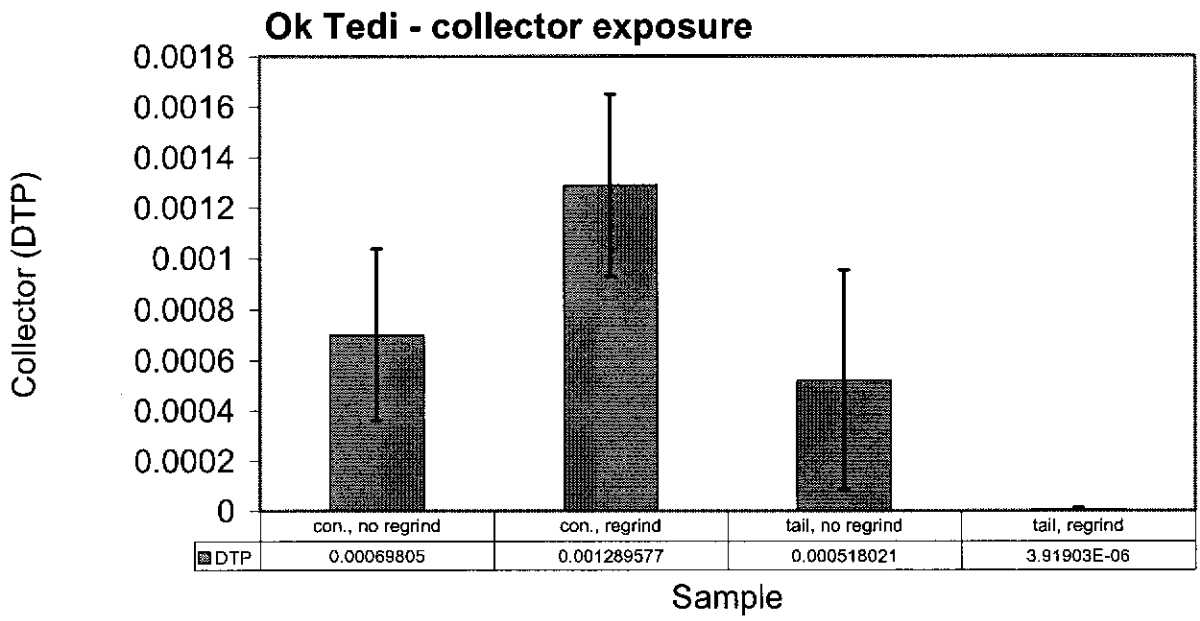

Figure 65.0: Selected spectral characteristics of chalcopyrite in cleaner tail and cleaner concentrate – effect of grinding (confidence intervals calculated for P=95%)

From the ToF-SIMS results of Figures 64.0 and 65.0, it is apparent that there is some overlap of the error bars for:

- Collector exposure for concentrate product in the absence of regrind and in the presence of regrind.
- Collector exposure for concentrate (regrind) and tail (no grind).
- Overall hydrophobicity index for concentrate (no regrind) and concentrate (regrind).

In this situation, a Student's't' test was undertaken for each pair to determine whether the differences between the means are significant. That is, the difference for the analysed pair is statistically significant only if the calculated value of t (t_{calc}) is larger than the corresponding critical one (t_{crit}). The results are provided in Table 40.0.

Table 40.0: Results of Student't' test

Samples	Measure	t_{calc}	t_{crit}		Test result
			95% significance	98% significance	
Con, unground Con, ground	Overall Hydrophob.	2.63	2.01	2.40	Different (even for 98%)
Con, unground Con, ground	Collector exposure	2.48	2.01	2.40	Different (even for 98%)
Con, unground Tail, ground	Collector exposure	2.87	2.02	2.43	Different (even for 98%)

The results show that the calculated value of t (t_{calc}) is larger than the critical values and that indicates that the difference is significant. Based on the statistical data the following concluding remarks are drawn:

- Regrind increased the overall hydrophobicity of chalcopyrite that reported to the cleaner concentrate (and therefore its flotation rate constant). This was due to the removal of oxide coatings.

- Regrind decreased the hydrophobicity (and rate constant) of chalcopyrite that reported to cleaner tailing. This was due to the absence of collector on reground tailings chalcopyrite. The reason may be that for no regrind, the presence of surface hydroxides or locked gangue balanced the presence of collector, resulting in transfer to tailings. After regrind, locked gangue or hydroxides were absent, and these collector coated particles went to the concentrate.
- The increase in hydrophobicity of chalcopyrite in the concentrate after regrind can be attributed to a net increase in surface hydrophobic species relative to hydrophilic. This was due to removal of hydroxide or composite particle and possibly collector adsorption. It is apparent that the increased exposure of clean chalcopyrite could facilitate an increased adsorption of collector.
- The decreased hydrophobicity of chalcopyrite in the tailing after regrind can be attributed to a lack of collector adsorption on these particles, along with increase oxide exposure on chalcopyrite surfaces relative to that in the concentrate stream.
- It is therefore apparent that the floatability of chalcopyrite in the cleaner circuit in the presence of regrind, is governed by the surface exposure of DTP collector, and hydroxide coatings.
- In the case of chalcopyrite flotation in the cleaner circuit in the absence of regrind, the surface exposure of DTP on chalcopyrite in the concentrate and tailings samples was statistically the same. That is, the chalcopyrite floatability was not governed primarily by collector adsorption, but by other factors (such as liberation and oxide coatings).
- The spectral intensities of Figure 64.0 also show that chalcopyrite floatability depends upon the surface exposure of iron and copper. The higher the exposure of copper, the higher the mineral floatability. In contrast, the higher the exposure of iron (oxide) the lower the mineral floatability.
- The spectra further indicate the presence of Al, Si, and Ca overlayers on chalcopyrite. Higher surface exposure of these species correlated with a lower hydrophobicity of chalcopyrite.

Based on these results, it is apparent that with regrind and the generation of fresh particles surfaces, the floatability of chalcopyrite was governed primarily by collector adsorption and liberation effects. This suggests that additional collector may further enhance

chalcopyrite recovery in the presence of regrind. Since chalcopyrite floatability was not governed by collector in the absence of regrind, a mineralogical investigation was performed to clarify whether chalcopyrite floatability was affected by poor liberation or other mineralogical effects. It may be noted that recovery by size data presented in section 7.2.2 had already hinted at a possible liberation effect.

7.2.5 Mineralogical Examination

Mineralogical examination of cleaner tail samples was performed to provide information to help explain the reason for copper losses (cf. Coe 2002). The specific objective was to further determine the mode of copper losses in cleaner tailing. Summaries of the point counting analysis are shown in Tables 41.0 and 42.0 and are expressed as total copper distribution in the various particle size ranges.

Table 41.0: Estimated percentages of total copper sulphide occurrence in the cleaner tail under the condition without regrinding of the cleaner feed (Coe 2002)

Category	Total copper sulphide distribution (%)			
	-212+150	-150+106	-106+38	-38+13
Copper sulphide middlings with non-sulphide minerals	67	64	84	34
Copper sulphide middlings with other sulphide minerals	33	34	11	12
Free copper minerals	0	2	5	54
Total	100	100	100	100

Table 42.0: Estimated percentages of total copper sulphide occurrence in the cleaner tail under the condition with regrinding of the cleaner feed (Coe 2002)

Category	Total copper sulphide distribution (%)			
	-212+150	-150+106	-106+38	-38+13
Copper sulphide middlings with non-sulphide minerals	54	75	63	16
Copper sulphide middlings with sulphide minerals	43	20	19	29
Free copper minerals	3	5	18	55
Total	100	100	100	100

The results presented in Table 41.0 and 42.0 show total copper sulphide occurrence in four size ranges. Based on the mineralogical data derived from the two tailings samples, it is apparent that the feed to the cleaner circuit contained middlings of copper sulphide/ non sulphide and copper sulphide/sulphide minerals. Liberated copper minerals were also present. From Tables 41.0 and 42.0, it is apparent that without regrind, the total copper occurrence in all the size ranges is relatively higher in the copper sulphide/non sulphide middlings. This suggests that copper losses in the cleaner tail may be partly attributed to poor liberation. Copper losses were also apparent with regrind, especially in the coarse size ranges (-212 +38 μm), again due to limited liberation. This further suggests that the efficiency of the regrind mill may be low, although the total proportion of these coarse particles is small. It should be noted that mineralogical analysis presented in Chapter 5 (section 5.3.7), also indicated similar trends. From the tables it is apparent that the proportion of copper as liberated or combined was similar in each survey, suggesting similar ore blends.

Further analysis of the total percent loss of copper and gold in each size fraction in the cleaner tail with and without regrind (R.G.) was performed, with results shown in Figure 66.0. It is apparent from the figure that in the absence of regrind, the major losses for copper were in the coarse composites, while the gold losses were evenly spread. In contrast, for the condition with regrind, major losses of copper and gold occurred in the fine size ranges. However, the total losses were only 30% for copper and 25% for gold when compared to the no regrind condition. Therefore, overall the total losses of copper and gold decreased after regrind. However, it would appear from Figure 66.0 that there may be some evidence of overgrinding for the regrind case. This suggests that there may be a trade off between particle size and liberation effects in flotation recovery. Since the p80 of the cleaner feed (cyclone overflow) was 103 μm, it is suggested that a coarser cyclone overflow cut size of between 110-115 μm should be trialed.

Significant copper losses in the fines were found during an examination of the effect of regrind at the Escondida and Disputada concentrators (Bulatovic et al. 1998). Also, considerable loss of copper and gold were reported in the ultrafine fraction as a result of regrinding at Bajo De Alumbrera (Harbort et al. 2000). At Red Dog, regrinding was found to improve sphalerite recovery only in the presence of collector in the zinc retreatment

plant (Runge et al. 2004). It is apparent that the floatability of value minerals can be retarded by regrinding due to over-grinding. Furthermore, additional collector after regrinding may be required to render minerals hydrophobic.

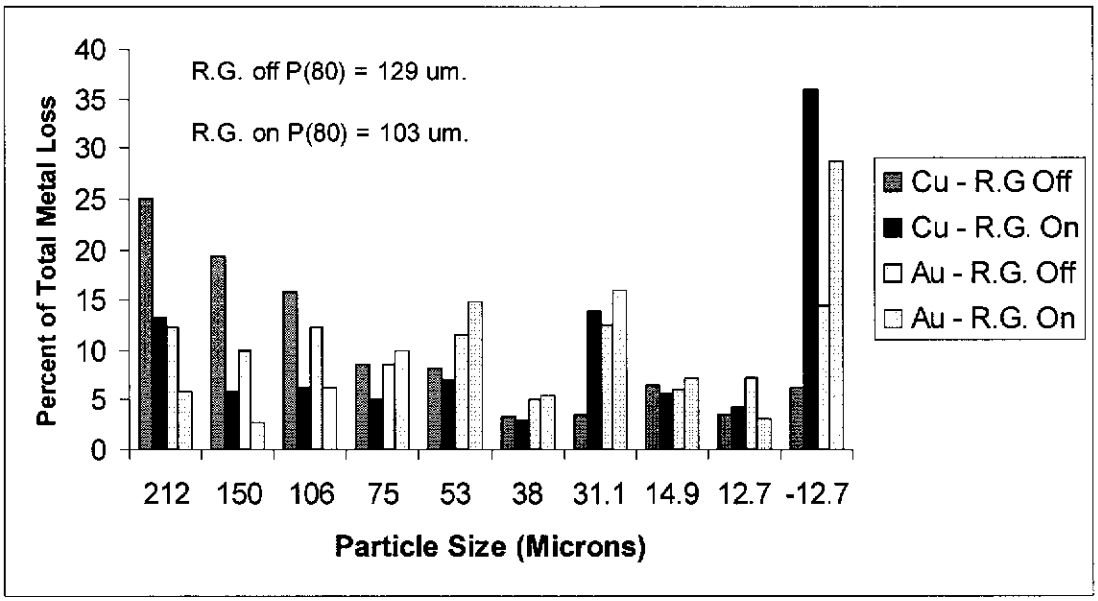

Figure 66.0: Distribution of total percent copper and gold losses in cleaner tailing with and without regrind

Photographs were taken for the polished sections used in mineralogical analysis of the tailings streams. Figures 67.0–72.0 show typical copper minerals and their mode of occurrence in the cleaner tailing with and without regrind conditions. Examples are shown of:

- Copper losses in the coarse size ranges as composites with non sulphide phases for both conditions.
- Liberated chalcopyrite and chalcopyrite in composite with non sulphides in the coarse size fractions with inclusions of gold particles.
- Gold inclusions with sulphides and non sulphides.

  This suggests that gold with non sulphides may not be recovered whilst losses associated with copper minerals may be recovered by flotation.

Furthermore, the presence of native copper (Figure 69.0) and traces of cuprite, including other oxide minerals were also found in the coarse size ranges (-212+38 μm). The presence of oxide copper minerals would increase the total percent of copper losses in the cleaner tailing.

Figure 67.0: Shows chalcopyrite/digenite with greater amount of /non-opaque gangue (-106+38 μm) in the cleaner tail with regrind

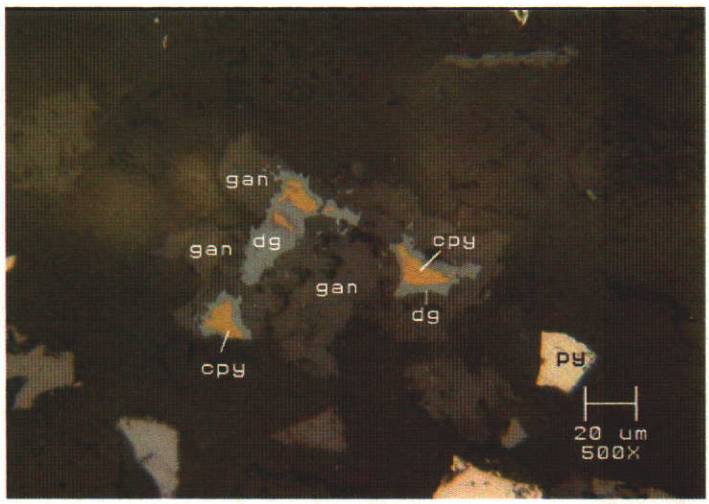

Figure 68.0: Shows gold locked in a particle with chalcopyrite/digenite (-212+150 μm) in the cleaner tail with regrind

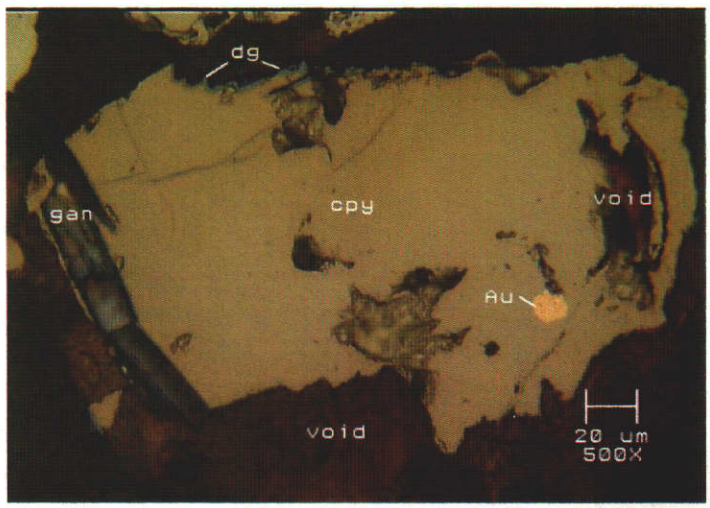

Figure 69.0: Shows a digenite/covellite particle and native copper (-150+106 μm) in the cleaner tail with regrind

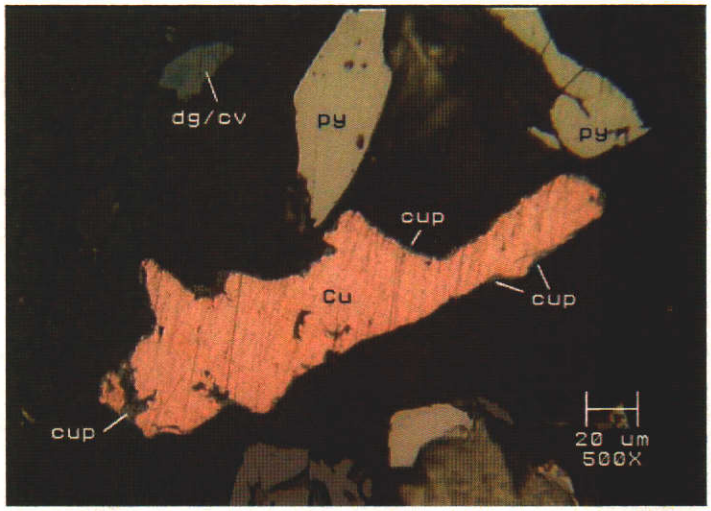

Figure 70.0: Shows a particle containing two gold grains locked with marcasite/chalcopyrite/non-opaque gangue (-212+150 μm) in the cleaner tail without regrind

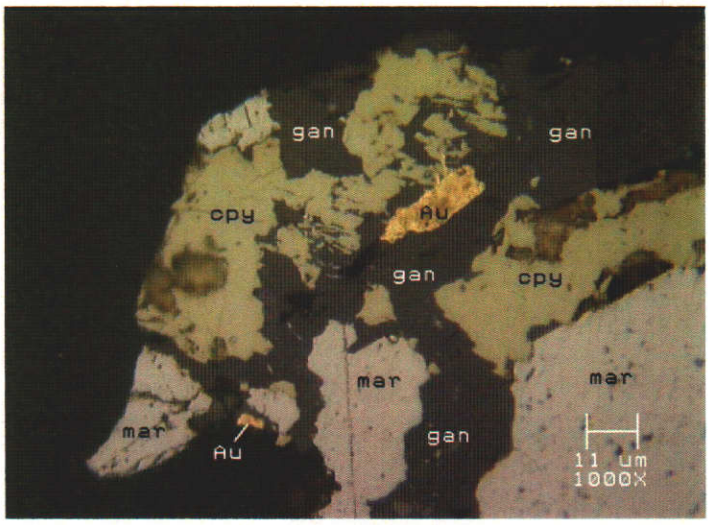

Figure 71.0: Shows two copper sulphide/non-opaque gangue middlings (-150+106 μm) in the cleaner tail without regrind

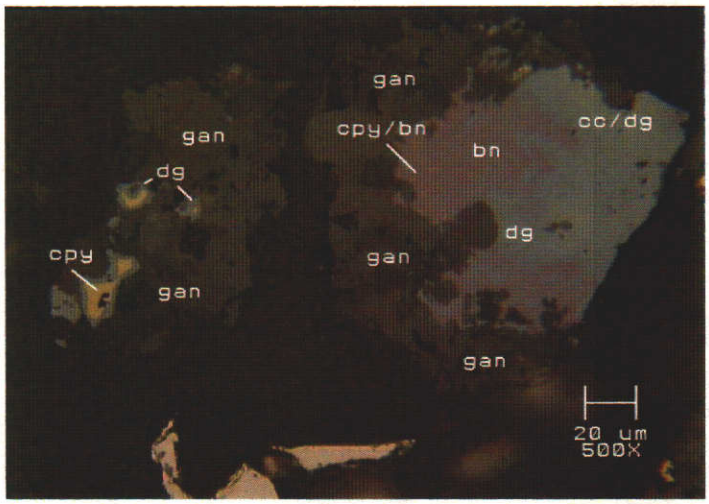

Figure 72.0: Shows chalcopyrite locked with non-opaque gangue and a free digenite/chalcopyrite particle (-38+13 μm) in the cleaner tail without regrind

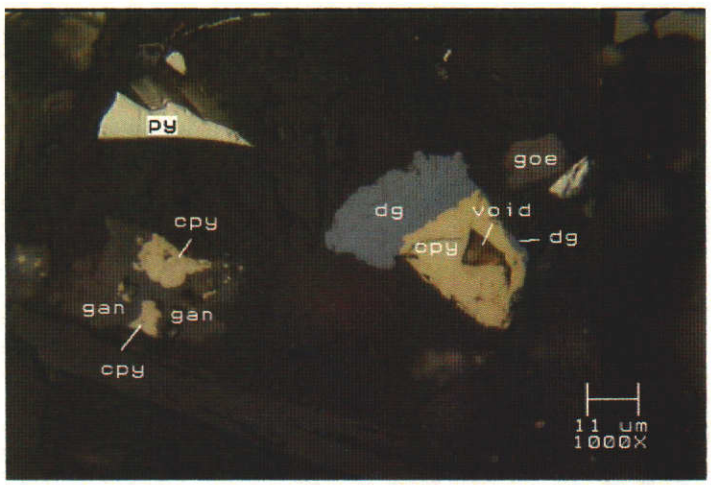

7.3 Conclusions and Recommendations

The mineralogical examination of un-ground and re-ground feed, with respect to cleaner flotation performance has shown evidence suggesting that regrinding is justified and beneficial to cleaner flotation. Regrind showed a high copper recovery of 97.9%, compared to 94.8% in the cleaner bank. Gold recovery remained unchanged, at 96% for both conditions. Possible reasons for the flotation behaviours with and without regrind are supported by the different analytical techniques:

- Size by size kinetics of the cleaner flotation circuit showed relatively low flotation rate constants for copper and gold with unground cleaner feed. This was attributed to the coarser particle size distribution (F80 of 129 μm) and probably composite particles in these coarse fractions. Pulp chemical analysis of the cleaner feed stream revealed a low oxygen demand, suggesting coated (passivated) particle surfaces. This is supported by the presence of slimes on the particle surface as indicated by EDTA analysis results. Furthermore, mineralogical examination of the cleaner tail samples revealed that total copper occurrence associated with sulphide and non sulphide middlings was relatively high across all size ranges (-212 +13 μm). This suggested that poor liberation was contributing to reduced copper recovery in the cleaners. Further, the total percent copper and gold distribution analysis in each size fraction in the cleaner tailing showed that a major loss of copper was in the coarse size fractions while gold was observed to be evenly spread in all size fractions. Particle surface analysis by time of flight secondary ion mass spectrometry (ToF-SIMS) analysis of chalcopyrite in the concentrate and tail revealed the same degree of hydrophobicity in the unground case. This suggested that the floatability of chalcopyrite was not dominated by collector in the un-ground case.

- When the cleaner flotation feed was subjected to regrind, a finer size distribution was produced (p80 of 103 μm). The flotation rate constants for copper and gold in the coarser fractions increased as a result, probably due to particle surface cleaning. The pulp chemical analysis revealed higher oxygen demand for the cleaner feed stream with less EDTA extractable ions after regrind. This suggests

that the particle surfaces were cleaner and more reactive to collector adsorption. Floatability of the particles would therefore be enhanced. ToFSIMS results indicated that the floatability of chalcopyrite was governed by the collector (DTP) adsorption in the reground case. Based on the hydrophobicity index of the chalcopyrite, a higher level of hydrophobicity was observed for chalcopyrite in the concentrate while a much low level was observed for chalcopyrite in the tail. In this case, as liberation is improved by regrinding, additional collector was required to render the minerals hydrophobic. Further, mineralogical examination of copper losses in the cleaner tail indicated that the copper losses were predominantly in the fines (-38+13 μm), with some as composites with non sulphides and sulphides in the coarse size range (-212+38 μm) after regrind. The total percent copper and gold distribution in each size fraction in the cleaner tailing after regrind indicated major losses of copper and gold in the ultrafines.

It is apparent that overall favourable flotation conditions resulted with regrind of cleaner feed pulp. For further developmental work, the addition of collector to the cleaner circuit is highly recommended as suggested by the ToFSIMS studies. Possible evidence of overgrinding for the reground case suggests a trade off between particle size and liberation effects may result from regrind. Further investigation is recommended with a trial of a coarser cyclone overflow cut size of 110-115 μm, along with mineral liberation analysis to determine the optimum liberation size.

CHAPTER 8: SUMMARY, CONCLUSIONS AND RECOMMENDATIONS

In this concluding chapter, the results of this investigation are briefly reviewed, and the implications for cleaner flotation performance summarised. Recommendations based on the findings are also presented, along with proposed further work.

8.1 Review of Project Outcomes

The aim of this research project was to investigate reasons for copper and gold losses from the cleaner tailings of the Ok Tedi Concentrator, and to examine methods for improved flotation performance in the cleaner bank. The project objectives therefore were to (1) characterize cleaner circuit performance, showing causal evidence for losses of valuable minerals to the cleaner tailings, (2) trial possible solutions in the laboratory, and (3) trial laboratory successes in the concentrator. Project outcomes in relation to these objectives are summarized in the following section.

8.1.1 Cleaner Circuit Characterization as a Function of Ore Blend

Cleaner circuit flotation performance was studied as a function of ore blend, blends being characterized as 'good' or 'bad' depending on the flotation response of the cleaner bank, all other variables being similar. Pulp and surface chemical analysis was used to correlate pulp parameters with flotation performance.

The findings with respect to the flotation response of 'good' and 'bad' ore blends were:

- ◊ Size by size kinetic analysis for the 'good' ore blend showed copper and gold recoveries between 95–98% in the particle size range between 22-100 μm. The flotation rate constant for copper was found to be high in this most floatable size ranges but was lower below 22 μm and above 100 μm, which is typical of mineral flotation systems. The flotation rate constant for gold particles was lower than for copper, with significant losses to cleaner tailing in all size ranges.

However, the highest gold losses were in the less floatable coarse (+100 μm) and fine (-22 μm) fractions, as for copper. Losses for both copper and gold were greatest in the coarse (+100 μm) fraction. Flotation rate constants for the 'bad' feed day, were lower than for the 'good' feed day.

- ◊ Surface chemical and pulp solution analyses for the 'good' ore feed survey, showed a high dissolved oxygen (DO) demand curve for the cleaner feed and concentrate streams and a low DO demand curve for the cleaner tail stream. The low DO demand of the tailing was found to correlate with increased concentrations of oxide, indicated by EDTA analysis. This suggested possible layers of oxide coatings on the particle surfaces. These results suggested that many particles in the cleaner feed stream were highly floatable because the sulphide surface was exposed for collector adsorption, and because there was little oxide depressant coatings on the surfaces of these sulphide particles. However, the sulphide particles with a greater coating of oxide depressant species on their surfaces tended to transfer to the cleaner tail stream.
- ◊ Surface analysis using ToF-SIMS supported EDTA analysis. A higher particle surface exposure of hydrophilic species (O, OH) was found on the chalcopyrite particle surfaces in the cleaner tail, relative to cleaner conc. ('good' feed blend). For the 'bad' feed blend, higher levels of oxide, and the deposition of copper on pyrite were observed, suggesting depressed flotation generally as indicated by a lower flotation rate constant, and also poor selectivity due to the copper activation of pyrite. Increase levels of collector were also observed on pyrite where copper was present.
- ◊ Pulp potentials were lower for the 'good' ore blend survey (200 mV SHE), compared to the 'bad' survey (350 mV SHE). This correlated with the consumption of oxygen by the exposed sulphide mineral surfaces for the 'good' ore, and passivated particles surfaces coated with oxides for the 'bad' ore.

From the above summary of results for 'good' and 'bad' surveys of the cleaner bank with regrind of cleaner feed, it was apparent that pulp and surface chemical analysis combined to give a clear picture of the reasons for poorer flotation performance on a 'bad' day. The primary reasons were ore related, with oxide coatings decreasing particle hydrophobicity,

and slowing flotation rate. Furthermore, concentrate grade was diluted by pyrite activated by oxide copper and collector. The formation of covellite rimming on pyrite (see pp.129, Figure 49.0) was a clear indication of pyrite activation in the pit, and makes the pyrite difficult to depress in flotation.

8.1.2 Cleaner Flotation Response with Un-ground Cleaner Feed

Cleaner flotation response was also characterized as a function of un-ground feed (without regrind). The objective was to establish whether regrinding of the cleaner feed was beneficial to cleaner flotation via the reduction of coarse composite particle numbers and a possible particle surface cleaning mechanism. Outcomes from this work included:

- ◊ A copper recovery of 94.8% was observed in the cleaner bank for the flotation of un-ground feed compared to 97.9% for re-ground cleaner feed. There was no observable difference for gold recovery in both conditions, suggesting that gold recovery may be governed by other factors.
- ◊ Lower flotation rate constants for copper and gold were observed without regrind, compared to the re-ground case. This was attributed to the coarser size distribution (F80 of 129 μm cf. 103 μm) with increased levels of coarse composite particles floating more slowly.
- ◊ Particle surface analysis by ToFSIMS, in the presence of regrind showed that the floatability of chalcopyrite was governed by the collector (DTP) adsorption. A higher level of DTP was observed on chalcopyrite, in the concentrate whilst a lower level was observed on chalcopyrite in the tail. The results suggest that loss of chalcopyrite in the cleaner tail could be partially affected by low hydrophobicity resulting from low DTP adsorption. Conversely ToFSIMS analysis without regrind showed similar levels of collector exposure on chalcopyrite in both the concentrate and tail. This result suggested that the floatability was not governed by collector adsorption for the un-ground case. Floatability of the unground case was more strongly influenced by particle size and hydrophilic surface coatings. Surface exposure of hydrophilic coatings on chalcopyrite was slightly higher in the absence of regrind.

- ◊ Mineralogical examination of the cleaner tail sample in the absence of regrind indicated that total copper occurrence associated with sulphide and non sulphide middlings was relatively high across coarse size ranges. These composite particles were less floatable due to reduced exposure of collector (which adsorbs electrochemically to copper sulphides). The percentage of ore in these size ranges was greater for the un-ground case. Therefore, poor liberation was contributing to reduced copper recovery, with major copper losses in the coarse size fractions. This contrasted with the re-ground case, where copper losses were predominately in the fines (-38 μm), with some losses as composites with non sulphides and sulphides in the coarse size ranges.

From the above summary of cleaner bank flotation performance as a function of regrind, it is apparent that regrind was beneficial, providing increased flotation recovery of copper and similar recovery of gold. Improved cleaner flotation performance was found to be due to the reduction in less floatable coarse composites as a percentage of the feed, and a freshening of particle surfaces (removal of oxide coatings). It is possible that an addition of collector to the regrind stage may have been beneficial, as there was reduced collector exposure on chalcopyrite in the cleaner tailing after regrind. However, over-grind is also a possibility if the correct cyclone balance is not obtained, potentially resulting in increased losses of ultra-fine particles after the regrind stage.

8.1.3 Laboratory Evaluation of Methods to Improve Cleaner Flotation Recovery

Laboratory flotation as a function of pulp chemical variables was performed on concentrator cleaner feed samples, with the objective of improving cleaner flotation performance. Outcomes included:

- ◊ A pH increase from 10.0 to 12.0, resulted in an increase in copper recovery from 94.0 to 98.0% and gold recovery from 90.0 to 94.0%. There was no apparent change in concentrate grade indicating that selectivity against gangue minerals such as pyrite was maintained.

- ◊ An addition of 27 g/t std collector relative to cleaner feed at pH 11.0, increased the recovery of copper from 96.3 to 98.9% and gold from 92.1 to 97.5%. This correlated with a slight decrease in concentrate grade. These results suggest that copper and gold recovery in the cleaner circuit may increase with addition of collector to cleaner feed.
- ◊ Laboratory flotation of cleaner feed as a function of hydrodynamic conditions including agitation rate and aeration rate were performed. Results for agitation tests suggested an optimum agitation rate could be found, balancing rates of particle–bubble collision and attachment against detachment at higher levels of pulp turbulence. The laboratory cell gave optimum flotation performance at 600 rpm and pH 11.0. The Eh was 235 mV (SHE) and no additional collector was added. Copper and gold recovery improved to 98% and 95%, respectively. The concentrate grade was not affected and was steady at 12% copper and 11 g/t gold. Similarly for aeration rate tests, the results indicated that at an optimum could be found, balancing attachment rate versus froth collapse at higher air additions. For lab tests, an aeration rate of 15 l/min, at pH 11.0 and Eh of 245 mV (SHE) with no additional collector, gave an optimal copper recovery of 97.8%. There was no observed change in gold recovery at 93.3 %. Concentrate grades were similar at 13% copper and 12 g/t gold. These flotation tests demonstrated the impact of hydrodynamic conditions on the efficiency of the flotation process, and the criticality of good cell mixing and aeration. It is difficult to alter agitation rates in the Cleaner bank, although alternative agitators for Denver DR500 cells are available. Aeration rates may be checked using instrumentation such as the JKTech Jg probe (Power et al. 2000).
- ◊ Cleaner flotation as a function of cell residence time was also assessed. An additional 2.25% copper and 2.86% gold recovery was achievable with extended flotation of the cleaner tail sample. This suggests that loss of copper and gold in the cleaner tail may be in part attributable to insufficient flotation time. It is apparent that 2-3% of Cu and Au particles in the cleaner feed have very low flotation rate constants under normal hydrodynamic conditions. These particles may be ultra fines, recovered with increased agitation rates (previous paragraph) or slow floating coarse composite particles.

8.1.3.1 Laboratory Trial Implications for Cleaner Circuit Performance

◊ Laboratory flotation tests indicated that increased lime and collector to cleaner feed would result in increased copper and gold recovery without loss of grade. These results were directly transferable to concentrator trials. Residence time trials were also performed in the concentrator cleaner bank as a function of plant throughput. Furthermore, tests on flotation cell hydrodynamic conditions suggested increased agitation and aeration may improve recovery. Cleaner bank cell aeration was studied using the JKTech Jg probe and gas holdup probe. Increased agitation rate however, was more difficult to trial in the plant and was not included in this study.

8.1.4 Plant Trials of Hydrodynamic Conditions and Residence Time

◊ Residence time investigations in the Concentrator cleaner bank determined that a mean residence time of 12 minutes was observed at a SAG throughput of 2148 dry tonnes per hour. This compared with a design value of 13.8 minutes for a dry tonnage of 1879 and suggest that loss of copper and gold in the cleaner tail is probably influenced by inadequate residence time, at higher SAG throughputs (above 1879 dry tonnes). Residence time issues were posted for future work.

◊ Aeration efficiency within the cleaner bank cells was investigated using Jg and Holdup probes. Results indicated that there was an uneven distribution of superficial gas velocity (J_g) and gas hold up (ϵ_g) across individual cells. This suggests that poor air dispersion is limiting the availability of bubbles for particle-bubble collision and the transfer of hydrophobic particles to the froth phase. Aeration and agitation issues were posted for future work.

8.1.5 Plant Trials of Collector and Lime to Improve Cleaner Flotation Recovery

Examination of the effect of collector and lime addition to the cleaner circuit was undertaken as a result of the ToFSIMS findings that showed: (i) the loss of chalcopyrite to tailings may have been due to low surface exposure of collector species on chalcopyrite, and (ii) the presence of activated pyrite in the cleaner concentrate. Furthermore, laboratory trials showed significantly improved cleaner flotation performance with additional collector or an increase in pH from 10.0 to 12.0.

The findings with respect to concentrator cleaner flotation trials included:

- ◊ Addition of lime increased both copper and gold recoveries by 5 and 6 percent, respectively, and with a 90% statistical confidence level.
- ◊ Addition of lime increased the Tank cell concentrate grade by 3% for copper and 4 g/t for gold with no affect on cleaner concentrate grade.
- ◊ Addition of collector to regrind (cleaner feed) resulted in a marginal (1%) improvement in gold recovery. Copper recovery was unchanged as were the cleaner concentrate copper and gold grades.

8.2 Conclusions and Recommendations

This project has followed the logical progression of cleaner bank characterization via plant surveys and pulp chemical and surface analysis techniques. Pulp and surface chemical techniques gave consistent evidence to explain poor flotation performance as resulting from oxide coatings, limited collector coverage and activation of pyrite by copper. Mineralogical analysis indicated liberation issues when regrind was not used. Laboratory flotation tests suggested lime and collector addition would improve cleaner flotation performance, along with improved hydrodynamic conditions.

Plant trials were then successfully implemented with increased lime addition to cleaner feed via the regrind stage, and were statistically verified. Both copper and gold recoveries were improved, with grades maintained. Collector trials did not show any verifiable improvement, although trends were as expected.
It is apparent therefore that at pH 12, the cleaner bank grade/recovery curves had shifted to the right, providing increased recovery of valuable minerals, with less associated gangue. Probable mechanisms for the depression of pyrite at pH 12 include:

- ◊ More $Ca(OH)_2$ precipitates on pyrite particle surfaces.
- ◊ Less collector adsorption to pyrite. Collector adsorption onto pyrite surfaces decreases exponentially beyond pH 10.

It may be noted that the maintenance of concentrate grade with increased recovery implies no increased recovery of coarse composite particles. Rather, additional recovery came from liberated particles, possibly from the finer fractions. A possible mechanism for the increased hydrophobicity of the finer particles as a function of increased pH, includes dispersion of hydroxide coatings of copper from value mineral sulphide particle surfaces as $Cu(OH)_3^-$. As the pH moves away from the iso electric point (point of zero charge) for $Cu(OH)_2$ ppt around pH 9.5-10, and towards pH 12, the concentration of $Cu(OH)_2$ ppt will decrease exponentially as the $Cu(OH)_3^-$ concentration increases.

The strong recommendation of this study therefore, is that the pH regime in the Ok Tedi concentrator cleaner bank be changed from a natural pH at cleaner feed of approx. 10.5, to

a controlled pH of 12. It is further recommended that future work be undertaken to confirm potential benefits observed in some tests of this study.

8.3 Future Work

A number of outcomes from the test results of this study warrant further investigation, as at present no clear conclusions can be made regarding potential benefits. Further work which may show benefit includes:

- ◊ Hydrodynamic characterization studies for the cleaner flotation cells as a function of air dispersion, and agitation are recommended. It may be noted that the Denver DR500 cells may be retrofitted with modified agitator mechanisms, some of which may be trialed at OTML. A study should be conducted to compare air dispersion (profile across the cell) and also flotation rate for adjacent cells in the same bank, comparing the old style and more recently designed modified agitators.
- ◊ Further development work is required to establish if additional cleaner cell capacity is warranted. A Supaflo pilot Tank cell is available on site for pilot scale trials to identify if increased recoveries are significant, and if the concentrate can be upgraded to final concentrate grade.
- ◊ Collector addition tests at laboratory scale showed significant improvement to recovery of copper in cleaner flotation. However, brief plant trials were inconclusive. It is possible that results were limited in the plant trials due to low collector addition rates. Further trials of collector addition to cleaner feed (low grade regrind) are recommended, including higher collector additions.

REFERENCES

Adam, K. & Iwasaki, I. 1984, 'Grinding media-sulfide mineral interaction and its effect on flotation', *Trans SME/AIME*, pp. 66-80.

Ahmed, N. & Jameson, G.J. 1989, 'Flotation kinetics', in *Frothing in Flotation*, J.S. Laskowski (ed), Gordon and Breach Science Publishers, New York, pp. 77-99.

Alexander, D. 2002, *Short course in hydrodynamic measurement*, Presented to Ok Tedi Mining Limited, JKTech, University of Queensland, Brisbane.

Allison, S.A., Harris, P.J. & Nicol, M.J. 1982, 'Interactions between sulphide minerals and metal ions in the activation, deactivation, and depression of mixed- sulphide ores', *Mintek*, no. M29, pp. 1-31.

Amdel 1999, *Mineralogical investigation of the Ok Tedi cleaner scavenger tailing*, Report to Ok Tedi Mining Limited, Dated 31st May 1999, Amdel, Adelaide.

AMTEL 2000, *Gold and copper deportment in the taranaki zone*, Report to Ok Tedi Mining Limited, Dated 15th May 2000, AMTEL, Canada.

Arbiter, N. 1984, 'The flotation cell - a critique', in M.H. Jones & J.T. Woodcock (eds), *Principle of Mineral Flotation,* The Australasian Institute of Mining and Metallurgy, Parkville, Vic., pp. 301-311.

Ata, S., Ahmed, N. & Jameson, G.J. 2002, 'Collection of hydrophobic particles in the froth phase', *International Journal of Mineral Processing*, vol. 64, no. 2-3, pp. 101-122.

Ball, B. & Rickard, R.S. 1976, 'The chemistry of pyrite flotation and depression', in *Flotation-A.M.Gaudin Memorial Volume*, M.C. Fuerstenau (ed), AIME, U.S.A.

Basilio, C.I, Kartio, I.J. & Yoon, R.H. 1996, 'Lead activation of sphalerite during galena flotation', *Minerals Engineering*, vol. 9, no. 8, pp. 869-879.

Bentli, I. & Kaya, M. 2000, 'Flotation hydrodynamics', in *Proceedings of the 8th International Mineral Processing Symposium*, Turkey, G. Ozbayoglu, C. Hosten, M.U. Atalay, C. Hicyilmaz, & A.I. Arol (eds), A.A. Balkema Publishers, U.S.A., pp. 263-268.

Boulton, A., Fornasiero, D. & Ralston J. 2003, 'Characterisation of sphalerite and pyrite flotation samples by XPS and ToF-SIMS', *International Journal of Mineral Processing*, vol. 70, pp. 205-219.

Buckley, A.N. & Woods, R. 1984, 'An X-ray photoelectron spectroscopic study of the oxidation of chalcopyrite', *Aust. J. Chem.*, 37, pp. 2403-2413.

Buckley, A.N. & Woods, R. 1997, 'Chemisorption - the thermodynamically favoured process in the interaction of thiol collectors with sulphide minerals', *International Journal of Mineral Processing*, 51, pp. 15-26.

Buckley, A.N., Goh, S.W., Lamb, R.N. & Woods, R. 2003, 'Interaction of thiol collectors with pre-oxidised sulphide minerals', *International Journal of Mineral Processing*, vol. 72, no. 1-4, pp. 163-174.

Bulatovic, S.M., Wyslouzil, D.M. & Kant, C. 1998, 'Operating practices in the beneficiation of major porphyry copper/molybdenum plants from chile: Innovated technology and opportunities, a Review', *Minerals Engineering*, vol. 11, no. 4, pp. 313-331.

Castro, S.H. & Mayta, P.E. 1994, 'A kinetics approach to the effect of particle size on the flotation of molybdenite', in *Proceedings of the IV Meeting of the Southern Hemisphere on Mineral Flotation; and III Latin-American Congress on Froth Flotation'*, S.Castro & J. Alvarez (eds), Flotation Volume II, A. Sutulov Memorial Volume, Chile, pp. 331-343.

Cecile, J.L. 1985, 'Application of XPS in the study of sulphide mineral flotation - a Review', in *Flotation of Sulphide Minerals*, K.S.E Forssberg (ed), Development in Mineral Processing, vol. 6, Elsevier, New York, pp. 61-80.

Chander, S & Khan, A. 2000, 'Effect of sulphide dioxide on flotation of chalcopyrite', *International Journal of Mineral Processing*, 58, pp. 45-55.

Chander, S. 1988, 'Electrochemistry of sulphide mineral flotation', *Minerals and Metallurgical Processing*, vol. 5, no. 3, pp. 104-113.

Chander, S. 1991, 'Electrochemistry of sulphide flotation: Growth characteristics of surface coatings and their properties, with special reference to chalcopyrite and pyrite', *International Journal of Mineral Processing*, 33, pp. 121-134.

Chen, G., Grano, S., Sobieraj, S. & Ralston, J. 1999, 'The effect of high intensity conditioning on the flotation of a nickel ore, Part 2: Mechanisms', *Minerals Engineering*, vol. 12, no. 11, pp. 1359-1373.

Cheng, X. & Iwasaki, I. 1992, 'Effect of chalcopyrite and pyrrhotite interaction on flotation separation', *Minerals and Metallurgical Processing*, pp. 73-79.

Cho, Y.S. & Laskowski, J.S. 2002, 'Effect of flotation frothers on bubble size and foam stability', *International Journal of Mineral Processing*, 64, pp. 69-80.

Clarke, P., Fornasiero, D., Ralston, J. & Smart, R. St. C. 1995, 'A study of the removal of oxidation products from sulfide mineral surfaces', *Minerals Engineering*, vol. 8, no. 11, pp. 1347-1357.

Coe, E.J. 2002, *A technical service report on copper and gold occurrences in cleaner tails from 'bad' feed survey # 2 and low grade regrind 'on' and 'off' tests from Ok Tedi mining limited*, Dated June 2002, Cytec, Mineral Processing Chemical, Stamford, U.S.A.

Cornish, B. 1997, *Flotation reconfiguration project-metallurgical justification*, Internal Memorandum, Ok Tedi Mining Limited, Papua New Guinea.

Cutting, G.W., Barber, S.P. & Newton, S. 1986, 'Effects of froth structure and mobility on the performance and simulation of continuously operated flotation cells', *International Journal of Mineral Processing,* 16, pp. 43-61.

Dai, Z., Fornasiero, D. & Ralston, J. 2000, 'Particle-bubble collision models: a Review', *Advances in Colloid and Interface Science*, 85, pp. 231-256.

Deglon, DA., Egya-Mensah, D. & Franzidis, J.P. 2000, 'Hydrodynamics and metallurgical characterization of industrial flotation banks for control purposes', *Minerals Engineering*, vol. 13, no. 3, pp. 235-244.

Derjaguin, B.V. & Dukhin, S.S 1961, 'Theory of flotation of small and medium size particles', *Transactions of the Institute of Mining and Metallurgy*, 70, pp. 221-246.

Dichmann, T.K. & Finch, J.A. 2001, 'The role of copper ions in sphalerite-pyrite flotation selectivity', *Minerals Engineering*, vol. 14, no. 2, pp. 217-225.

DiFeo, A., Rao, S.R. & Finch, J.A. 2004, 'Interpretation of high base consumption in the flotation of gypsum-containing ores', *Minerals Engineering*, 17, pp. 557-559.

Dunglison, M. 2000, *Unit 1 flotation surveys*, Report to Ok Tedi Mining Limited, JKTech, Dated August 2000, University of Queensland, Brisbane.

Dunglison, M., Alexander, D. & Stark, S. 2001, *Characterisation of the Ok Tedi flotation Circuit–MLA Report*, Report to Ok Tedi Mining Limited, JKTech, Dated April 2001, University of Queensland, Brisbane.

Ekmekci, Z. & Demirel, H. 1997, 'Effects of galvanic interaction on collectorless flotation behaviour of chalcopyrite and pyrite', *International Journal of Mineral Processing*, 52, pp. 31-48.

Engelbrecht, J.A. & Woodburn, E.T. 1975, 'The effects of froth height, aeration rate, and gas precipitation on flotation', in *Journal of The South African Institute of Mining and Metallurgy*, pp. 125-131.

England, J.K. 1993, Copper concentrator practice at Ok Tedi mining limited, Papua New Guinea, in *Proceedings of the Australasian Institute of Mining and Metallurgy*, J.T.Woodcock, & J.K. Hamilton (eds), The Sir Maurice Mawby Volume, Second Edition, The Aus.I.M.M., Melbourne, pp. 661-665.

Erepan, P. 2000, Recovery of gold and copper from tailings at the Ok Tedi mining limited, *Postgraduate Diploma Thesis in Metallurgy*, W.A. School of Mines, Curtin University of Technology, Western Australia.

Finch, J.A. & Dobby, G.S. 1990, *Column flotation,* Pergamon Press, New York.

Finch, J.A., Xiao, J. & Gomez, C.O. 2000, 'Gas dispersion properties: bubble surface area flux and gas holdup', *Minerals Engineering*, vol. 13, no. 4, pp. 365-372.

Finkelstein, N.P. & Allison S.A. 1976, 'The Chemistry of activation, deactivation and depression in the flotation of zinc sulfide: a Review', in *Flotation-A.M.Gaudin Memorial Volume*, M.C. Fuerstenau (ed), AMIE, U.S.A., vol. 1, pp. 414-450.

Finkelstein, N.P. 1997, 'The activation of sulphide minerals for flotation: a Review', *International Journal of Mineral Processing*, 52, pp. 81-120.

Forrest, K. 1998, Optimisation of gold recovery by selective gold flotation, *B Eng Thesis*, W.A. School of Mines, Curtin University of Technology, Western Australia.

Frew, J.A. & Davey, K.J. 1993, 'Effect of liberation on the flotation performance of a complex ore, in *Proceedings of the XVIII International Mineral Processing Congress*, Sydney, pp. 905-912.

Fuerstenau, D.W. 1982a, 'Activation in the flotation of sulphide minerals', in R.P. King (ed), *Principles of Flotation*, South African Institute of Mining and Metallurgy, Johannesburg, pp. 183-198.

Fuerstenau, D.W. 1982b, 'Mineral-water interfaces and the electrical double layer', in R.P. King (ed), *Principles of Flotation*, South African Institute of Mining and Metallurgy, Johannesburg, pp. 17-51.

Gardner, J. R. &Woods, R. 1979, 'An electrochemical investigation of the natural floatability of chalcopyrite', *International Journal of Mineral Processing*, 6, pp. 1-16.

Gaudin, A.M. 1939, *Principles of Mineral Processing*, Chapter 16, McGraw-Hill, New York.

Goncalves, K.L.C, Andrade, V.L.L. & Peres, A.E.C. 2003, 'The effect of grinding conditions on the flotation of a sulphide copper ore', *Minerals Engineering*, vol. 16, no. 11, pp. 1213-1216.

Gorain, B.K., Franzidis, J.P. & Manlapig, E.V. 1995, 'Studies on impeller type, impeller speed and air flow rate in an industrial scale flotation cell. Part 1: Effect of bubble size distribution', *Minerals Engineering*, vol. 8, no. 6, pp. 615-635.

Gorain, B.K., Franzidis, J.P. & Manlapig, E.V. 1996, 'Studies on impeller type, impeller speed and air flow rate in an industrial scale flotation cell. Part 3: Effect on superficial gas velocity', *Minerals Engineering*, vol. 9, no. 6, pp. 639-654.

Gorain, B.K., Burgess, F., Franzidis, J.P. & Manlapig, E.V. 1997a, 'Bubble surface area flux-a new criterion for flotation scale-up, in *Proceedings of the Sixth Mill Operators' Conference*, Aus.I.M.M., Madang, Papua New Guinea, pp. 141-148.

Gorain, B.K., Franzidis, J.P. & Manlapig, E.V. 1997b, 'Studies on impeller type, impeller speed and air flow rate in an industrial scale flotation cell. Part 4: Effect of bubble surface area flux on flotation performance', *Minerals Engineering*, vol. 10, no. 4, pp. 367-379.

Gorain, B.K., Harris, M.C., Franzidis, J.P. & Manlapig, E.V. 1998, 'The effect of froth residence time on the kinetics of flotation', *Minerals Engineering,* vol. 11, no. 7, pp. 627-638.

Grano, S., Ralston, J. & Smart, R.St.C. 1990, 'Influence of electrochemical environment on the flotation behaviour of Mt. Isa copper and lead-zinc ore', *International Journal of Mineral Processing*, 30, pp. 69-97.

Grano, S.R., Wong, P.L.M., Skinner, W., Johnson, N.W. & Ralston, J. 1994, 'The effect of autogenous and ball mill grinding on the chemical environment and flotation of the copper ore of Mount Isa mines limited, Australia', in *Proceedings of the IV Meeting of the Southern Hemisphere on Mineral Flotation; and III Latin-American Congress on Froth Flotation*, S. Castro, & J. Alvarez (eds), Flotation Volume II, A. Sutulov Memorial Volume, Chile, pp. 351-367.

Greet, C.J., Grano, S.R., Netting, A.K.O. & Ralston, J. 1994, 'Surface analysis of plant flotation streams in the lead circuit of the Hellyer mine of Aberfoyle resources limited, Australia', in *Proceedings of the IV Meeting of the Southern Hemisphere on Mineral Flotation; and III Latin-American Congress on Froth Flotation*, S.Castro & J.Alvarez (eds), Flotation Volume II, A. Sutulov Memorial Volume, Chile, pp. 269-293.

Gron, P. 2001a, *Ok Tedi Flotation Circuit Optimisation Project, Progress Report II*, OTML Internal Memorandum, Dated 13th February 2001.

Gron, P. 2001b, *Ok Tedi Flotation Circuit Optimisation Project, Progress Report IV*, OTML Internal Memorandum, Dated 22nd June 2001.

Guo, H. & Yen, W.T. 2003, 'Pulp potential and floatability of chalcopyrite', *Minerals Engineering*, vol. 16, no. 3, pp. 247-256.

Guy, P.J. & Trahar, W.J. 1985, The effects of oxidation and mineral interaction on sulphide flotation, in *Flotation of Sulphide Minerals*, K.S.E. Forssberg (ed), Development in Mineral Processing, vol. 6, Elsevier, New York, pp. 91-110.

Harbort, G., Lauder, D., Miranda, J. & Murphy, A. 2000, 'Size by size analysis of operating characteristics of Jameson cell cleaners at the Bajo De Alumbrera copper/gold concentrator', in *Proceedings of the Seventh Mill Operators' Conference*, Aus.I.M.M., Kalgoorlie, Western Australia, pp. 207-220.

Harris, C.C. & Khandrika, S.M. 1985, 'Flotation machine design: Important hydrodynamic effects; Slight geometrical causes', *Powder Technology*, 43, pp. 243-248.

Harris, C.C. 1976, 'Flotation Machine', in *Flotation-A.M.Gaudin Memorial Volume*, M.C. Fuerstenau (ed), AMIE, U.S.A., vol. 2, pp. 753-815.

Hartati, F., Mular, M., Steward, A. & Gorken, A. 1997, 'Increased gold recovery at PT Freeport Indonesia using Aero 7249 promoter', in *Proceedings of the Sixth Mill Operators' Conference*, Aus.I.M.M., Madang, Papua New Guinea, pp. 165-168.

Hayes, P. 1993, *Process principles in minerals & materials production*, Hayes Publishing Co, Brisbane, pp. 107-108.

Hayes, R.A. & Ralston, J. 1988, 'The collectorless flotation and separation of sulphide minerals by Eh control', *International Journal of Mineral Processing*, 23, pp. 55-84.
Healy, T.W. 1984, 'Pulp chemistry, surface chemistry, and flotation', in M.H. Jones & J.T. Woodcock (eds), *Principle of Mineral Flotation,* The Australasian Institute of Mining and Metallurgy, Parkville, Vic., pp. 43-55.

Heiskanen, K. 2000, 'On the relationship between flotation rate and bubble surface area flux', *Minerals Engineering*, vol. 13, no. 2, pp. 41-149.

Heyes, G.W. & Trahar, W.J. 1977, 'The natural floatability of chalcopyrite', *International Journal of Mineral Processing*, 4, pp. 317-344.

Hintikka, V.V. & Leppinen, J.O. 1995, 'Potential control in the flotation of sulphide minerals and precious metals', *Minerals Engineering*, vol. 8, no. 10, pp. 1151-1158.

Jasieniak, M. 2003, *Investigation of pyrite and chalcopyrite by ToFSIMS*, Report to Ok Tedi Mining Limited, Dated 31st January, Ian Wark Research Institute, University of South Australia, Adelaide.

Jenkins, B.M. & Adair, B.M. 1996a, *The characterisation of six sulphide skarn ores from the Ok Tedi mine, using QEM*SEM*, Report to Ok Tedi Mining Limited, CSIRO Division of Minerals Report, DME 489, Australia.

Jenkins, B.M. & Adair, B.M. 1996b, *The characterisation of three porphyry ores from the Ok Tedi mine, using QEM*SEM*, Report to Ok Tedi Mining Limited, CSIRO Division of Minerals Report, DME 488, Australia.

JKMRC 1988, 'Flotation Manual', in *The optimization of mineral processes by modelling and simulation*, Submitted to AMIRA PL9, JKMRC, University of Queensland, Brisbane.

JKTech, 2001, *Characterisation of the Ok Tedi flotation circuit*, Report to Ok Tedi Mining Limited, Dated April 2001, JKTech, University of Queensland, Brisbane.

Kanau, J.L. & Katom, M. 1997, 'Operations and control of 32 feet diameter SAG mills', in *Proceedings of the Sixth Mill Operators' Conference*, Aus.I.M.M., Madang, Papua New Guinea, pp. 37-53.

Kant, C., Rao, S.R. & Finch, J. A. 1994, 'Distribution of surface metal ions among the products of chalcopyrite flotation', *Minerals Engineering*, vol. 7, no. 7, pp. 905-916.

Kelly, E.G. & Spottiswood, D.J. 1982, *Introduction to Mineral Processing*, John Wiley and Sons, New York, pp. 310-311.

Klimpel, R.R. 1999, 'Industrial experiences in the evaluation of various flotation reagent schemes for the recovery of gold', *Minerals and Metallurgical Processing*, vol. 16, no. 4, pp. 1-8.

Kuopanportti, H., Suorsa, T. & Pollanen, E. 1997, 'Effects of oxygen on kinetics of conditioning in sulphide ore flotation', *Minerals Engineering*, vol. 10, no. 11, pp. 1193-1205.

Kuopanportti, H., Suorsa, T., Dahl O & Niinimaki, J. 2000, 'A model of conditioning in the flotation of a mixture of pyrite and chalcopyrite ores', *International Journal of Mineral Processing*, vol. 59, pp. 327-338.

Laajalehto, K., Kartio, I. & Suoninen, E. 1997, 'XPS and SR-XPS techniques applied to sulphide mineral surfaces', *International Journal of Mineral Processing*, 51, pp. 163-170.

Laplante, A.R., Toguri, J.M. & Smith, H.W. 1983, 'The effects of air flow rate on the kinetics of flotation. Part 1: The transfer of material from the slurry to the froth', *International Journal of Mineral Processing*, 11, pp. 203-219.

Laskowski, J.S. 2001, *An electrokinetic investigation of the activation of sulphide minerals*, Lecture notes, W.A. School of Mines, Curtin University of Technology, Western Australia.

Lins, F.F. and Adamian, R. 1993, 'The influence of some physical variables on gold flotation', *Minerals Engineering*, vol. 6, no. 3, pp. 267-277.

Liu, Q. & Zhang, Y. 2000, 'Effect of calcium ions and citric acid on the flotation separation of chalcopyrite from galena using dextrin', *Minerals Engineering*, vol. 13. no. 13, pp. 1405-1416.

Luttrell, G.H. &Yoon, R.H. 1984, 'Surface studies of the collectorless flotation of chalcopyrite', *Colloids and Surfaces*, 12, pp. 239-254.

Lynch, A.J., Johnson, N.W., Manlapig, E.V. & Thorne, C.G. 1981, *Mineral and coal flotation circuits*, Volume 3, Elsevier Scientific Publishing Company, New York.

Majima, J. 1969, 'How oxidation affects selective flotation of complex sulphide ores', *Canadian Metallurgical Quarterly*, vol. 8, no. 3, pp. 269-273.

Met Engineers Ltd. 1999, *An Assessment of Flotation Performance*, Report to Ok Tedi Mining Limited, Dated August 1999, Met Engineers Ltd., Canada.

Morey, M.S & Grano, S.R. 2000, *Plant surveys on current skarn and porphyry sulfide ores at Ok Tedi*, Report to Ok Tedi Mining Limited, Dated September 2000, Ian Wark Research Institute, University of South Australia, Adelaide.

Morey, M.S., Grano, S.R., Ralston, J., Prestidge C.A. & Verity, B. 2001, 'The electrochemistry of Pb^{II} activated sphalerite in relation to flotation', *Minerals Engineering*, vol. 14, no. 9, pp. 1009-1017.

Morey, M.S. 1998, Improving galena/sphalerite selectivity at Hellyer: The lead activation of sphalerite; mechanisms and solutions, *Doctor of Philosophy Thesis in Applied Science in Chemical Technology*, Ian Wark Research Institute, University of South Australia, Adelaide.

Morizot, G., Conil, P., Durance, M.V. & Badri, F.G. 1997, 'Liberation and its role in flotation-based flowsheet development', *International Journal of Mineral Processing*, 51, pp. 39-49.

Nagaraj, D.R. & Brinen J.S. 2001, 'SIMS study of adsorption of collectors on pyrite', *International Journal of Mineral Processing*, vol. 63, pp. 45-57.

Neething, S.J. & Cilliers, J.J. 2002, 'The entrainment of gangue into a flotation froth', *International Journal of Mineral Processing*, 64, pp. 123-134.

Nguyen, A.V., Schulze, H.J. & Ralston, J. 1997, 'Elementary steps in particle-bubble attachment', *International Journal of Mineral Processing*, 51, pp. 183-195.

Ninduara, J. 2002, Personal Communication, Geologist at Ok Tedi Mining Limited, 04th April, 2002.

O'Connor, C.T., Botha, C., Walls, M.J. & Dunne, R.C. 1988, 'The role of copper sulphate in pyrite flotation', *Minerals Engineering*, no. 1, pp. 203-212.

Orwe, D. 2000, The influence of sodium hydrogen sulphide on porphyry sulphide copper recovery at Ok Tedi, *Master of Applied Science Thesis*, Ian Wark Research Institute, University of South Australia, Adelaide.

Orwe, D., Grano, S.R & Launder, D.W. 1998, 'Increasing fine copper recovery at the Ok Tedi concentrator, Papua New Guinea', *Minerals Engineering*, vol. 11, no. 2, pp. 171-187.

Orwe, D., Grano, S.R. & Lauder, D.W. 1997, 'Chalcocite oxidation and its influence on fine copper recovery at the Ok Tedi concentrator, Papua New Guinea', in *Proceedings of the Sixth Mill Operators' Conference*, Aus.I.M.M., Madang, Papua New Guinea, pp. 85-95.

Paki, O.K. & Erepan, C.P. 1997, 'Implementation of flash flotation in the Ok Tedi grinding circuit', in *Proceedings of the Sixth Mill Operators' Conference*, Aus.I.M.M., Madang, Papua New Guinea, pp. 125-132.

Pang, J. & Chander, S. 1992, 'Electrochemical characterization of the chalcopyrite/solution interface', *Minerals and Metallurgical Processing*, vol. 9, no. 3, pp. 131-136.

Pang, J. & Chander, S. 1993, 'Properties of surface films on chalcopyrite and pyrite and their influence in flotation', in *Proceedings of the XVIII International Mineral Processing Congress*, Sydney, pp. 669-677.

Peng, Y., Grano, S., Fornasiero, D. & Ralston, J. 2003, 'Control of grinding conditions in the flotation of chalcopyrite and its separation from pyrite', *International Journal of Mineral Processing*, vol. 69, no. 1-4, pp. 87-100.

Piantadosi, C. & Smart, R. St. C. 2002, 'Statistical comparison of hydrophobic and hydrophilic species on galena and pyrite particles in flotation concentrates and tails from TOF-SIMS evidence', *International Journal of Mineral Processing*, vol. 64, pp. 43-54.

Piantadosi, C., Jasieniak, M. & Smart, R.St.C. 2001, 'ToF-SIMS statistical analysis of surface hydrophobic/hydrophilic species and contact angle estimation in real ore systems', in *Proceedings of the Fourth UBC- McGill International Symposium on Fundamentals of Mineral Processing*, Canadian Institute of Mining, Metallurgy and Petroleum, Toronto, Canada, pp. 305-323.

Poling, G.W. & Beattie, M.J.V. 1984, 'Selective depression in complex sulphide', in M. H. Jones & J.T. Woodcock (eds), *Principle of Mineral Flotation*, The Australasian Institute of Mining And Metallurgy, Parkville, Vic., pp. 137-146.

Poling, G.W. 1976, 'Reactions between thiol reagents and sulphide minerals', in *Flotation-A.M.Gaudin Memorial Volume*, M.C. Fuerstenau (ed), AMIE, U.S.A., Volume 1, pp. 334-357.

Power, A., Franzidis, J-P. & Manlapig, E.V. 2000, 'The characterisation of hydrodynamic conditions in industrial flotation cells', in *Proceedings of the Seventh Mill Operators' Conference*, Aus.I.M.M., Kalgoorlie, Western Australia, pp. 243-255.

Ralston, J. & Grano, S. 1995, *Short course in the chemistry of sulphide mineral flotation*, Presented to Ok Tedi Mining Limited, Ian Wark Research Institute, University of South Australia, Adelaide.

Ralston, J. 1991, 'Eh and its consequences in sulphide mineral flotation', *Minerals Engineering*, vol. 4, no. 7-11, pp. 859-877.

Ramadan, A.M., Saleh, A.M. & Moharam, M.R. 1998, 'Parameters affecting hydrodynamics of conventional flotation cell, in *Proceedings of the 7th International Mineral Processing Symposium*, S. Atak, G. Onal, & M.S.(eds), Innovations in Mineral and Coal Processing, A.A. Balkema Publishers, U.S.A., pp. 241-244.

Rao, S.R., Labonte, G. & Finch, J.A. 1992, 'Electrochemistry in the plant', in *Innovations in Flotation Technology*, P.Mavoros & K.A. Matis (eds), Kluwer Academic Publishers, Netherlands, pp. 57-100.

Rao, S.R., Moon, K.S. & Leja, J. 1976, 'Effect of grinding media on the surface reactions and flotation of heavy metal sulphides', in *Flotation-A.M.Gaudin Memorial Volume*, M.C. Fuerstenau (ed), AMIE, U.S.A., Volume 1, pp. 509-527.

Ritcey, G.M. 1989, *Tailings management: problems and solutions in the mining industry*, Elsevier, New York, pp. 249-250.

Ritchie, I.M., Bailey, S. & Woods, R. 1999, 'The metal-solution interface', *Advances in Colloid and Interface Science*, 80, pp. 183-231.

Ross, V.E. 1998, 'Mechanisms operating in flotation froths', in *Frothing in Flotation II*, J.S. Laskowski & E.T.Woodburn (eds), Chapter 4, Gordon and Breach Science Publishers, The Netherlands.

Rubinstein, J.B. & Samygin, V.D. 1998, 'Effect of particle and bubble size on flotation kinetics', in *Frothing in Flotation II*, J.S. Laskowski & E.T.Woodburn (eds), Chapter 2, Gordon and Breach Science Publishers, The Netherlands.

Rumball, J.A. & Richmond G.D. 1996, 'Measurement of oxidation in a base metal flotation circuit by selective leaching with EDTA', *International Journal of Mineral Processing*, 48, pp. 1-20.

Runge, K., Manlapig, E. & Franzidis, J.P. 2004, 'Optimisation of flotation pulp selectivity utilising nodal analysis', in *Proceedings of the 36th Annual Meeting of the Canadian Mineral Processors*, The Canadian Institute of Mining, Metallurgical Petroleum, Ottawa, Canada, pp. 575-597.

Runge, K.C., Harris, M.C., Frew, J.A. & Manlapig, E.V. 1997, 'Floatability of streams around the Cominco Red Dog lead cleaning circuit', in *Proceedings of the Sixth Mill Operators' Conference*, Aus.I.M.M., Madang, Papua New Guinea, pp. 157-163.

Rush, P.M. & Seegers, H.J. 1990, 'Ok Tedi copper-gold deposits in geology of the minerals deposits of Australia and Papua New Guinea', F.E.Huges (ed), in *Proceedings of the Aus.I.M.M.*, Melbourne, pp. 1747-1754.

Schubert, H. & Bischofberger, C. 1978, 'On the hydrodynamics of flotation machines', *International Journal of Mineral Processing*, 5, pp. 131-142.

Schubert, H. & Bischofberger, C. 1998, 'On the microprocesses air dispersion and particle-bubble attachment in flotation machines as well as consequences for the scale-up of microprocesses', *International Journal of Mineral Processing*, 52, pp. 245-259.

Senior, G.D. & Trahar, W.J. 1991, 'The influence of metal hydroxides and collector on the flotation of chalcopyrite', *International Journal of Mineral Processing*, 33, pp. 321-341.

Senior, G.D., Trahar, W.J. & Guy, P.J. 1995, 'The selective flotation of pentlandite from a nickel ore', *International Journal of Mineral Processing*, 43, pp. 209-234.

Shannon, L.K. & Trahar, W.J. 1986, 'The role of collector in sulphide ore flotation', in P. Somasundaran (ed), *Advances in Mineral Processing*, pp. 408-425.

Sis, H. & Chander. S. 2003, 'Improving froth characteristics and flotation recovery of phosphate ores with nonionic surfactants', *Minerals Engineering*, vol. 16, no. 7, pp. 587-595.

Smart, R.St.C, Jasieniak, M., Prince, K.E. & Skinner, W.M. 2000, 'SIMS studies of oxidation mechanisms and polysulfide formation in reacted sulfide surfaces', *Minerals Engineering*, vol. 13, no. 8-9, pp. 857-870.

Smart, R.St.C. 1991, 'Surface layers in base metal sulphide flotation', *Minerals Engineering*, vol. 4, no. 7-11, pp. 891-909.

Song, S., Lopez-Valdivieso, A., Reyes-Bahena, J.L. & Lara-Valenzuela, C. 2001, 'Floc flotation of galena and sphalerite fines', *Minerals Engineering*, vol. 14, no. 1, pp. 87-98.

Subrahmanyam, T.V. & Forssberg, K.S.E. 1993, 'Mineral solution-interface chemistry in minerals engineering', *Minerals Engineering*, vol. 6, no. 5, pp. 439-454.

Sui, C.C., Brienne, S.H.R., Ramachandra Rao, S., Xu, Z. & Finch, J.A. 1995, 'Metal ion production and transfer between sulphide minerals', *Minerals Engineering*, vol. 8, no. 12, pp. 1523-1539.

Sui, C.S, Brienne, S.H.R., Xu, Z. & Finch, J.A. 1997, 'Xanthate adsorption on Pb contaminated pyrite', *International Journal of Mineral Processing*, 49, pp. 207-221.

Sutherland, D.N., Gottlies, P., Heyes, G.W. & Jackson, B.R. 1988, 'The influence of mineral locking on the flotation behaviour', in *Proceedings of the XVI International Mineral Processing Congress*, E.Forssberg (ed), Elsevier Science Publishers, Amsterdam, pp. 535-545.

Sutherland, K.L. & Wark, I.W. 1955, *Principles of flotation*, Australasian Institute of Mining and Metallurgy (Inc.), Melbourne, pp. 154-210.

Trahar, W.J. 1981, 'A rational interpretation of the role of particle size in flotation', *International Journal of Mineral Processing*, 8, pp. 289-237.

Trahar, W.J. 1984, 'The Influence of pulp potential', in M.H. Jones & J.T. Woodcock (eds), *Principle of Mineral Flotation*, The Australasian Institute of Mining and Metallurgy, Parkville, Vic., pp. 147-183.

Voigt, S., Szargan, R. & Suoninen, E. 1994, 'Interaction of copper (II) ions with pyrite and its influence on ethyl xanthate adsorption', *Surface and Interface Analysis*, vol. 21, no. 8, pp. 526-536.

Wang, X.H. & Xie, Y. 1990, 'The effect of grinding media and environment on the surface properties and flotation behaviour of sulphide minerals', in *Proceedings of Mineral Processing and Extractive Metallurgy Review*, vol. 7, pp. 49-79.

Warman International Ltd. 1981, *Cyclosizer instruction manual*, 2nd Revision, Warman International Limited, Sydney.

Weisener, C. & Gerson, A. 2000a, 'An investigation of the Cu (II) adsorption mechanism on pyrite by ARXPS and SIMS', *Minerals Engineering*, vol. 13, no. 13, pp. 1329-1340.

Weisener, C. & Gerson, A. 2000b, 'Cu (II) Adsorption mechanism on pyrite: An XAFS and XPS study', *Surface and Interface Analysis*, 30, pp. 454-458.

Weller, K.R., Gottlieb, P., Davey, K.J. & Richmond, G.D. 1997, 'An assessment of the role of regrinding in lead cleaner flotation at the Hellyer concentrator, Tasmania', *Erzmetallurgy*, no. 9, pp. 572-584.

Wills, B.A. 1997, *Mineral Processing Technology*, Pergamon Press, Sixth Edition, pp. 274-275.

Win, U.N. & Yan, D.S. 1992, 'Factors affecting the recovery and grade of complex lead-zinc ores by flotation', in *Proceedings of the Extractive Metallurgy of Gold and Base Metals*, Aus.I.M.M., Kalgoorlie, pp. 221-229.

Wiseman, D. 1997, *Technical software and process control applications for mineral industry*, Blackwood, South Australia.

Woods, R. 1984, 'Electrochemistry of sulphide flotation', in M.H. Jones & J.T.Woodcock (eds), *Principle of Mineral Flotation*, The Australasian Institute of Mining and Metallurgy, Parkville, Vic., pp. 91-115.

Yan, D.S. 1999, *Mineral processing course notes*, W.A. School of Mines, Curtin University of Technology, Western Australia.

Yelloji Rao, M.K. & Natarajan, K.A. 1989, 'Effect of electrochemical interactions among sulfide minerals and grinding medium on chalcopyrite flotation', *Minerals & Metallurgical Processing*, pp. 146-151.

Yianatos, J., Bergh, L., Condori, P. & Aguilera, J. 2001, 'Review of hydrodynamics and gas dispersion in flotation cells on South African platinum concentrators', *Minerals Engineering*, vol. 14, no. 9, pp. 1033-1046.

Yoon, R.H. 2000, 'The role of hydrodynamic and surface forces in bubble-particle interaction', *International Journal of Mineral Processing*, 58, pp. 129-143.

Zhang, Q., Xu, Z., Bozkurt, J. & Finch, J.A. 1997, 'Pyrite flotation in the presence of metal ions and sphalerite', *International Journal of Mineral Processing*, 52, pp. 187-201.

APPENDICES

APPENDIX #1

LABORATORY TESTWORK

Unit #1 Cleaner flotation bank residence time measurement

1.1 Concentration of salt tracer showing residence time of cleaner bank ('Bad' feed survey)

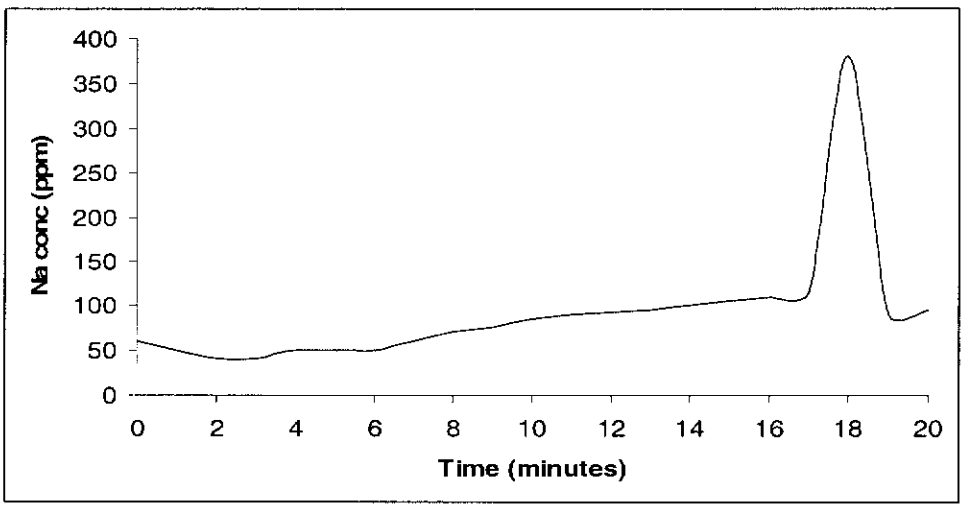

The mean residence time is indicated by the peak. The analysis indicates that the mean residence of the cleaner bank was 18 minutes at a SAG throughput of 2,232 dry tonnes per hour.

1.2 Concentration of salt tracer showing residence time of cleaner bank ('Good' Feed survey)

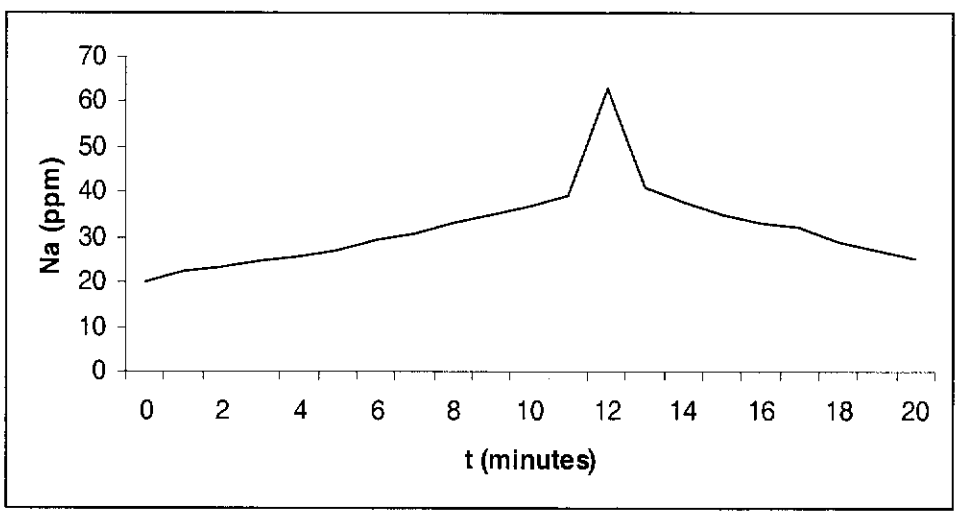

The mean residence time is indicated by the peak. The analysis indicates that the mean residence of the cleaner bank was 12 minutes at a SAG throughput of 2,148 dry tonnes per hour.

1.3 Pulp chemical data (plant feed & tail pulp)

1.3.1 Calibration data

Eh in Zobell solution	430 mV
Calibration Eh	416 mV
Offset Eh (Calibration Eh – Reference Eh)	14 mV
Reference potential Eh	199 mV
pH in Buffer	10.05

Pulp Eh conversion to SHE = Offset Eh + 199 mV + pulp Eh

1.3.2 Cleaner feed pulp

Time (sec)	Eh (mV)	Eh (SHE) (mV)	pH	DO (%)
0	35	248	10.7	98
10				95.4
20				91
30				84.3
40				78.4
50				73.2
60	-19	194	10.7	68.8
80				60.8
100				53.6
120	-26.6	186.4	10.7	48.6

1.3.3 Cleaner tail pulp

Time (sec)	Eh (mV)	Eh (SHE) (mV)	pH	DO (%)
0	216	429	10.96	102
10				88.1
20				86.5
30				85.3
40				84.7
50				84.1
60	161	374	11.2	84
80				81.9
100				80.2
120	129	342	11.2	78.7

APPENDIX #2

CLEANER CIRCUIT CHARACTERISATION STUDIES

2.1 Pulp chemical data (Cleaner circuit characterisation studies as a function of good feed)

2.1.1 Calibration data (survey on 02/08/01)

Eh in Zobell solution	430 mV
Calibration Eh	420 mV
Offset Eh (Calibration Eh – Reference Eh)	10 mV
Reference potential Eh	199 mV
pH in Buffer	10.05

Pulp Eh conversion to SHE = Offset Eh + 199 mV + pulp Eh

2.1.2 Cleaner feed pulp

Time (sec)	Eh (mV)	Eh (SHE) (mV)	pH	DO (%)
0	84	293	10.3	96.1
10				91.5
20				85.4
30				82.8
40				81.9
50				81
60	-12.2	196.8	10.5	80.1
80				78.5
100				76.7
120	-16.1	192.9	10.5	75.5

2.1.3 Cleaner cell #1 concentrate pulp

Time (sec)	Eh (mV)	Eh (SHE) (mV)	pH	DO (%)
0	-45	164	10.3	97.2
10				94.6
20				71.5
30				67
40				63.6
50				60.2
60	- 56	153	10.5	56.4
80				52.1
100				48.9
120	-55.4	153.6	10.5	46.1

2.1.4 Cleaner tail pulp

Time (sec)	Eh (mV)	Eh (SHE) (mV)	pH	DO (%)
0	30.7	239.7	10.2	99
10				89.8
20				89.7
30				88.3
40				87.1
50				87
60	2.7	211.7	10.7	86.2
80				85.6
100				85.2
120	3.3	212.3	10.7	84.7

2.1.5 Cleaner feed pulp (survey on 23/08/01)

Time (sec)	Eh (mV)	Eh (SHE) (mV)	pH	DO (%)
0	41	250	10.7	98.2
10				90.9
20				87.4
30				86.3
40				85.4
50				84.7
60	-5.8	203.2	10.9	83.1
80				82
100				80.7
120	-12.8	196.2	10.9	78.9

2.1.6 Cleaner cell #1 concentrate pulp

Time (sec)	Eh (mV)	Eh (SHE) (mV)	pH	DO (%)
0	-45	164	10.9	92
10				85.9
20				74.7
30				71
40				68.4
50				66
60	-44.9	164.1	10.9	64.2
80				61.9
100				61.6
120	-44	165	10.9	59.6

2.1.7 Cleaner tail pulp

Time (sec)	Eh (mV)	Eh (SHE) (mV)	pH	DO (%)
0	30.7	239.7	10.9	99
10				89.8
20				89.7
30				88.3
40				87.1
50				87
60	2.7	211.7	10.9	86.2
80				85.6
100				85.2
120	3.3	212.3	10.9	84.7

2.1.8 EDTA data

2.1.8.1 Good feed survey on 23/08/01

	Cu ppm	Fe ppm	Ca ppm	S Ppm	Solid mass gms	Sol'n vol. ml	EDTA Cu %	EDTA S %	EDTA Ca %	EDTA Fe %
feed	9	21.2	63.7	16.5	1.67	100	0.159	0.153	47.091	1.537
con	28	66.1	52	12.2	7.29	100	0.012	0.005	39.628	0.414
tail	7	29	64.6	22.5	1.45	100	1.222	0.543	51.804	3.630

2.1.8.2 Good feed survey on 02/08/01

	Cu ppm	Fe ppm	Ca ppm	S ppm	Solid mass gms	Sol'n vol. ml	EDTA Cu %	EDTA S %	EDTA Ca %	EDTA Fe %
feed	20	10.4	62.3	12.7	2.16	100	0.144	0.039	84.831	0.370
con	110	66.7	84.5	26.2	8.53	100	0.052	0.010	55.035	0.374
tail	11.5	14.1	44.2	16.1	1.41	100	3.021	0.238	87.076	1.767

2.1.9 ToFSIMS data ('good' feed case)

2.1.9.1 +SIMMS spectra of copper for: A – pyrite activated with copper; B – chalcopyrite in the cleaner tail

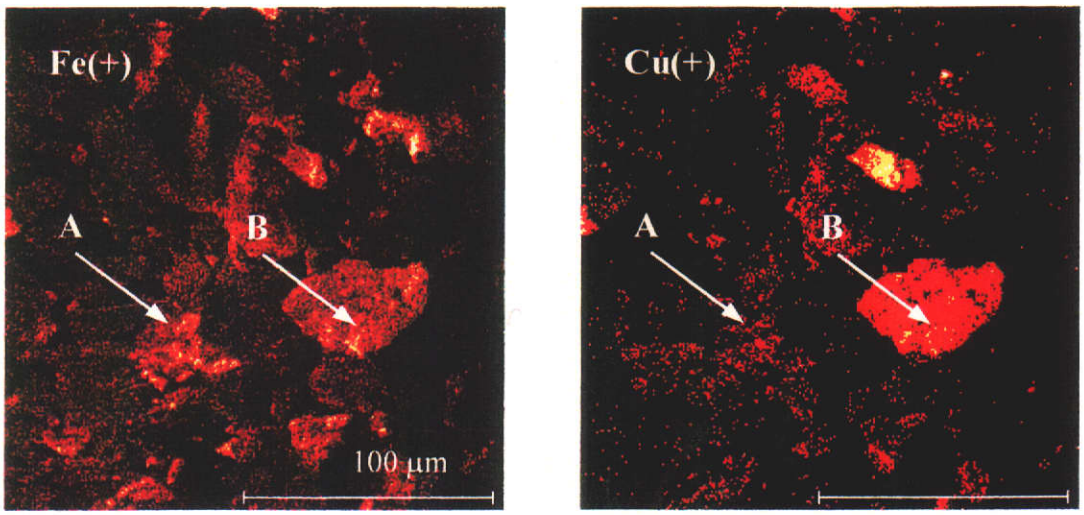

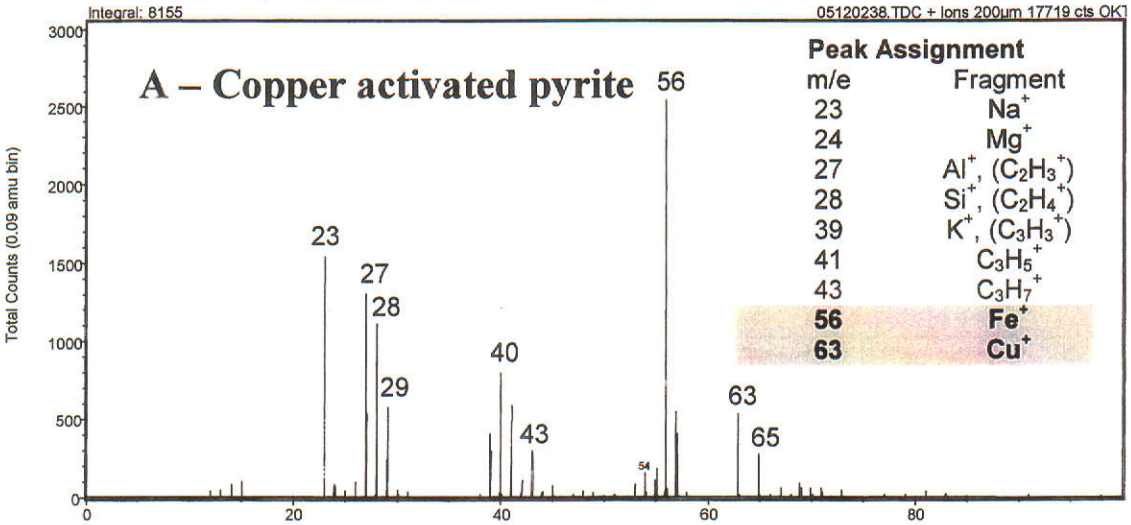

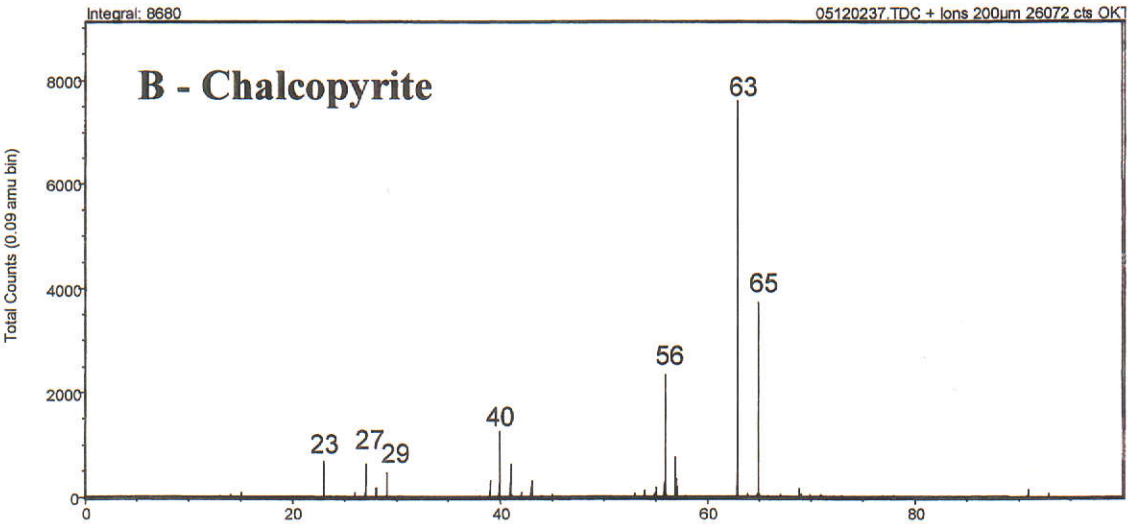

2.1.10 MATBAL Summary

2.1.10.1 Copper results ('good' feed survey on 23/08/01)

2Cct road side bank survey #3 - 23/08/01						
	Total Stream		cu			
StreamName	Weight	Weight%	Original	Adjusted	Residual	Recovery
feed	100	100	2.74	2.74	0	100
cell 1 conc	3.02	3.02	31.32	31.32	0	34.52
cell 1 tail	96.98	96.98	1.85	1.85	0	65.48
cell 2 conc	3.41	3.41	22.7	22.7	0	28.26
cell 2 tail	93.57	93.57	1.09	1.09	0	37.22
cell 3 conc	2.81	2.81	16.61	16.61	0	17.02
cell 3 tail	90.76	90.76	0.61	0.61	0	20.21
cell 4 conc	1.29	1.29	7.56	7.56	0	3.55
cell 4 tail	89.47	89.47	0.51	0.51	0	16.65
cell 5 conc	2.76	2.76	4.91	4.91	0	4.94
cell 5 tail	86.72	86.72	0.37	0.37	0	11.71
cell 6 conc	1.45	1.45	3.9	3.9	0	2.06
cell 6 tail	85.27	85.27	0.31	0.31	0	9.65
cell 7 conc	1.75	1.75	2.7	2.7	0	1.72
cell 7 tail	83.52	83.52	0.26	0.26	0	7.93
cell 8 conc	0.41	0.41	2.29	2.29	0	0.34
cell 8 tail	83.11	83.11	0.25	0.25	0	7.58

2.1.10.2 Gold results ('good' feed survey on 23/08/01)

2Cct road side bank survey #3 - 23/08/01						
	Total Stream		gold			
StreamName	Weight	Weight%	Original	Adjusted	Residual	Recovery
feed	100	100	3.74	3.74	0	100
cell 1 conc	20.76	20.76	13.17	13.17	0	73.09
cell 1 tail	79.24	79.24	1.27	1.27	0	26.91
cell 2 conc	2.02	2.02	11.22	11.22	0	6.05
cell 2 tail	77.23	77.23	1.01	1.01	0	20.86
cell 3 conc	2.75	2.75	9.96	9.96	0	7.31
cell 3 tail	74.48	74.48	0.68	0.68	0	13.54
cell 4 conc	1.02	1.02	5.01	5.01	0	1.36
cell 4 tail	73.46	73.46	0.62	0.62	0	12.18
cell 5 conc	0.43	0.43	3.99	3.99	0	0.46
cell 5 tail	73.03	73.03	0.6	0.6	0	11.72
cell 6 conc	1.56	1.56	3.81	3.81	0	1.59
cell 6 tail	71.47	71.47	0.53	0.53	0	10.13
cell 7 conc	3.61	3.61	2.22	2.22	0	2.14
cell 7 tail	67.86	67.86	0.44	0.44	0	7.98
cell 8 conc	3.19	3.19	2.67	2.67	0	2.28
cell 8 tail	64.67	64.67	0.33	0.33	0	5.71

2.1.10.3 Copper results ('good' feed survey on 02/08/01)

Unit1Cct road side survey #2-02/08/01						
	Total Stream		copper			
StreamName	Weight	Weight%	Original	Adjusted	Residual	Recovery
feed	100	100	7.11	7.11	0	100
cell 1 conc	7.55	7.55	31.1	31.1	0	33.04
cell 1 tail	92.45	92.45	5.15	5.15	0	66.96
cell 2 conc	11.6	11.6	19.71	19.71	0	32.17
cell 2 tail	80.84	80.84	3.06	3.06	0	34.79
cell 3 conc	5.9	5.9	20.08	20.08	0	16.66
cell 3 tail	74.94	74.94	1.72	1.72	0	18.13
cell 4 conc	4.78	4.78	11.12	11.12	0	7.47
cell 4 tail	70.17	70.17	1.08	1.08	0	10.66
cell 5 conc	0.5	0.5	13.69	13.69	0	0.96
cell 5 tail	69.67	69.67	0.99	0.99	0	9.7
cell 6 conc	1.95	1.95	9.67	9.67	0	2.65
cell 6 tail	67.72	67.72	0.74	0.74	0	7.05
cell 7 conc	2.14	2.14	6.26	6.26	0	1.88
cell 7 tail	65.58	65.58	0.56	0.56	0	5.17
cell 8 conc	0.42	0.42	5.17	5.17	0	0.31
cell 8 tail	65.16	65.16	0.53	0.53	0	4.86

2.1.10.4 Gold results ('good' feed survey on 02/08/01)

1Cct roadside bank survey #2 - 02/08/01						
	Total Stream		gold			
StreamName	Weight	Weight%	Original	Adjusted	Residual	Recovery
feed	100	100	4.29	4.29	0	100
cell 1 conc	5.36	5.36	18.78	18.78	0	23.45
cell 1 tail	94.64	94.64	3.47	3.47	0	76.55
cell 2 conc	9.16	9.16	13.17	13.17	0	28.14
cell 2 tail	85.48	85.48	2.43	2.43	0	48.42
cell 3 conc	8.09	8.09	8.46	8.46	0	15.95
cell 3 tail	77.39	77.39	1.8	1.8	0	32.47
cell 4 conc	8.85	8.85	6.06	6.06	0	12.5
cell 4 tail	68.54	68.54	1.25	1.25	0	19.97
cell 5 conc	1.45	1.45	10.05	10.05	0	3.39
cell 5 tail	67.1	67.1	1.06	1.06	0	16.58
cell 6 conc	1.22	1.22	8.1	8.1	0	2.3
cell 6 tail	65.88	65.88	0.93	0.93	0	14.28
cell 7 conc	1.11	1.11	5.58	5.58	0	1.45
cell 7 tail	64.76	64.76	0.85	0.85	0	12.83
cell 8 conc	0.42	0.42	6.99	6.99	0	0.68
cell 8 tail	64.35	64.35	0.81	0.81	0	12.15

2.1.11 Size by size data

2.1.11.1 Size by size recovery ('good' feed survey on 23/08/01)

Size (um)	Feed				Tail				Concentrate				Recovery by Size	
	Wt	%Wt..	%Cu	g/tAu	Wt. g.	%Wt..	%Cu	g/tAu	Wt (tph)	%Wt..	%Cu	g/tAu	%Cu	%Au
106	31.7	5.3	2.12	3.53	36.6	6.1	0.26	0.45	1.39	3.85	7.35	12.19	90.95	90.60
75	32.2	5.4	3.73	5.32	36.3	6.1	0.21	0.49	1.50	4.16	12.83	17.80	95.94	93.36
53	71.1	11.9	4.38	3.58	45	7.5	0.25	0.36	7.06	19.60	7.19	5.77	97.69	95.93
38	49.7	8.3	3.66	3.34	39	6.5	0.18	0.23	4.12	11.43	7.18	6.48	97.53	96.54
21.9	42.5	7.1	3.31	3.1	45.1	7.5	0.17	0.21	2.27	6.31	9.96	9.22	96.51	95.40
14.9	34	5.7	2.03	2.46	39.3	6.5	0.15	0.21	1.48	4.11	7.35	8.83	94.54	93.69
12.7	104	17.4	2.56	3.03	118	19.7	0.29	0.39	4.79	13.30	8.53	9.97	91.79	90.67
-12.7	234	39.1	2.2	3.43	241	40.1	0.45	0.65	13.40	37.23	5.55	8.76	86.56	87.55
Total	600	100.0	2.79	3.40	600	100.0	0.319	0.466	36.00	100.0	7.18	8.61	93.94	92.97

2.1.11.2 Size by size recovery ('good' feed survey on 02/08/01)

Size (um)	Feed				Tail				Concentrate				Recovery by Size	
	Wt	%Wt..	%Cu	g/tAu	Wt. g.	%Wt..	%Cu	g/tAu	Wt (tph)	%Wt..	%Cu	g/tAu	%Cu	%Au
106	38	7.59	11	13	24	4.80	2.9	3.1	4.47	12.77	16.97	20.64	89.45	90.49
75	41	8.19	9.8	10	28	5.59	1	1.3	4.56	13.02	16.85	17.33	95.57	94.23
53	44	8.74	11	8.1	36	7.17	0.5	0.7	4.08	11.65	23.08	16.60	97.63	95.28
38	33	6.63	11	7.8	34	6.81	0.2	0.5	2.20	6.29	32.19	22.64	98.64	96.16
21.9	83	16.66	12	6.9	69	13.86	0.5	1	7.64	21.84	26.43	13.81	97.73	92.28
14.9	29	5.81	4.5	4.1	33	6.55	0.3	0.8	1.55	4.43	15.84	13.22	94.89	85.91
12.7	78	15.68	3.3	2.7	93	18.67	0.5	0.7	3.54	10.12	12.95	9.52	88.09	79.64
-12.7	154	30.71	3.3	3.5	183	36.55	1	1.5	6.96	19.87	11.12	10.50	77.22	67.95
Total	500	100.0	7.18	5.97	500	100.0	0.781	1.156	35.00	100.0	19.07	14.90	92.40	87.74

2.1.12 Pulp chemical data (cleaner circuit characterisation studies as a function of 'bad' feed)

2.1.12.1 Calibration data

Eh in Zobell solution	430 mV
Calibration Eh	420 mV
Offset Eh (Calibration Eh – Reference Eh)	10 mV
Reference potential Eh	199 mV
pH in Buffer	10.05

Pulp Eh conversion to SHE = Offset Eh + 199 mV + pulp Eh

2.1.12.2 Cleaner feed pulp (pyrite skarn/porphyry feed blend)

Time (sec)	Eh (mV)	Eh (SHE) (mV)	pH	DO (%)
0	168	377	10.6	95.1
10				84.4
20				81.8
30				80.9
40				80.9
50				80.0
60	124	333	10.6	79.1
80				77.5
100				75.7
120	128	337	10.6	74.5

2.1.12.3 Cleaner cell#1 concentrate pulp

Time (sec)	Eh (mV)	Eh (SHE) (mV)	pH	DO (%)
0	156.6	365	10.7	98
10				95
20				93
30				81
40				79
50				76.5
60	4.3	213	10.7	72.4
80				66
100				67
120	4.7	214	10.6	64

2.1.12.4 Cleaner tail pulp

Time (sec)	Eh (mV)	Eh (SHE) (mV)	pH	DO (%)
0	150	359	10.6	98
10				88.8
20				88.7
30				87.3
40				86.1
50				86
60	112	321	10.6	85.2
80				84.6
100				84.2
120	111	320	10.5	83.7

2.1.12.5 Cleaner feed pulp (magnetite skarn/porphyry feed blend)

Time (sec)	Eh (mV)	Eh (SHE) (mV)	pH	DO (%)
0	9	218	10.8	100
10				82.2
20				79.1
30				76.4
40				62.0
50				60.9
60	-16	193	10.7	57.9
80				54.9
100				53.7
120	-19	190	10.8	47.4

2.1.12.6 Cleaner cell #1 concentrate pulp

Time (sec)	Eh (mV)	Eh (SHE) (mV)	pH	DO (%)
0	-33	176	10.7	98
10				95
20				93
30				81
40				79
50				76.5
60	-38	171	10.7	72.4
80				66
100				67
120	-39	170	10.8	64

2.1.12.7 Cleaner tail pulp

Time (sec)	Eh (mV)	Eh (SHE) (mV)	pH	DO (%)
0	5	214	11.7	100
10				89
20				87.7
30				86.9
40				86.1
50				84.9
60	-11	198	10.7	83.8
80				82.9
100				81.0
120	-12	197	10.7	79.4

2.1.13 EDTA data

2.1.13.1 'Bad' feed survey on 31/12/01

	Cu ppm	Fe ppm	Ca ppm	S Ppm	Solid mass gms	Sol'n vol. ml	EDTA Cu %	EDTA S %	EDTA Ca %	EDTA Fe %
feed	36	34.6	80.7	16.1	1.72	100	0.951	0.067	59.39	1.45
con	180	98.9	95.4	19.7	10.99	100	0.050	0.023	51.06	0.386
tail	56	36.3	70.9	10.3	2.98	100	1.59	0.017	54.07	0.583

2.1.13.2 'Bad' feed survey on 27/11/01

	Cu ppm	Fe ppm	Ca Ppm	S Ppm	Solid mass gms	Sol'n vol. ml	EDTA Cu %	EDTA S %	EDTA Ca %	EDTA Fe %
feed	16.5	74.3	137.6	12.7	3.84	100	0.021	0.014	65.12	0.744
con	29.5	114	129.7	16.6	10.1	100	0.010	0.005	67.59	0.397
tail	13.5	53.5	209	15.2	6.3	100	0.055	0.044	32.52	0.801

2.1.14 ToFSIMS data ('bad' feed case)

2.1.14.1 Selective (+) and (-) ion images showing chalcopyrite inclusions in pyrite in the cleaner concentrate

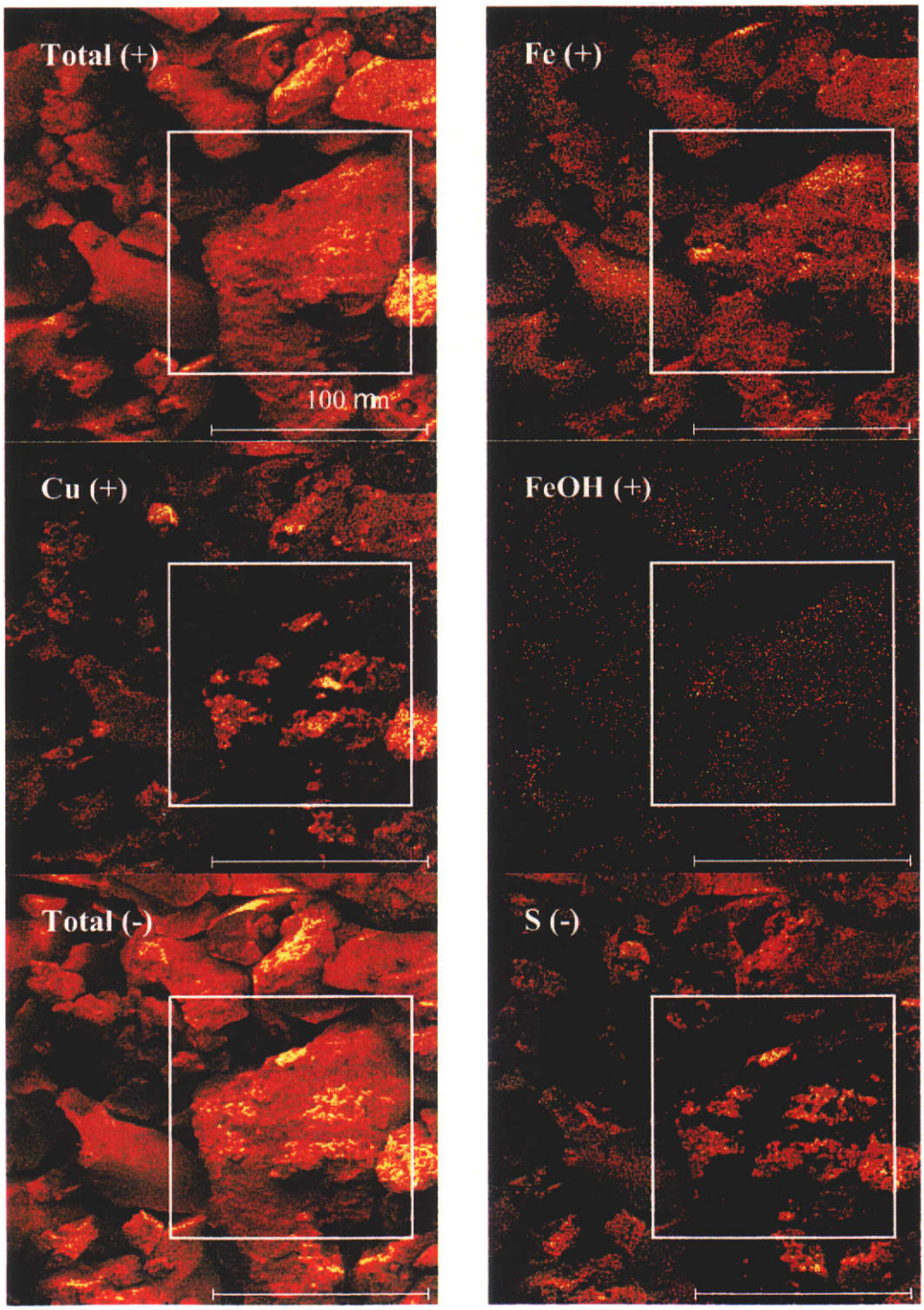

2.1.14.2 Selective (+) and (-) ion images illustrating a high floatability of non-sulfide gangue mineral in the cleaner concentrate

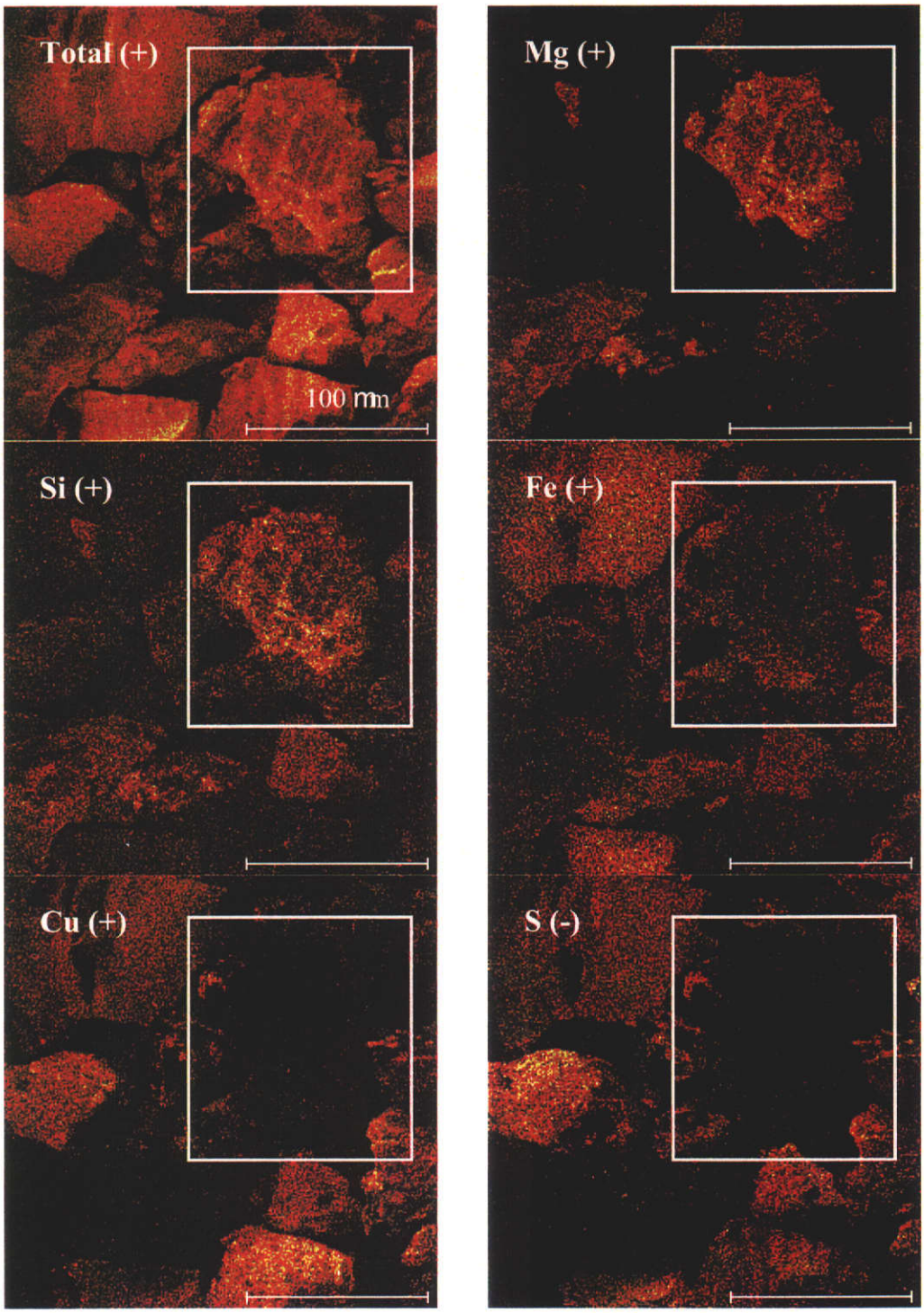

2.1.15 MATBAL summary

2.1.15.1 Copper results (pyrite skarn/porphyry feed blend)

Bad Feed Survey #1 _Roadside Cleaner Flotation Bank						
	Total Stream		copper			
StreamName	Weight	Weight%	Original	Adjusted	Residual	Recovery
cleaner feed	100	100	19.4	19.4	0	100
cell 1 conc	11.14	11.14	29.85	29.85	0	17.14
cell 1 tail	88.86	88.86	18.09	18.09	0	82.86
cell 2 conc	3.76	3.76	30.07	30.07	0	5.84
cell 2 tail	85.1	85.1	17.56	17.56	0	77.02
cell 3 conc	19.36	19.36	29.07	29.07	0	29.01
cell 3 tail	65.74	65.74	14.17	14.17	0	48.01
cell 4 conc	13.65	13.65	27.64	27.64	0	19.45
cell 4 tail	52.09	52.09	10.64	10.64	0	28.57
cell 5 conc	1.08	1.08	25.29	25.29	0	1.41
cell 5 tail	51.01	51.01	10.33	10.33	0	27.16
cell 6 conc	3.53	3.53	26.61	26.61	0	4.84
cell 6 tail	47.48	47.48	9.12	9.12	0	22.32
cell 7 conc	0.98	0.98	27.2	27.2	0	1.37
cell 7 tail	46.5	46.5	8.74	8.74	0	20.95
cell 8 conc	1.41	1.41	28.25	28.25	0	2.05
cell 8 tail	45.09	45.09	8.13	8.13	0	18.9

2.1.15.2 Gold results (pyrite skarn/porphyry feed blend)

Bad Feed Survey #1 _Roadside Cleaner Flotation Bank						
	Total Stream		Au			
StreamName	Weight	Weight%	Original	Adjusted	Residual	Recovery
cleaner feed	100	100	12.75	12.75	0	100
cell 1 conc	14.08	14.08	18.06	18.06	0	19.94
cell 1 tail	85.92	85.92	11.88	11.88	0	80.06
cell 2 conc	8.89	8.89	17.34	17.34	0	12.09
cell 2 tail	77.03	77.03	11.25	11.25	0	67.97
cell 3 conc	20.65	20.65	16.74	16.74	0	27.11
cell 3 tail	56.39	56.39	9.24	9.24	0	40.87
cell 4 conc	13.42	13.42	16.35	16.35	0	17.21
cell 4 tail	42.97	42.97	7.02	7.02	0	23.66
cell 5 conc	0.74	0.74	15.57	15.57	0	0.9
cell 5 tail	42.23	42.23	6.87	6.87	0	22.75
cell 6 conc	3.89	3.89	15.45	15.45	0	4.71
cell 6 tail	38.34	38.34	6	6	0	18.04
cell 7 conc	1.73	1.73	11.7	11.7	0	1.59
cell 7 tail	36.61	36.61	5.73	5.73	0	16.45
cell 8 conc	5.9	5.9	9.63	9.63	0	4.46
cell 8 tail	30.7	30.7	4.98	4.98	0	11.99

2.1.15.3 Copper results (magnetite skarn/porphyry feed blend)

Bad Feed Survey #2 _Roadside Cleaner Flotation Bank						
	Total Stream		copper			
StreamName	Weight	Weight%	Original	Adjusted	Residual	Recovery
cleaner feed	100	100	18.03	18.03	0	100
cell 1 conc	21.05	21.05	32.66	32.66	0	38.12
cell 1 tail	78.95	78.95	14.13	14.13	0	61.88
cell 2 conc	11.12	11.12	27.73	27.73	0	17.11
cell 2 tail	67.83	67.83	11.9	11.9	0	44.77
cell 3 conc	17.49	17.49	23.87	23.87	0	23.16
cell 3 tail	50.34	50.34	7.74	7.74	0	21.61
cell 4 conc	9.17	9.17	19.15	19.15	0	9.73
cell 4 tail	41.17	41.17	5.2	5.2	0	11.87
cell 5 conc	3.36	3.36	13.18	13.18	0	2.46
cell 5 tail	37.81	37.81	4.49	4.49	0	9.42
cell 6 conc	0.83	0.83	23.76	23.76	0	1.09
cell 6 tail	36.98	36.98	4.06	4.06	0	8.33
cell 7 conc	0.49	0.49	17.6	17.6	0	0.47
cell 7 tail	36.5	36.5	3.88	3.88	0	7.85
cell 8 conc	0.72	0.72	17.8	17.8	0	0.71
cell 8 tail	35.78	35.78	3.6	3.6	0	7.14

2.1.15.4 Gold results (magnetite skarn/porphyry feed blend)

Bad Feed Survey #2 _Roadside Cleaner Flotation Bank						
	Total Stream		gold			
StreamName	Weight	Weight%	Original	Adjusted	Residual	Recovery
cleaner feed	100	100	7.82	7.82	0	100
cell 1 conc	26.57	26.57	13.68	13.68	0	46.47
cell 1 tail	73.43	73.43	5.7	5.7	0	53.53
cell 2 conc	1.9	1.9	10.23	10.23	0	2.48
cell 2 tail	71.54	71.54	5.58	5.58	0	51.05
cell 3 conc	19.52	19.52	9.15	9.15	0	22.84
cell 3 tail	52.01	52.01	4.24	4.24	0	28.2
cell 4 conc	7.58	7.58	8.58	8.58	0	8.31
cell 4 tail	44.44	44.44	3.5	3.5	0	19.89
cell 5 conc	4.18	4.18	6.39	6.39	0	3.41
cell 5 tail	40.26	40.26	3.2	3.2	0	16.47
cell 6 conc	1.57	1.57	10.08	10.08	0	2.03
cell 6 tail	38.68	38.68	2.92	2.92	0	14.44
cell 7 conc	1.7	1.7	7.92	7.92	0	1.72
cell 7 tail	36.98	36.98	2.69	2.69	0	12.72
cell 8 conc	3.04	3.04	8.04	8.04	0	3.13
cell 8 tail	33.94	33.94	2.21	2.21	0	9.59

2.1.16 Size by size data

2.1.16.1 Size by size recovery (pyrite skarn/porphyry feed blend)

Size (um)	Feed				Tail				Concentrate				Recovery by Size	
	Wt	%Wt..	%Cu	g/tAu	Wt. g.	%Wt..	%Cu	g/tAu	Wt (tph)	%Wt..	%Cu	g/tAu	%Cu	%Au
106	75.2	7.5	10	11.3	151	15.1	5.88	5.13	0.74	1.34	47.94	67.80	46.96	58.94
75	103	10.3	19.9	12	113	11.3	12.2	6.81	5.20	9.45	27.42	17.15	69.67	71.97
53	143	14.3	22.9	14.3	89.2	8.9	9.78	4.56	10.25	18.63	27.97	18.12	87.95	91.02
38	111	11.1	21.6	15.7	118	11.8	3.56	2.56	5.77	10.50	38.22	27.84	92.10	92.19
21.9	195	19.5	23.3	15.1	125	12.5	6.47	3.78	13.90	25.28	30.18	19.72	92.00	92.79
14.9	56.2	5.6	19.7	12.7	51.7	5.2	5.07	4.28	3.29	5.99	30.09	18.58	89.36	86.00
12.7	100	10.0	18	11.8	103	10.3	8.94	6.64	5.41	9.84	25.65	16.13	77.05	73.99
-12.7	216	21.6	15.7	14.9	249	24.9	10.5	10.3	10.44	18.98	21.20	19.73	65.29	64.11
Total	1000	100.0	19.31	13.93	1000	100.0	8.165	6.194	55.00	100.0	28.43	20.26	77.55	78.88

2.1.16.2 Size by size recovery (magnetite skarn/porphyry feed blend)

Size (um)	Feed				Tail				Concentrate				Recovery by Size	
	Wt	%Wt..	%Cu	g/tAu	Wt. g.	%Wt..	%Cu	g/tAu	Wt (tph)	%Wt..	%Cu	g/tAu	%Cu	%Au
106	107	10.7	16.6	16.1	134	13.4	8.4	7.36	6.07	9.34	22.97	22.85	78.02	80.12
75	94.2	9.4	21.1	12.3	72.7	7.27	8.14	3.82	6.87	10.57	25.83	15.38	89.56	91.58
53	236	23.6	22.4	8.82	137	13.7	3.65	1.78	18.83	28.97	27.24	10.62	96.69	95.90
38	54.8	5.5	22.3	8.16	40.3	4.03	2.11	0.87	4.07	6.26	29.24	10.69	97.56	97.26
21.9	113	11.3	25.2	12.2	63.4	6.34	4.12	3.12	9.11	14.02	30.37	14.46	96.80	95.01
14.9	128	12.8	14.1	5.55	139	13.9	2.11	1.95	7.94	12.21	21.40	7.76	94.30	86.65
12.7	82.8	8.3	9.01	3.96	115	11.5	3.01	1.98	4.26	6.56	14.67	5.83	83.79	75.73
-12.7	183	18.3	8.81	2.22	299	29.9	4.08	1.5	7.84	12.07	15.12	3.18	73.53	61.38
Total	1000	100.0	17.31	8.25	1000	100.0	4.419	2.685	65.00	100.0	24.25	11.25	88.78	85.45

APPENDIX #3

EFFECT OF UNGROUND FEED

3.1 Pulp chemical data

3.1.1 Calibration data

Eh in Zobell solution	430 mV
Calibration Eh	420 mV
Offset Eh (Calibration Eh – Reference Eh)	10 mV
Reference potential Eh	199 mV
pH in Buffer	10.05

Pulp Eh conversion to SHE = Offset Eh + 199 mV + pulp Eh

3.1.2 Cleaner feed pulp (unground feed condition)

Time (sec)	Eh (mV)	Eh (SHE) (mV)	pH	DO (%)
0	45.5	254	10.6	100
10				79.0
20				74.6
30				72.6
40				70.5
50				68.2
60	-13.6	195	10.7	66.1
80				59.9
100				56.3
120	-39.4	170	10.7	55.2

3.1.3 Cleaner tail pulp (unground feed condition)

Time (sec)	Eh (mV)	Eh (SHE) (mV)	pH	DO (%)
0	15.5	224	10.5	100
10				83.4
20				79.5
30				78.8
40				76.3
50				74.0
60	-37.8	171	10.6	73.2
80				71.4
100				69.5
120	-43.3	166	10.6	67.4

3.1.4 Cleaner feed pulp (ground feed condition)

Time (sec)	Eh (mV)	Eh (SHE) (mV)	pH	DO (%)
0	17.5	226	10.5	100
10				87.0
20				84.0
30				83.0
40				81.0
50				79.8
60	-32.6	176	10.7	75.7
80				73.8
100				70.1
120	-50.4	159	10.7	68.4

3.1.5 Cleaner tail pulp (ground feed condition)

Time (sec)	Eh (mV)	Eh (SHE) (mV)	pH	DO (%)
0	12	221	10.5	100
10				92.2
20				88.9
30				87.8
40				87.2
50				86.8
60	-50	159	10.6	85.4
80				79.9
100				79.4
120	-52	157	10.6	78.5

3.2 ToFSIMS data

3.2.1 Selected (-) ion images for chalcopyrite particle in the cleaner concentrate (ground feed)

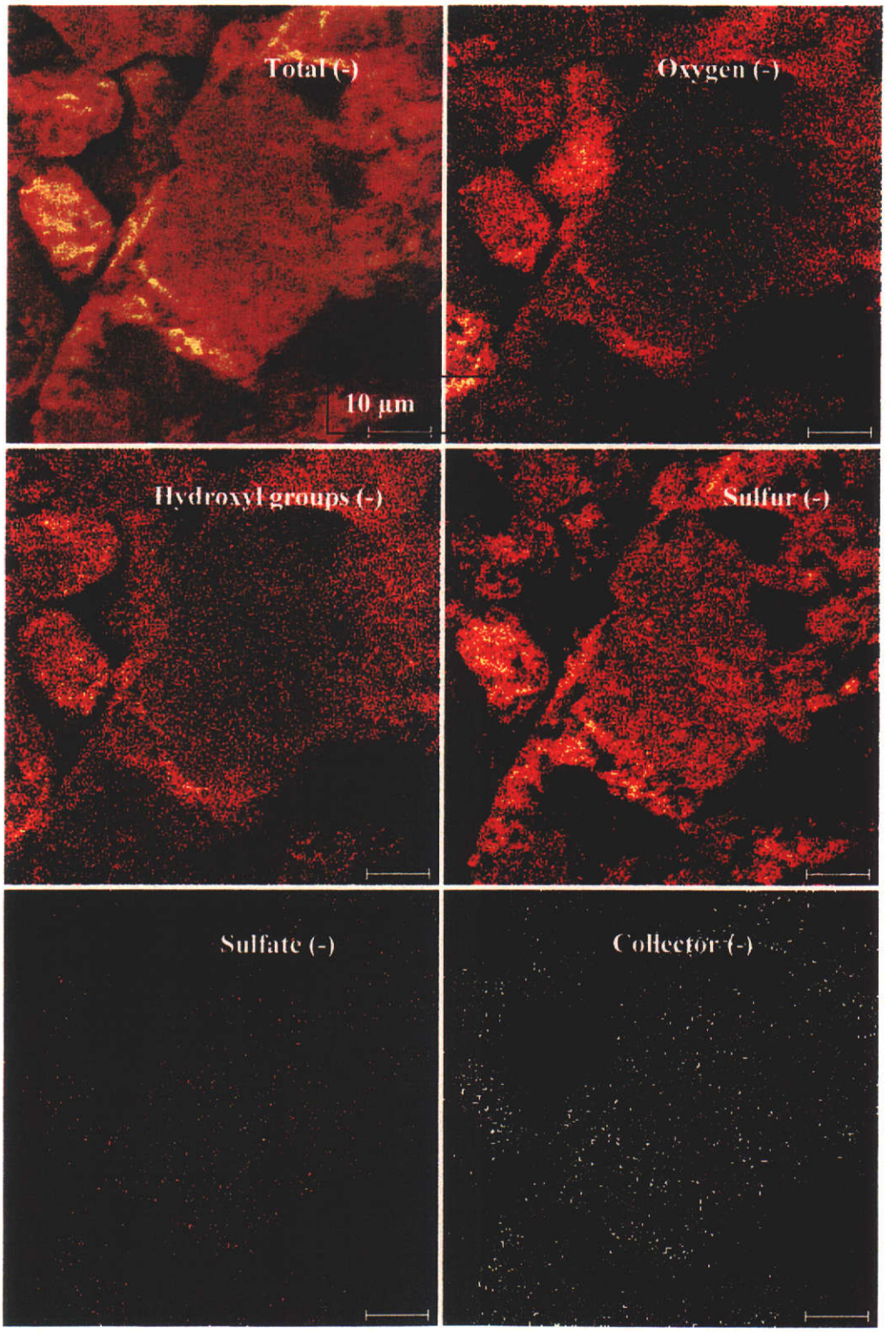

3.2.2 Selected (+) ion images for chalcopyrite particle in the cleaner concentrate (ground feed)

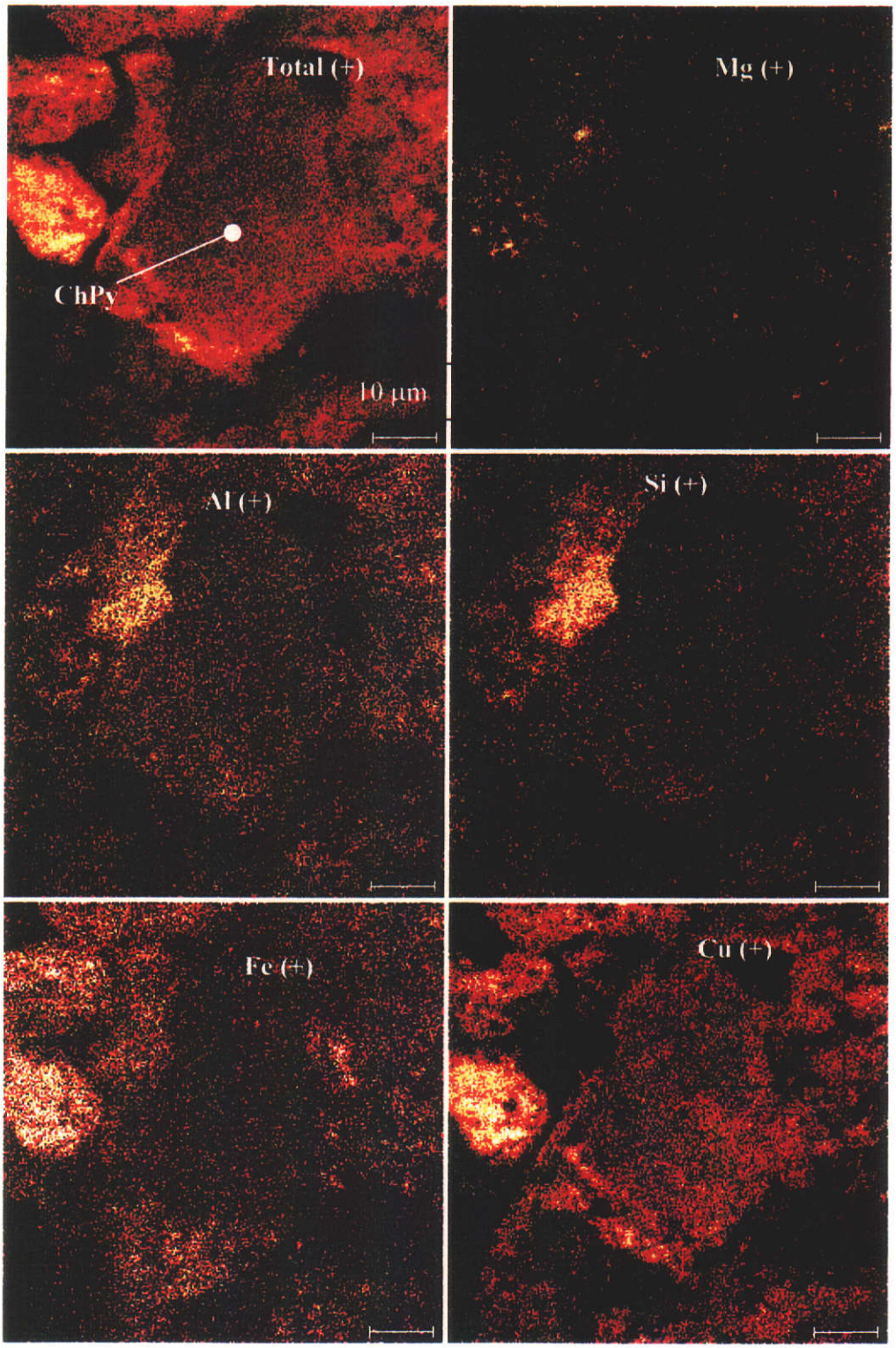

3.2.3 Evidence of the liberation problems in the cleaner concentrate (unground feed)

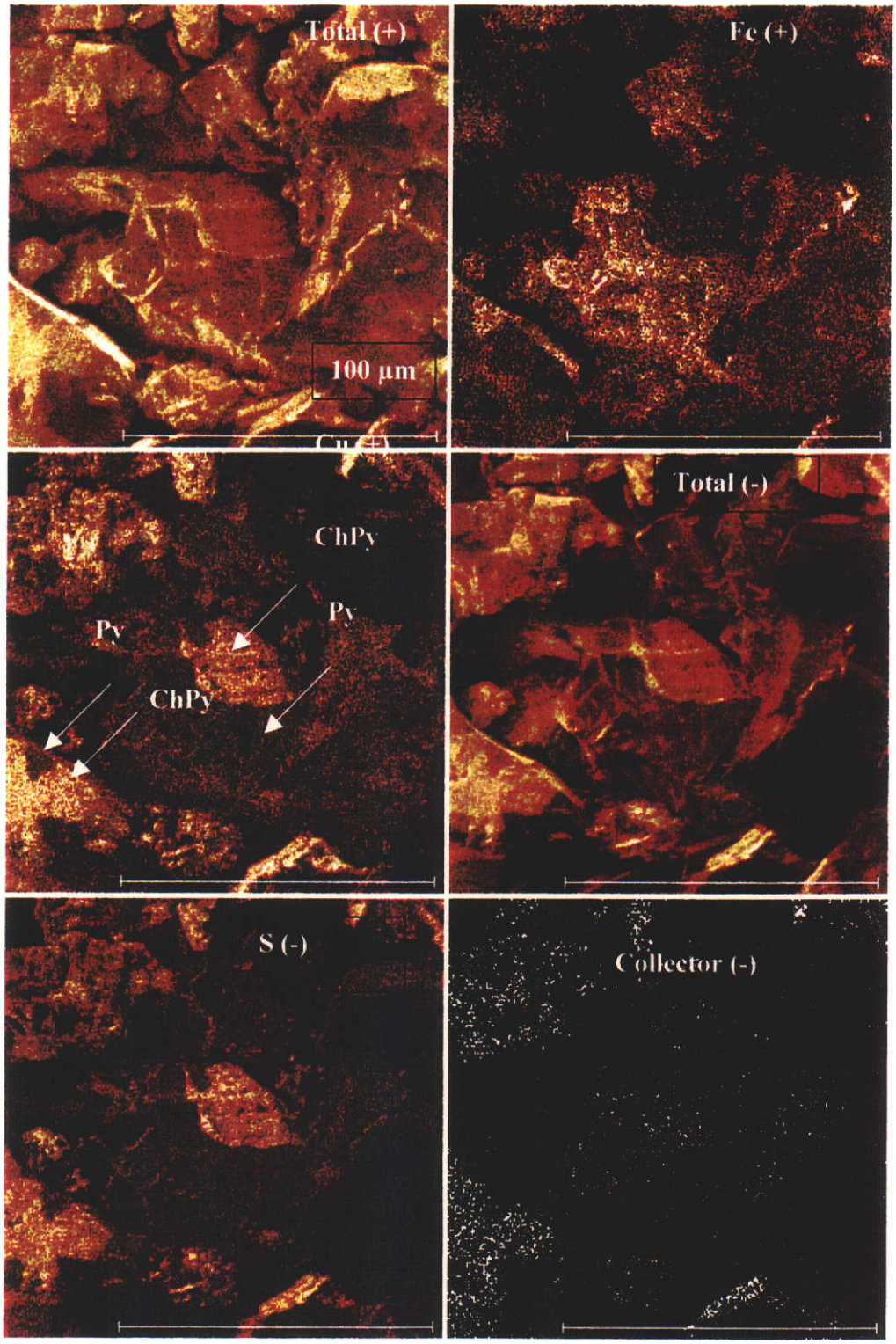

3.2.4 Selected (-) ion images for pyrite particle in the cleaner concentrate (ground feed)

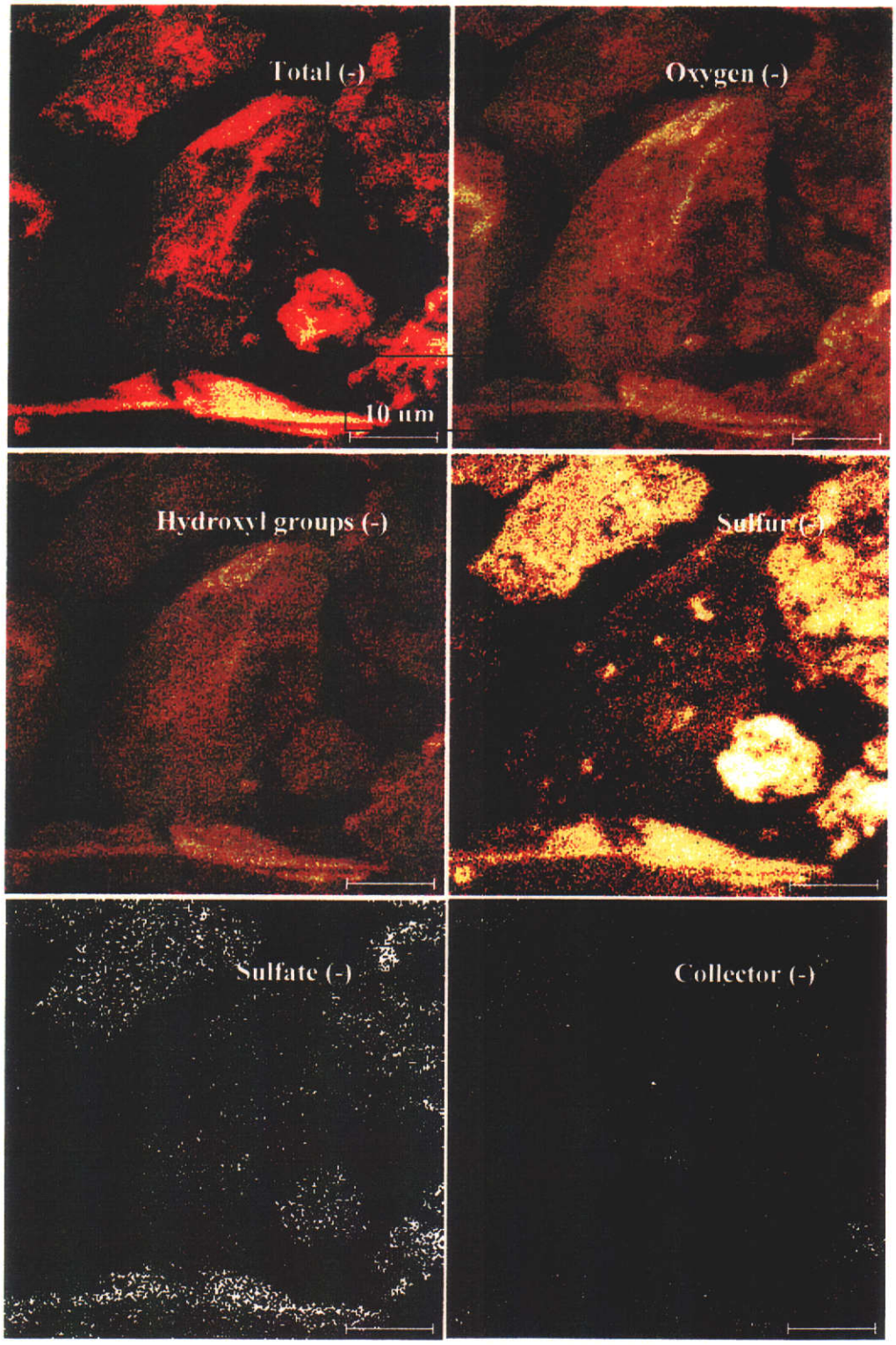

3.2.5 Traces of collector present on chalcopyrite particles in the cleaner concentrate (ground feed)

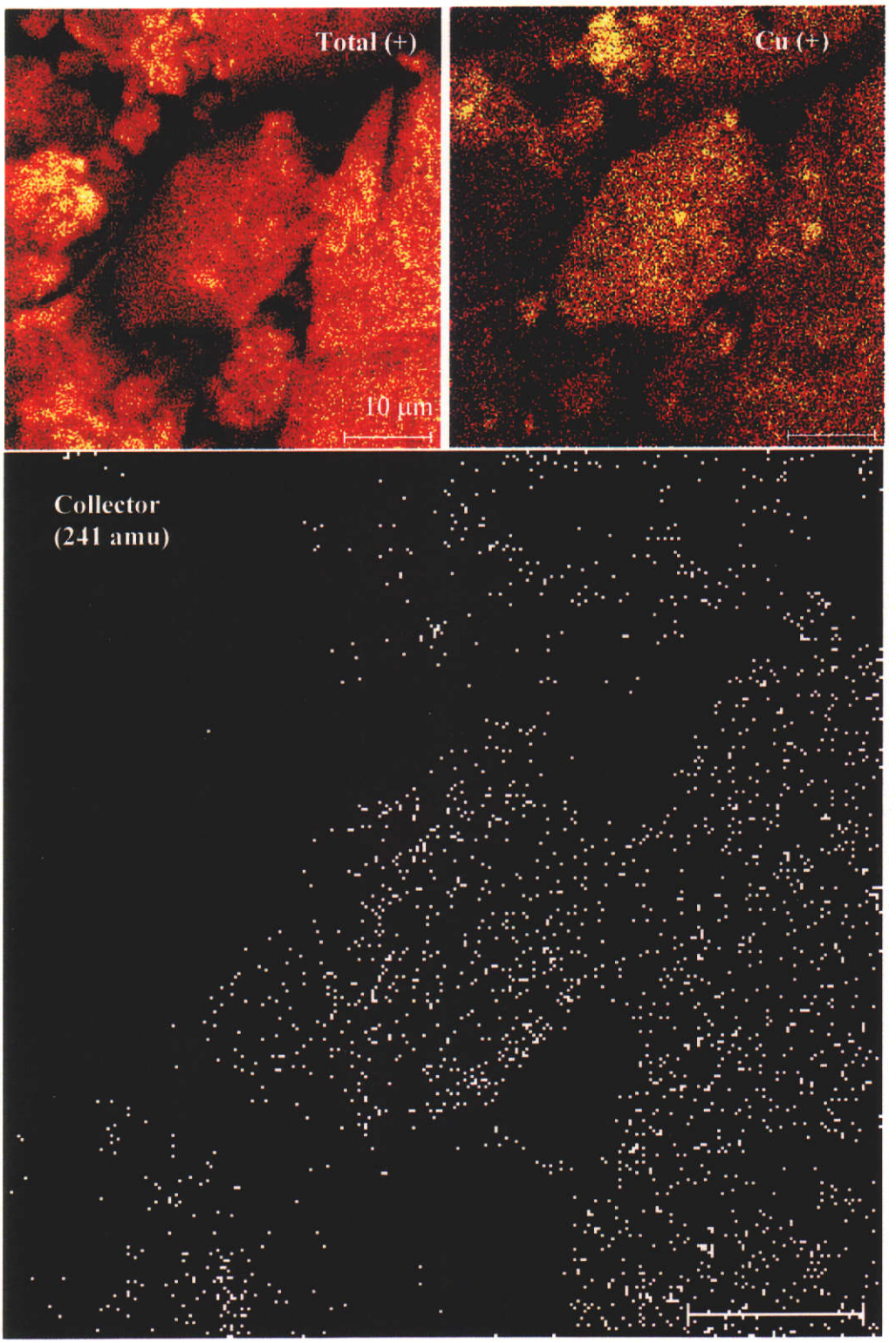

3.2.6 Virtually only fine chalcopyrite particles reported to the cleaner tails; observe no collector in chalcopyrite (ground feed)

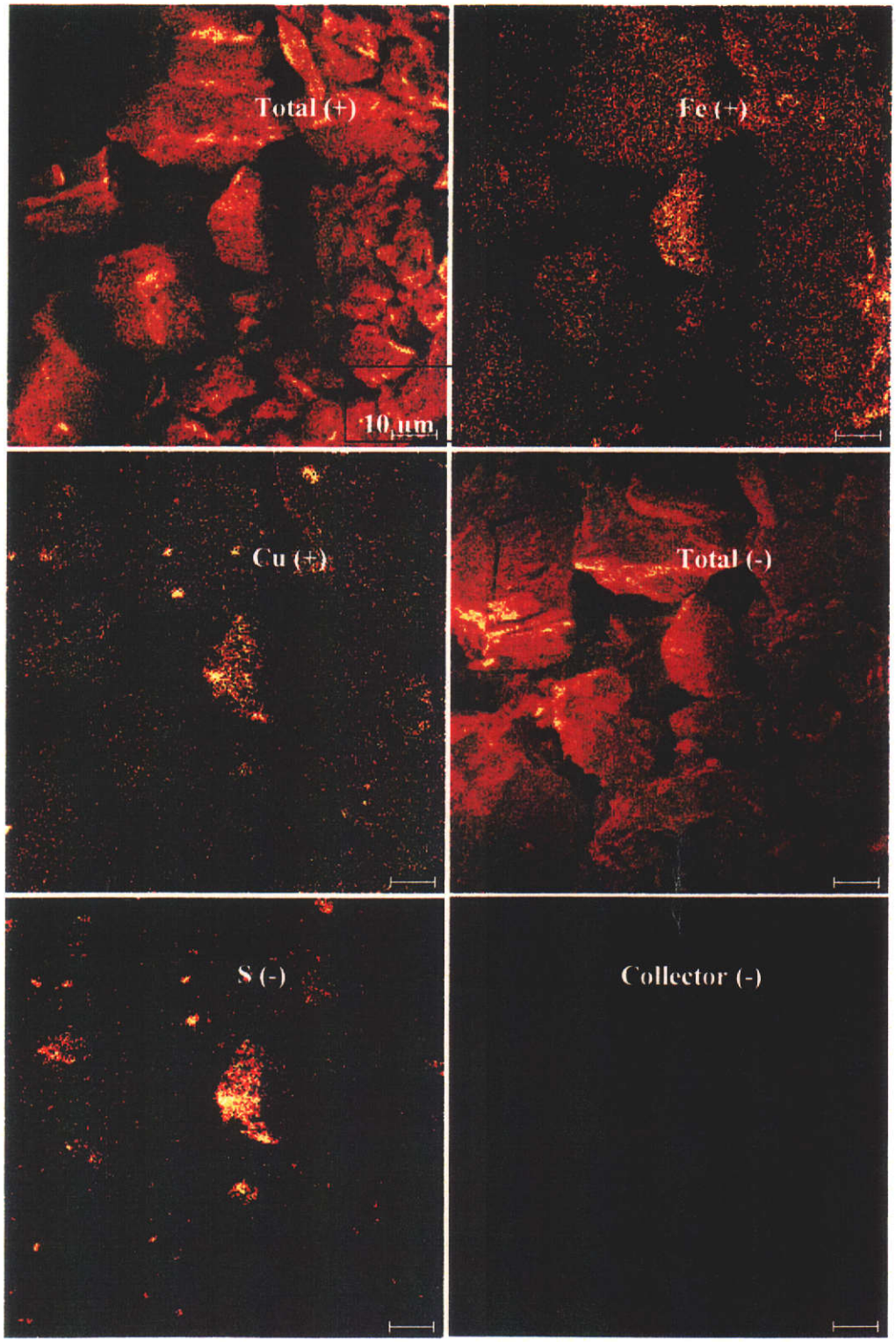

3.3 MAT BAL summary

3.3.1 Copper results (unground feed)

Regrind Off Survey _Roadside Cleaner Flotation Bank						
	Total Stream		copper			
StreamName	Weight	Weight%	Original	Adjusted	Residual	Recovery
cleaner feed	100	100	11.54	11.54	0	100
cell 1 conc	2.04	2.04	23.52	23.52	0	4.17
cell 1 tail	97.96	97.96	11.29	11.29	0	95.83
cell 2 conc	13.62	13.62	22.68	22.68	0	26.77
cell 2 tail	84.33	84.33	9.45	9.45	0	69.06
cell 3 conc	4.29	4.29	23.63	23.63	0	8.78
cell 3 tail	80.04	80.04	8.69	8.69	0	60.27
cell 4 conc	22.8	22.8	16.22	16.22	0	32.05
cell 4 tail	57.24	57.24	5.69	5.69	0	28.22
cell 5 conc	13.15	13.15	11.49	11.49	0	13.09
cell 5 tail	44.09	44.09	3.96	3.96	0	15.13
cell 6 conc	0.07	0.07	16.14	16.14	0	0.1
cell 6 tail	44.02	44.02	3.94	3.94	0	15.03
cell 7 conc	6.72	6.72	12.48	12.48	0	7.27
cell 7 tail	37.29	37.29	2.4	2.4	0	7.76
cell 8 conc	3.57	3.57	8.25	8.25	0	2.55
cell 8 tail	33.72	33.72	1.78	1.78	0	5.2

3.3.2 Gold results (unground feed)

Regrind Off Survey _Roadside Cleaner Flotation Bank						
	Total Stream		gold			
StreamName	Weight	Weight%	Original	Adjusted	Residual	Recovery
cleaner feed	100	100	9.94	9.94	0	100
cell 1 conc	27.18	27.18	15.54	15.54	0	42.49
cell 1 tail	72.82	72.82	7.85	7.85	0	57.51
cell 2 conc	14.18	14.18	14.8	14.8	0	21.11
cell 2 tail	58.65	58.65	6.17	6.17	0	36.4
cell 3 conc	0.19	0.19	15.26	15.26	0	0.3
cell 3 tail	58.45	58.45	6.14	6.14	0	36.11
cell 4 conc	16.67	16.67	10.7	10.7	0	17.95
cell 4 tail	41.78	41.78	4.32	4.32	0	18.16
cell 5 conc	5.85	5.85	8.19	8.19	0	4.82
cell 5 tail	35.93	35.93	3.69	3.69	0	13.34
cell 6 conc	1.68	1.68	12.23	12.23	0	2.07
cell 6 tail	34.25	34.25	3.27	3.27	0	11.27
cell 7 conc	5.16	5.16	7.95	7.95	0	4.13
cell 7 tail	29.09	29.09	2.44	2.44	0	7.14
cell 8 conc	4.77	4.77	6.93	6.93	0	3.32
cell 8 tail	24.32	24.32	1.56	1.56	0	3.82

3.3.3 Copper results (ground feed)

Regrind On Survey _Roadside Cleaner Flotation Bank						
	Total Stream		copper			
StreamName	Weight	Weight%	Original	Adjusted	Residual	Recovery
cleaner feed	100	100	11.94	11.94	0	100
cell 1 conc	13.51	13.51	29.1	29.1	0	32.92
cell 1 tail	86.49	86.49	9.26	9.26	0	67.08
cell 2 conc	9.88	9.88	27.01	27.01	0	22.36
cell 2 tail	76.61	76.61	6.97	6.97	0	44.72
cell 3 conc	4.98	4.98	25.68	25.68	0	10.7
cell 3 tail	71.63	71.63	5.67	5.67	0	34.02
cell 4 conc	7.73	7.73	19.55	19.55	0	12.66
cell 4 tail	63.9	63.9	3.99	3.99	0	21.35
cell 5 conc	9.94	9.94	13.44	13.44	0	11.18
cell 5 tail	53.96	53.96	2.25	2.25	0	10.17
cell 6 conc	6.82	6.82	7.57	7.57	0	4.33
cell 6 tail	47.14	47.14	1.48	1.48	0	5.84
cell 7 conc	4.5	4.5	7.16	7.16	0	2.7
cell 7 tail	42.64	42.64	0.88	0.88	0	3.14
cell 8 conc	1.84	1.84	6.64	6.64	0	1.02
cell 8 tail	40.79	40.79	0.62	0.62	0	2.12

3.3.4 Gold results (ground feed)

Regrind On Survey _Roadside Cleaner Flotation Bank						
	Total Stream		gold			
StreamName	Weight	Weight%	Original	Adjusted	Residual	Recovery
cleaner feed	100	100	9.63	9.63	0	100
cell 1 conc	47.6	47.6	13.89	13.89	0	68.66
cell 1 tail	52.4	52.4	5.76	5.76	0	31.34
cell 2 conc	0.33	0.33	13.68	13.68	0	0.47
cell 2 tail	52.07	52.07	5.71	5.71	0	30.87
cell 3 conc	5.5	5.5	14.34	14.34	0	8.2
cell 3 tail	46.57	46.57	4.69	4.69	0	22.68
cell 4 conc	8.15	8.15	10.35	10.35	0	8.75
cell 4 tail	38.42	38.42	3.49	3.49	0	13.92
cell 5 conc	6.2	6.2	9.36	9.36	0	6.03
cell 5 tail	32.22	32.22	2.36	2.36	0	7.9
cell 6 conc	3.74	3.74	5.63	5.63	0	2.19
cell 6 tail	28.47	28.47	1.93	1.93	0	5.71
cell 7 conc	1.58	1.58	6.53	6.53	0	1.07
cell 7 tail	26.9	26.9	1.66	1.66	0	4.64
cell 8 conc	2.16	2.16	6.23	6.23	0	1.4
cell 8 tail	24.73	24.73	1.26	1.26	0	3.24

3.4 Size by size data

3.4.1 Size by size recovery (unground feed)

Size (um)	Feed				Tail				Concentrate				Recovery by Size	
	Wt	%Wt..	%Cu	g/tAu	Wt. g.	%Wt..	%Cu	g/tAu	Wt (tph)	%Wt..	%Cu	g/tAu	%Cu	%Au
212	47.6	4.8	18.2	12.6	33.3	3.3	12.4	9.56	3.66	5.50	19.99	13.54	84.33	82.52
150	91	9.1	16.1	11.8	28.9	2.9	9.4	8.13	8.15	12.24	16.92	12.20	93.89	92.75
106	144	14.4	15.7	10.1	41	4.1	5.32	5.14	13.04	19.58	16.73	10.57	96.80	95.19
75	114	11.4	15.8	10.5	41.3	4.1	3.1	3.09	10.08	15.14	17.53	11.49	97.66	96.49
53	158	15.8	14.5	9.73	77.9	7.8	2.53	2.16	13.20	19.82	16.81	11.21	97.16	96.38
38	60.8	6.1	13	9.14	40.6	4.1	2.19	1.8	4.74	7.12	16.02	11.21	96.29	95.67
31.1	74.1	7.4	10.4	9.72	45.8	4.6	3.97	3.45	5.90	8.86	12.06	11.33	92.22	92.76
14.9	97.8	9.8	8.05	5.45	162	16.2	2.21	1.51	4.43	6.66	15.10	10.20	84.99	84.85
12.7	61.4	6.1	6.5	4.62	143	14.3	1.87	1.3	1.41	2.12	22.1	15.8	77.83	78.32
-12.7	151	15.1	6.93	2.76	386	38.6	2.01	0.87	1.97	2.96	38.6	14.9	74.90	72.72
Total	1000	100.0	12.48	8.36	1000	100.0	1.86	1.54	66.59	100.0	17.26	11.53	89.61	88.77

3.4.2 Size by size recovery (ground feed)

Size (um)	Feed				Tail				Concentrate				Recovery by Size	
	Wt	%Wt..	%Cu	g/tAu	Wt. g.	%Wt..	%Cu	g/tAu	Wt (tph)	%Wt..	%Cu	g/tAu	%Cu	%Au
212	38.2	3.8	14.5	12.8	36.7	3.7	5.29	5.51	2.36	3.92	20.16	17.37	85.95	83.50
150	56.3	5.6	15.2	13	29.7	3.0	5.1	4.91	4.44	7.40	17.93	15.12	92.95	92.03
106	96.2	9.6	14.4	13.9	52	5.2	2.14	3.33	7.54	12.56	17.83	16.80	96.80	94.82
75	100	10.0	15.9	12.6	59.9	6.0	0.74	1.95	7.63	12.71	20.61	15.95	98.88	96.31
53	152	15.2	15.3	11.1	110	11.0	0.49	1.21	10.81	18.01	21.31	15.13	99.08	96.86
38	65.2	6.5	14.1	10.4	50.8	5.1	0.54	0.87	4.49	7.47	20.30	14.73	98.80	97.39
31.1	152	15.2	12.4	10.2	112	11.2	1.42	1.51	10.73	17.87	17.05	13.88	96.63	95.65
14.9	42.6	4.3	9.43	5.03	101	10.1	0.79	0.5	0.22	0.37	168.62	88.50	92.05	90.57
12.7	63.1	6.3	6.63	3.36	133	13.3	1.03	0.65	1	1.67	36.36	17.75	86.93	83.72
-12.7	234	23.4	7.39	4.31	315	31.5	2.81	1.81	10.8	18.02	12.71	7.21	79.58	77.44
Total	1000	100.0	12.08	9.18	1000	100.0	1.84	0.72	60.05	100.0	18.89	14.16	92.76	90.83